



The interaction of building energy use, ventilation performance and urban noise under future climate scenarios

Michael Barclay

Supervisors: Professor Jian Kang and Professor Steve Sharples

Submitted for the degree of PhD

School of Architecture

Submitted October 2012

Abstract

This thesis studies the interaction of building energy use, ventilation performance and urban noise under future climate scenarios, comparing in particular the noise and climatic influences on non-domestic natural ventilation cooling. The main objective is to determine the level of climate change temperature increase that a noise reduction measure would mitigate. This involves quantifying the tension between maximising natural ventilation and maintaining good acoustic conditions.

Methods are linked that are appropriate to a number of scales: ventilation aperture, whole-building, urban area, and the climate scale. Using the Finite Element Method (FEM), it was found that the sound transmission of ventilation apertures varied by up to 8dB across the frequencies considered. Noise mapping and whole building thermal performance were used to quantify natural ventilation potential and the impact of noise reduction measures.

Three future climate data sets were compared and it was found that all sets provided acceptable information about future natural ventilation performance. The difficulty of adopting natural ventilation with the warming present in all the data sets was clear from the high levels of future overheating.

Using these methods and a representative future weather data set, a number of design implications were illustrated, such as the reduction in sensible cooling per unit of ventilation airflow with higher summer temperatures. The main comparison of acoustic and climatic environmental influences showed that a 10dB noise reduction measure affecting natural ventilation could mitigate a summer temperature increase due to climate change of between 2.0°C and 3.4°C.

List of Abbreviations

Abbreviations used in this document:

- ACH Air Changes per Hour
- AIVC Air Infiltration and Ventilation Centre
- AOGCM Atmosphere-Ocean Global Circulation Models
- BEM Boundary Element Method
- BRE Building Research Establishment
- CCP Climatic Cooling Potential
- CFD Computation Fluid Dynamics
- CIBSE Chartered Institution of Building Services Engineers
- COPSE CO-incident Probabilistic climate change weather data for a Sustainable Environment
- CNSF Coalition for National Science Funding
- DSY Design Summer Year
- END Environmental Noise Directive
- EPSRC Engineering and Physical Sciences Research Council of the UK
- FEM Finite Element Method
- GCM General Circulation Model
- HadRM3 Met Office Hadley Centre Regional Climate Model 3
- HVAC Heating, Ventilation, and Air Conditioning
- PET Potential Evapotranspiration
- PMV Percentage Mean Vote
- PPD Percentage of Persons Dissatisfied

- PROMETHEOUS The Use of Probabilistic Climate Change Data to Future-proof Design Decisions in the Building Sector
- RCM Regional Climate Models
- SBEM Simplified Building Energy Modelling
- SRI Sound Reduction Index
- TL Transmission Loss
- TRY Test Reference Year
- UKCIP02 United Kingdom Climate Impacts Programme 2002 report
- UKCP09 United Kingdom Climate Projections from 2009

Acknowledgments

First of all I would like to thank my tutors, Professor Jian Kang and Professor Steve Sharples whose help and support were crucial to the completion of this thesis. I would like to thank the EPSRC for financial support for this work: grant number (ref. EP/F038100/1) and also partly the CNSF (50928801). Additional thanks go to the Chartered Institute of Building Services Engineers (CIBSE) and the COPSE and PROMETHEUS projects for the provision of future hourly weather data. I would also like to thank the following people for their help and input Richard Watkins, Nader Pourmosavi, Hongsoek Yang, Owen Bodger, Huahua Huang, Bo Wang (who provided the sources of Figure 5.5) and Hu Du. Also many thanks go to the following people for helping in the final stages of thesis writing: Mark Westmoquette, Dave Carswell, Luzia Barclay, John Barclay, Paula Barclay, John Chapman, Simon Williams, Brendan Campbell, Last but not least thank you Sylvia Noorbhai for proof reading and putting up with my mood swings while writing up.

Table of Contents

Abstract.....	i
List of Abbreviations	ii
Acknowledgments.....	iv
Table of Contents.....	v
List of Tables	xi
List of figures.....	xiii
1 Introduction.....	1
1.1 Background	1
1.2 Aims and objectives	4
1.3 Overview of thesis structure.....	5
2 Literature Review.....	8
2.1 Thermal building modelling.....	9
2.1.1 Thermal building simulation software	12
2.1.2 The simulation software package EnergyPlus	14
2.1.3 Natural ventilation	15
2.1.4 Night ventilation	18
2.1.5 Local climate.....	21
2.1.6 Sensitivity and uncertainty of ventilation	24
2.1.7 Thermal comfort	26
2.1.8 Weather data inputs for building modelling	29

2.2	Climate change.....	31
2.2.1	Climate change modelling	34
2.2.2	Incorporating climate projections into weather data.....	35
2.2.2.1	Morphing method	36
2.2.2.2	Stochastic weather generator method	38
2.2.3	UKCP09 Projections.....	40
2.2.3.1	Eleven member RCM	41
2.2.3.2	Wind from PET	42
2.2.4	Dynamic building simulation with future weather data.....	43
2.3	Influence of acoustics on natural ventilation.....	48
2.3.1	Building noise criteria.....	50
2.3.2	Noise criteria for naturally ventilated buildings	53
2.3.3	Noise mapping	55
2.3.4	Noise reduction measures	61
2.3.5	Sound insulation.....	65
2.3.6	Acoustic Transmission Loss of Apertures	68
2.3.7	Finite Element modelling of ventilation aperture	71
2.4	Conclusions	73
3	Methodology.....	75
3.1	Climate scale modelling output.....	77
3.2	Urban area scale	79

3.3	Whole building scale.....	80
3.4	Ventilation aperture scale.....	84
3.5	Conclusions.....	85
4	Numerical modelling of ventilation apertures	86
4.1	Ventilation aperture dimensioning.....	87
4.2	Sound transmission of façade panel.....	89
4.3	FEM acoustic simulation.....	93
4.3.1	Meshing of the domain	98
4.3.2	Boundary definition	99
4.4	Ventilation aperture finite element model set up	100
4.5	Validation of finite element model.....	102
4.5.1	Wilson Soroka approximation	102
4.5.2	Validation results	103
4.6	Results for SRI of ventilation aperture.....	105
4.7	Façade combined sound insulation	108
4.8	Discussion	110
4.9	Conclusions.....	111
5	Combining noise mapping and building thermal performance.....	113
5.1	Tolerated internal noise level	114
5.2	Example thermal building modelling.....	115
5.3	Mixed mode cooling.....	119

5.4	Manchester noise map	120
5.5	Building noise exposure	122
5.6	Combining noise mapping and thermal building modelling	124
5.7	Cooling energy variation with noise tolerance results	125
5.7.1	Quantifying for location	127
5.7.2	Quantifying for noise reduction method	128
5.7.3	Zone level cooling	130
5.8	Discussion	136
5.9	Conclusions	138
6	Comparison of future weather data sets	140
6.1	Details of the compared future weather data sets	141
6.1.1	UKCIP02	143
6.1.2	UKCP09	144
6.2	Wind speed projection	145
6.2.1	11 member Regional Climate Model	146
6.2.1.1	Comparison of ensemble variant wind speed change	148
6.2.1.2	Climate sensitivity	152
6.2.2	Wind from weather generator potential evapotranspiration	154
6.2.3	Comparison of change in wind speed	157
6.3	Comparison method	159
6.3.1	Example building models	159

6.3.2	Adaptive comfort	161
6.3.3	Performance indicators	164
6.4	Building performance with different weather files	167
6.4.1	Comparison of ventilation rates across TRY's	167
6.4.2	Wind direction	169
6.4.3	Sensitivity to change in wind direction.....	171
6.4.4	Thermal comfort	172
6.5	Discussion	180
6.6	Conclusions	181
7	Performance implications	183
7.1	Climate change implications on natural ventilation cooling.....	184
7.1.1	Sensible heat loss background	184
7.1.2	Sensible heat loss results.....	186
7.1.3	Mixed mode results.....	195
7.2	Construction materials.....	198
7.2.1	Thermal performance of the construction materials	199
7.2.2	Construction material sound insulation	205
7.3	Comparing the influences of noise and climate on building thermal performance	208
7.3.1	Comparing the effects of noise tolerance and climate warming on mixed mode cooling	208
7.3.2	Quantifying the influence of a 10dB noise reduction measure.....	212
7.4	Discussion	215

7.5	Conclusion.....	217
8	Conclusions.....	218
8.1	Overview of contribution	219
8.2	Future work	222
9	Publication list	224
10	Appendix A.....	225
11	References.....	227

List of Tables

Table 2.1. Reproduced from (Field 2010) Recommended background noise limits for unoccupied mechanically ventilated spaces from the following standards Standard BS8233 (BSI 1999), (ASHRAE 2007), AS2107 (Australian Standard 2000).	51
Table 3.1. Shows which thesis chapters deal with which scales.	75
Table 4.1. Construction material sound insulation values (dB).	109
Table 5.1. Details of the example buildings.	117
Table 5.2 Influence of a 10dB acoustic treatment on mixed mode cooling energy consumption. Percentage change relative to cooling energy consumption before the implementation of 10dB treatment and a corresponding increase in ventilation opening to maintain noise ingress at 34dBA.	129
Table 6.1. Details of the 11 member RCM ensemble taken from (BADC et al. 2008).	153
Table 6.2. Monthly wind speed change factors (%).	158
Table 6.3. Category temperature limits (Θ_{max}) reproduced from Annex A of (CEN & BSI 2007) equations defining Θ_{rm} are given in the text.	163
Table 6.4. Explanation of categories reproduced from (CEN & BSI 2007).	163
Table 7.1 Comparison of standard maximum permitted U-values of construction elements specified in UK Building Regulations from 1965 to 2002 taken from (Chow & Levermore 2010).	199
Table 7.2. Physical properties of three classes of thermal weight, reproduced from (Chow & Levermore 2010).	203
Table 7.3. Construction material SRI values (dB). Measured according to ISO 140-3 (ISO 1995).	206
Table 7.4. Weather files used for the comparison ranked by their average summer temperature.	209

Table 7.5. Results showing the equivalent temperature where the acoustic factors equal the climatic factors.....215

List of figures

Figure 1.1. Framework drawing showing how the thesis chapters link together.....	7
Figure 2.1. Results for ACH sensitivity reproduced from the study by Horan & Finn (2008). Wind speeds and orientations indicated in the legend.	26
Figure 2.2. Illustration of improved spatial resolution of climate models of Europe. (FAR 1990; AR4 2007). Reproduced from (Hacker et al. 2009).	35
Figure 2.3. Contours showing required insulation performance in $D_{nT,A,2}$. Reproduced from (Kurra & Dal 2011).....	60
Figure 2.4. Air flow path and sound transmission representation of the staggered window system.	64
Figure 2.5. Maximum TL of an enclosure as a function of the opened surface reproduced from (Miller & Montone 1978).....	67
Figure 2.6. Representation of circular aperture sound transmission in a finite thickness wall.	69
Figure 2.7. SYSNOISE model mesh (Oldham et al. 2005)	72
Figure 3.1. Framework showing how methods link together. Highlighting colour indicates the scale, with colours assigned according to Table 3.1.....	76
Figure 4.1. Window aperture configuration.....	88
Figure 4.2. TL of a slit for normal plane wave incidence ($\theta=0^\circ$), oblique plane wave incidence ($\theta=45^\circ$) and diffuse incidence. Where k_0 is the wave number and b is the aperture height. Reproduced from (Sgard et al. 2007).....	90
Figure 4.3. Illustration of linear shape functions and the interpolation of the approximate solution for acoustic pressure.....	96

Figure 4.4. Finite element model set-up representing a plane wave incident on the ventilation aperture and sound transmission through it. Left hand side is source side and right hand side is receiving side.....	101
Figure 4.5. Comparison of SRI against ke for a circular aperture of radius 11mm and depth 220mm. two calculation methods are indicated in the legend.	104
Figure 4.6. Comparison of SRI for the two calculation methods. The trend line is the average of the numerical data points.....	105
Figure 4.7. SRI for a slit aperture representing 40mm window opening, spectrum values and octave band averages.	106
Figure 4.8. SRI averaged over the octave bands for different sized ventilation apertures (aperture width indicated in the legend).	107
Figure 4.9. Combined SRI variation with frequency and ventilation opening size indicated in the legend.....	110
Figure 5.1. Floor plan of office Building 5.1.....	118
Figure 5.2. Floor plan of simple deep plan office building (Building 5.2).....	118
Figure 5.3. Floor plan of the simple shallow plan office building (Building 5.3).....	119
Figure 5.4. Area of Manchester used for noise mapping (Ordnance Survey 2012). The example Locations A and B are marked on the figure.....	121
Figure 5.5. Contours of noise levels at building façade - (i) Building 5.1 in Location A. (ii) Building 5.1 in Location B. (iii) Building 5.2 in Location A. (iv) Building 5.2 in Location B. (v) Building 5.3 in Location A. (vi) Building 5.3 in Location B.....	123
Figure 5.6. Traffic sound level spectra reproduced from (BSI 1997) levels are A-weighted and normalized to 0dB.....	124
Figure 5.7. Comparison of Building 5.1 in different noise locations.....	126
Figure 5.8. Comparison of Building 5.2 in different noise locations.....	126

Figure 5.9. Comparison of Building 5.3 in different noise locations.....	127
Figure 5.10. Zone level mixed mode cooling for Building 5.1 in Location A. Zone 8 from the ground floor is highlighted.....	131
Figure 5.11. Zone level mixed mode cooling for Building 5.1 in Location B. Zones 5 and 2 from the 3 rd floor is highlighted.	133
Figure 5.12. Zone level mixed mode cooling for Building 5.2 in Location A. Zones 1 and 2 from the 1 st floor are highlighted.	134
Figure 5.13. Zone level mixed mode cooling for Building 5.2 in Location B. Zones 1 and 2 from the 1 st floor are highlighted.	134
Figure 5.14. Zone level mixed mode cooling for Building 5.3 in Location A. Zones 1 and 2 from the 1 st floor are highlighted.	135
Figure 5.15. Zone level mixed mode cooling for Building 5.3 in Location B. Zones 1 and 2 from the 1 st floor are highlighted.	135
Figure 5.16. Representation of usual relationship between noise and mixed mode chiller use.	137
Figure 6.1. Change in wind speed between the control period and 2020 time period, for the 11 RCM variants which are indicated in the key.	149
Figure 6.2. Change in wind speed between the control period and 2050 time period, for the 11 RCM variants which are indicated in the key.	149
Figure 6.3. Change in wind speed between the control period and the time period indicated in the legend, for the 11 RCM. Error bars indicating scatter across the 11 member RCM.	150
Figure 6.4. Change in wind speed between the control period and 2080 time period, for the 11 RCM variants and UKCIP02 which are indicated in the key.	151
Figure 6.5. Ensemble variant change in wind speed plotted against climate sensitivity.	153

Figure 6.6. Representation of example buildings used in the study. (A) is Building 6.1 and (B) is Building 6.2 (note solar shading).....	160
Figure 6.7. Comparison of air exchange rates for weather data sets. Crosses indicate occupied zone summer air exchange rate. Black squares indicate mean values and triangles indicate plus and minus one standard deviation.	168
Figure 6.8. Wind direction distributions given as frequency of occurrences (%) for 30 degree increments of the compass.	170
Figure 6.9. Sensitivity of air exchange rate to change in wind direction for control TRY. Black squares indicate mean values and bars represent \pm one standard deviation.	171
Figure 6.10. Percentage hours over threshold comfort temperature for the control period..	173
Figure 6.11. Percentage hours over threshold comfort temperature for the 2050's under the high emission scenario.	174
Figure 6.12. Percentage of occupied hours over threshold comfort temperature for the 2080's under the high emission scenario.	175
Figure 6.13. Percentage of occupied hours above thermal comfort threshold against mean summer temperature legend for two percentiles (50 th and 90 th) of the PROMETHEUS DSY's and the COPSE DSY. Each series consists of a control, 2050 and 2080 under the high emission scenario.	177
Figure 6.14. Overheating plotted against mean summer external temperatures for the CIBSE DSY weather data set.....	179
Figure 6.15. Overheating plotted against mean summer external temperatures for the weather generator derived data sets.....	180
Figure 7.1. Sensible heat loss for Building 6.1 against average summertime temperature for a number of weather files from datasets marked in the legend.	186

Figure 7.2. Sensible heat loss for Building 5.2 against average summertime temperature for a number of weather files from datasets marked in the legend.	188
Figure 7.3. Average air exchange rate for Building 6.1 against average summertime temperature for a number of weather files from datasets marked in the legend.....	189
Figure 7.4. Average air exchange rate for Building 5.2 against average summertime temperature for a number of weather files from datasets marked in the legend.....	189
Figure 7.5. sensible heat loss per unit volume of infiltration for Building 6.1 against summer external temperature for a number of weather data sets.	191
Figure 7.6. Sensible heat loss per unit volume of infiltration for Building 5.2 against summer external temperature for a number of weather data sets.	192
Figure 7.7. sensible heat loss per unit volume of infiltration for Building 6.2 against summer external temperature for a number of weather data sets.	194
Figure 7.8. Sensible heat loss for a mixed mode Building 6.1 against average summertime temperature for a number of weather files from datasets marked in the legend.....	196
Figure 7.9. Average air exchange rate for Building 6.1 against average summertime temperature for a number of weather files from datasets marked in the legend.....	197
Figure 7.10. Average summer chiller electricity use against average summer temperature for Building 5.2 with the construction standards indicated in the legend.	201
Figure 7.11. Average summer chiller electricity use against average summer temperature for Building 5.3 with the construction standards indicated in the legend.	202
Figure 7.12. Average summer chiller electricity use against average summer temperature for Building 5.2 with the construction weight indicated in the legend.....	204
Figure 7.13. Average summer chiller electricity use against average summer temperature for Building 5.3 with the construction weight indicated in the legend.....	204
Figure 7.14. Comparison of construction materials for Building 5.3 in Location B.	207

Figure 7.15. Comparison of chiller electricity for Building 5.1 in Location A and with the weather file’s average summer temperature indicated in the legend.210

Figure 7.16. Comparison of chiller electricity for Building 5.2 in Location A and with the weather file’s average summer temperature indicated in the legend.211

Figure 7.17. Comparison of chiller electricity for Building 5.3 in Location A and with the weather file’s average summer temperature indicated in the legend.211

Figure 7.18. Illustration of how the change in chiller electricity due to a 10dB noise reduction measure is calculated.213

Figure 7.19. Comparison of chiller electricity difference for Building 5.1, in Location A against climate temperature increase, relative to the control period. difference due to 10dB acoustic treatment is compared with difference due to climate change temperature rise.....214

1 Introduction

1.1 Background

The quality of the built environment is of central importance to the wellbeing and sustainability of any society. Internal building comfort conditions contribute significantly to an occupant's impression of the success or otherwise of a building, and a large part of building design effort and energy use is dedicated to creating and maintaining comfort conditions. Two aspects of occupant comfort are dealt with in this thesis - thermal and acoustic comfort, both of which have implications for building energy use.

There is a drive by the UK government to reduce building energy consumption through a variety of initiatives and legislation, for example through the Energy Act (DECC 2011) of October 2011. Through the green deal consumers can pay for improvements in building energy efficiency through a charge on energy bills rather than upfront costs. This legislation also sets energy efficiency standards for rented properties. Building energy efficiency certificates and the increasing use of environmental rating systems aim to raise the profile of building energy efficiency, and promote measures that will reduce building energy use.

One heat transfer mechanism impacting on energy use in buildings is natural ventilation. Natural ventilation is a simple but important approach whereby air is driven into and out of buildings by natural forces. It is the dominant approach in domestic buildings in the UK and, if carefully designed, this can be an effective way to cool non-domestic buildings (Awbi 1991; Allard 1998). Although comfort cannot always be ensured by natural ventilation alone, it can become part of a mixed mode strategy whereby natural ventilation air flows are

supplemented, when required, by mechanical ventilation systems. Maximising the time a building relies on natural ventilation has real benefits in terms of air quality, occupant comfort and energy use through the replacement of mechanical ventilation and air-conditioning. It can be difficult to do this as the natural forces driving ventilation are often weak (Sharples & Chilengwe 2006), making it difficult to produce the flow rates that would provide sufficient cooling for non-domestic buildings. Variability in the external environment leads to inconsistent results, and peak cooling demands can often coincide with lower natural ventilation driving forces and a lower cooling effect.

The surrounding urban environment is very important to naturally ventilated buildings, as by their very nature they are more connected to the external surroundings - both in terms of their climatic environment and their surrounding noise environment. The climatic environment describes the combination of weather conditions viewed over a long timescale, the longer timescale being relevant to buildings due to their long lifespan. Any changes to temperature and wind characteristics are of particular importance to natural ventilation. Projections for climate change are being updated regularly. The latest set of United Kingdom Climate Projections from 2009 (UKCP09) (Murphy et al. 2009), give a large amount of information about future climate. The noise environment is defined here as the distribution and type of noises that cause annoyance to building occupants. An example of this could be excessive traffic noise (Kang 2007). Mapping the distribution of such noise has been mandated by EU directives (European Union 2002) giving a potentially rich source of information about building noise exposure. For basic naturally ventilated building facades where, for example, windows are open, there is little resistance to the noise. It is not always clear which environmental factor, acoustic or climatic, is the most relevant to the potential adoption of natural ventilation for a specific situation.

With refurbishment periods of maybe tens of years, problems with comfort and energy use will often persist for some time. Rectifying problems may be difficult and expensive, and so it is worth expending considerable effort to avoid creating them in the first place. To help with this, computer simulation tools have been developed to aid in the design of buildings (Clarke 2001). The dynamic nature of building thermal physics, with daily and seasonal cycles, means that simulation is required to properly understand the energy transfer processes. The underlying fundamentals of building physics are generally well understood in isolation. Complexity is increased when interrelationships, sometimes with feedback effects, are important. An example of this is the interrelationship of natural ventilation and internal temperatures. Natural ventilation can change the internal temperature, and in turn, internal temperatures affect ventilation rates due to changes in thermal density differences. Ventilation modelling is now integrated into much widely used building thermal modelling software (LBNL 2010), and may often affect design decisions.

The combining of ventilation performance and acoustic performance has been demonstrated for building façades (De Salis et al. 2002; Oldham et al. 2004). This is useful for building designers as it quantifies interrelationships and can be used to optimise the response to problems of air freshness, thermal comfort and acoustic comfort. This approach could be extended to include detailed information about the specific building and surrounding area. The integration of a number of specialist tools can create a fuller picture of building behaviour. The choice of tool for a particular purpose needs to be carefully considered, as scale is important both in terms of time and space. For example, in acoustics simulation different tools are needed for the modelling of building components, as opposed to those needed for larger scale urban noise mapping. Both scales are important to understanding what noise levels building occupants are exposed to, and so the linking of tools is needed.

1.2 Aims and objectives

This thesis therefore compares acoustic and climatic environmental influences on natural ventilation, to determine which factors have the most effect on a building's ability to maintain comfort conditions by natural ventilation. This is an important question as both acoustic and climatic environmental factors affect the viability of natural ventilation, now and in the future. To achieve this, a number of methods will be developed; these will also be useful in their own right for quantifying relationships that can inform building design priorities.

The central objective of this thesis is to:

- Quantify the level of climate change temperature increase that a noise reduction measure mitigates.

This can contribute to the motivation for applying noise reduction measures, the method used to achieve this can be summarised as follows. First the Sound Reduction Index (SRI) of the naturally ventilated façade is calculated (see page 89 for more on SRI). Then the thermal performance of the building is linked to noise mapping exposure through the natural ventilation opening patterns over the building façade. Parametric calculations are conducted according to noise tolerance. These calculations are driven by weather data with a range of climate change included. Possible sources for future weather data need to be compared so that a representative range can be assembled. This allows an example noise reduction measure to be quantified in terms of equivalent external temperature increase due to climate change. These methods are of appropriate complexity, combining a sound physical basis with practical ease of use that can aid design. An example of an appropriate simplification is the use of temperature set-points to represent control of windows.

The novel contributions of each of the main chapters are:

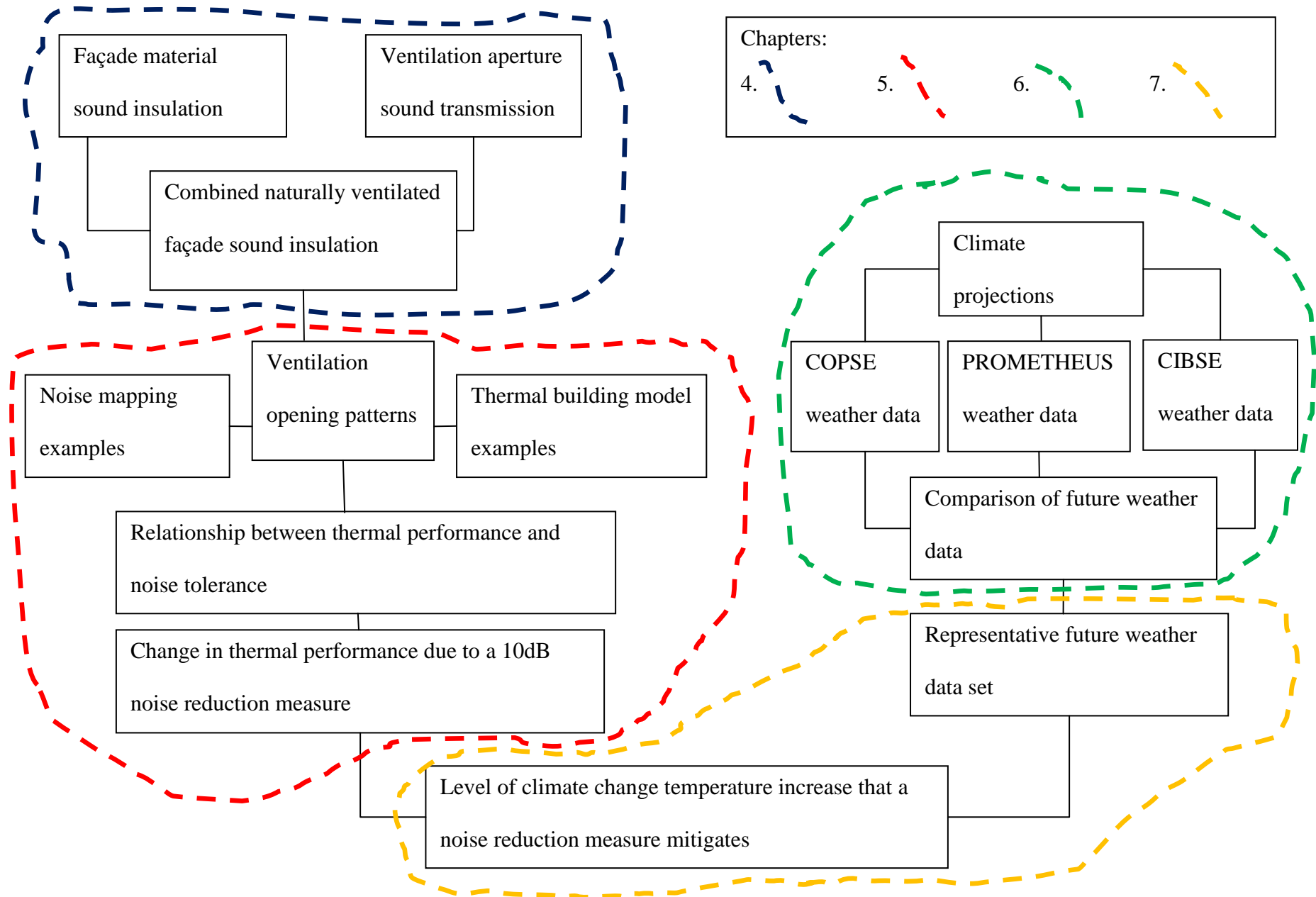
- Chapter 4; Determine the sound insulation of the naturally ventilated facade by means of a robust and well validated method.
- Chapter 5; Show the relationship between noise tolerance and thermal performance
- Chapter 6; Determine which future weather data sets should be used to represent future thermal performance.
- Chapter 7; Illustrate design implications using the new methods and data.

1.3 Overview of thesis structure

Chapter 2, the literature review, is by necessity relatively broad-ranging, due to the multidisciplinary nature of the research presented. It covers key literature on building thermal modelling, climate change, and the influence of acoustics on natural ventilation. Chapter 3, the methodology section, presents the framework of the research conducted and introduces the different methods adopted for the different scales covered in this thesis, highlighting the potential for automation and the efficient use of information sources. Details of the methods used are covered in the relevant main chapters, along with results. Chapter 4 deals with the calculation of acoustic Transmission Loss (TL) of the ventilation aperture and a description of the FEM approach used for this analysis. The results from Chapter 4 are used in Chapter 5, where noise mapping and building energy modelling are combined for three representative case study buildings in two urban locations.

The large amount of data from UKCP09 means that there are a number of possible options for adopting future weather scenarios. Chapter 6 analyses and compares a number of these to determine which sets give an appropriate representative range of future weather. Chapter 7 then uses the chosen sets to illustrate the implications for natural ventilation performance with a range of climatic changes, using the methods developed throughout the thesis to consider design implications for different levels of environmental influence. This includes a final comparison of the relative size of the acoustic and the climatic influence on natural ventilation, to calculate what level of climate change temperature rise a noise reduction measure could mitigate. The main findings and conclusions from the study are presented in Chapter 8. A framework drawing showing an overview of how the thesis chapters fit together is given in the Figure 1.1.

Figure 1.1. Framework drawing showing how the thesis chapters link together



2 Literature Review

Through this literature review research relevant to environmental influences on building natural ventilation are covered. The success of buildings can be evaluated in a number of different ways, for example, energy consumption, cost, comfort and occupant approval. Different methods can be used to investigate the success of these different aspects. Some approaches aim to get a sense of the occupants impression, examples of some aspects of this approach can be found in thermal comfort surveys presented by de Dear and Brager (2002) and occupant surveys of users' perceptions of acoustic conditions by Baird and Dykes (2010). Other approaches focus on the measureable physical variables such as temperature and energy consumption. The many interacting aspects of building performance mean that simulation is a widely used tool, (Santamouris et al. 2010; Hacker et al. 2009).

Building energy modelling is one of the most widely used methods to quantify natural ventilation of buildings; and is used for new building design, retrofit, refurbishment and research. Thus in the first section, Section 2.1, work done relating to building energy modelling and natural ventilation calculation will be introduced. This type of simulation is the basis for much of the results presented in this thesis. Then in Section 2.2, the work done on climate change predictions and the generations of climate projections that aim to give information about the most likely future scenarios is reviewed. Finally in Section 2.3 a review of some relevant research done on the interaction of acoustics and natural ventilation is presented in preparation for the work done in this thesis on integrating environmental noise and natural ventilation calculation methods.

2.1 Thermal building modelling

In the future a changing climate will affect thermal comfort (people's perception of how comfortable the temperature is) and building energy use, for example in a study by Chow and Levermore (2010) it was shown that both heating and cooling loads would change. They found that for some buildings the increases in cooling load will be more than compensated for by a reduction in heating load. The potential to provide more comfortable buildings and reduce energy consumption significantly by the appropriate use of simulation tools has been available since the 1980s. The benefits have been documented by McElroy et al. (2001). This is true for the design of new buildings and the improvement of existing buildings. The various individual aspects of building energy use have undergone much research and are relatively well understood. Understanding the whole building as an energy system is a more complex proposition. Factors such as occupancy level and weather all interact to determine the energy use and indoor environment of the building, as is outlined in the introduction to the esp-r software package (Hand 2008). Simulation has developed as a way to deal with this complexity and it has become increasingly used in building design. This is useful for parametric studies of design options where the reproducibility of the conditions can be ensured for all runs and the factors of interest can be isolated. It was also used by Santamouris et al. (2010) to enable the inter comparison of a large number of case study buildings by ensuring consistent boundary conditions.

Dynamic building modelling is a term given to the simulation of processes in buildings where changes occurring through time are represented by calculating results at discrete time steps, the previous conditions influencing the results of the current time step. For building simulation this usually centres on a heat balance based solution. Modelling the individual processes in building physics are relatively simple; the complication comes from the

simultaneous linking together of the many different processes through time. This requires a substantial degree of data organisation to enable feedback between the different aspects of building physics and the central heat balance calculation (LBNL 2010).

An example of a common approach to numerical integration in dynamic building simulation is the finite difference method. The buildings condition at the previous time-step along with information about the weather conditions and building use are used to calculate the conditions at the next time-step. The use of this method for long time periods could be problematic due to the build-up of truncation errors. But due to the diurnal cycle that building temperature undergoes, these errors during the day are the opposite of the errors during the night so that no net accumulation of error occurs (LBNL 2010). The external weather conditions that the building is subjected to are represented by the weather data. The requirements for weather data for dynamic building simulation were discussed by Crawley and Hand (1999). They suggested a format that allowed the full range of variables that might be needed and allowed for a range of temporal resolutions, as required. It was noted that buildings could be sensitive to sub-hourly changes in solar and wind variables. Solar radiation and the glazing of the building have a key influence on the heat flow through the building and therefore the thermal comfort. Air-flow through the building is also key to the thermal flows due to temperature differences of the air masses. For the UK, CIBSE is the standard source of these weather data for building performance evaluation by dynamic thermal simulation (CIBSE 2002). Weather data is discussed in more detail in Section 2.1.8.

Dynamic simulation allows some of the complexity of occupant interactions with a building to be representation. This is commonly done with schedules that represent the patterns of

regular occupant action through the simulated period (DesignBuilder Software Ltd 2009). Some occupant or plant actions can be linked to the internal condition as well as time period, an example of this is set-point temperatures. This concept was refined by Tuohy et al. (2007) with the window opening patterns being driven by thermal comfort. The further complexity of occupant interaction with the buildings was looked at by Yun and Steemers (2010) for night time ventilation. With the statistical representation of window opening patterns, seen in field studies, being investigated. It was found that the Markov chains and Monte Carlo based behaviour algorithm agreed well with observations revealing how building design and occupant behaviour affect thermal performance. The study also showed that the provision of secure ventilation leads to more frequent use of the window.

The level of detail in the modelling should be appropriate to the task. Dynamic building simulation is described in contrast to the Simplified Building Energy Modelling (SBEM) methods in the national calculation methodology (DCLG 2010). SBEM is constrained in dealing with properties which vary non-linearly over periods of the order of an hour.

Examples given where this can be the case are:

- Buildings with ventilated double-skin facades
- Automatic blind control
- Light transfer between highly glazed internal spaces such as atrium or lightwells

Dynamic simulation tools were also said to be more suited for design support tools as opposed to SBEM which was developed for compliance and certification calculations. The following section looks at the different programs that implement dynamic building energy simulation.

2.1.1 Thermal building simulation software

A large number of dynamic thermal simulation software packages have been developed by various organisations and businesses. These whole-building simulation programs are used to calculate key building performance indicators such as temperature, energy use, airflow and thermal comfort indicators. These programs are the core tool for people looking into building energy use such as in design studies, building design refinement and to evaluate retrofit opportunities (Hacker & Holmes 2005). In their study of the impacts of climate change on the built environment, Hacker and Holmes focussed on performance indicators relating to the level of summertime overheating and the associated changes in energy consumption and carbon emissions. The computer program ENERGY2 (E2) was chosen for the study which was developed by Arup research and development. The reasons for this choice were given as:

- The need to modify the code for rule based control.
- Large number of simulations.
 - Use of batch simulation techniques
 - Fast simulation speed
- Need to customise output
- Gave predictions close to the median of validation tests

Comparison is often difficult due to different capabilities and priorities across the many software programs available. The capabilities and features of twenty major thermal building simulation programs were contrasted by Crawley & Hand (2006). The study does not make judgements about the software performance but it is a useful single source of information about their features and capabilities. The software included EnergyPlus (LBNL 2010), which is used to derive many of the results in this thesis. This study was based primarily on vendor supplied information with little peer reviewing undertaken, even so this amounted to a large amount of information being processed and presented in a number of tables to compare

simulation programs. These tables were organised systematically and they are informative about what the key issues relating to building energy simulation are.

The following aspects are compared by Crawley & Hand (2006). General modelling features which included tools for geometry production and visualisation and solution time step frequency. Zone loads gives an overview of the physics, this was usually based on heat balance, the approach for convection exchange and the calculation approach to plant sizing is also indicated. Building envelope and daylighting, including the interaction of the sky and the ground with the building. Infiltration, ventilation and multi-zone airflow was included which covers how air movement is treated and whether a pressure network model is employed. Other included aspects were renewable energy systems, electrical systems, Heating, Ventilation, and Air Conditioning (HVAC) systems HVAC equipment, environmental emissions, economic evaluation, climate data evaluation, results reporting, validation, user interface, the availability of the software and its ability to link with other programs.

It was found that the lack of a common language used by the building simulation community encouraged the use of individual vendor jargon and resulted in a large degree of ambiguity in what programs can do. One of the main aims of Crawley & Hand in their work was to start the development of a common language and comparison methodologies in the simulation community, and the hope was that this would progress in the future. It was found that most users only used one simulation tool for a variety of simulation activities. Greater productivity could be expected from the use of a suite of programs suited to different types of simulation. These might be used to inform the initial design decisions such as massing of the building or

degree and position of glazing. These simulation requirements would be in contrast to the requirements for the detailed design of building plant components. The ambiguity about the performance of the different software was a central reason for adopting the well-established simulation program EnergyPlus for the results produced in this thesis. This is a modular program made up of the most popular parts of the mature simulation programs BLAST, DOE-2 and COMIS (LBNL 2010) and is well validated (Henninger & Witte 2009).

2.1.2 The simulation software package EnergyPlus

EnergyPlus has undergone extensive development over a number of years by the USA's Department of Energy and is widely used in research and practice. Numerous validation exercises have been carried out, for example, by Henninger and Witte (2009). The development of EnergyPlus has concentrated on the calculation engine with the development of more sophisticated user-interfaces being generally left to commercial organisations. An example of this kind of software is DesignBuilder (DesignBuilder Software Ltd 2009), where EnergyPlus can be used as the program's calculation engine. This commercial user-interface has data templates, visualisation and import tools that aid the generation of building energy models. The accuracy of the input parameters describing construction materials, occupant schedules and external climate are of central importance to the simulation validity. Data templates aid the efficient and accurate allocation of this information.

With EnergyPlus, the ventilation calculations, which are often central to results reported in this thesis, are carried out by the network airflow module which models bulk airflow. This is based on the most popular components of a multi-zone infiltration program. The program was the output from a workshop called Conjunction of Multi-zone Infiltration Specialists

(COMIS) and the resultant program was then named after the workshop. Feustel (1999) introduces COMIS along with reference to the difficult but important work done to evaluate its accuracy (Furbringer et al. 1996).

2.1.3 *Natural ventilation*

Air flow through buildings has a strong influence on the heat flows and comfort in these buildings, therefore natural ventilation is an important part of a passive cooling strategy (Santamouris & Asimakopoulos 1996). The pressure differences that drive air flow through a building can be characterised as due to the stack effect or wind pressure. The stack effect comes from the inlet and outlet height difference and the temperature driven density differences between inside the building, and outside. Wind around a building will produce a positive pressure on the windward side and a corresponding negative pressure on the leeward side. A review of the different designs that encourage wind driven natural ventilation is given by Khan et al. (2008). Many of the reviewed studies make use of natural ventilation numerical modelling techniques.

Two numerical modelling techniques are widely used to simulate the movement of air in buildings. The first is network airflow modelling or zonal modelling such as is implemented in COMIS and the second is Computation Fluid Dynamics (CFD). Network airflow is well adapted to building energy analysis with each zone being combined with the assumption of full air mixing. For the more detailed simulation of air flow which would be useful for the analysis of comfort and air quality, CFD is more appropriate. In a network airflow model the building is modelled as a collection of nodes representing rooms, parts of rooms, equipment connection points, ambient conditions etc. The paths between these nodes then represent the

cracks, doors, fans etc. (Clarke 2001). The mass flow rate between nodes is given as a function of pressure difference, and the conservation of mass at each node gives the set of equations that can be solved at successive time steps. This type of pressure network approach is usual for whole-building modelling.

CFD is a more general method for looking at fluid behaviour. When looking at the internal building space it is mostly used to model the movement of air, vapour or pollutants (Clarke 2001). The investigated domain is generally much more finely discretized than the network airflow model and numerical methods are used to give a solution for fields such as temperature, pressure and velocity at the nodes of the mesh. The two methods can be linked with each other. Network airflow results for the whole building are used to provide the boundary conditions to the CFD calculation of a specific area of interest within the building. In general, however, detailed CFD simulations are too computationally expensive for whole buildings over a simulated year or season.

Some background to the central ventilation equations are given in this section. The heat loss due to ventilation is given by the equation (2.1).

$$\dot{\phi}_v = \frac{1}{3} NV\Delta T \quad (2.1)$$

where N is number of air changes per hour or ACH (h^{-1}), V is the volume of the room (m^3) and ΔT is the difference between indoor and outdoor temperatures ($^{\circ}\text{C}$). The flow rate through each opening is driven by the pressure differences. In the case of natural ventilation, this is caused by wind pressures or buoyancy. Calculations for flow rate through openings are given

by Liddament (1996) as part of a guide to energy efficient ventilation. An example of a calculation linking flow rate to pressure difference is given in equation (2.2) (CIBSE 2007).

$$Q = C(\Delta P)^n \quad (2.2)$$

where Q is the flow rate through the opening ($\text{m}^3 \cdot \text{s}^{-1}$), C is the flow coefficient (which is related to the opening size) ($\text{m}^3 \cdot \text{s}^{-1} \cdot \text{Pa}^{-n}$), ΔP is the pressure difference across the opening (Pa) and n is the flow exponent varying from between 0.5 for fully turbulent flow to 1.0 for laminar flow. For orifice type opening for example those used in the example buildings used in this study the common orifice flow equation can be used which is given in equation (2.3) (CIBSE 2007).

$$Q = C_d A (2\Delta P / \rho)^{0.5} \quad (2.3)$$

Where C_d is the discharge coefficient and A is the area of the opening (m^2) and ρ is the density of air ($\text{kg} \cdot \text{m}^{-3}$).

It can be seen how opening area and pressure differences are the main factors effecting natural ventilation flow rate. The opening areas are related to building design and occupant control of the openings. The pressure differences are a product of building shape, surrounding topography and the climate - particularly the wind conditions and temperature. The stack effect is dominant during periods of low wind speed and reduces in summer periods when temperature differences are minimal (Khan et al. 2008). Wind driven natural ventilation is more important for these periods and a number of design measures to encourage this type of ventilation where reviewed, such as wind catchers, rotating wind cowl, rotating turbine ventilators, and the strategic placement of openings relative to the surrounding environment. A number of urban environmental factors that influence natural ventilation were investigated by Ghiaus et al. (2006). Models were developed in this study to help with initial calculations

to assess the viability of natural ventilation in urban areas. To enable this, wind, temperature, noise attenuation and pollution transfer were measured for a number of urban areas. By urban area it is assumed that the authors meant from a terrain roughness of sub urban to full city centre. Although pollution ingress is an issue for natural ventilation in urban areas, noise is the issue focused on in this thesis.

It is widely known that in summer, and for low rise buildings, wind driven ventilation through windows and other openings is the predominant type of natural-ventilation (Karava et al. 2007). The importance of the wind characteristics to the design and position of ventilation openings was illustrated by the work of Mochida et al. (2005). The surrounding environment of the building was also focussed on, such as planted tree arrangements around the building, opening locations and the size of openings. The strategic positioning of openings was described as a way of optimising wind driven ventilation. This could be done by looking at flow patterns around buildings and the changes in ventilation rates. It should be noted though, that ventilation opening exposure to prevailing wind and sheltering is not the only environmental consideration for natural ventilation design. Such factors as exposure of the building façade to noise would also have an impact on the success of the natural ventilation strategy.

2.1.4 Night ventilation

The effectiveness of natural ventilation can be increased as part of a night ventilation strategy. A night ventilation cooling strategy is where cooler air during the night is encouraged to flow through the building, cooling the internal air and building fabric. This acts as a heat sink so that internal daytime temperatures are reduced. The simplicity of this

strategy makes it appealing and it could yield attractive benefits in certain climates and with appropriate design. Later in Chapter 6 night ventilation is utilized in the example passive office building (Building 6.2). A number of studies have looked into how and where night ventilation can be used to most affect.

Flow rate was also identified as a factor by Santamouris et al. (2010) with this explained as determining the usability of stored cooling potential in the buildings fabric. Although some limits to how central flow rate was to night ventilation performance were suggested by Finn et al. (2007). It was found that increasing ventilation rates above 10 Air Changes per Hour (ACH) did not bring further improvements. The work of Artmann et al. (2008) found that the critical airflow rate at which no further improvements are found depends on the building construction and heat gains. The use of additional cooling measures is included in some of the studies of night ventilation with results indicating the effect on the cooling load that night ventilation has (Kolokotroni et al. 2006; Santamouris et al. 2010). Additional measures were incorporated by Breesch & Janssens (2010) to help improve the probability of good thermal comfort, including increased flow rate by day, top cooling of air supplied by mechanical ventilation, additional thermal mass and increased ventilation flow rate in combination with top cooling. All measures were determined to significantly decrease the uncertainty of thermal comfort in warm weather.

Another issue that would seem to be important to a night ventilation strategy is the heat sink potential of the building fabric. The convective heat transfer characteristics of the internal building elements are described by the internal convective heat transfer coefficients by natural convection (Breesch & Janssens 2010). These are partly defined using semi-empirical

coefficients which have been determined by, for example (Awbi & Hatton 1999). The convective heat transfer coefficients are not necessarily valid for highly ventilated areas; however in the night ventilation study by Blondeau et al. (1997), predicted indoor temperature did not seem to be sensitive to increased heat transfer coefficients and still air values were therefore used. In a separate study by Artmann et al. (2008), significant sensitivity to heat transfer was found only for total heat transfer coefficients below about $4\text{W/m}^2\text{K}$.

A natural ventilation strategy where occupants were encouraged to leave windows open during the night was investigated by Yun & Steemers (2010) A key feature of the strategy employed in this field study, was that window systems did not present security issues when left open during the night. Security was maintained by a system of fixed louvres that prevented possible office break in during the night. In this study, emphasis was on occupant's behaviour and this included monitoring of the two field studies and modelling window opening behaviour patterns using statistical models. This is a more complex representation of night ventilation control than is employed by for example Kolokotroni et al. (2006) where the night ventilation control was described as follows. Start at 21:00 and end at 7:00 plus as long as the inside temperature is greater than the heating set-point of 18°C and the outside air temperature is greater than 12°C . The main motivation for employing this control was to avoid over-cooling, which was also the reason for the controls implemented in (Artmann et al. 2008).

Most of the studies of night ventilation have focussed on commercial buildings only few have looked at residential buildings (Golneshan & Yaghoubi 1990; Santamouris et al. 2010). The

large study by Santamouris et al. (2010) presented data on 214 residential buildings. Most office buildings are unoccupied during the operation of a night ventilation strategy but this is not the case for residential buildings and so the comfort of residential occupants during the night must be taken into account. As well as the issue of over cooling during the night acoustic considerations for the areas of the building where occupants are sleeping would be relevant. The effect of road noise and ventilation noise was compared in a study by Öhrström & Skånberg (2004). It was found that exposure to road noise reduced the sleep quality by 22% opposed to the ventilation system noise that reduced it by 12%. Noise ingress from road noise, ventilation rates and cooling load were linked by Barclay et al. (2010) and a similar approach could be used for the night cooling potential of residential buildings in specific urban area. This section has outlined issues relating to the use of the cooling strategy used in Chapter 6.

2.1.5 Local climate

The surrounding area is a major factor for natural ventilation: when the wind flows over a building, pressure differences relative to the internal pressure encourage ventilation. In building simulation programs this is represented with wind pressure coefficient distributions. Accurate wind pressure coefficient distributions need to take the surrounding area into account, such as terrain roughness and sheltering. Cóstola et al. (2009) presents an overview of the main sources of wind pressure coefficients. The review splits the sources into primary and secondary. Examples of primary sources are:

- full-scale measurements
- reduced-scale windtunnel tests
- CFD simulations.

Secondary sources are said to be those sources that were generated based on primary sources. The most common sources are databases of collected wind pressure coefficients data for a limited set of generic buildings. Some examples of these sources are.

- Air Infiltration and Ventilation Centre (AIVC) database (Liddament 1986)
- ASHRAE Handbook of Fundamentals (ASHRAE 2004)

These secondary sources are often used for convenience but it should be noted that they are meant for simple buildings, Cóstola states that primary sources are generally preferable. For example, wind pressure coefficients from the AIVC table data (Liddament 1986) are used in the models produced by DesignBuilder and are meant for cubic buildings up to 3 storeys high. Although CFD or other methods such as wind tunnel experiments can be used for more complex situations, the more convenient table data are often used for initial simulation.

The effect of local climate on the potential for night-time ventilation cooling was investigated by Artmann et al. (2007) using 259 stations across Europe. A high potential was found for night ventilation cooling over the whole of Northern Europe and still significant potential in Central, Eastern and even some regions of Southern Europe. Local climatic effects are important to night ventilation potential, in particular the difference in day and night temperatures. Higher night temperatures are a key characteristic of the urban heat island effect, the impact of which is discussed by Santamouris et al. (2001). A specific investigation into the effect of the London heat island on stack night ventilation strategy is given by Kolokotroni et al. (2006). Notional offices were modelled for two sites, an urban site and a rural site. Stack ventilation was investigated as this was said to be the most suitable night ventilation strategy for urban offices due to it being largely independent of wind variations

which are affected by local urban morphology. Measured air temperature data was used from a network of monitoring stations to describe the external conditions. In particular the observed differences between rural and urban temperatures were focused on. Ratios of required cooling energy, illustrating the effect of night ventilation and building position, were presented with and without the optimisation of the thermal mass, solar protection glazing ratio, internal heat gains, infiltration and day airflow rate. The effect of improving the design options were therefore indicated for urban and rural environments. In the study, a thermal and air flow simulation tool specifically designed for offices in London, was used. The software was based on the Building Research Establishment's (BRE) 3TC program and included control based on occupancy and temperature. The results showed that the rural reference office cooling load was 84% to 73% of the urban office cooling load, depending on the level of optimisation.

The local topography of an urban area has a central influence on the local wind speeds that a building is exposed to. A large part of the uncertainties in wind pressure coefficients come from the difficulties in determining these local wind speeds. This can be done with descriptions of terrain roughness. A method for this is given in the ASHRAE handbook (ASHRAE 2009) which uses coefficients representing a number of terrain types such as, suburban, city, open country and woodland. Descriptions of these parameters are difficult to define accurately for a specific site. They do, though, allow the adjustment of wind speed station data (which is usually taken at exposed positions) to be adjusted to something more realistic for a building site. As well as general terrain effects, the local obstacles, such as surrounding buildings, are incorporated into the "CP generator" method by TNO (2010). This method produced wind pressure coefficients based on extensive lab testing which included obstacles. Obstacles can have a strong influence on ventilation depending on wind direction.

2.1.6 *Sensitivity and uncertainty of ventilation*

Warming was found to affect the uncertainty of thermal comfort in buildings with night ventilation strategies. The use of weather data which would be expected to occur once every 10 years significantly increased the uncertainty of thermal comfort, compared to that with a standard weather data set (Breesch & Janssens 2010). The aim of the study by Breesch & Janssens (2010) was to develop a method to predict the performance of night ventilation strategies that took into account the associated uncertainty in a wide range of key parameters. The weighted temperature excess hours (WTE) thermal comfort model was used by van der Linden et al. (2002) as the main indicator of performance. The method also employed a building energy simulation model of a generic office building and uncertainty and sensitivity analysis. WTE thermal comfort for no night ventilation, single-sided, cross, and stack was compared, first for the deterministic single values and then also with probability distributions. It was found that the single-sided night ventilation strategy showed the largest uncertainty for thermal comfort. Uncertainty for the stack and cross ventilation strategies were said to be substantially smaller. It is somewhat surprising that the cross ventilation strategy showed a similar level of uncertainty to the stack strategy due to the variability of wind, though this could be due to larger openings being used to model this strategy.

The use of Monte Carlo analysis enabled key parameters to be ranked according to their importance for thermal comfort for the cases modelled. Internal heat gains, solar heat gain coefficients of sun blinds, internal convective heat transfer coefficients, thermophysical properties related to thermal mass, temperature set-point control of openings, the discharge coefficients of openings, and wind pressure coefficients were established as the dominant parameters (Breesch & Janssens 2010). A separate study of which parameters had the most

influence on the effectiveness of night ventilation strategies was conducted by Artmann et al. (2008). It found that climate conditions and the night time airflow rate had the most effect.

The uncertainty associated with surface averaged wind pressure coefficient table data was investigated by Cóstola et al. (2010). Although the uncertainty due to the use of surfaced averaged wind pressure coefficients was found to be high, they can still be appropriate depending on the situation. They may be appropriate for example, when performance indicators that are predominantly sensitive to the higher flow rates are the focus or performance indicators related to cooling or thermal comfort. They may also be appropriate when the aim is a comparative study rather than the representation of specific existing buildings.

The sensitivity of building Air Change Rates (ACH) to wind orientation was looked at by Horan & Finn (2008). This paper describes a CFD study of a naturally ventilated atrium space where the influence of variation in the external wind speed and direction is examined. The atrium simulated was from a two story building with a series of entry vents on one wall and roof vents. A range of wind speeds from 25% to 250% of the mean site wind speed were examined and a roughly linear relationship to ACH was reported. Wind directions were then examined and a non-linear response in the ACH was reported. The sensitivity of ACH to the wind direction appeared to be larger at the higher wind speeds as shown in Figure 2.1.

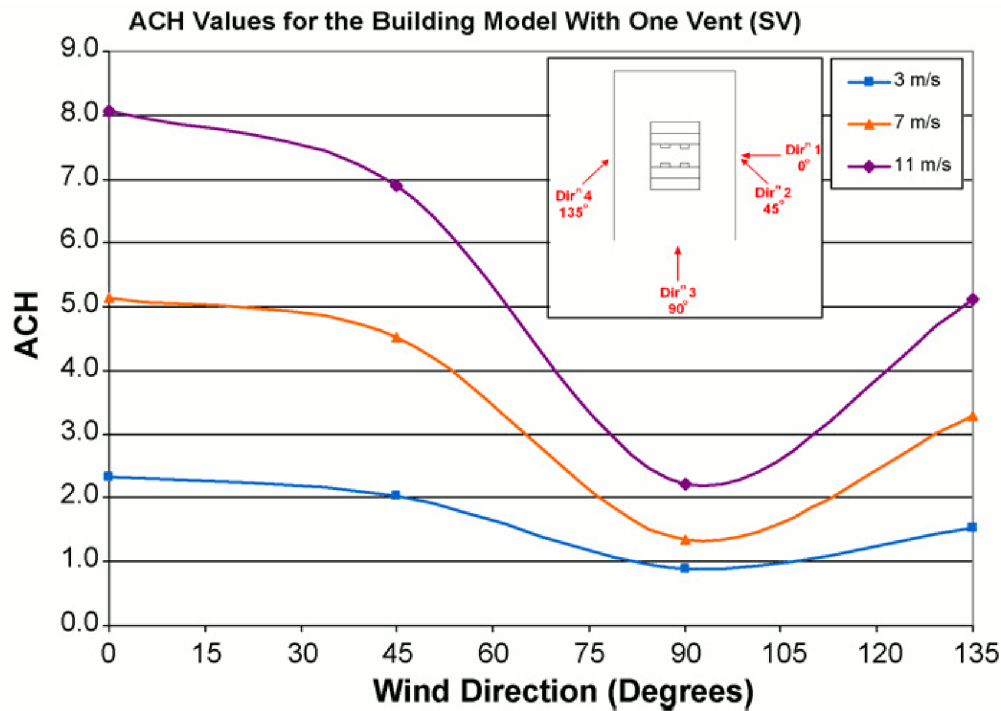


Figure 2.1. Results for ACH sensitivity reproduced from the study by Horan & Finn (2008). Wind speeds and orientations indicated in the legend.

The building was modelled as having wall vents in one side of the building each with an opening area of 1.0m^2 and roof vents each with 2.6m^2 opening area. The position of the vents was highlighted as a key factor in the difference in sensitivity of the models. Such differences in opening position could be expected for a façade subject to uneven noise distribution. Acoustic ventilation interaction is explored in more detail in Section 2.3. For residential buildings noise ingress at night is an issue due to sleep disturbance and this would be an issue for night ventilation cooling strategies.

2.1.7 Thermal comfort

Thermal comfort is an important concept for buildings; it determines the heating and cooling requirements of a building and therefore has important implications for building energy use

as well as the wider success of the building as perceived by its occupants. Thermal comfort measures are often a key output of building simulation software. To aid building and plant design and to enable the setting of thermal comfort standards, researchers have developed mathematical comfort models. These were developed by monitoring the environmental variables and physiological variables that affect peoples' impressions of thermal comfort.

The first, and still one of the most widely used mathematical models of thermal comfort was developed by Fanger (1970) This model, called Percentage Mean Vote (PMV), makes up much of the information given in BS EN ISO 7730:2005 (CEN & BSI 2005). It is based on a heat balance model of the human body and relates this to the expected mean value of votes given by a large group of people on a thermal comfort scale. The scale used has 7 points as follows +3 hot, +2 warm, +1 slightly warm, 0 neutral, -1 slightly cool, -2 cool -3 cold. The model was developed by many experiments where the subjects were exposed to various environments. The model enables the prediction of what comfort vote would arise from a set of environmental conditions given a certain clothing insulation and metabolic rate. The relevant environmental variables are air temperature, radiant temperature, relative air velocity and humidity. This approach has led to the traditional thermal comfort criteria that can be found in the standards and guidance that deal with this subject. As well as PMV, the concept of Percentage of Persons Dissatisfied (PPD) is used to define thermal acceptability criteria. For example 80% or 90% acceptability are used as a limiting acceptability criterion. A widely used relationship leads to 20% dissatisfaction corresponding to ± 0.85 PMV and 10% dissatisfaction corresponding to ± 0.5 PMV.

The Chartered Institution of Building Services Engineers (CIBSE) guide A: Environmental design (CIBSE 2007) gives guidance for the design of buildings and plant; this includes environmental criteria including thermal comfort criteria and is the main source of guidance for U.K. practitioners in this area. The guide is meant for industry use, so as far as possible simple criteria are presented that can easily be adopted by practitioners. For buildings that are fully air-conditioned, guide A recommends operative temperature ranges for different buildings and activity levels. For example, for general offices during the summer an operative temperature range of 22°C to 24°C is recommended, assuming activity levels of 1.2met and clothing levels of 0.7clo.

Guide A acknowledges that for buildings with free running modes where air conditioning is not exclusively relied on for summertime comfort, higher internal temperatures are acceptable. This is looked at in more detail in Chapter 6, Section 6.3.2, which covers adaptive comfort. A general indoor comfort temperature for offices is said to be 25°C during warm conditions. The guide also acknowledges that this is not a fixed target and it may not be possible to achieve these temperatures under all conditions without the use of mechanical cooling. It suggests that and the risk of overheating should be analysed instead. Clear criteria for overheating are difficult to define and the method commonly recommended by CIBSE is to define bench mark temperatures related to thermal discomfort, productivity, or health, and consider the periods of time that the building exceeds these. If these periods of time exceed a certain level the building is said to be overheating. In the UK the only fully agreed overheating criteria relates to schools (DfES 2003). Guide A does include guideline criteria but due to issues relating to climate change CIBSE will keep this under review. The guideline criteria for overheating in office buildings is that 28°C internal operative temperature is exceeded for 1% of the building's occupied hours.

Over the last few years there has been more discussion about whether the laboratory-testing-derived heat balance thermal comfort models given in BS EN ISO 7730:2005 (CEN & BSI 2005), are necessarily appropriate for naturally ventilated buildings (Brager & de Dear 2000; de Dear & Brager 2002). In fact it has been difficult to meet the narrow definitions of thermal comfort without mechanical cooling. This has led to the development of adaptive comfort models for thermal comfort in naturally ventilated buildings. With these models there is a tension between the desire to produce a model that is as rigorous as possible, but which will also be readily usable for practitioners. The following expression was proposed for the optimum comfort temperature T_{comf} , given a mean monthly external dry bulb temperature $T_{\text{a,out}}$ in equation (2.4) (ASHRAE 2004).

$$T_{\text{comf}} = 0.31T_{\text{a,out}} + 17.8 \quad (2.4)$$

The use of this PMV – PPD relationship leads to a comfort zone band of 5°C for 90% acceptability and 7°C for 80% acceptability. This corresponds to a PPD value of 10% and 20% respectively. An alternative standard to ASHRAE 55 that includes an adaptive thermal comfort model is European standard BS EN 15251:2007 (CEN & BSI 2007). The European adaptive comfort overheating criteria are used in Chapter 6 and more detailed information about this is given in Section 6.3.2.

2.1.8 Weather data inputs for building modelling

A key input into building energy modelling is hourly weather data. This is a description of the external climate that a building is subject to through a year. It allows building designers to test a design in the appropriate weather conditions. In the area of building energy consumption, the CIBSE have been producing weather data for the UK since the 1980's (Holmes & Hitchin 1978) with guide J (CIBSE 2002) describing typical years and near

extreme warm summers. To calculate average energy consumption over a year hourly weather data is often used and the usual approach is to use year-long weather time series. As well as the CIBSE TRY data other sources for such data exist, such as (ASHRAE 2001).

A number of file formats for the weather files have been used, one of the most popular is the tmy and tmy2/epw file formats. The format is widely used by building energy simulation software and was first proposed by Crawley & Hand (1999). This paper was an attempt to standardise the weather file formats and enables the use of more variables and sub-hourly data if desired. In the UK CIBSE provides yearlong hourly weather data of two types, the Design Summer Years (DSY) and Test Reference Years (TRY). The DSY is a near extreme year which is used for overheating calculations, the year is chosen that has summer temperatures which are the centre of the upper quartile of the climate period this is the year with the third highest average summer temperature. The TRY is used, for example, for calculations of average energy use; it is a year of data made up of the most typical months joined together.

The method of production for the design summer years is given by Levermore & Parkinson (2006) and this has provided a practical way to test a building under near extreme summer conditions. For this study a TRY drawn from 1983 to 2005 was used and the DSY was 1999 which was chosen from the period 1983 to 2004. The design summer year has received some criticism as it produces a full intact year based only on near extreme nature in terms of summertime temperatures. In their paper, Jentsch & Bahaj (2008) noted the differences between measured data and the local DSY. This has led to the development of a Design Reference Year (Watkins et al. 2012; Du et al. 2012).

As part of the study by Jentsch & Bahaj (2008) software tools were produced and distributed to aid the production of future weather data. One tool incorporated climate predictions into hourly weather data, while the other was a base file creator which could produce the necessary weather base file in the CIBSE format. It was said that both research and professional communities should be able to undertake climate change assessments (Jentsch & Bahaj 2008). There are restrictions on the future weather data due to licensing and copyright of the weather data and climate predictions. The climate change weather file generator tool was therefore created by Jentsch & Bahaj as a spread sheet macro that could produce climate change weather data once the required base data had been obtained. The methods employed by this tool will be covered in more detail in Section 2.2.2.1.

2.2 Climate change

Anthropogenic climate change is now generally accepted as the most likely cause of global warming (IPCC 2007). Over the years the Intergovernmental Panel on Climate Change (IPCC) has published a series of reports bringing together and summarising the state of knowledge on climate change. In (IPCC 2007) it is stated that global average surface temperatures can be expected to rise, for the different scenario ranges, between 1.1°C –6.4°C compared to temperatures in the 1990s. From the UK Climate Impacts Programme 2002 scientific report (UKCIP02) by (Hulme & Jenkins 2002) that presented the projected future climate change scenarios specifically for the UK, an average warming per decade varying between 0.1°C to 0.3°C for a low emissions scenario and 0.3°C to 0.5°C for a high emissions scenario was predicted. The UK Meteorological Office recently published its research into recent trends Jenkins et al. (2009); it found that UK summer temperatures have increased by between 1°C and 2°C since the 1960s. This indicates that even with concerted mitigation efforts climate change will be a growing challenge. The seriousness with which climate

change is now viewed by the government is indicated by the ambitious target of reducing CO₂ emissions to 60% of 1990 levels by 2050 (DTI 2003).

Climate change presents a challenge to those dealing with the built environment both in terms of reducing emissions and in terms of adaptation to this changed climate. The goals of mitigation and adaptation are not helped by the fact that building stock changes relatively slowly. The built environment is responsible for approximately 40% of the UK energy consumption (EC 2005) and possibly over 50% of the UK's carbon emissions (Defra 2008). This area is therefore of vital importance in reducing the UK's climate emissions. A review of the built environment section of the fourth IPCC report was undertaken by Levermore (2008). It was concluded that the document was a useful reference for those looking at the implications of climate change on building design. A recent overview of the various strategies for reducing energy consumption and emissions from buildings is given by for example, Clarke & Johnstone (2008). This included strategies for improving the efficiency of old and new buildings and future technology and design tools such as simulation. A more specific look at thermal comfort and energy can be found in the work of Holmes & Hacker (2007) which concluded that sustainable design should take into account future performance.

Reviews of climate change impacts on the built environment have collected evidence for four main areas: urban ventilation and cooling, urban drainage and flood risk, water resources and outdoor spaces (Roberts 2008; Wiley 2007). Of particular interest in these studies is the impact on the indoor environment. A popular method to assess the impact of climate change on thermal comfort is to use future climate change weather data along with thermal building simulation techniques. Examples of work that includes future performance analysis of case

study buildings are (Holmes & Hacker 2007; Jentsch & Bahaj 2008; Hacker & Holmes 2005). These studies suggest that, with the expected future temperature rises, providing a comfortable summertime indoor environment without a heavy reliance on mechanical cooling will be one of the major challenges. This is partly due to the potential of summertime natural ventilation to cool building interiors being diminished by the higher external temperatures (Sharples & Lee 2009).

The impact of climate change night ventilation, ventilation which increases cooling of the building fabric during the night, was investigated by Artmann al. (2008). A Climatic Cooling Potential (CCP) quantity is introduced which is derived from degree-hours based on a building temperature that varied within a standardised range of thermal comfort. Degree-hours are similar to the commonly used degree-days but with a finer temporal resolution. This was done to keep the method as general as possible, enabling the comparison of climate data; it was not meant as a replacement of detailed simulation of specific buildings that would be more appropriate for design purposes. 30 regional climate models (RCMs) from the European PRUDENCE project (Christensen et al. 2007) were used to predict the climate across Europe up to the year 2100. The results showed clearly that night ventilation would no longer be sufficient to maintain thermal comfort for southern and central Europe though the potential remained for northern Europe at least for the next few decades. The marked divergence of CCP with different future climate scenarios illustrated some of the uncertainty about the future and need for flexible buildings design.

2.2.1 *Climate change modelling*

The climate change scenarios that have been published contain information derived from ever more complex computer climate models. The starting point for modelling the future behaviour of the climate is the generation of “emission scenarios” which are story lines describing possible future paths for the anthropogenic factors that affect the climate. In the IPCC Special report on emissions scenarios (Swart & Nakicenovic 2000), six widely used key scenarios are presented. These scenarios use different assumptions about the demographic, economic and technological trends of the future to give a set of emission rates. Emission scenarios provided the radioactive forcing for the climate change predicted for the UK in UKCIP02 (Hulme & Jenkins 2002) and in the 2009 projection (UKCP09) (Murphy et al. 2009). The climate models, also known as General Circulation Models (GCMs) or Atmosphere-Ocean Global Circulation Models (AOGCMs), simulate the physical, chemical and biological processes that drive the climate. The range of processes that the successive models (IPCC 1990; IPCC 1995; IPCC 2001; IPCC 2007) incorporate has become more extensive and complex. As well as this, the increase in computational resources available to run these simulations has enabled finer horizontal resolution of the models. This is illustrated by the improvement from a 500km grid (IPCC 1990) to a 110km grid (IPCC 2007) resolution for northern Europe. Figure 2.2 illustrates how this improvement in resolution improves the topographical representation.

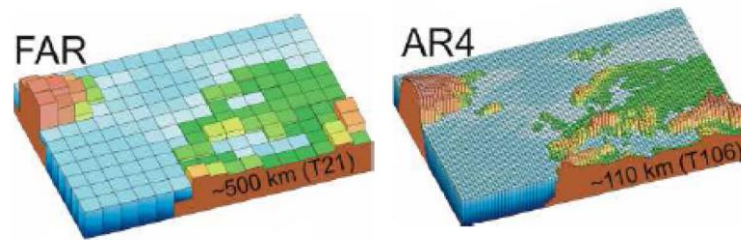


Figure 2.2. Illustration of improved spatial resolution of climate models of Europe. (FAR 1990; AR4 2007). Reproduced from (Hacker et al. 2009).

To obtain more detailed information about the climate for a particular part of the world such as the UK, RCMs can be used. These use global models for the boundary conditions, allowing the RCMs to cover a smaller area with a finer mesh that will enable better representation of the topography, and importantly coastline morphology. Increasing the spatial and temporal resolution of GCMs and AOGCMs is called downscaling. For reference the Met Office Hadley Centre regional climate model (HadRM3) used for UKCIP02 (Hulme & Jenkins 2002) had a grid size of 50km.

2.2.2 *Incorporating climate projections into weather data*

To enable the evaluation of building performance in weather conditions expected for the future, predictions about the future must be incorporated into weather data; A recent review of the methods for this is given by Guan (2009). One of the simplest methods is to extrapolate statistical historical weather data for a single measure to predict future weather conditions. This has been used to give the change to “heating degree day” (Hulme & Jenkins 2002; Rosenthal & Gruenspecht 1995). This method is simple and fast but gives only coarse information about the future and thus has limited applicability. Of particular interest here are the methods that provide the type of data that can be used in energy simulation. This requires

further downscaling from a RCM to give predictions at a finer temporal and spatial resolution. Two such methods are described in the next sections.

2.2.2.1 Morphing method

Morphing, or time series adjustment, was the term given to a method of imposing the climate change predictions onto a chosen weather time series representing the current weather (Belcher et al. 2005). The change to the weather variable is imposed by either a shift or a stretch or both depending on the relevant variable. This methodology was evaluated by comparing the heating degree day of morphed weather data to that given directly in UKCIP02 (Hulme & Jenkins 2002). It was found that the heating degree days calculated from morphed data corresponded well to the UKCIP02 data and this was thought to providing some confidence that this method was appropriate for producing future weather data (Belcher et al. 2005). The method has since been used widely due to its simplicity and tools that have been made available for its implementation.

Morphing incorporates the climate change projections into a current weather data time series by one of the following three processes, depending on the variable. These are described as a shift, a linear stretch or combination of both and are presented as follows (Belcher et al. 2005):

- A ‘shift’ which adds the UKCIP02 predicted absolute monthly mean change

$$x = x_0 + \Delta x_m \quad (2.5)$$

where x is the future climate variable, x_0 the original present day variable and Δx_m the absolute monthly change according to UKCIP02. This method is for atmospheric pressure.

- A ‘linear stretch’ of hourly weather data parameter by scaling it with the UKCIP02 predicted relative monthly mean change (Belcher & Hacker, 2005).

$$x = a_m x_0 \quad (2.6)$$

where a_m is the fractional monthly change according to UKCIP02. This method is used for wind speed.

- A combination of a ‘shift’ and a ‘stretch’. An hourly weather data parameter is ‘shifted’ by adding the UKCIP02 predicted absolute monthly mean change and ‘stretched’ by the monthly diurnal variation of this parameter:

$$x = x_0 + \Delta x_m + a_m(x_0 - \langle x_0 \rangle_m) \quad (2.7)$$

where $\langle x_0 \rangle$ is the monthly mean related to the variable x_0 , and a_m is the ratio of the monthly variances of Δx_m and x_0 . This method is used for dry bulb temperature. It uses the UKCIP02 predictions for the monthly change of the diurnal mean, minimum and maximum dry bulb temperatures in order to include predicted variations of the diurnal cycle.

As part of a separate study, the program called “ccgenerator” was produced that would carry out the morphing procedure for a desired weather time series and set of change factors (Jentsch & Bahaj 2008). This automated the morphing procedure through an excel spreadsheet macro, which uses the UKCIP02 climate change factors and a weather data file. The morphing method was used to produce the CIBSE future weather years (CIBSE & Met Office 2009); this incorporated the UKCIP02 projections into the CIBSE set of hourly simulation weather data for 14 sites around the UK (Hacker 2009). As part of the UKCP09 projections a fundamentally different downscaling method was used, stochastic weather

generators. Stochastic weather generator output was made available that incorporates the probabilistic projections. Stochastic weather generators are discussed in the next section.

2.2.2.2 Stochastic weather generator method

A stochastic weather generator produces synthetic time series of weather that represents both the stochastic or random nature of weather and also key statistical properties of the observed meteorological record such as daily means, variances and covariances, and frequencies. This is in contrast to the deterministic calculation methods employed by, for example the building energy modelling methods described previously. Stochastic weather generators have been widely used in water engineering design and in agricultural, ecosystem and hydrological impact studies. They have been used for the in-filling of missing data or for producing long synthetic weather time series from finite station records (Wilks & Wilby 1999). Weather generators have also more recently been used for the statistical downscaling of regional climate change scenarios and this is what is focussed on here. As part of the BETWIXT project (Harpham & Goodess 2006), hourly stochastically generated future weather data was produced and is available on-line from the “betwixt” website (Betwixt 2008). The weather data incorporates the four generic IPCC SRES emissions scenarios and the UKCIP02 scenarios (Hulme & Jenkins 2002). A version of this weather generator was also used to statistically downscale the UKCP09 projections (Jones et al. 2009).

A stochastic weather generator works by using past hourly meteorological observations at a site to estimate the model parameters. These are then used in a stochastic model to generate streams of hourly weather variables. Precipitation is the primary variable and is generated using the RainClim software, from which all the other variables are derived with regression

relationships or direct calculations. Most stochastic weather generators focused on precipitation due to the high importance of rainfall to many environmental processes and due to the complexity of building internally consistent, Multi-variable models (Wilks & Wilby 1999). At least 10 years of observed meteorological data must be available for a site to train the generator and estimate the model parameters. Six UK locations had the appropriate observed data to produce the hourly generated weather data for the BETWIXT project (Betwixt 2008).

The Climatic Research Unit (CRU) hourly weather generator which was used in the BETWIXT project produced data for the following variables; precipitation, temperature, vapour pressure, relative humidity, wind speed and sunshine duration. The data available is for 30 simulated years; these do not correspond to past calendar years due to the stochastic nature of the generator, but the distribution and statistical characteristics of the aforementioned variables are matched to the training period. 50 runs of each simulation set have been run for validation purposes with the time series from the middle of each distribution being made available. To incorporate the climate change predictions into the weather generator outputs, “change factors” calculated from the HadRM3H regional climate simulation, were applied to mean daily precipitation. RainClim uses predicted changes to the mean, variability and skewness of precipitation to produce the synthetic data. The CRU daily generator uses changes to the mean and variability of the maximum and minimum temperature. Hourly data is produced with the assumption that the relationship between daily and hourly variables will stay the same in the future. In this way, the weather generator method was used by the environment agency rainfall and weather impacts generator (Kilsby & Jones 2007). To extend coverage of this generator, beyond the selected sites mentioned previously, continuous coverage across the UK at a 5km resolution is provided.

A minimum of 100 runs of the desired 30 year time period are recommended when using stochastic weather generator output (Jones et al. 2009). These large amounts of weather data can be processed to produce building simulation weather years such as typical years and design summer years. Two methods for this are studied in this thesis (Watkins et al. 2011; Eames et al. 2011) and these are compared in Chapter 6. Such methods are required to produce weather data usable for thermal building simulation from the large volumes of data that are available as part of the UKCP09 probabilistic projections.

2.2.3 UKCP09 Projections

There are a number of uncertainties in the scenarios presented in UKCIP02 (Hulme & Jenkins 2002) such as those stemming from the emission scenarios chosen and modelling approach adopted by the RCM (Jenkins & Lowe 2003). In an attempt to quantify and communicate the modelling uncertainties in climate predictions, a probabilistic approach was adopted for UKCP09 (Murphy et al. 2009). An earlier example of this probabilistic approach is shown in the “Ensembles” project (Hewitt & Griggs 2004). Probabilistic projections of climate change for London Heathrow airport are presented by Hewitt & Goodess (2009). These studies link the ensembles of RCMs results with a stochastic weather generator.

The general approach of probabilistic projections is to sample the range of uncertainty in parameters and modelling approach, and then present how these propagate through to the results. These are often presented as probability distributions. UKCP09 is the first major climate projections that attach probabilities to different levels of climate change (Murphy et al. 2009). The probabilistic projections for UKCP09 are largely based on an ensemble of multiple variants of the Hadley Centre Met Office climate model HadRM3, as well as climate

models from other centres. The projections are presented in a variety of formats through a user interface (UKCP 2009), which includes maps and probabilistic plots. In addition, a stochastic weather generator that can produce weather data time series at daily or hourly resolution is available.

Some weather variables, including wind are excluded from the standard output of UKCP09. Wind was excluded as there is a large amount of variability and no systematic trends are observed for this variable. This is a problem for building energy evaluation as wind is a key driver of natural ventilation. There are, though, other sources of future wind information linked to UKCP09. Firstly it is possible to backward calculate wind by using the Potential Evapotranspiration (PET) variable (Ekström 2007) which is still given as an output from the weather generator. Secondly wind speed is available directly from the RCM output that the probabilistic projections are largely based on.

2.2.3.1 Eleven member RCM

For the highest spatial resolution simulations in UKCP09, RCMs are used for the climate modelling, giving projections down to the 25km scale. As part of the information gathered for UKCP09, 11 variants of the HadRM3 model were produced. The outputs from these were continuous daily time series from 1950 to 2099 and were driven by the UKCP09 medium emission scenario. The RCM outputs are available via the LINK project (BADC et al. 2008) and these time series are spatially coherent between grid squares. The 11 different variants of the RCM represent 11 different representations of climate physics; in this way some of the uncertainty in climate modelling was sampled. One aspect to bear in mind is that they are all based only on one HadRM3 model so they do not take into account as much uncertainty as

the full UKCP09 output, which also includes results from other institutions. In this way some uncertainty due to modelling approach is sampled.

A wind technote by (Brown et al. 2009) assesses the information from the 11 member RCM, focussing in particular on wind speed. Biases were noted including lower than observed speeds over mountainous regions of Scotland and Wales and higher than observed speeds over low lying regions of England. The report concluded that these were most likely due to the representation of topography and surface roughness. It was suggested however that the biases were unlikely to significantly influence the changes in wind speed as this was determined mainly by large scale physical processes affecting the circulation of the free atmosphere. The reasoning was that the projected patterns of future change in surface winds are similar for both the regional and global model projections. As is the convention when using climate projections, it was recommended that fractional changes in wind speed between 30 year climate periods were calculated. This is then a similar approach to UKCIP02, but with 11 variants. In summary it was found that changes in wind speed were in the range of +10% to -15%. Such outputs were of interest for this study of building performance as they provide a source of information about future behaviour of wind.

2.2.3.2 Wind from PET

Wind is a key driver of natural-ventilation so it needs to be taken into account when considering a buildings' thermal performance. Wind data is a necessary component of the weather information needed to run thermal building simulation so that air flows through the building can be properly represented. As mentioned in Section 2.2.2.2, inter-variable relationships are preserved by the stochastic weather generator method. Consistency between

wind speed and the other weather variables is important due to the tendency for peak overheating conditions to occur when high temperatures and low wind speeds coincide. With weather generator wind data, the occurrences of high wind speeds during warm spells should be statically representative of that seen in the observed climate period. Methods for the calculation of wind data from PET were proposed by Eames et al. (2011b) and Watkins et al. (2011). The motivation for this is that wind speed produced from the weather generator method was used as one of the terms in the PET calculation. The formula used is a version of the Penman method modified by the Food and Agriculture Organization of the United Nations. The method is described by Ekström (2007).

Although wind data consistent with the other weather variables is available from this method, it should be noted that uncertainties about the future behaviour of wind speed still remain. Although the approaches of (Eames et al. 2011) and (Watkins et al. 2011) both involve backward calculation of wind speed, differences do occur. This is due to the additional steps needed to produce data usable for building evaluation. One such step was the production of wind direction. Also PET values are available at a daily time scale; whereas hourly wind data is needed; both methods adopted different strategies to deal with this. Care must be taken to validate the output due to the rather complex method used to gain wind data. For example rounding errors for near zero PET values can produce unrealistic wind speeds that need to be corrected.

2.2.4 *Dynamic building simulation with future weather data*

To determine the likely future performance of buildings and building designs, dynamic building simulation can be run with future weather data. Results from building simulations

with future weather data have been published in a number of studies (Jentsch & Bahaj 2008; Du et al. 2010; Hacker & Holmes 2005; Hacker et al. 2009; Jenkins et al. 2011). This is a useful way of looking into the resilience of building design to projected changes in the climate. CIBSE future weather years (CIBSE & Met Office 2009) were used in the work of (Du et al. 2010), where a range of buildings of different types were modelled with UKCIP02 scenarios. These weather files make use of the morphing procedure which was also used by Hacker & Holmes (2005) for CIBSE TM36. 13 case study buildings, some with adaption strategies such as advanced natural ventilation systems, were investigated to study building performance with future weather data. The results suggested that for dwellings with very good control of solar shading, ventilation and internal heat gains, thermal comfort targets can be met until the 2050s. For office buildings, modelling suggested that it would be difficult to meet the thermal performance targets as the climate warms using passive measures alone (Jentsch & Bahaj 2008).

Future performance analysis can be used to determine the effectiveness of mitigation measures such as reducing internal heat gains. The importance of internal heat gains was highlighted in the work of (Jenkins 2009) where esp-r models of office buildings were used with morphed weather data. It was shown that reductions in internal heat gains could significantly reduce cooling loads and might alleviate problems due to climate change. A zero cooling office building in London was said to be very difficult to achieve, even with internal heat gain minimisation. The options for producing future weather data were summarised in the work of Jentsch & Bahaj (2008). These authors also introduced a tool to aid the implementation of the morphing procedure (described in section 2.2.2.1). Morphed weather data was used to investigate the future performance of a case study building, the Faraday Tower in the University of Southampton was used. It was found that with the full use of solar

shading and night natural ventilation, the future climate conditions likely to be experienced towards the end of the building's design life should be addressed. A detailed monitoring regime was implemented for the tower with logged data at 5 minute intervals being collected. The simulation results were compared with this logged data and it was found that performance under current extreme summer conditions can indicate future summer performance. To determine what contribution noise reduction measures could play in climate change mitigation is a central goal of this thesis.

Simplifying future performance analysis is an attractive goal. Coley & Kershaw (2010) found a linear relationship between external climate and the internal temperature of buildings, for a wide range of building models representing an array of architecture and building use types such as domestic house, school apartment and office, over a range in thermal mass, glazing, U-value and ventilation. With the different weather files used, which included extreme future scenarios, 400 different combinations of building model and morphed weather file were tested. The resulting linear relationships enabled the authors to produce climate change amplification factors which they said "fully describe the change in the internal environment of an architecture given a seasonal or annual change in external climate". This could greatly simplify calculations used to judge the resilience of particular designs and aid the future proofing of buildings in response to climate change. These linear relationships were confirmed in the study by (Du et al. 2010), which, in addition to domestic buildings, also found the same applied to a wide range of no-domestic buildings. The results were also said to give an indication of when additional mechanical cooling might need to be adopted. These linear relationships between average internal and external temperatures could be linked to building energy use. Whether these relationships continue to hold when probabilistic

projections are used is not clear, or when the more complex issue of thermal comfort is considered.

Fewer building performance studies have been published using the UKCP09 dataset than with UKCIP02. This is due to the more recent release of the UKCP09 projections and also the difficulty in making this data usable for building simulation, such as the calculation of wind speed from PET as described in Section 2.2.3.2. One example by Hanby & Smith (2012) presented an analysis of the probabilistic scenarios released under UKCP09, together with a detailed building plant simulation of case a study building with evaporative cooling systems. It was found there was a high probability that evaporative cooling will still be a viable technique in to the 2050s. Results which have used the more recent UKCP09 scenarios were also presented by (Du et al. 2011). In this study, future TRYs were produced from the UKCP09 weather generator and used in EnergyPlus dynamic building simulations. Interestingly the authors found that the prediction from UKCIP02 and UKCP09 gave similar building performance. This was the case, even though very different techniques were used to produce the future weather data for each set (the UKCIP02 set applied the morphing method and UKCP09 set was derived from the stochastic weather generator).

The UKCP09 weather generator makes available for download 3000 (30 years x100 runs) of weather data. To enable this to be used for dynamic building simulation some kind of simplification is required. This inevitably causes a tension between practical considerations and ease of use for industry practitioners against the fullest representation of climate conditions and associated uncertainties. In the work of (Du et al. 2011) traditional single-year TRYs are produced, whereas other studies suggest a different use of the probabilistic

information. For example the method proposed by (Jenkins et al. 2011) involves the use of a large database of climate data. This is available from the weather generator and is used to produce a probability curve of future overheating risk for a building. It aims to transfer the uncertainty represented in the probabilistic projections through into the building performance predictions. The method aims to produce probability curves to represent such things as overheating risk that can be considered as part of building design. The steps of the method are as follows:

- 100 randomly chosen years of climate chosen for a given climate scenario.
- Hourly temperature is obtained from building simulation with these 100 years.
- Regression relationships obtained between hourly climate data and hourly internal temperatures by principle component analysis.

Part of the motivation for this was said to be that deterministic representation of the future climate such as that given by the morphing method, imply a level of certainty about the future climate that does not really exist. With this release of the probabilistic information in UKCP09, an indication of the level of certainty is given. With the method proposed by this paper the uncertainty is transferred down through to the building simulation results. It is not clear though whether this approach will become a widely used part of the design process.

This method is somewhat in contrast to the use of UKCP09 weather data for building simulation represented in (Watkins et al. 2011; Eames et al. 2011a), where yearlong data files were produced. In the work of Kershaw & Coley a separate yearlong weather file for a number of climate percentile was produced so. Typical questions of concern to practising building services engineers are, for example, the hours over 28°C and annual energy use. Single-year reference years produce distributions for these parameters that show a good

match with the full 3000 set according to (Kershaw et al. 2011). However, it was said by Watkins et al. (2011) that the use of a large number of weather files was not necessarily a benefit. Providing an excess of options to building designers could defeat the object of a TR Y year, which was to provide a common practical weather year that all designers can use to compare building designs.

2.3 Influence of acoustics on natural ventilation

Natural ventilation strategies are difficult to implement for buildings in urban areas for a number of reasons, such as lower wind speeds, higher temperatures due to the urban heat island effect, pollution and noise. A number of different influences on natural ventilation were investigated by Ghiaus et al. (2006). In their work, street canyon situations were addressed with measurements being taken outside the façade at different heights above street levels. Relationships were then defined between street aspect ratio, height above street level and noise levels at which occupants might be motivated to close the windows. This demonstrated how the influence of noise on ventilation changes with position on the building façade. The openings in a naturally ventilated façade are a natural acoustic weak point in the building façade and tend to increase a building's susceptibility to environmental noise. The interrelated environmental problems of noise, temperature, air quality and light level were investigated for schools in the Heathrow airport flight path by Montazami et al. (2012). The temperature, air quality and noise were monitored quantitatively, along with the other factors that were assessed by subjective surveys using interviews and questionnaires. It was found that schools in the vicinity of Heathrow Airport were more likely to experience overheating and poor air quality due to aircraft noise.

The pressure differences that drive natural ventilation, wind and or buoyancy effects, are very weak, typically less than 10Pa. The easiest way to achieve the least restriction of a ventilation path is to open large areas of the façade (Oldham et al. 2004). This leads to the conflict between attempts to reduce noise ingress and the maximizing of natural ventilation rates. De Salis et al. (2002) related ventilation opening area percentage to the façade sound insulation and the airflow rates due to a 5Pa pressure difference. This was done in order to review the combined performance (acoustic and airflow rate) of various noise control techniques. A product of this investigation was a set of curves relating sound insulation and air flow rate. In their method, the SRI of the aperture was assumed to be 0 at all frequencies to simplify the calculations. It is acknowledged that the SRI of smaller openings such as cracks and other perforations can vary quite significantly between the resonant and anti-resonant frequencies, depending on the aperture width to depth ratio. The authors assume this effect will be negligible for the purposes of their study, although no estimation of the possible relative size of the deviations due to this effect was given. Chapter 4 will calculate the SRI of ventilation apertures as a new contribution to this approach.

Further details of the interaction of acoustic and airflow performance was investigated by Oldham et al. (2004) using a combined theoretical and experimental approach. The motivation for this study was that designers need information about the acoustic performance of a ventilator alongside the airflow performance. This was presented in terms of design charts, which can be used with the suggested design methodology. For a given façade construction, a chart is compiled, which gives the sound insulation to road traffic noise for a given flow rate. Relationships were produced representing different acoustic treatments such as acoustic louvers, lined ducts and lined duct plus active noise control. When specific flow rates and sound insulation are required, the opening area for a specific pressure differential

can be determined from the chart or the pressure differential for a given opening area. Another practical use of these design curves would be to establish a façade opening and natural ventilation flow rate according to a given façade sound insulation. The choice of which façade sound insulation is required, depends on the exposure of the building and also the levels of noise ingress that are acceptable. Although there are established guidance on noise criteria, (as will be introduced in the next section) these are not necessarily appropriate for naturally ventilated buildings.

2.3.1 Building noise criteria

An example of the impact of noise on health is its link to cardiovascular disease (Babisch 2000). As well as health factors, speech intelligibility, speech privacy and general annoyance can be problems, particularly for non-domestic buildings such as offices. The type of building use is important to the level of noise ingress that may be appropriate. Office buildings may have more flexibility about noise than schools, as teaching is more likely to be disturbed by noise than most office activities. Clear communication between teachers and students is required through much of the day. For England and Wales, specific limits for schools have been introduced (Hopkins et al. 2003), partly on the grounds of disabilities discrimination concerns. This gives internal limits of unoccupied classrooms, but is not specifically aimed at naturally ventilated buildings.

CIBSE Guide A (CIBSE 2007) gives a recommended allowable background noise that can be generated by the building services installations. This allowable background noise is prescribed as an NR value due to the high tonal component of the noise often produced by components of building services, for example fans. NR 35 is recommended for open plan

offices. To calculate an NR value the spectrum is compared with the standard curves and the value is taken from the curve that the spectrum does not break. This procedure is also used for other standard curves such as the NC curves which are used in the America. Noise levels are more commonly given in dBA, which indicates a frequency weighting that mimics the hearing response of the human ear, and has been used for many years. The study of noise issues has led to a number of international standards bodies publishing guidelines (BSI 1999; Australian Standard 2000; ASHRAE 2007). These relate to, for example, standard office buildings and give recommended internal background noise levels. The comparison of these noise limits is given in Table 2.1. where L_{Aeq} is the equivalent continuous A-weighted sound pressure level (equivalent in terms of average sound energy). This is given on the decibel scale using the standard value of 2×10^{-5} Pa as the reference pressure.

Table 2.1. Reproduced from (Field 2010) Recommended background noise limits for unoccupied mechanically ventilated spaces from the following standards Standard BS8233 (BSI 1999), (ASHRAE 2007), AS2107 (Australian Standard 2000).

Occupancy type	BS8233 (L_{Aeq} , dB)		AS2107 (L_{Aeq} , dB)		ASHRAE (NC) ¹	
	Satisfactory	Maximum	Satisfactory	Maximum	Satisfactory	Maximum
Private office	35	40	40	50	25	35
Meeting Room	30	40	35	40	25	35
Open plan office	40	45	45	50	30	40

1. For comparison purposes, the NC rating was said to be typically 5dB below the L_{Aeq} .

Noise tolerance, though, is difficult to define exactly due to the complex psychological component of annoyance and factors such as climate. In the work of (Wilson & Nicol 1994) it was found that occupants of naturally ventilated buildings in the United Kingdom and Pakistan had different noise tolerances. In their study occupants were surveyed and measurements of office noise levels were taken. The UK survey showed 70% of respondents

were dissatisfied with break-in noise levels of 51-55dBA. In contrast the Pakistan study showed that 53% of respondents were disturbed by break-in noise levels of 62-64dBA. It was not possible to determine whether the climate was responsible for this due to insufficient data and a number of confounding variables relating to building use. It did though, illustrate the substantial differences that can occur between countries and was consistent with the findings published by Berenek (1971). Berenek reported that tolerances to environmental noise differed between northern Europe (England and Scandinavia) and southern Europe (France and Italy). These differences were attributed to the amount of time windows are left open in the different climatic zones.

In the UK, guidance for the consideration of noise in the planning process is given in Planning Policy Guidance 24 (PPG24) (DCLG 1994). This includes planning applications for noise sensitive developments and developments that could generate noise. The guidance uses the concept of noise exposure categories which apply to dwellings. Ranges of noise from a number of sources are given that define the Noise Exposure Category (NEC). The category determines how noise should be considered for planning. The options are: that planning should be refused, that noise should not be a consideration or two middle categories where planning could be granted once levels of protection have been ensured. PPG 24 advised that these NEC principles were not appropriate for noise sensitive buildings other than dwellings, such as offices, schools and hospitals. This is due to such developments being large and with areas of varying noise sensitivity. For these buildings internal noise standards are recommended such as in BS 8233 (BSI 1999), though, these may not be appropriate for naturally ventilated buildings (Field 2010).

2.3.2 Noise criteria for naturally ventilated buildings

External noise levels are given by (Wilson & Nicol 1994) as a common justification for air-conditioning buildings. Lambert et al. (1984) studied the patterns of behaviour due to road noise of 1500 people. It was shown that traffic noise can lead to the closing of windows to shut out the noise. There is therefore a tension between efforts to encourage the design of sustainable buildings and acoustic requirements. The question of whether the established noise limits from Table 2.1 are suitable for the design of sustainable buildings that have a large reliance on natural ventilation was investigated by Field (2010). In this study a review of the acoustic criteria was undertaken, with the main internationally recognised limits for background noise being compared. The result was that these noise criteria generally assume that the building is sealed and air conditioned, and are not necessarily appropriate for naturally ventilated buildings.

A review of noise surveys carried out by (Ghiaus & Allard 2005) recommended a noise threshold of 55dBA to 60dBA for open plan offices. This is somewhat higher than all the maximum levels reported in Table 2.1. It was proposed by Field (2010) that occupants of naturally ventilated buildings had a lower sensitivity to noise for the following reasons.

- The expectation of a low noise level environment is lower.
- The appreciation of non-acoustic benefits that natural ventilation provides, as part of an overall sustainable design strategy, promotes occupant acknowledgement that there is the inability to control internal noise levels to the same degree as a sealed, mechanically ventilated building.
- Office layouts (open plan) in green buildings provide occupants with greater awareness and therefore tolerance of surrounding activities.

- Climate – people in countries where windows are customarily open for most of the year seem to be more tolerant of noise.

The aim of maximising natural ventilation is usually driven by a desire to increase the sustainability of the building. A building is required to function satisfactorily; one can question whether a building that is not acoustically comfortable, and therefore not fit for purpose, is really sustainable? The two building rating tools Green star (GBCA 2011) and Breeam (BRE 2011) include points for meeting acoustic criteria. These criteria though are derived from the standards covered in Table 2.1 and the issue, discussed previously, of whether they apply to naturally ventilated buildings is therefore relevant.

The question of whether occupants found sustainable buildings to be acoustically comfortable was focused on in the work of Baird & Dykes (2010). In this, paper the results of a worldwide survey of users' perceptions of acoustic conditions in sustainable buildings is reported. This extensive post-occupancy survey covered 36 sustainable buildings in 11 different countries. A mixture of fully sealed and air conditioned naturally ventilated and - mixed mode buildings was studied. The category of noise sources from outside referred to noise sources exterior to the buildings such as: nearby traffic, open air performances, and distant industrial and agricultural operations. It was found that the occupants' perceptions of acoustic conditions in sustainable buildings were slightly better than for the conventional buildings. This was an interesting result, due to the scale of the survey. The tendency of sustainable buildings to incorporate natural or mixed mode cooling strategies had not decreased an occupant's perception of the acoustic conditions. One issue that was not addressed was whether the noise exposure differed between the sets of buildings. It was not

clear from the study whether, for example, buildings built with sustainable aspirations tended to be situated in quieter areas. The noise exposure of a building can be complex and can vary from building surface to surface, opening to opening with additional variation through time. Including measurements of this as part of a large survey becomes a substantial task.

Variation in the noise criteria and in the noise exposure is the motivation for the work of Kurra & Dal (2011). The use of noise maps for the design of sound insulation was proposed. In their method strategic noise maps are utilised to determine the required sound insulation of a building's external elements, this is then displayed graphically. The variation of noise criteria is taken into account by the categorisation of different areas of the building. These differences in criteria were due to room use in Kurra & Dal's study. In addition, variations due to cooling requirements could also be useful, which would require linking with building energy simulation and involve more information at the sub-building scale. To achieve a good degree of natural ventilation and an appropriately comfortable internal noise environment a more sophisticated approach could be useful. This may need to take into account such things as differences in building use, site exposure, cooling demands and the paths by which air tends to flow through the building.

2.3.3 *Noise mapping*

Noise mapping is a map of how noise is distributed; it gives information about noise levels through an urban area. Noise levels are represented spatially, usually in the form of interpolated isocontours. Noise map information can be from either modelled or measured information about noise levels through an urban area. Both the multiple sources of noise and its propagation through the urban area lead to complex distributions. Well produced noise

maps that give accurate descriptions of the noise levels at a location can be used to provide noise trend data, establish exposure levels of a population, identify pollution hotspots and quiet areas, predict the effectiveness of noise management schemes, and indicate management/legislative/policy changes that might be required (Kang 2007). A case study of noise mapping in Brazil was presented in the work of Zannin & Sant'Ana (2011). The maps were said to be extremely helpful for environmental management and decision making by public authorities to enable the solution of potential urban noise risks. Noise maps can be used for the early prediction of noise problems, this can be done during planning and design phases. The early prediction of noise problems is important as solutions at construction tend to be much easier and cheaper than trying to solve problems post-construction.

In Europe, noise mapping became a legislative requirement for agglomerations along major transportation routes and major industrial premises, as part of the Environmental Noise Directive (END) (European Union 2002). This dealt with the following key aspects of assessing and managing environmental noise:

- Monitoring the environmental problem.
- Informing and consulting the public.
- Addressing local noise issues.
- Developing a long-term EU strategy.

A distinction was made between the wider strategic noise maps and noise maps more focused on representing noise distribution spatially. Noise mapping was said to enable a global assessment of noise exposure in an area, and information concerning the production of strategic noise mapping was given. Noise mapping was defined in the END as 'the presentation of data on an existing or predicted noise situation in terms of a noise indicator,

indicating breaches of any relevant limit value in force, the number of people affected in a certain area, or the number of dwellings exposed to certain values of a noise indicator' (European Union 2002). Part of the aim of the END was to help make noise control information openly available. That has been partly accomplished by making some initial maps available through a website (EEA 2012). The noise maps need to be updated every five years to ensure the information stays relevant; they therefore provide a readily available source of information on the distribution of noise through urban areas.

The European Commission Working Group Assessment of Exposure to Noise (WG-AEN) outlines the current good practice for noise mapping (EC 2006). This document was designed to balance the need for specific advice with being flexible enough to allow for differences between member states. The good practice guide encourages the use of computational methods for noise map production, when possible. It was advised that measurements be used for the validation of computed results, although maps based on measurements are technically allowed in the END. A method implemented in computational noise mapping in the UK and Ireland is the Calculation of Road Traffic Noise (CRTN) (DfT 1988). This method was intended for regulatory and planning use where road noise needed to be calculated some distance from the highway. It gives calculated noise levels in terms of L_{10} , which is the noise level exceeded for 10% of the time of the measurement duration. Conversion methods have been developed to comply with the END (European Union 2002) for example (O'Malley et al. 2009). This issue was highlighted by (Murphy & King 2010) in a paper exploring methodological issues surrounding the implementation of the END. It was suggested that these be considered in future amendments to the legislation.

As well as issues surrounding sound descriptors, there are also some concerns about the accuracy of noise mapping. (Kang & Huang 2005) found that the accuracy of noise maps were highly dependent on the importance of reflected noise to a specific noise map. Efforts have been made to improve robustness and harmonise calculation methods across Europe so that results are more comparable. The IMAGINE project and its predecessor the HARMONOISE project investigated improvements to calculation methods. A reference model was developed and described by Salomons & Heimann (2004); this modelled sound propagation to a good degree of accuracy but with high computational expense. A simpler engineering model was described by Nota et al. (2005) which enabled efficient production of large scale noise mapping. In addition, updated source models were described for example by Peeters & Blokland (2007).

Although these projects ended successfully some time ago the HARMONOISE/IMAGINE methods have not yet been officially recommended for noise assessments in the European Union. Part of the reason for the delay in using these new methods was the difficulties in the clear application of these methods into software. Hartog van Banda & Stapelfeldt (2007) investigated the uncertainty due to the software implementation of the method which was produced from the HARMONOISE project. They found that although improvements were made, the inclusion of unclear phrases and inconsistencies and incomplete information in the documentation meant that the method was not robust enough for software implementation. The consequences of these findings could lead to the continuation of different software packages giving inconsistent results for simple situations even when based on the same calculation methods, as has been the case for previous methods. In its current form, the HARMONOISE method is highly complex with, for example, several choices for vehicle type and meteorological class. The number of input variables required exceeds the level of

data that is currently required for many existing national calculation methods (Murphy & King 2010).

While efforts to improve noise mapping for EU wide legislative purposes progress, software exists that implement current national calculation methods. An example of a popular noise mapping software is CADNA (DataKustik GmbH 2006), which has many features that aid the production of noise maps, calculate the noise distribution and present results (usually in the form of isocontours). The versatility of this kind of software was demonstrated by (Wang & Kang 2011) where it was used in a study of urban morphology. The CRTN method was one of the calculation configurations used for this study, and was shown to produce results that were consistent with measured noise levels at different floor levels in the work of Mak et al. (2010). It could be said that noise mapping can be more representative than short term measurements as it predicts a longer term noise exposure. It also allows for the inclusion of buildings that are not completed yet.

In the work done by Kurra & Dal (2011), the noise maps were used for the purpose of assigning sound insulation of the external elements of buildings according to the calculated noise exposure. The sound insulation requirements are displayed graphically (an example of which is given in Figure 2.3), clearly showing the uneven variation of insulation requirement throughout the surface exposed to noise source. Contours are given in terms of standardized weighted level difference ($D_{nT,A,2}$). The calculation of which is given in ISO 140-4 (ISO 1998) and is a single figure level difference normalised for the receiving room reverberation.

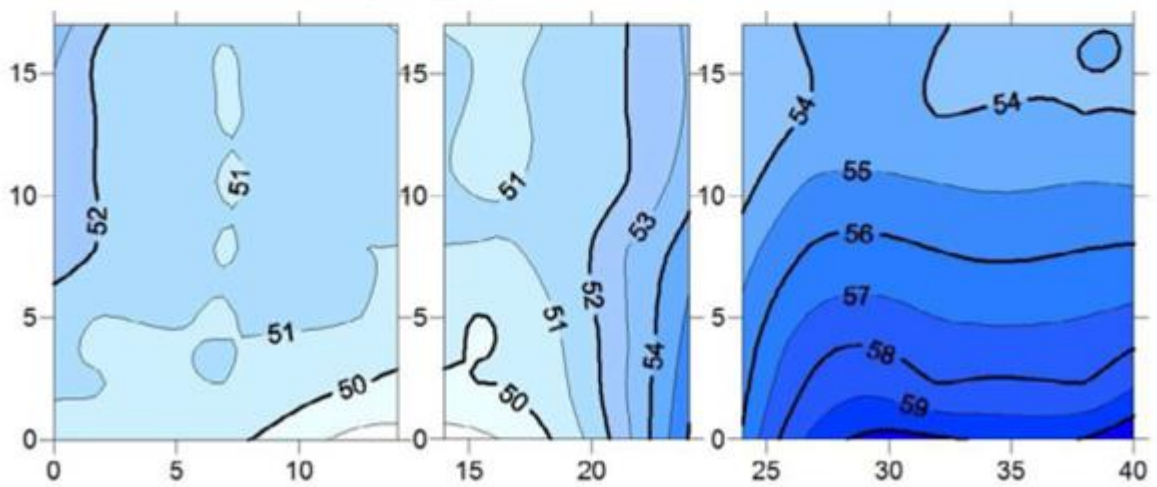
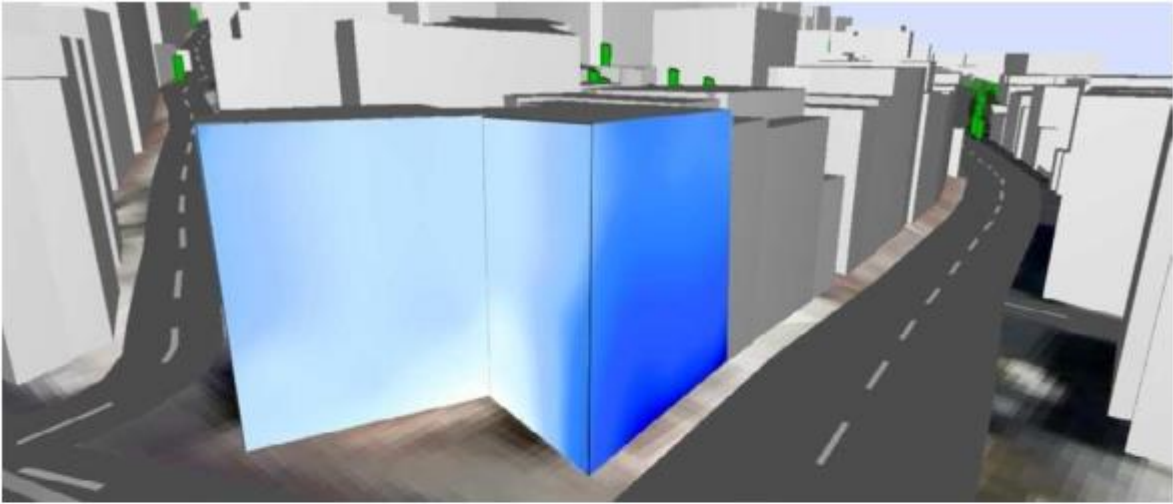


Figure 2.3. Contours showing required insulation performance in $D_{nT,A,2}$. Reproduced from (Kurra & Dal 2011).

Additional façade sound insulation is considered in this study as a noise reduction measure. The effect of openings in the façade, such as those for ventilation, is not considered. Neither are measures to reduce sound transmission through these openings. This use of noise mapping to show building sound insulation requirements has some similarities to the use of noise mapping exposures in this thesis. Thermal performance is not considered and this will be done in Chapter 5.

2.3.4 Noise reduction measures

Noise reduction measures are reviewed in this section as quantifying their thermal performance benefits are a central aim of this thesis. A reduction in noise not only has benefits to, building thermal performance, health and well-being, but also to the economy. The effects of noise abatement measures were monetised as part of a cost benefit analysis carried out by Nijland et al. (2003). The following types of measures were covered.

- Measures to reduce the sources of noise, examples being the introduction of more low-noise kinds of cars or by reducing traffic speed or traffic volume.
- Noise can be reduced by enlarging the distance between source and recipient
- Hampering noise propagation, for example construction of noise barriers
- Influencing the time of day of noise emission
- Additional acoustic insulation of building façades

It was found that the costs of implementing noise reduction measures were surpassed by the benefits. Noise ingress through building façades, in particular the effect of natural ventilation opening, is the main area focused in Chapter 5. A number of studies on noise reduction measures are reviewed through this section to determine how they can be related to thermal building performance.

A review of combined acoustic and airflow performance of a number of noise reduction methods was given by De Salis et al. (2002). Existing and future techniques that might be applied to large, non-domestic, open plan office buildings were covered in this study. The following noise reduction measures were mentioned: The first was simply to locate the building in a low noise area or position the ventilation apertures away from direct noise paths. Both of these would require good information of an area's noise distribution; although not

mentioned in this study, a possible source of this information could be noise mapping techniques (covered in Section 2.3.3).

Noise reduction measures can also be applied to the ventilation openings themselves. Curves have been produced to aid the design of building façades by illustrating the change in acoustic insulation against air flow for different levels of opening of façades (De Salis et al. 2002; Oldham et al. 2004). As an example, this enabled Oldham et al. (2004) to estimate the benefit of introducing double louvres to the ventilation opening as an example. It was calculated that the untreated apertures would give the façade a SRI of 20dB, whereas the same airflow could be provided with double louvres that gave the façade an SRI of 31dB. These values were for the acoustic insulation of road traffic noise. Other treatments of simple ventilation apertures were also covered and can be grouped as passive, reactive and active measures. Examples are absorbing linings, active noise treatments which use anti-noise to cancel out noise, quarter wave resonators and Helmholtz resonators. The use of absorbing materials is the most common method used and each method is most effective at attenuating noise from a particular part of the spectrum.

From (De Salis et al. 2002) it can be seen that the most popular passive measures such as screening and louvres are most effective for high frequencies and that a combination of approaches would be needed for most effective noise treatment of broad band noise such as road traffic noise. The combination of treatments suggested by Oldham et al. (2004) had the potential to provide flow rates of $30\text{m}^3/\text{h}/\text{Pa}^{0.5}$ (per m^2 of the façade) while only reducing the sound insulation of the façade to road traffic noise by 2dB relative to the wall with no aperture. Quarter wave resonators were investigated by Field & Fricke (1998), and found that

6-7dB extra attenuation was achieved. The ability of Helmholtz resonators to target specific frequencies was used by Mao & Pietrzko (2010), tuned Helmholtz resonators reduced noise passing through a double glazing example window. The experimental investigation of active noise control applied to a double glazed window was reported by Jakob & Möser (2003). It was concluded that a noise reduction of between 3-7dB was possible depending on the set up.

A staggered window system that employed micro perforated absorbers was proposed by Kang & Brocklesby (2005), Figure 2.4 shows a representation of this system. The aim was to provide a combination of natural ventilation and daylighting along with good reductions of noise ingress. The theoretical background to the micro perforated absorbers was covered, including the acoustic absorption at frequencies of interest. This was related to the configuration of the micro perforations in the absorbers. The window system incorporating layers of the micro perforated absorbers between staggered glazing was tested in a semi-anechoic chamber. As well as the additional attenuation achieved from incorporating the micro perforated absorbers in different configurations, air-flow and light transmission measurements were taken. It found that the window system gave an average level difference of 28.9dB at 500-8000Hz, this could be increased further even when using additional standard un-optimised absorbers. Airflow through the system at normal rates did not appear to affect the noise transmission greatly. Light transmission was reduced with multiple layers of the micro perforated material but it was noted that in some cases this could be beneficial for the reduction of solar gains if overheating was an issue.

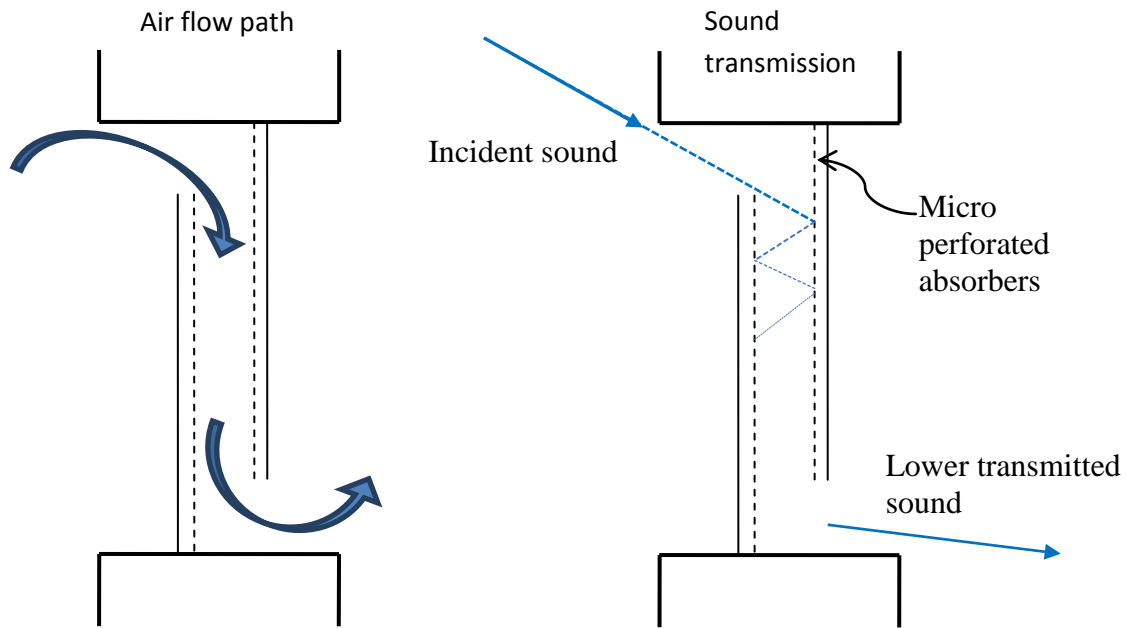


Figure 2.4. Air flow path and sound transmission representation of the staggered window system.

A parametric study was later carried out on the staggered window system to optimise aspects of the window system configuration (Kang & Li 2007). A FEM model was set up to replicate the test configuration and level differences calculated (Kang & Brocklesby 2005). In general an average level difference without absorbers of 20dB at 125-1000Hz was calculated for the window system, with further increases depending on the application of absorbers.

Calculations were also conducted with the staggered window system and louvres between the sheets of glass and with the inclusion of a hood outside the opening. It was found that the hood gave the better improvement in sound level difference. Computational fluid dynamics calculations of airflow at a number of pressure differences across the window system were conducted in 2D. These gave for example 2D flow of $0.014\text{m}^2/\text{s}$ to $0.061\text{m}^2/\text{s}$ at a pressure difference of 4Pa and an air gap of 240mm between the glass. From these simulations it was

concluded that this window system can meet the ventilation requirements for background ventilation and comfort.

To further increase the effectiveness of the window system, a combination of active treatments were also included into the window system in the work of (Huang 2011). An analytical model was developed based on the modal expansion method and validated using the finite elements method. The numerical calculations were also compared to a 1:2 scale physical model. Low frequencies were focused on in this work so the impact of the micro perforated absorbers is ignored as these have negligible effect at these frequencies. The analytical model assumed that the incident sound is planar and of normal incidence. This simplified the method and was considered appropriate as the road traffic source is usually several wavelengths from the window. The extra attenuation from the active noise control was found to be up to 20dB for 100-390Hz, suggesting a combined system could provide substantial attenuation of broadband sound such as road traffic noise. The reviewed studies show the range of attenuation noise reduction measures can provide. A mid-range noise reduction measure from those reviewed gave an attenuation of 20dB (Kang & Brocklesby 2005), this can be seen as 10dB extra, on top of the 10dB that an open window would, approximately, give (Hopkins et al. 2003). 10dB is therefore used as the example noise reduction measure in this thesis.

2.3.5 *Sound insulation*

The sound insulation of building construction materials is central to restricting the ingress of external noise into a building. Calculation methods are standardized by the International Organization for Standardization (ISO). Site measurement procedures are given in (ISO

1998), where the level difference between the source and receiving rooms can be used to give the apparent SRI. This physical test procedure is carried out in reverberation chamber test facilities. The requirements for the facilities are given in ISO 140-1 (ISO 1997) and the procedure for sound insulation testing is outlined in ISO 140-3 (ISO 1995). The SRI is defined as ten times the base 10 logarithm of the ratio of the sound power which is incident on a partition under test to the sound power transmitted through the specimen. This therefore gives a sound insulation value on the decibel scale, as more sound power is transmitted through the façade the SRI value reduces. This definition is used to define the sound insulation of the naturally ventilated façade in Chapter 4.

Information on material sound insulation is can be provided by the manufacturer in some cases (Oldham et al. 2005). As part of the acoustic design of schools guidance (Hopkins et al. 2003), the acoustic insulation values for a number of generic building materials are given to aid rough initial calculations. These have been assembled from a range of previous sources such as (DfEE 1975; Templeton 1993), and these values are used for this thesis. The intention was to update this information with averaged data for future generic construction materials. It was recommended that for non-generic construction materials sound insulation data would have to be obtained from the manufacturer. A related issue when looking at the acoustic insulating properties of different materials is their sustainability, Yu & Kang (2009) looked at this by considering the embodied and operational eco points of five residential building types.

Façades of building are usually composed of more than one construction type, for example the wall and the window, plus also a window opening if opened for natural ventilation. Ford & Kerry (1973) investigated the sound insulation of partially open double glazing for road

traffic noise and aircraft noise. A series of laboratory experiments were conducted for both horizontal and vertical sliding windows. It was found that the sound level difference for partially opened double glazing is in the region of 10dBA better than partially open single glazing. Openings and leaks significantly reduce the sound insulation of a material, this is the case for specialist acoustic enclosures, which was the subject of (Trompette et al. 2009), but also for building façades. Figure 2.5 shows the change in the enclosure acoustic efficiency as the opening area changes, this behaviour is due to the sound power that can be transmitted through larger openings. TL and SRI are similar quantities although SRI has a specific measurement procedure given in ISO 140-3 (ISO 1995).

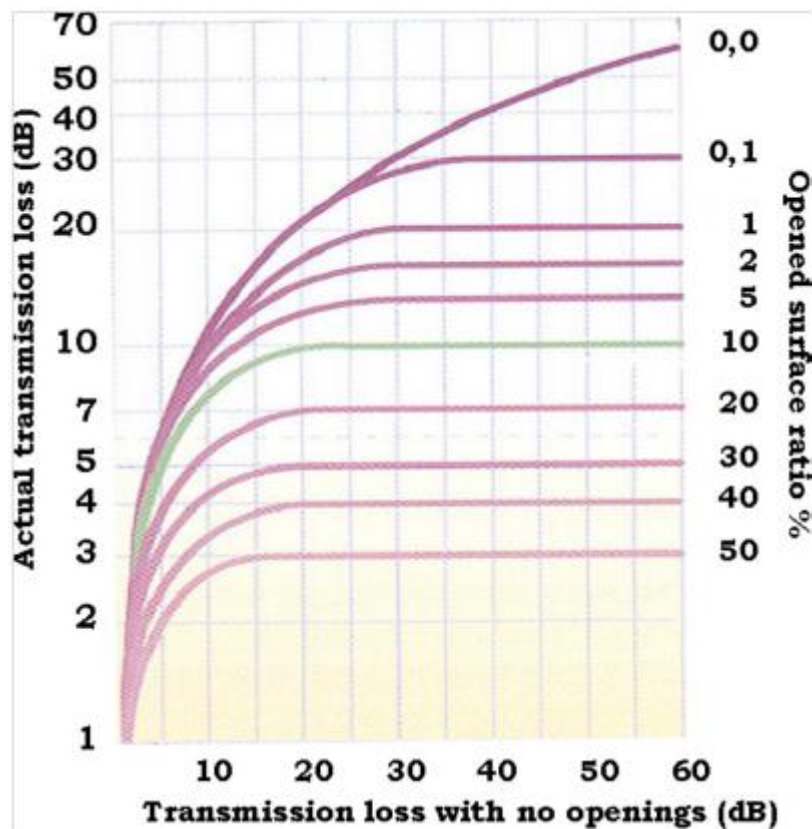


Figure 2.5. Maximum TL of an enclosure as a function of the opened surface reproduced from (Miller & Montone 1978).

A similar relationship to that seen in Figure 2.5 is implicit in the method of (De Salis et al. 2002; Oldham et al. 2004). In this study a combined sound insulation is calculated to create curves showing change in ventilation flow rate against sound insulation. The method used the SRI and relative areas, of each component, including the construction material and the ventilation aperture. The simplifying approximation of 0 SRI for the apertures at all frequencies is used. In practice the sound reduction varies with frequency and the geometry of the aperture. For apertures of small dimensions there can be substantial variation with frequency, determining the size of this variation is the aim of Chapter 4. This behaviour can be quantified by a number of methods including exact analytical formulae, simplified formulae and FEM and Boundary Element Method (BEM).

2.3.6 Acoustic Transmission Loss of Apertures

The calculation of acoustic TL through apertures in walls has been the subject of study for some time. Initially solutions for infinitely thin walls were developed, for example by (Bouwkamp 1941). When the assumption of an infinitely thin wall is not valid the solution becomes more complex. The exact solution for TL through a circular aperture in a wall of finite thickness was established by Nomura & Inawashiro (1960) although the method is complicated involving the evaluation of infinite series. The simplifying assumptions used also limited the range of frequencies and aperture dimensions that can be calculated from this method.

Additional approximate solutions have been produced that are more practical to use, (Gomperts 1964) produced an approximate method of calculation of the transmission coefficient of circular and slit shaped apertures in walls of finite thickness. Figure 2.6 shows

a representation of the circular aperture. This is done by relating the velocity potential in the aperture to the velocity potential of a spherical wave which is assumed to be transmitted from the aperture. The acoustic velocity is the gradient of the velocity potential. The transmission coefficient is then derived from trigonometric functions and end correction of a cylindrical tube from the aperture dimensions. The results for circular apertures were compared to the exact solution (Nomura & Inawashiro 1960), and with experimental results. This approximate solution was said to be of reasonable practical accuracy for $e/\lambda < 0.24$, where λ is the wavelength and e is the radius of the aperture (Gomperts 1964).

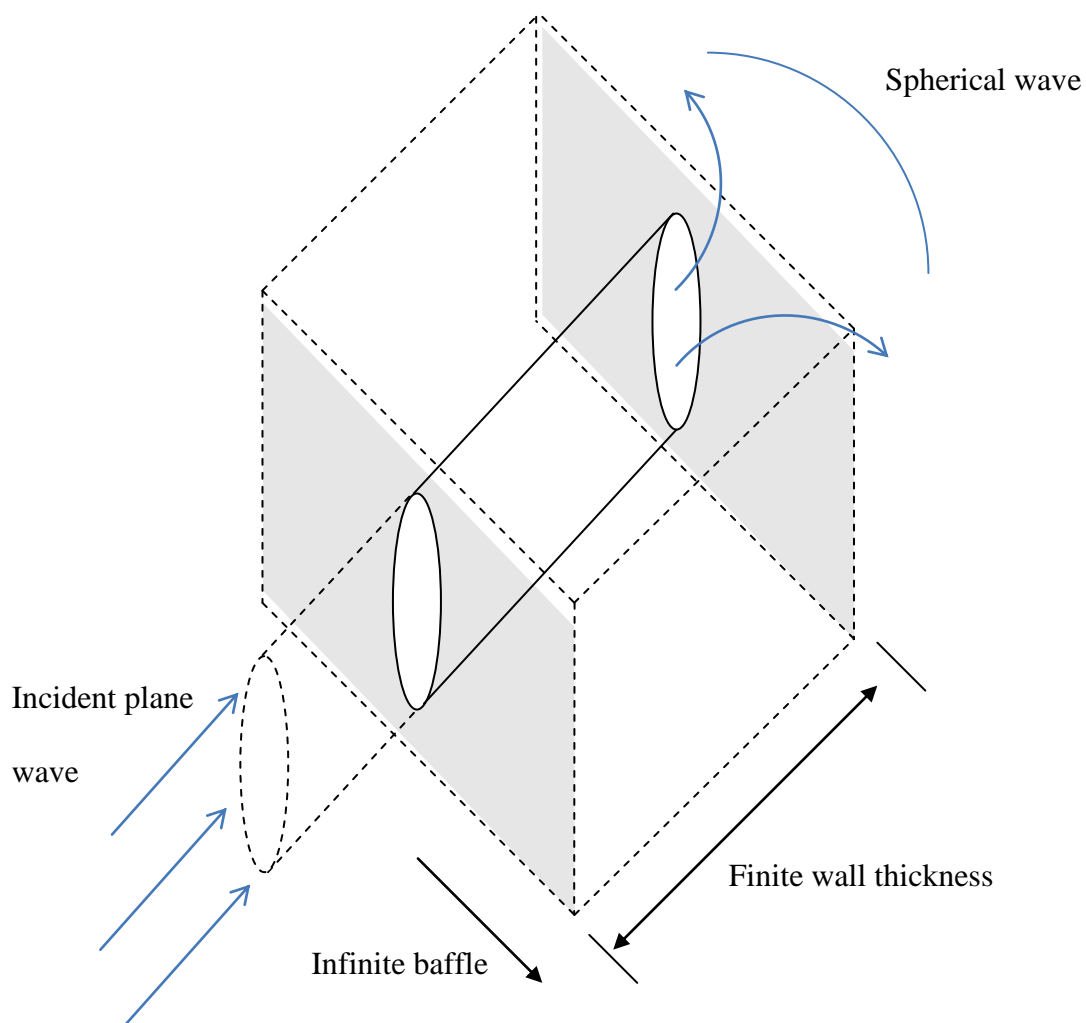


Figure 2.6. Representation of circular aperture sound transmission in a finite thickness wall.

(Wilson & Soroka 1965) developed a different method which assumes a plane wave propagating within the aperture and uses the impedance function of rigid weightless pistons at either end of the aperture. This coupled the internal conditions of the aperture with the external environment and was shown to compare well against the exact solution and experimental results (Oldham & Zhao 1993). The method assumes a plane wave within the aperture which was presumed to invalidate the approximate solution for apertures where the wavelength was shorter than the aperture diameter. Experimental results suggested wider usability with experimental results being found to be within 2dB of the plane wave dependant calculation for $e/\lambda=4.0$. The calculation approach was also extended to rectangular slit shaped apertures (Sauter & Soroka 1970).

The previously covered methods were included in a comprehensive review of aperture TL studies (Sgard et al. 2007), which had the aim of aiding the design of acoustic enclosures. In this study a general method to predict the diffuse field aperture TL was proposed and then compared to classic, mostly normal incidence, models. A diffuse sound field being where the sound has random angle of incidence rather than a clear direction such as normally incidence. A comparison of this new solution showed good agreement with the classic models, apart from Gompert's solution at higher frequencies. At their core, the previously reviewed models have an assumption of normal incidence of sound on the aperture. The diffuse field TL and normal incidence TL were compared for four different geometric configurations, two types of aperture cross-section and for the frequency range 100-5000Hz. The TL for normal incidence was consistently 2.2dB higher than for diffuse field TL for low frequencies (frequencies below about 1 kHz). The differences then tended toward 0 for the higher frequencies, this was the case for all the configurations (Sgard et al. 2007).

2.3.7 *Finite Element modelling of ventilation aperture*

The previous section reviewed derived approximate expressions for aperture TL (Gomperts 1964; Wilson & Soroka 1965), these have assumptions about the aperture dimensions incorporated into their formulation. A more flexible approach in terms of aperture dimensions is FEM, which has been used for some cases of ventilation opening sound transmission (Oldham et al. 2005; Kang & Brocklesby 2005; Huang et al. 2011). The FEM was used by (Huang et al. 2011) as part of the study of a staggered glazing window design with active noise control. Due to the heavy use of memory and long calculation time required to undertake FEM calculations at mid to high frequencies (for example 500Hz), an analytical model was developed. The effectiveness of their analytical model was then validated using FEM, with the Comsol simulation program (Comsol Multiphysics 2008). The source side was set up to represent an infinite baffle and the receiving side then represented a room. Both plane wave and point source excitations were modelled with discrepancies between the proposed analytical model and the FEM simulation found to be between 0.01dB and 1.39dB. This, they concluded, was sufficient to validate the analytical model.

FEM modelling of apertures and absorbers was conducted in the work of Oldham et al. (2005); this was done to establish the optimum configuration for ventilation apertures in relation to acoustic and air flow performance. The study concentrated on ventilation apertures in the building wall, the length of the aperture was determined by the depth of the wall (typically 200 – 450mm). Armafoam (expected to be representative of other open celled foams) was used for the aperture lining, the parameters of which were obtained from the manufacturer. The SYSNOISE simulation package was used for the acoustic FEM modelling and FLUENT was used for the CFD modelling of airflow. Figure 2.7 shows the SYSNOISE model used.

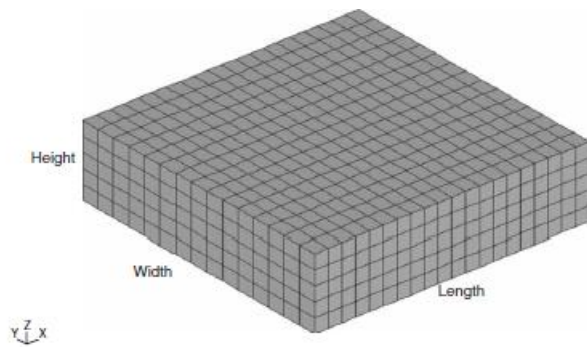


Figure 2.7. SYSNOISE model mesh (Oldham et al. 2005)

The SYSNOISE calculation was undertaken with a FEM rather than the BEM approach as although the results with both methods were similar FEM was said to be more appropriate to situations where sound could propagate within the porous material. It was recommended that for SYSNOISE, acoustics simulations with at least 6 elements per wavelength should be used (Oldham et al. 2005). The source was modelled as a plane wave incident on the aperture; this was done by prescribing the frequency of a vibrating panel on the source side. The outlet side was prescribed as an anechoic termination, anechoic meaning the full absorption of all sound and thereby eliminating reflections. The insertion loss of different geometrical configurations and absorbing liners was calculated. A variety of aperture dimensions were investigated and it was found that the aperture width did not have a large influence on the acoustic performance. It was concluded that these apertures could be treated as two dimensional devices with only height and depth being of importance.

In order to make the findings of the research of practical use for the optimisation of acoustic and airflow performance, sound insulation was described by single-figure values (Oldham et al. 2005). The acoustic performance is transformed into a single-figure value by using the method described in ISO 717-1 1997 (BSI 1997). The airflow characteristics were defined in

terms of their open or free area, which was determined by setting up a CFD model based on the standard test procedure for passive ventilators given in ISO BS EN 13141-1 (BSI 2004). It was found that for aperture heights greater than 40mm, the effective free area was similar but slightly greater than the actual cross sectional area. For reductions of aperture height below 40mm the effective free area then reduced much more rapidly. In contrast to the acoustic performance, increasing the aperture length had little effect. Oldham et al. (2005) concluded by noting that the sound reduction of the simple apertures was assumed to be zero for their study at all frequencies and that in fact reductions would occur due to the inlet and outlet. The calculation of the sound reduction across simple ventilation apertures will therefore be included in Chapter 4, where the combined sound insulation of a naturally ventilated façade will be calculated.

2.4 Conclusions

From reviewing the literature it has been concluded that the best way to represent whole-building thermal and ventilation behaviour is to use the software EnergyPlus and DesignBuilder, due to the mature nature and validation history of this software. Climate change projections have been incorporated into hourly weather data, so these can be used to drive the thermal building models. A comparison will be undertaken in Chapter 6 to enable a representative set to be assembled, which will be used in Chapter 7 to determine design implications. Work on the tensions between natural ventilation and acoustic comfort has been reviewed, showing the importance of this area. Previous work on linking the acoustic and ventilation performance of a façade has been covered and this will be extended to provide whole-building level results in Chapters 4 and 5. The availability of noise mapping for noise exposure information was identified. Approaches to sound insulation have been reviewed, including those for apertures, which will feed into the methods detailed in Chapters 4 and 5.

A mid-range noise reduction measure from those reviewed gave an attenuation of 20dB, this is 10dB extra, on top of the 10dB that an open window gives. It is therefore concluded that noise reduction measures that add an extra 10dB of noise attenuation are of medium effectiveness and this will be used as the example reduction measure in Chapters 5 and 7.

3 Methodology

This thesis spans a number of different scales in its aim of integrating and comparing different environmental factors affecting natural ventilation. These scales are both spatial and temporal. Different calculation methodologies have to be used for different scales as different physical processes and relationships are important, and also the requirements for accuracy differ. The linking of these different scales is necessary to answer the main question: determine what level of climate change a 10dB noise reduction measure would mitigate. The framework for the methods employed and the way they are linked is outlined in this chapter, with the details of individual methods then covered in the following relevant chapters. Table 3.1 illustrates which scales are relevant to which chapters and Figure 3.1 is a framework drawing showing how the methods at different scales fit together.

Table 3.1. Shows which thesis chapters deal with which scales.

Scale	Chapter
Climate scale	6,7
Urban scale	5,7
Building scale	5, 6 and 7
Aperture scale	4

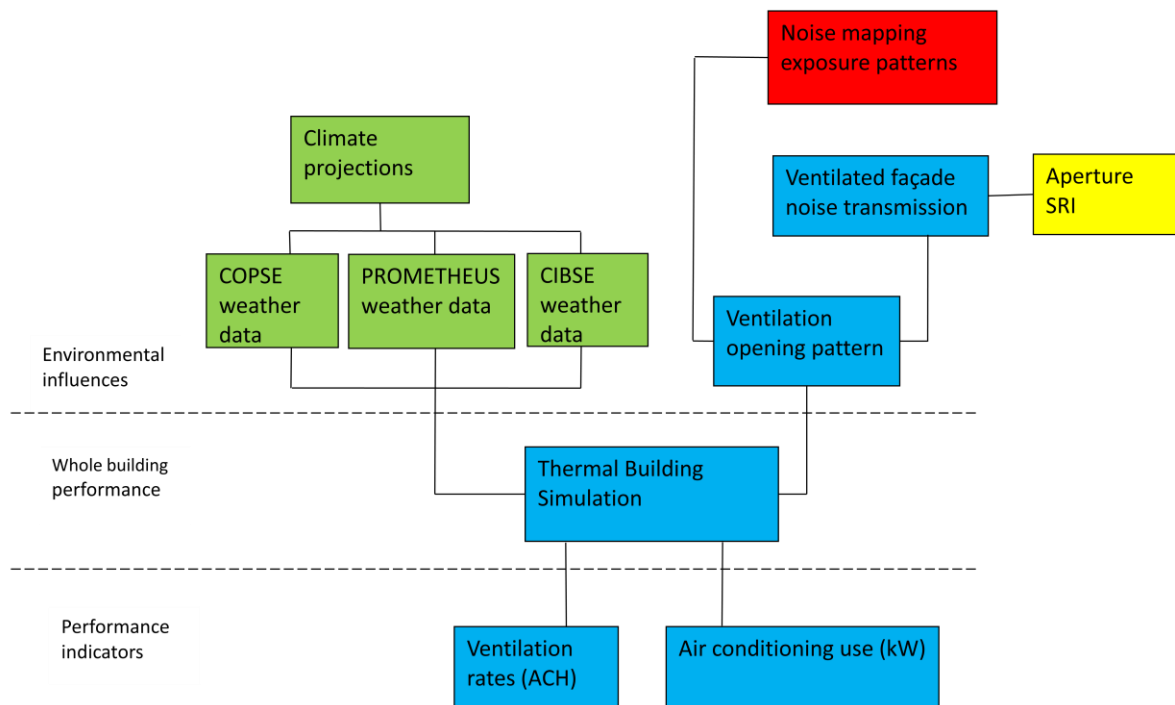


Figure 3.1. Framework showing how methods link together. Highlighting colour indicates the scale, with colours assigned according to Table 3.1.

The first section will outline how the largest climate scale is dealt with; the modelling of this is conducted globally, regionally and over many decades. This is linked to building energy modelling through the simulation weather data. Information about the local urban environment also feeds into building energy modelling through local micro climate effects such as sheltering from wind. This urban area scale is dealt with in Section 3.2, where noise mapping is a key tool used at this scale. Noise mapping is linked to the building scale by giving the noise exposure on the building façade. The whole-building scale is discussed in Section 3.3, many of the end results are produced at this key scale. These results give details of natural ventilation performance through thermal building modelling. The smallest scale considered covers the ventilation aperture and this is discussed in Section 3.4. This helps link the façade noise level, from noise mapping, to noise a building occupant would be exposed

to. The linking between the scales is an important part of the research presented here and enables the answering of the main thesis question.

3.1 Climate scale modelling output

The climate scale is the largest scale dealt with in this thesis and is both spatial and temporal and is central to the comparison conducted in Chapter 6. The information comes from global climate models of the atmospheric system which link to finer representation with regional climate models. By definition climate is the statistics of weather over 30 year periods. This kind of large scale modelling requires super computer resources and so is conducted by large specialist research groups. In this thesis the UKCP09 projections are used which draw predominately on the Met Office Hadley Centre climate models such as HadRM3. These projections give information about the changing climate in a wide range of forms due to the wide range of interested parties in such information. Examples are those interested in drainage, flood management, agriculture and tourism as well as built environment researchers.

All climate information used in this thesis needed to be processed into consistent hourly weather data in a format that could be used with the building scale modelling which is covered in Section 3.3. This enables the linking of the climate projections with building level ventilation. Two types of future climate information were used for this research, raw 11 member RCM data and processed stochastic weather generator data. Raw wind data was accessed through the BADC link project (BADC et al. 2008) giving 11 continuous daily modelled wind speed values from 1960 to 2099. Wind was extracted in this fashion as it is missing from UKCP09. As part of the extraction process, relative change needed to be

calculated. The morphing method (Belcher et al. 2005) was used with CIBSE weather files (CIBSE & Met Office 2009a) to produce building simulation weather data that had future wind changes included. This was done with a small BASIC program, the details of which can be found in Chapter 6.

Chapter 6 also includes the comparison of ready processed future hourly weather data sets which have been produced from published methodologies (Eames et al. 2011a; Watkins et al. 2011). These can immediately be used to drive thermal building models with little or no additional processing. Natural ventilation airflow characteristics and overheating metrics from a number of case study buildings were compared via this method. Wind was particularly focused on due to methodological differences in the production of the data for this variable. Future wind speed and direction data were analysed directly as well as its effect on building ventilation. This enables a range of future weather scenarios to be chosen that where in a format compatible with building thermal modelling. The chosen data sets were used to give design implications and compared with noise environment influences in Chapter 7.

There are a number of options when choosing weather data set these include: emission scenario, future time slice and probability level resulting in a large number of possible weather years. The aim in Chapter 7 is to use a representative range, but also keep the number of weather files to a manageable level. Data sets were ranked by average summertime temperature and then six were chosen that represented an even spread of summer temperature. Manchester is used as the location, due to the availability of weather data for this location, it also gives an alternative to London which has been the subject of many studies. Many aspects of the climate are adjusted by the local surroundings; two

examples are temperature which is adjusted by the urban heat island and the sheltering of wind. These are two important drivers of natural ventilation. Some local urban area effects are included in the UKCP09 climate data where some degree of urban heat island is included. Due to the coarseness of the 5km grid size this could only ever give a rough representation and so most local urban scale environmental effects are represented in other ways. Another example is wind which is affected by obstacles on the local urban scale.

3.2 Urban area scale

Consideration of the urban area scale is important to the conditions that individual buildings are exposed to. The urban area scale is here defined as a scale that covers one street to another or part of a city and takes into account surrounding buildings and other obstacles. One of the main effects on natural ventilation from the surrounding area is the change from the weather station wind speed to a reduced local wind speed that a building is usually exposed to. Wind measurements that go into the building simulation weather data are taken at open locations, whereas most buildings are situated in areas with significantly rougher terrains. A function that many building simulation software employ is to adjust the weather data wind speed according to the terrain roughness of the surrounding area.

In this thesis adjustments for local wind speed are made according to the ASHRAE method (ASHRAE 2009) as part of the calculation of wind pressure coefficients in EnergyPlus. A suburban terrain roughness is assumed which matches the terrain around the example location in Manchester. More details of the example location can be found in Chapter 5. As well as the availability of future climate data for this location, there was the availability of noise maps for Manchester from a study by (Wang & Kang 2011). Consideration of this urban area

scale is particularly important to determine the acoustic environment a particular building is exposed too. Noise maps show the uneven noise distribution due to urban noise sources and noise propagation paths. Their availability should increase as work for the EU directive progresses. A $500 \times 500\text{m}$ noise map of this area, south of Manchester city centre was used, the flatness of the area aided the noise mapping. Also the mapped area had a variety of possible noise exposure levels, so a noisy and relatively quiet location could be contrasted from the same noise map.

The external noise is linked to internal building acoustic conditions and whole-building ventilation rates through the ventilation openings. This is a key method developed in this thesis. The detail of the method linking noise mapping and building energy performance is given in Chapter 5. External surface dimensions of the three example buildings were added to the existing noise map and façade noise levels calculated in contour form. This was done to get the noise level at each window of the building. In this way the noise mapping results were linked to building level ventilation calculations to assess which environmental factor has the greatest influence on natural ventilation. The process of matching the surfaces of the building in noise mapping and building thermal simulation could in theory be automated. This would make the integration of the two types of simulation much more efficient for the end user but would require some coordination between the two fields.

3.3 Whole building scale

The whole-building scale is a central scale for this thesis. It covers aspects of building behaviour that happen within the building envelope. Many of the key results reported in Chapters 5, 6 and 7 are from this scale. One of the main focuses of these results is the thermal

behaviour of the building as a whole. Whole building thermal behaviour is now usually calculated with thermal building models, these are used by building services engineers to determine whether mechanical cooling is required. They are also increasingly used by architects to give an early indication of the energy use and comfort consequences of building form decisions. The wide use of such building models means that their results in themselves have an effect on the built environment and are therefore of interest. This is the case even before the accuracy is considered, and is why, for many of the final results building thermal simulation outputs are used.

In building thermal modelling a building is split up into thermal zones, with the models used in this thesis, where each room was treated as a separate thermal zone. The timescale used for the simulation of building thermal physics is covered with time steps of several minutes. This is sufficient to describe dynamic thermal flows and allow full years to be simulated without excessive computational expense. The well validated thermal modelling software EnergyPlus (Henninger & Witte 2009), was used to give natural ventilation information and is the source of the main results in Chapters 5 to 7. EnergyPlus version 6 is used throughout this thesis to ensure consistency of the results. The production of the example models given in Chapters 5 and 6 was aided by the software DesignBuilder and the EnergyPlus Sketchup plug-in, OpenStudio. The example models were all of office building and had a representative range of forms and constructions.

As well as a solely naturally ventilated cooling approach, mixed mode was used in Chapters 5 and 7. Mixed mode zones are naturally ventilated until an operative temperature of 26°C is reached, the zone then changes over to a fan coil cooling system (this is explained in section

5.2). The method for interpreting results from these thermal model outputs was to focus on some key performance indicators. To interpret the airflow characteristics of the example building, the number of ACH was used. Both room-level and building-level were used. Thermal comfort was interpreted by looking at the percentage of hours over a thermal comfort threshold temperature; more details on the two thresholds used are given in Chapter 6. The average electrical energy used by the mixed mode cooling system through the summer was also used.

Natural ventilation calculations take significantly longer to run compared to the thermal models where airflow is not given by pressure network calculations. Each model can take from between 10 minutes and 2 hours to calculate for a summertime period, depending on the size of the example building. Large sets of model outputs are needed to represent the range of environmental influences affecting the example buildings. To represent a range of future weather data, up to 27 different weather files (from CIBSE, COPSE and PROMETHEUS data sets) were run with each example building. Up to six model runs were needed to show the change in ventilation with noise tolerance for a single location. Each of these building models had a different window opening pattern, determined by the noise exposure. Running these large numbers of thermal models manually can therefore be a laborious undertaking. To aid the running of batches of models EnergyPlus has a batch simulation tool that allows a list of models to be described with solutions written out to different paths. A batch can be left to run without any further user input. To speed up the modelling further each model can be run simultaneously on each core of a multi-core processor.

Output from the batches of model runs are hourly values of chosen variables, such as operative temperature or electrical energy use. These need to be processed and plotted to produce the results reported in the following chapters. A custom BASIC script was developed to read and process the output from the batch simulations. An example of the processing needed is described for the production of average occupied summertime chiller electricity use. First, the occupied summertime periods needed to be found and then the chiller electricity at these times (given as W at each hour) was averaged and converted to kW. A similar procedure is used to produce the other outputs from Chapters 5, 6 and 7. The customisable post processing script also enabled non-standard performance indicators to be used. For example, in Chapter 6 the percentage above adaptive comfort threshold temperatures could be calculated, this is not currently possible with post processing from the thermal simulation software packages due to the adaptive comfort methodology still being the subject of research and not yet widely used in industry.

For most of the results it was thought most appropriate to use the following statistical measures: mean values, standard deviation, correlation coefficients, and linear regression gradients. These were calculated from Excel or open office calc spreadsheet software, which were also used for plotting graphs. This level of statistical analysis was considered appropriate to analyse the results derived from deterministic thermal building models. Further statistical analysis was restricted to results dealing with the weather data sets in Chapter 6. Here, due to the stochastic representation of the weather variables, the calculation of statistical significance (p) was appropriate. This was calculated with the statistical software package R (R Development Core Team 2011).

In building natural ventilation models the opening area is usually defined by the types of windows. The method developed in Chapter 5 links whole-building ventilation behaviour and acoustics with the use of a tolerated noise level, this describes at which level occupants would reduce window opening due to the ingress of noise. Different tolerated levels, resulted in different opening patterns, depending on the uneven noise exposure from the urban surroundings, here determined by noise mapping. This required the matching of façade surfaces between noise mapping and building thermal models. To link the noise mapping and ventilation calculations in Chapter 5 the concept of a tolerated noise level is used. Tolerated noise level is the noise level that occupants would tolerate before closing the ventilation openings to reduce noise ingress. A range of noise tolerances produces a range of ventilation opening patterns each needing a separate building model to describe the corresponding natural ventilation behaviour. A good description of noise transmission through ventilation openings is needed to determine what level of noise building occupants are exposed to.

3.4 Ventilation aperture scale

To enable the calculation of sound transmission through the ventilation openings, the area and geometry of the opening should be taken into account; both affect the level of noise transmitted through the building façade. The opening geometry is important as the transmission of sound is dependent on the opening dimensions and the frequency of sound being transmitted. The ventilation aperture scale is the smallest considered in this thesis, spanning 10s of mm. Calculations at this scale require the consideration of sound as a wave phenomenon as described by the wave equations. The openings from the example buildings in Chapter 5 are from sliding windows, the size of which determines both the air flow and acoustic transmission of the façade. The ventilation aperture scale is therefore important to linking the urban area noise exposure to whole-building ventilation.

In this thesis natural ventilation air flow through the opening was calculated as part of the thermal building simulation results. The acoustic transmission was calculated by the FEM described in the following chapter, Chapter 4, rather than derived expressions for generic apertures such as by (Gomperts 1964). The software COMSOL (Comsol Multiphysics 2008) was used to build, run and post-process the aperture models. The method used was first validated by a comparison with the method by (Wilson & Soroka 1965). A BASIC program needed to be written to calculate the infinite series terms that were part of the Wilson and Soroka expression. After validation, a number of ventilation aperture models were run with different opening widths and tuned for different portions of the acoustic spectrum. The aim was to gain acoustic TL, which is sound level drop due to the presence of the aperture, rather than an open field. These values could then be combined with façade construction material sound insulation values to give the combined sound insulation of the naturally ventilated façade needed for Chapter 5.

3.5 Conclusions

In this chapter four relevant scales have been identified that need to be modelled with different approaches. The whole-building scale is identified as the central scale with results and data from aperture sound transmission, noise exposure from noise mapping and climate weather data feeding into the whole-building thermal performance at this scale. Results from whole-building EnergyPlus simulation gave the performance indicators of natural ventilation flow rate, overheating and mixed mode chiller use. These performance indicators make up many of the results presented in the following chapters and enable the aims of the thesis to be met. Although the method outlined here can seem quite cumbersome there is a potential for automating much of the linking procedure, also the use of existing information sources means the process could be efficient and worthwhile.

4 Numerical modelling of ventilation apertures

The ventilation apertures used in building energy modelling are an acoustic weak point in the façade of a building. In Chapter 5 thermal building models are used with natural ventilation openings created by the operation of horizontally sliding windows, these are long thin slits. In order to establish the effective sound insulation of the façade the sound transmission of these slits has to be taken into account and combined with the sound insulation of the other components of the façade. Acoustic insulation values for construction materials can be obtained from manufacturers and design guidelines; these have usually been established through physical testing. The SRI of the aperture is sometimes assumed to be zero at all frequencies although, in fact, this is not the case. The exact sound transmission changes with frequency and is difficult to determine accurately as it depends on the aperture dimensions. Finite element approximation will be used in this chapter as it is difficult to calculate exact analytical solutions due to these methods having restrictions on the dimensions and frequency range that a solution can be calculated for.

The aim of this chapter is to determine accurately and in detail the SRI of representative ventilation apertures by numerical simulation. These values are then combined with the façade construction material values. The result of this will be the effective sound insulation of a section of facade which will be used to combine natural ventilation and acoustic performance of buildings (Barclay et al. 2012). As the dimensions of the aperture are dependent on the degree of window opening a number of aperture sizes will be used relating to DesignBuilder models from Chapter 5. Section 4.1 details the aperture dimensions that will be investigated. The finite element model of the aperture was set up with COMSOL (Comsol Multiphysics 2008) and background to the numerical simulation methods employed will be

covered in Section 4.3. A validation of the adopted numerical approach is presented in Section 4.5, after which the results for ventilation aperture are combined with the façade materials in Section 4.7.

4.1 Ventilation aperture dimensioning

A common configuration of the ventilation apertures which make up the airflow network component of the EnergyPlus thermal building models is a vertical slit. This is formed from a horizontally sliding window. Windows used in the building models presented in Chapter 5 have dimensions auto-generated with DesignBuilder (DesignBuilder Software Ltd 2009). The dimensions of the ventilation apertures are therefore dependant on the software's auto generation process. The DesignBuilder software package has a number of ways to define the window dimensions; the models produced for this thesis employ the preferred height method. With the preferred height method a standard height, standard separation and percentage glazing are defined and then the exact window dimensions are auto-generated by the software. All the example buildings used in Chapter 5 have a standard height of 1.5m, a standard separation of 5m and a percentage glazing of 30%. These values were similar to the DesignBuilder examples and were considered representative. The opening of the windows is defined by the percentage of glazing which opens and this can be set in 1% increments, the largest percentage opening used in Chapter 5 is 5%. This is now sufficient information to give the widths of all the ventilation apertures that the example buildings will use. The window frame thickness is also important to the TL of an aperture as it defines the aperture depth. A frame thickness of 100mm is adopted for all the windows.

This then results in the dimensions of the aperture being defined as a 1500mm long slit with a depth of 100mm and opening width dependant on the degree of window opening. The basic method for describing window ventilation opening areas in the DesignBuilder modelling tool is to prescribe the percentage of glazing that opens for each window. For the building model windows in Chapter 5 this is between 0% and 5% open. The level of opening chosen for each window will depend on the sound exposure by a method given Chapter 5. In addition, whether the window is open at all will depend on the standard natural ventilation temperature controls (24°C set point temperature) and occupation schedules following office hours. The possible opening widths increase from 0mm to 200mm in 5 equal 40mm increments. The unsuitability of the standard approximate solutions for these dimensions is a reason why finite elements will be used in this chapter to determine sound transmission.

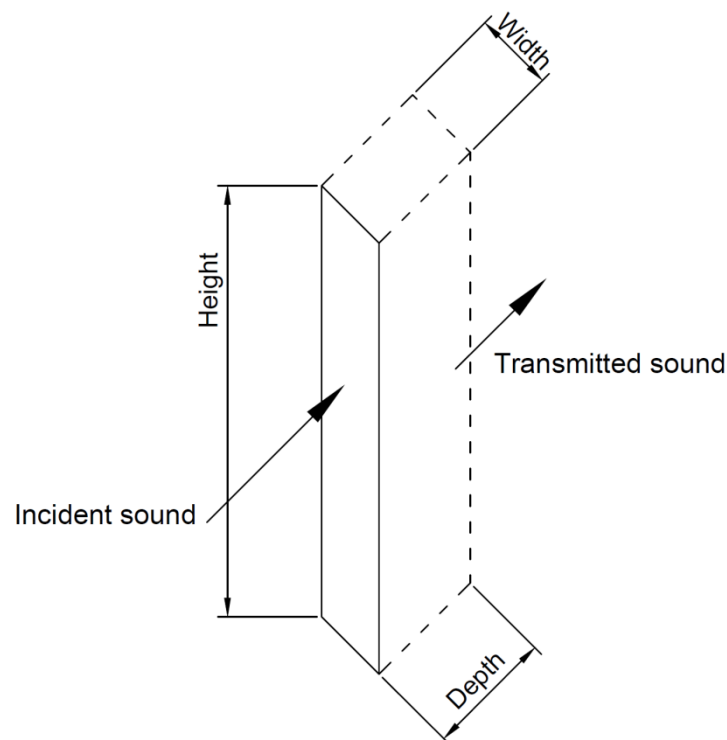


Figure 4.1. Window aperture configuration.

4.2 Sound transmission of façade panel

The physical test procedure to calculate the sound transmission of a construction component specimen is outlined in ISO 140-3 (ISO 1995). This procedure is carried out in a reverberation chamber with sound power on either side of the façade panel being measured. The sound insulation property is often given in terms of SRI or a similar unit and is defined as ten times the common logarithm of the ratio of the sound power which is incident on a partition under test to the sound power transmitted through the test panel. This SRI test procedure assumes random incidence of the source and the conventional use of the term SRI therefore suggests measurements taken with a diffuse source field.

Figure 4.2 shows the TL for an aperture with three different source types, normal plane wave incidence, oblique plane wave incidence and a diffuse source field. The Mechel slit calculation method and a new calculation method is compared for different source conditions (θ). The x-axis is in terms of the wave number (k_0) which is equal to $2\pi/\lambda$. It can be seen from the results that the difference in TL due to the source condition is 1dB or less (Sgard et al. 2007). 1dB or less is small enough to not significantly affect the results reported in this study, as it is not audible. The model used later in this chapter to calculate the TL of the ventilation aperture has a source with normal incidence. Due to the insignificant effect of source condition, it is concluded that the TL of apertures with normal source incidence can be described as the aperture SRI (SRI_A) this is ten times the log of the ratio of sound power incident on the aperture to sound power transmitted through the aperture. SRI_A can be used along with construction material SRI values to give the combined SRI of the façade.

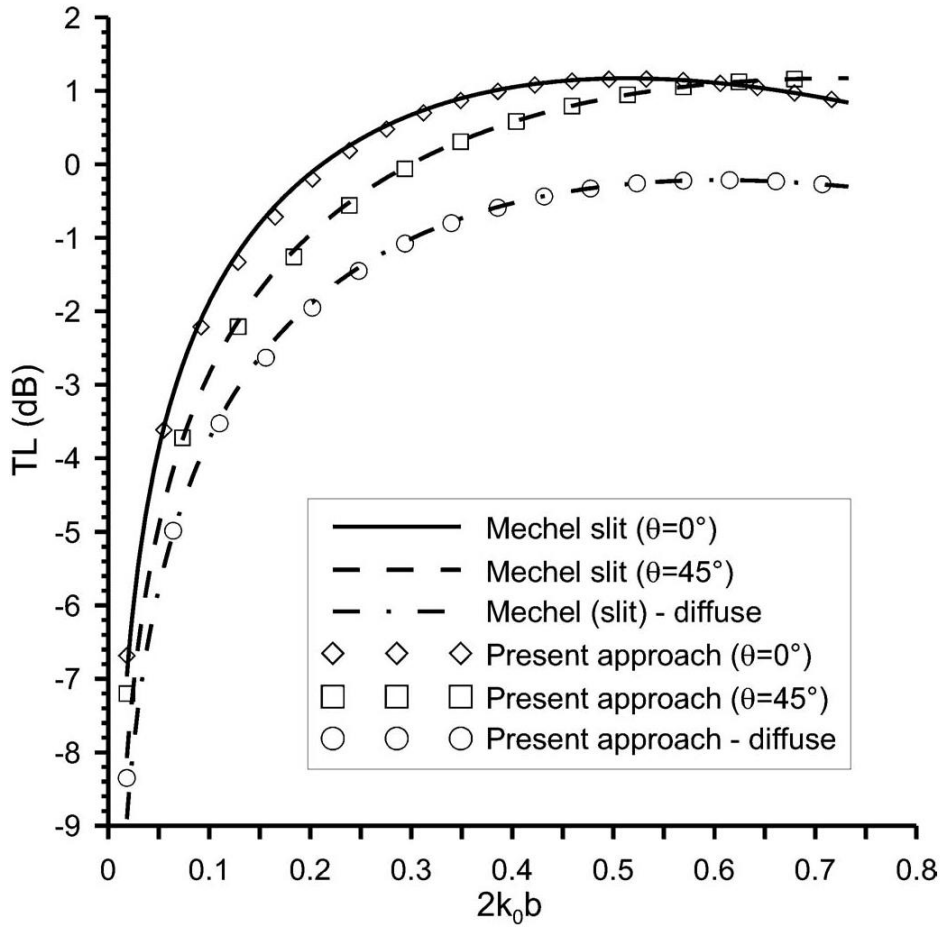


Figure 4.2. TL of a slit for normal plane wave incidence ($\theta=0^\circ$), oblique plane wave incidence ($\theta=45^\circ$) and diffuse incidence. Where k_0 is the wave number and b is the aperture height. Reproduced from (Sgard et al. 2007).

The same calculation used to calculate construction material SRI is here extended to calculate the SRI_A of apertures created in a building's façade by the opening of a window. SRI_A is generally significantly lower than for solid facades as there is little to interfere with the sound wave, but it is not zero for all frequencies. An expression for SRI_A is given formally by equation (4.1).

$$SRI_A = 10 \log_{10} \left(\frac{1}{r} \right) \text{ dB} \tag{4.1}$$

$$r = \frac{W_0}{W_i} \tag{4.2}$$

where r is the transmission coefficient, which is the ratio between energy incident on the aperture $W_0(W)$ and energy transmitted through the aperture $W_t(W)$. When $r = 1$, $SRI_A = 0$, indicating that all the acoustic energy incident on the aperture passes through to the receiving side.

In previous studies SRI_A was assumed to be zero for all frequencies (De Salis et al. 2002; Oldham et al. 2004), but resonance and anti-resonance cause the SRI to change periodically with frequency. Negative values of SRI_A represent the cases where more acoustic energy passes through the aperture than is directly incident on its opening area - this was observed in the experimental results of Oldham & Zhao (1993). The frequencies at which this occurs depend on the aperture width and depth and is due to a reflected wave issuing from the aperture entrance. As part of the development of this approach for this chapter the frequency-dependant sound transmission of the apertures will be calculated.

A number of methods that describe the sound transmission through an aperture in terms of the aperture dimensions. For circular apertures in a wall of finite thickness and for normal incidence of the sound source, an exact mathematical solution for sound transmission has been given (Nomura & Inawashiro 1960). This exact solution is complicated and so more practically useful approximate solutions have also been developed (Gomperts 1964; Wilson & Soroka 1965). These approximate solutions show good agreement with the experimental results for circular apertures up to values of $e/\lambda < 0.24$, where λ is the wavelength and e is the radius of the aperture (m). There does not appear to be an exact solution for sound transmission through slit shaped apertures, although Gomperts does suggest an approximate solution that matches the experimental results with acceptable accuracy for some cases

(Gomperts 1964). Oldham and Zhao found that this approximation fitted the experimental results to within 1.5dB for $d/\lambda < 0.32$, where d is the width of the slit aperture (m) (Oldham & Zhao 1993).

Some of the range of opening widths and frequency ranges that are useful to determine the attenuation of road traffic noise lie outside this d/λ condition for the approximate solutions so numerical techniques are adopted in this thesis which can have a wider range of solutions. Another issue is that the approximate solutions are for a continuous slit whereas the building model apertures have a height of 1500mm. Also numerical techniques present the possibility of investigating apertures with geometries more like those found in practice. They also give the opportunity to incorporate the noise reduction impact of absorbing materials.

A distinction is made between the approximate methods, mentioned previously, which derived approximate equations that are simplifications of the fundamental problem of sound transmission through apertures in walls of finite thickness and numerical methods such as the FEM. The numerical solution of the wave equations gives the acoustic wave propagation through the aperture. The FEM approximates the acoustic pressure at the mesh nodes and these pressures can be used to calculate the required energies to determine SRI_A from equation (4.1). This is done by calculating the following integrals of pressure over the relevant surface. For equation (4.3) p_0 is the prescribed acoustic pressure source at the surface directly in front of the aperture entrance. The plane wave source with normal incidence travels through this surface; this represents the energy incident on the aperture. Equation (4.4) uses the summation of pressures p at the aperture exit to calculate the energy transmitted.

$$W_0 = \int_{\delta\Omega_0} \frac{p_0^2}{2\rho c} dA \quad (4.3)$$

$$W_i = \int_{\delta\Omega_i} \frac{|p|^2}{2\rho c} dA \quad (4.4)$$

where ρ ($\text{kg} \cdot \text{m}^{-3}$) is the density of air and c is the speed of sound in air ($\text{m} \cdot \text{s}^{-1}$), $\delta\Omega_0$ is the surface directly in front of the aperture entrance, $\delta\Omega_i$ is the surface at the aperture exit.

Equations (4.3) and (4.4) show how the ISO definition of SRI used for the measurement of acoustic insulation can be expressed in terms of acoustic pressure. This can be the dependant variable of a finite element formulation and with nodal approximations of acoustic pressure calculated at the relevant surfaces the SRI quantity can be calculated. In the next section some background will be given on how this finite element formulation is derived.

4.3 FEM acoustic simulation

As was shown previously the opening sizes of ventilation apertures are not within the appropriate range for derived methods (Gomperts 1964; Wilson & Soroka 1965). For this reason the FEM was used to calculate the acoustic transmission of apertures. In this section the fundamentals of acoustic simulation with the FEM is presented to illustrate why this method offers flexibility with geometry. Derived methods needed to incorporate assumptions about the problem geometry into the formulation and this limits its applicability. Splitting the geometry up into elements and applying a formulation of the governing wave equations over a discretized domain, FEM avoids these limitations. This also illustrates the cause of some challenges such as the computational expense of building such models. By showing the fundamental formulation, this section also demonstrates how the validation exercise (Section

4.5) conducted on a small circular aperture also applies to the larger ventilation apertures which are the main results of this chapter.

The starting point for the calculation of acoustic pressure is the governing wave equation which comes from the conservation of mass, momentum and energy. For most acoustics cases perturbations are several orders of magnitude smaller than the equilibrium values of the medium. This is certainly the case for road noise impacting buildings, which is the focus of this thesis. The basic wave equation describing the propagation of acoustic over pressure in a stationary medium is given in equation (4.5). As pressure differences are small, sound is very nearly an adiabatic phenomenon so damping terms can be ignored.

$$\nabla^2 p - \frac{1}{c^2} \frac{\partial^2 p}{\partial t^2} = 0 \quad (4.5)$$

where c is the speed of sound in air ($\text{m} \cdot \text{s}^{-1}$). To simplify this relationship further we can concentrate on the special case where a stable time harmonic wave varies with time according to equation (4.6). The harmonic response results from a harmonic excitation and is a common simplification if transient effects are not important as can be assumed for the case of steady background road noise. The harmonic response results can therefore be used to determine road noise sound transmission through the ventilation apertures.

$$p(x, t) = p(x)e^{i\omega t} \quad (4.6)$$

where ω is the angular velocity which can also be expressed in terms of frequency f in Hz as follows, $\omega = 2\pi f$.

This means that the wave equation can be written in the inhomogeneous Helmholtz form as shown in equation (4.7). Time can be eliminated from the equation and instead ω becomes a

parameter. As the pressure is now a known function of time, a solution can be calculated for a single frequency. To find the solutions across the portion of the spectrum that is of interest a separate solution needs to be calculated with a different harmonic load. In COMSOL this can be automated by sweeping over a number of frequencies with the parametric solver.

$$\nabla^2 p - \frac{\omega^2 p}{c^2} = 0 \quad (4.7)$$

The stationary solver used for the modelling presented in this chapter uses a type of weighted residual method to arrive at a robust approximate solution. To illustrate the weighted residual method the governing equation (4.7) is represented in the very compact and general form of equation (4.8) using $L(\cdot)$ to represent the differential function acting on the real solution (u). If the approximate solution (\hat{u}) is sought it introduces an error called the residual R_Ω which is the difference between the real (u) and approximate solution.

$$R_\Omega = L(\hat{u}) - L(u) \quad (4.8)$$

R_Ω is dependent on the position in the domain, so to reduce the residual overall, this method requires that an appropriate number of integrals of the residual, weighted in different ways, be zero (Zienkiewicz & Morgan 1983). The solution is sought that satisfies equation (4.9).

$$\int_{\Omega} w_i (L(\hat{u}) - L(u)) \, d\Omega = 0 \quad (4.9)$$

Where w_i is the weighting function and in the popular method of finite element formulation called the Galerkin method this is taken to be an arbitrary or virtual function ϕ that incorporates the element shape functions N as follows $\phi = \sum_{i=1}^n \psi_i N_i$ with ψ as arbitrary coefficients that satisfy the boundary conditions (Chandrupatla & Belegundu 2001).

Shape functions are central to how the physics of the problem can be spread over the elements. By building up a mesh of elements, the geometry of the ventilation aperture can be formed while still retaining a sound description of the physics of acoustic wave propagation.

Figure 4.3 shows an illustration of shape functions N .

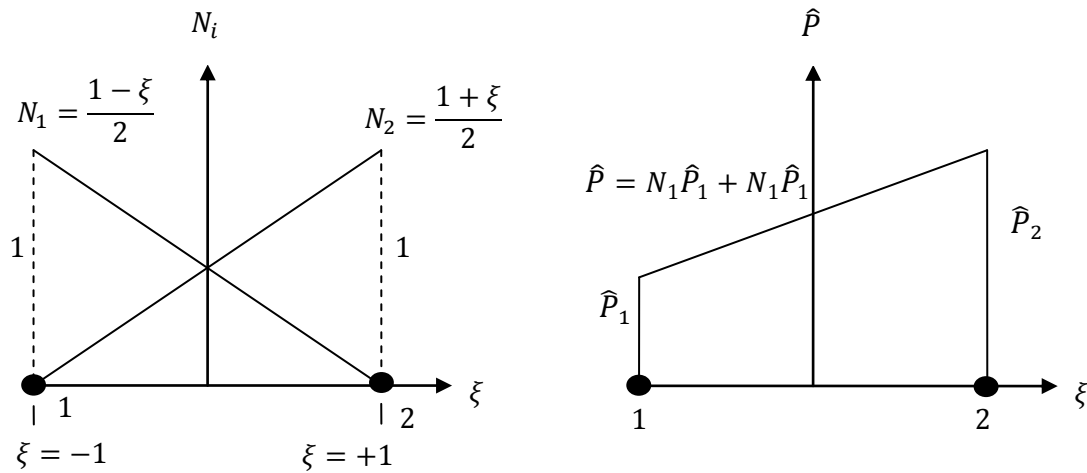


Figure 4.3. Illustration of linear shape functions and the interpolation of the approximate solution for acoustic pressure.

where \hat{P} is the approximate acoustic pressure, ξ is the unit of the natural coordinate system which is relative to the centre coordinate of the element. The example in Appendix A illustrates a simple one-dimensional case. The one-dimensional example is focused on for conciseness but the principles presented can be extended for more dimensions, for the ventilation aperture a three-dimensional model is produced. The approach is to use the Galerkin method to convert the problem into a linear system of equations that will yield to computer processing. The final system of equations is given in equation (4.10).

$$\mathbf{K}\hat{\mathbf{P}} - \frac{\omega^2}{c^2}\mathbf{M}\hat{\mathbf{P}} = \mathbf{F} \quad (4.10)$$

where \mathbf{K} is the global stiffness matrix, \mathbf{M} is the global mass matrix and \mathbf{F} is the global force vector. This can now be solved for $\hat{\mathbf{P}}$. If greater accuracy is required then higher order

elements can be used meaning that the shape functions are higher order polynomials which can better approximate the solution over the domain. In return additional processing is needed to arrive at a solution. One-dimensional elements are too crude to properly represent the geometry of many real world problems. In order to properly describe the ventilation aperture, the problem geometry is built up with four node tetrahedral elements which also had quadratic shape functions. Essentially the same Galerkin method can be extended to the three-dimensional case. This forms the bases for the results in this chapter. For example the following would need to be satisfied.

$$\int_V \phi \left[\frac{d^2 \hat{p}}{dx^2} + \frac{d^2 \hat{p}}{dy^2} + \frac{d^2 \hat{p}}{dz^2} + \frac{\omega^2}{c^2} \hat{p} \right] dV = 0 \quad (4.11)$$

This expansion would be extensive and the introduction of the more complex three-dimensional shape functions for tetrahedral elements would also increase the complexity, but essentially the same procedure as shown previously would be used. The formulation would lead again to $[\mathbf{K} - k^2 \mathbf{M}] \hat{\mathbf{P}} = \mathbf{F}$ but where \mathbf{K} and \mathbf{M} are assembled from larger element matrices. The use of four node tetrahedral elements would mean $\mathbf{k} = V_e \mathbf{B}^T \mathbf{B}$ is assembled from 6×12 element B matrices and the element mass matrix would be a symmetrical 12×12 matrix and V_e is the element volume. The steps shown in this section have demonstrated how the governing wave equations and problem boundary conditions can be formed into systems of simultaneous equations based on element connectivity. These can be assembled into matrices and solved globally.

As has been shown the finite element approach is robust in terms of its physical representation of the wave phenomena. It is more flexible than the derived expressions in terms of the geometric configurations and the ability to introduce absorbing materials (Oldham et al. 2005). The reasons for this flexibility have been demonstrated in this section

by showing the way the governing wave equations are spread over the problem domain by the connectivity of the elements. This is why it has been used for the calculation of aperture SRI. It has been necessary to show this background to FEM so that it is clear that the validation exercise (Section 4.5.1) also applies to other configurations. The validity of the larger ventilation aperture models can be inferred from the positive results for the smaller circular aperture. One of the main issues affecting accuracy of FEM is mesh quality. This had to be carefully considered due to resolution of the waves and the effect on computational expense.

4.3.1 Meshing of the domain

The method described earlier requires the problem geometry to be split up into a mesh of small units or elements that have a simple shape. This needs to be generated so that the geometry of the domain is as faithfully represented as possible. A finer mesh with a larger number of smaller elements tends to produce a more accurate approximation. It should be remembered, though, that an excessively fine mesh increases the degrees of freedom of the model and thereby increases the sizes of the global matrices that need to be solved, for example those in equation (4.10). The computational resources needed to compute a solution are dramatically increased with larger degrees of freedom and so if there is a limit to the resources required, this needs to be avoided. The same is true for all finite element models.

Acoustics finite element simulations also have an element size requirement that relates to the acoustic frequency. The acoustic pressure waves have to be sufficiently resolved to ensure that the gradient of the variable solved for is not too large over one element. This is particularly important for lower order elements. The guidance for this suggests not having

less than 6 elements per wavelength (Oldham et al. 2005). This dictates the maximum element size relative to the highest frequency that is modelled as part of the parametric sweep. The meshing of the model in this Chapter was undertaken with the meshing tool in the simulation program COMSOL. This has a number of parameters that can be defined to control mesh generation size and quality. Models run for frequencies of 1000Hz had a mesh with over 700 000 degrees of freedom. For the computers used (Viglen Genie I5 Quad Core, 4gb Ram), this resulted in over 24 hours of computer simulation time. Further increases in the degrees of freedom would have made the simulation impractical so changes to the model were made to ensure degrees of freedom kept to about 700 000.

4.3.2 *Boundary definition*

Boundary conditions are important to achieving valid results and take some careful consideration. There are a number of ways of representing the acoustic boundary conditions. The approaches used in this chapter are the sound hard condition, perfectly matched layer (PML) and a prescribed pressure source. The boundary conditions are often expressed in terms of the particle velocity (velocity due to the acoustic wave); the normal component of which is zero for particles at a hard boundary, so the following is true:

$$\mathbf{N} \cdot \frac{\nabla p}{\rho_0} = 0 \quad (4.12)$$

where \mathbf{N} is the vector normal to the surface, p is acoustic pressure (Pa) and ρ_0 is the air density ($\text{kg} \cdot \text{m}^{-3}$).

A pressure source is where the acoustic pressure p_0 is specified. For the time harmonic calculations that are conducted in this chapter this acoustic pressure is the amplitude of the source pressure wave. The PMLs are a way of modelling infinity boundary conditions, that is,

waves travel into the region but do not reflect back into the physically representative part of the model. With PMLs, a volume is meshed and given absorbing properties that are tuned to absorb all reflections.

4.4 Ventilation aperture finite element model set up

The ventilation aperture described in Section 4.1 was simulated with models set up in the COMSOL pre-processor. The models were set up to represent a normal incident plane wave acting on an infinite area of wall with a finite thickness of 100mm and incorporating a regular aperture. A plane wave was introduced at one side of the model with its direction incident on the wall with the aperture. The wall and internal aperture surfaces were represented as fully acoustically hard. Then areas on the source side and receiving side that represented infinity conditions were modelled with PMLs. This set up is shown in Figure 4.4. The assumption of a normal plane wave impacting on the aperture was considered appropriate given the needs of this investigation, particularly as the road traffic source would be at least several wavelengths away from the window in any case. This is also the boundary assumption used in the Wilson-Soroka method.

By using equation (4.1), and the model illustrated in Figure 4.4, SRI_A can be calculated. It should be remembered that according to Figure 4.2 SRI_A can be assumed to be the same as the aperture TL. The apertures modelled with this technique corresponded to the ventilation openings of the building models described in Section 4.1, this model replicates air borne acoustic transmission through the ventilation aperture and therefore the model domain represents the air volume surrounding the building. some of these were outside the limits of aperture dimensions for the approximate solutions (Gomperts 1964; Wilson & Soroka 1965).

For numerical calculations these limits should not apply, so wider and shallower apertures can be modelled. For numerical calculations the main concern is to ensure that the acoustic

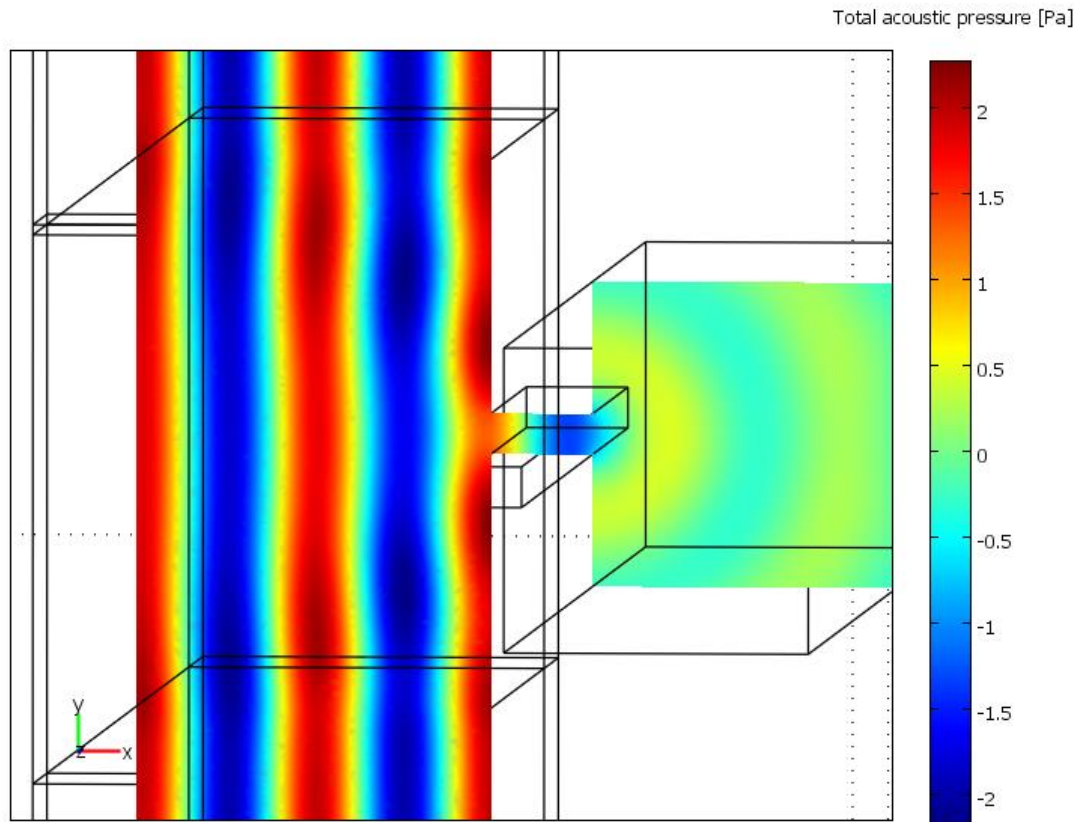


Figure 4.4. Finite element model set-up representing a plane wave incident on the ventilation aperture and sound transmission through it. Left hand side is source side and right hand side is receiving side.

waves are sufficiently resolved with at least six elements per wavelength (Oldham et al. 2005). For some configurations, and at high frequencies, this required substantial computational resources. Separate models had to be produced with each one meshed for a specific section of the frequency domain. The results for each frequency sweep are then joined together to produce the results presented in this chapter.

4.5 Validation of finite element model

The finite element modelling was validated in two ways. An initial check ensured that the results were mesh independent, the mesh size was reduced incrementally and the results were compared. It was found that changes in results were insignificant with discrepancies many times smaller than a 1dB. Therefore the recommended mesh size of 6 elements per wavelength was sufficient for the accuracy of this model. The main validation of the modelling approach for this acoustics aperture model was done by comparing a finite element results for a circular aperture with a well-established approximate model. This had in turn been validated by comparison with an exact analytical solution and experimental measurements.

4.5.1 *Wilson Soroka approximation*

The established approximate solution used for the model validation was proposed by (Wilson & Soroka 1965) and included comparison with the Nomura & Inawashiro (1960) exact solution. It also compared well with experimental results presented by Oldham & Zhao (1993) and for these reasons it is taken as the true solution in the validation work presented here. This method is derived using the concept of pistons at the entrance and exit of the aperture which move like the air particles at these positions. This assumes they are massless, infinitely thin plane pistons. The transmission coefficient r is given in terms of the normalised radiation resistance R_0 and reactance X_0 by equation (4.13). The resistance being the quantity opposing the sound transmission and reactance is the quantity causing the sound to be out of phase with the source.

$$r = \frac{4R_0}{4R_0^2(\cos kh - X_0 \sin kh)^2 + [(R_0^2 + X_0^2 + 1) \sin kh + 2X_0 \cos kh]^2} \quad (4.13)$$

Where h is the depth of the aperture. The values R_0 and X_0 (units $N \cdot s \cdot m^{-3}$) are computed in terms of $2ke$ by means of the infinite series functions indicated in equations (4.13) and (4.14) below.

$$R_0(x) = \frac{x^2}{2 \cdot 4} - \frac{x^4}{2 \cdot 4^2 \cdot 6} + \frac{x^6}{2 \cdot 4^2 \cdot 6^2 \cdot 8} - \frac{x^8}{2 \cdot 4^2 \cdot 6^2 \cdot 8^2 \cdot 10} \quad (4.14)$$

$$X_0(x) = \frac{4}{\pi} \left[\frac{x}{3} - \frac{x^3}{3^2 \cdot 5} + \frac{x^5}{3^2 \cdot 5^2 \cdot 7} - \frac{x^7}{3^2 \cdot 5^2 \cdot 7^2 \cdot 9} \right] \quad (4.15)$$

This approach was also extended to rectangular slit-shaped apertures by Sauter & Soroka (1970). Both of these approximate solutions compare favourably to the measurements of sound intensimetry conducted by Oldham & Zhao (1993). Although the slit aperture approximate method did not have the options of comparison with an exact solution as this does not appear to be available. This was possible for the circular aperture method and so the circular case was chosen as it was considered a more robust validation of the FEM model setup.

4.5.2 Validation results

The validation results presented in this section are a direct comparison of SRI from finite element calculation with that from the Wilson Soroka method for a circular aperture of radius 11mm and depth of 220mm. These dimensions were chosen as they were used by Gomperts (1964) in an example of this method and were thought appropriate for approximate calculation methods. In addition it was ensured that the finite element model was sufficiently resolved for the frequencies shown in the results. A circular aperture version of the finite element set up shown in Figure 4.4 was built and nodal acoustic pressures were calculated for the surface directly in front of the circular aperture and at the aperture exit. These were used

to calculate SRI according to equation (4.1) and compared to the approximate solution calculated from equation (4.13). Figure 4.5 shows the comparison and also illustrates the nature of aperture SRI.

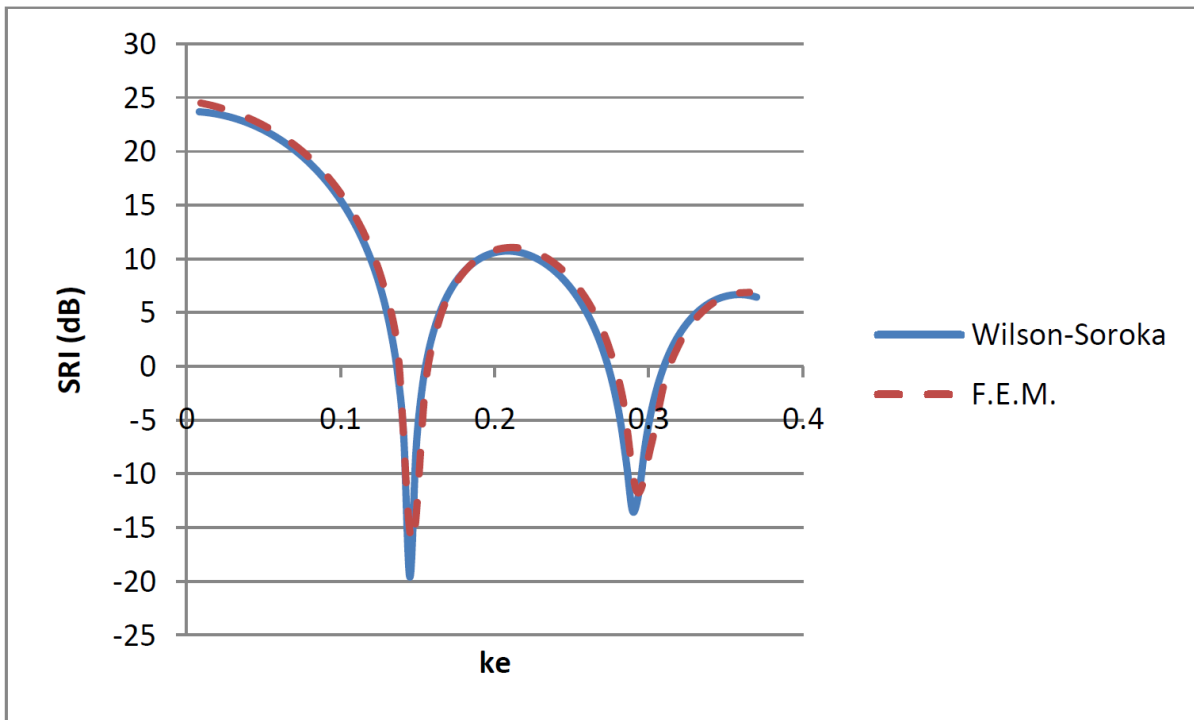


Figure 4.5. Comparison of SRI against ke for a circular aperture of radius 11mm and depth 220mm. two calculation methods are indicated in the legend.

It can be seen that there was good agreement between the finite element model and the Wilson-Soroka method. As well as showing the good accuracy, Figure 4.5 also demonstrates how the SRI varies with frequency with resonant (the maximums) and anti-resonant (the minimums) behaviour. An additional comparison plot is given in Figure 4.6 to illustrate where agreement is better and worse.

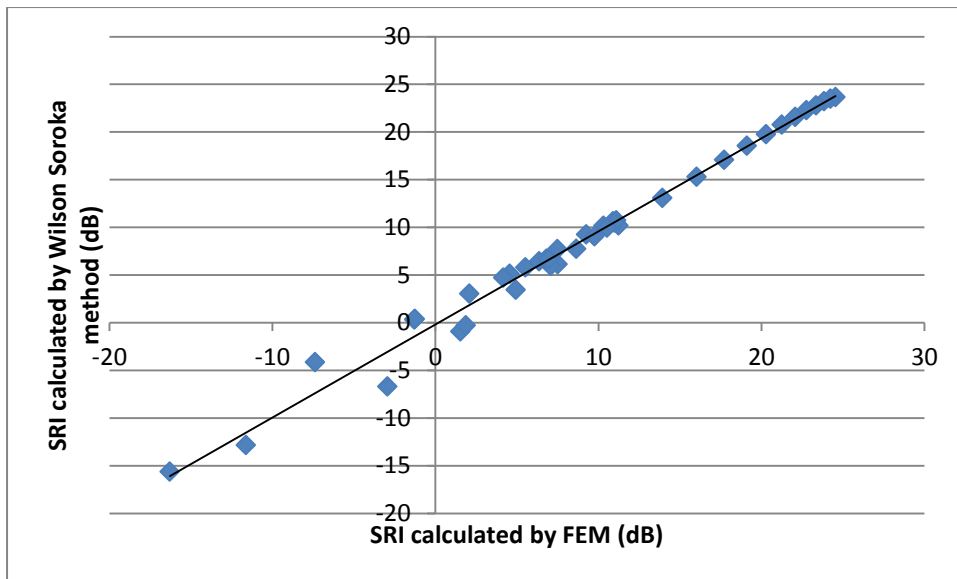


Figure 4.6. Comparison of SRI for the two calculation methods. The trend line is the average of the numerical data points.

Agreement is generally good with the results in Figure 4.6 following a gradient very close to one. The main deviation from this occurs between 0 and -10dB, in this region results alternate either side of the trend line. Figure 4.5 shows that this region is where rapid changes in SRI occur with frequency. This steeper gradient accounts for the larger disagreement in SRI results between the methods. There is good agreement in the frequency at which resonances and anti-resonances occur and overall the scatter in the results is small with a correlation coefficients (R^2) of 0.99. This gave confidence that the numerical model could be used to describe the SRI of the ventilation apertures.

4.6 Results for SRI of ventilation aperture

In this section the SRI of apertures corresponding to the sliding window ventilation openings of the example buildings used in Chapter 5 are presented. This is important as the combined SRI of the façade is dominated by the poor performance of the ventilation openings (De Salis

et al. 2002). Figure 4.7 shows the calculated SRI obtained from finite element analysis of an aperture of width 40mm. This represents a 1% opening of one of the example building's windows which is the increment of opening of the building energy model's windows. As well as the series representing the acoustic spectrum with small frequency intervals, octave band average SRI is also plotted

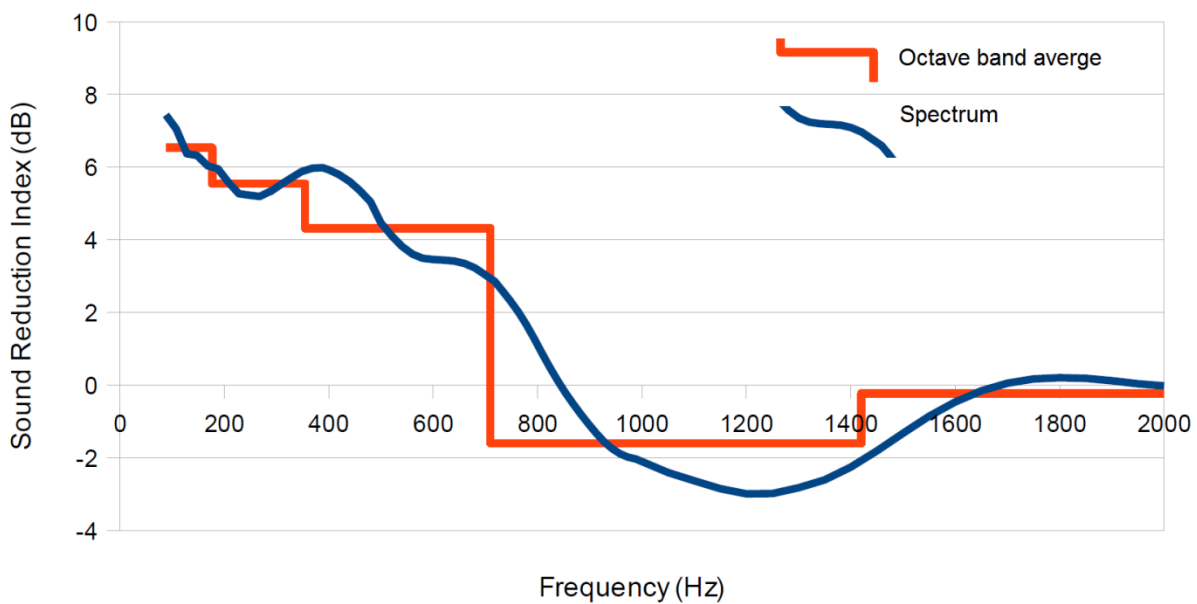


Figure 4.7. SRI for a slit aperture representing 40mm window opening, spectrum values and octave band averages.

The variation of SRI with frequency is evident from Figure 4.7. As mentioned previously, the negative SRI values are due to reflected waves from the aperture and can be observed in experimental results (Oldham & Zhao 1993). The oscillations are somewhat different to those seen for a circular aperture in Figure 4.5. The oscillations are not as regular and this is most likely due to the top and bottom of the slit aperture causing additional reflections which do not occur for circular apertures. To enable the practical use of the SRI results octave band averages are taken of the spectrum value. This includes some level of aperture frequency

response in the calculation of sound reduction but does not add undue complexity. Figure 4.8 shows the octave band averages of apertures of widths from 40mm to 200mm - this represents the 1% to 5% opening of the example building model's window area.

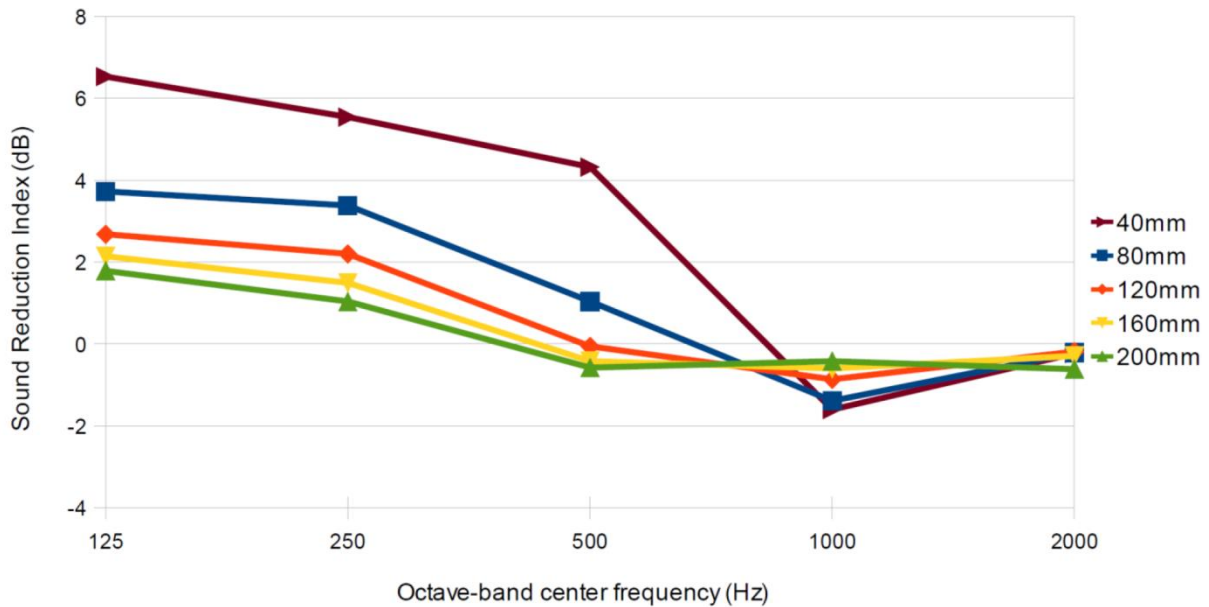


Figure 4.8. SRI averaged over the octave bands for different sized ventilation apertures (aperture width indicated in the legend).

Due to computational expense the apertures were not modelled beyond 2000Hz. This was seen as an acceptable simplification, with half the last octave band of interest being modelled. Fluctuations of SRI with these higher frequencies were well within 1.5dB of no sound reduction and the trend is for the amplitude of oscillations to reduce as frequencies increase. Published results from (Gomperts 1964; Oldham & Zhao 1993) are in agreement with this, showing that the difference between SRI at the resonances and anti-resonances tends to decrease as the frequency is increased. It is assumed that any change due to extending the calculation into the higher frequencies would not affect the results significantly. The crossing

of the lines in Figure 4.8 is due to the size of the aperture influencing the frequency at which resonances and anti-resonances occur. The largest differences between maximum and minimum aperture SRI occur with the smaller apertures. For the 40mm aperture this is from 6.5 to -1.6dB which is enough difference to have real implications for natural ventilation, as is shown in Chapter 5.

4.7 Façade combined sound insulation

The method presented in Chapter 5 requires a combined façade sound insulation to be calculated that indicates which level of environmental noise ingress occurs and which level occupants are exposed to. The combined sound insulation includes that of the window aperture presented in the previous section. This will be combined with the insulation of the other components of the façade. The external noise levels are attenuated by the acoustically insulating properties of the façade which can be described as the SRI. It is possible to combine different parts of the façade, the standard equation for the SRI of a composite panel (SRI_{combined}) is given in equation (4.16). A similar approach has previously been used to calculate combined sound insulation of a naturally ventilated wall (De Salis et al. 2002; Oldham et al. 2004).

$$SRI_{\text{combined}} = -10 \log \left[\frac{A_{\text{wall}} 10^{\left(\frac{-SRI_{\text{wall}}}{10}\right)} + A_{\text{window}} 10^{\left(\frac{-SRI_{\text{window}}}{10}\right)} + A_A 10^{\left(\frac{-SRI_A}{10}\right)}}{(A_{\text{wall}} + A_{\text{window}} + A_A)} \right] \quad (4.16)$$

where the aperture has area A_A and SRI_A , the wall has area A_{wall} and SRI_{wall} , and the window has area A_{window} and SRI_{window} .

In this work SRI_{wall} , and SRI_{window} values were adopted from the acoustic design of schools guidance (Hopkins et al. 2003). Standard construction type were used, 4/12/4mm double glazing and two leaves of 102.5mm brickwork with a 50mm cavity. These construction materials had the sound insulation properties shown in Table 4.1.

Table 4.1. Construction material sound insulation values (dB).

	Frequency (Hz)				
	125	250	500	1000	2000
Double glazing (Hopkins et al. 2003)	24	20	25	35	38
Cavity brick wall (DfEE 1975)	41	45	48	56	58

It can be seen that the insulation properties of the construction material in Table 4.1 are far larger than for the apertures given in Figure 4.8. The dominant influence of the poorer performing aperture on the combined sound insulation of the façade is represented in equation (4.16). With the use of equation (4.16), the values provided for construction material SRI given in Table 4.1, aperture SRI results shown in Figure 4.8 and the proportions of the façade made up of wall, glazing and opening, a composite SRI value can be calculated. These values are presented in Figure 4.9.

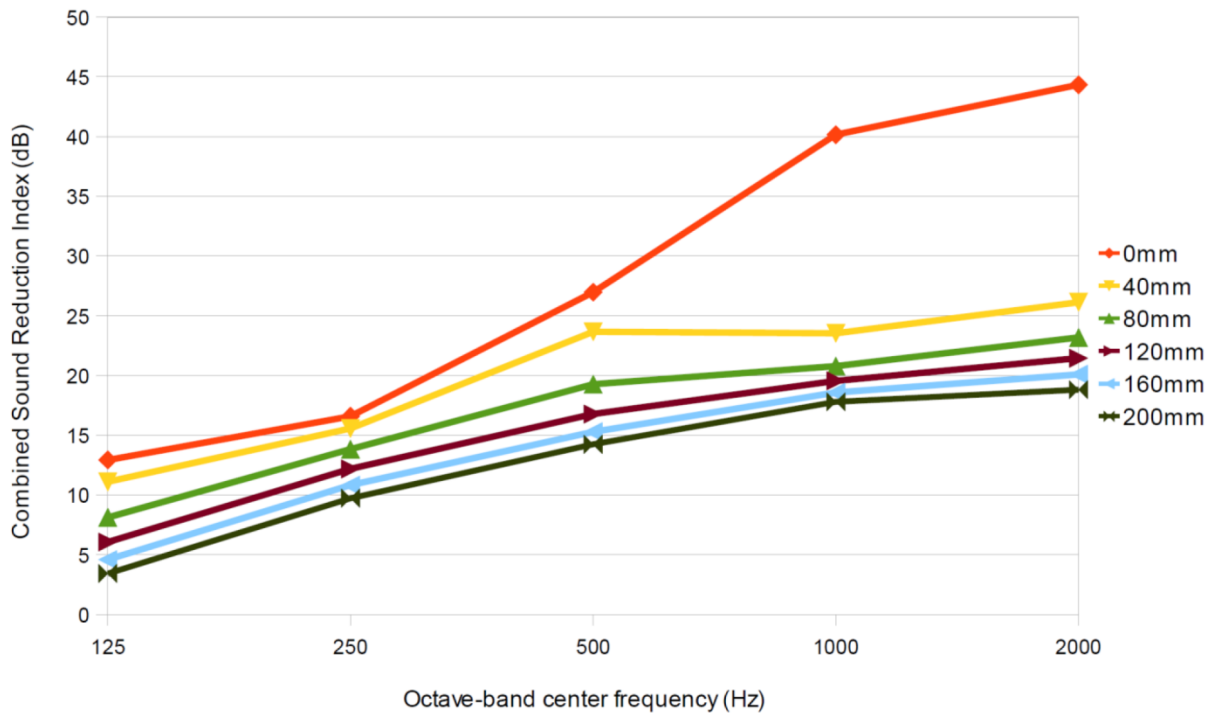


Figure 4.9. Combined SRI variation with frequency and ventilation opening size indicated in the legend.

Most variation across frequencies in SRI occurs between the opening widths of 0mm and 80mm, for the higher frequencies this difference is up to about 20dB. After that the subsequent extra opening has a smaller and more regular effect in reducing SRI with increases in aperture generally resulting in a 1 to 2dB change in SRI. BB93 (Hopkins et al. 2003) includes the guidance that a façade with an open window will give between 10dB and 15dB of sound insulation, this fits with the more open facades shown in Figure 4.9.

4.8 Discussion

With an even exposure of noise on the façade of a building it is now possible to quantify the balance between natural ventilation and the ingress of noise. The exposure of a façade to noise is generally not even though, as it is heavily dependent on the location and power of the

noise sources and the configuration of the urban surroundings. For example, the position of surrounding buildings or trees may provide shielding or conversely increases in noise exposure may occur due to reflections. A method for calculating noise distribution in urban areas has been produced and used as part of a European directive and is given the name of noise mapping. Exposure patterns from these methods will be used in Chapter 5 so that ingress from each section of façade with a window opening can be calculated using the results from this chapter.

The variation in SRI seen in slope seen Figure 4.8 and Figure 4.9 is due to both the size of the aperture and the frequency in question. Although a smooth inside face of the ventilation aperture is assumed for this work as it is the simplest and most widely applicable. Other arrangements could be adopted depending on the specifications of the frame, for example notches or other more complex geometries could be modelled. Flexibility with the geometry is a major advantage of numerical approaches such as the FEMs. An additional advantage would be the testing of noise mitigation methods such as the staggered window arrangement plus the adoption of absorbing materials, the properties of which can be simulated with impedance boundary conditions as was proposed by Kang & Brocklesby (2005). This system used micro perforated absorbers.

4.9 Conclusions

In conclusion to this chapter the following objectives have been met:

- The SRI of ventilation apertures were successfully calculated via a novel approach with FEM.

- The combined SRI for naturally ventilated facades was calculated.

In this chapter finite element models were used to define the frequency-dependant SRI of ventilation apertures. This was calculated for a number of apertures, the opening sizes of which were multiples of 40mm, corresponding to the degree of opening of the thermal building models in Chapter 5. It was found that SRI_A values varied by up to 8dB across the frequencies considered. It was shown that these values could be combined with façade material values to give the combined $SRI_{combined}$ of a ventilated façade. These results will be used in Chapter 5 to produce ventilation opening patterns.

5 Combining noise mapping and building thermal performance

In the previous chapter detailed modelling of the ventilation opening was undertaken, these results are used in this chapter where the scale will be increased to the surrounding area and whole-building performance. Combining noise mapping and building energy performance produces results relevant to building design and which are for specific areas and buildings. In Chapter 4, the transmission loss of the ventilation aperture was calculated. These results were combined with the sound insulation of the other components of the façade to give the SRI_{combined} . This was, in turn, used to link how external noise ingress is affected by the size of the ventilation opening. Results are presented, demonstrating how information about the link between tolerated noise level and thermal performance can be used to aid decisions in building design, such as when noise reduction measures have the most effect on natural ventilation and cooling.

Section 5.1 will introduce the new concept of the tolerated noise level, and how different uneven façade opening pattern distributions are produced by comparing the internal room noise level to the tolerated noise level. After this, the example thermal building models are introduced in Section 5.2, and details are given of the mixed mode cooling system that is used. Then the two example noise mapping locations from Manchester are introduced in Section 5.4 along with some comments on noise mapping. This is followed by Section 5.5, which gives the building noise exposure patterns in colour contour form. Details of the steps taken to integrate these noise mapping outputs with the example buildings thermal models are given in Section 5.6 before the results are presented and discussed in Section 5.7.

5.1 Tolerated internal noise level

The tolerated noise level is the level of noise ingress that is tolerated, before ventilation openings are reduced; this includes only the external noise that enters the building through the façade. The level of allowable noise ingress that is prescribed depends on a number of factors such as building use and is also the subject of some discussion (Field 2010). The concept of tolerated noise level is used so that a building's response to complex noise exposure and ingress can be summarised and incrementally changed, giving an indication of the trend and sensitivity for a particular building and location. Tolerated noise levels are sampled at regular increments between, at one extreme all ventilation openings being fully closed, and at the other all being open to their maximum. The use of tolerated noise level is a new approach, and could encourage a more flexible approach, in contrast to simply sticking to rigid fixed levels of noise ingress, which were criticised for not being relevant to naturally ventilated buildings (Field 2010; Baird & Dykes 2010).

With the method developed in this chapter, room noise levels in excess of the tolerated noise level cause ventilation openings to be restricted. The degree of ventilation opening to a room is determined by the traffic noise levels in the room, this is calculated with the use of $SRI_{combined}$ which was defined / discussed previously in Chapter 4. The level of traffic noise in a room is calculated by equation (5.1).

$$L_R = L_0 - SRI_{combined} + 10\log(S/A) \quad (5.1)$$

where L_R is the sound level in the room, L_0 is the sound level at the façade, $SRI_{combined}$ is the combined SRI of all elements of the façade, S is the surface area of the façade (for the example models used in this study there was a window for each $17.5m^2$ of façade area). A is the room absorption area and is assumed to be a standard $10m^2$. The ratio of façade surface to

absorption area will stay relatively constant, as will the last term of equation (5.1). With the use of the values above, the expression for the sound level in the room is as follows:

$$L_R = L_0 - SRI + 2.4 \quad (5.2)$$

In this method, L_0 at the centre position of each window opening is given by noise mapping. L_R can then be compared to the tolerated level. The window openings in a thermal building model are adjusted so that L_R is as close to the tolerated noise level as possible. Each sampled tolerated noise level corresponds to an uneven ventilation opening distribution over the building façade and therefore needs a separate thermal building model simulation.

5.2 Example thermal building modelling

Whole building level air flow patterns and cooling energy consumption were modelled for an extended summertime period to produce the results in this chapter. DesignBuilder software (DesignBuilder Software Ltd 2009) was used for this, where EnergyPlus is employed as the simulation engine. EnergyPlus is a thermal building calculation tool that has been widely used and tested (Henninger & Witte 2009), this software was further discussed in Section 2.1.2. It provides a heat-balance-based solution to the heating and cooling loads required to maintain the thermal conditions within a building. Various modules link into this core calculation to enable the representation of the building and its processes. This includes the calculation of solar heat gains and the airflow network module that was the focus of this work. The air flow rate through each opening is driven by the pressure differences that, in the case of natural ventilation, are caused by wind pressures and buoyancy.

For the example buildings used in this study a large degree of overheating was evident under free running conditions, i.e. where no heating or cooling systems are introduced into the

model but heat gains from occupants and the external climate are represented. For the example buildings, the percentage of occupied hours above 28°C are well above the CIBSE 1% guideline (CIBSE 2007) to determine whether a building is said to be overheating. For example building 5.1 overheating is 30% of occupied hours. This was the case even with the window opening at its maximum level - in this work (Section 5.7) mixed mode buildings (part natural/part mechanical ventilation) were simulated. In a mixed mode building, the internal comfort conditions are primarily maintained by natural ventilation. When this is inadequate, active cooling is introduced. The cooling energy consumption of the air handling unit will therefore be used to indicate the extent to which the acoustic environment has affected the natural ventilation potential. For all building models, a natural ventilation set-point of 24°C was used as this is the central adaptive comfort temperature from (ASHRAE 2004). A 2°C difference between cooling and natural ventilation set-points is recommended (DesignBuilder Software Ltd 2009), so a cooling set-point of 26°C was used for all the example buildings in this Chapter. The simulations were run over a June to August time period (summer in the UK) with typical weather data covering these months (CIBSE weather data for Manchester was used). The same set of weather data and surrounding terrain roughness characteristics were used for all the results to ensure that the window opening was responsible for the different calculated ventilation rates and cooling energy consumption.

The window opening for these buildings followed an office operation schedule of Monday to Friday, 08:00 to 18:00. Modelled window opening was controlled by this operation schedule and the fixed temperature set-points. When internal temperatures exceeded this set-point of 24°C windows were opened as long as external temperatures were lower than the internal temperatures. In addition to this standard modelled window opening behaviour, the opening percentage was adjusted so that the noise ingress was as close to the tolerated level as

possible. This was done so that a range of openings between fully open to fully closed could occur over the façade, depending on the noise distribution. For the building models used in this work, wind pressure coefficients from an AIVC document (Liddament 1986) were used. They represented a good initial approximation and were therefore considered acceptable for this comparative study. For more accurate representations of specific buildings wind pressure coefficients from scale model testing or CFD simulation would be required. Standard template descriptions of construction and HVAC equipment were used including a fan coil cooling system. The construction template had cavity walls and coated double glazed windows.

The three idealised office building types are used in this study and shown in Figures 5.1, 5.2 and 5.3. The building details were informed by buildings studied by colleagues on the COPSE project and discussions with Architects at the Sheffield School of Architecture. The footprint of Building 5.1 was 65.4m × 13.4m and it has five floors. Buildings 5.2 and 5.3 are two simple 3 floor office blocks with square footprints of dimensions 20m × 20m and 13m × 13m respectively. The details are summarised in Table 5.1. floor plans for these last two office buildings have contrasting room depths but otherwise the layouts were kept as similar as possible. Three to Five floors were found to be representative of the buildings in the mapped area of Manchester.

Table 5.1. Details of the example buildings.

	Length (m)	Depth (m)	Floor area (m ²)	Number of floors
Building 5.1	64.4	13.4	4314.8	5
Building 5.2	20	20	1200	3
Building 5.3	13	13	507	3

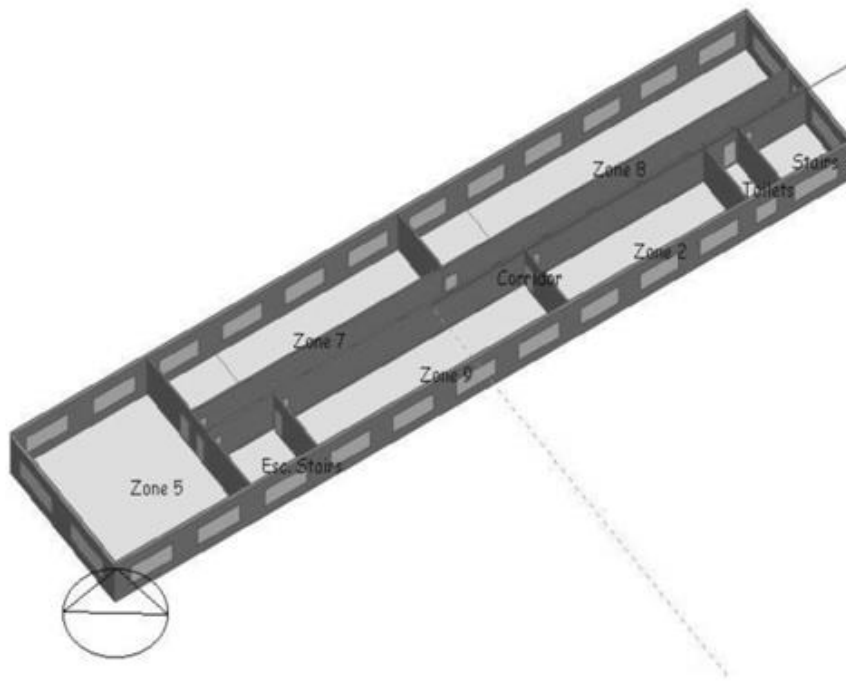


Figure 5.1. Floor plan of office Building 5.1.

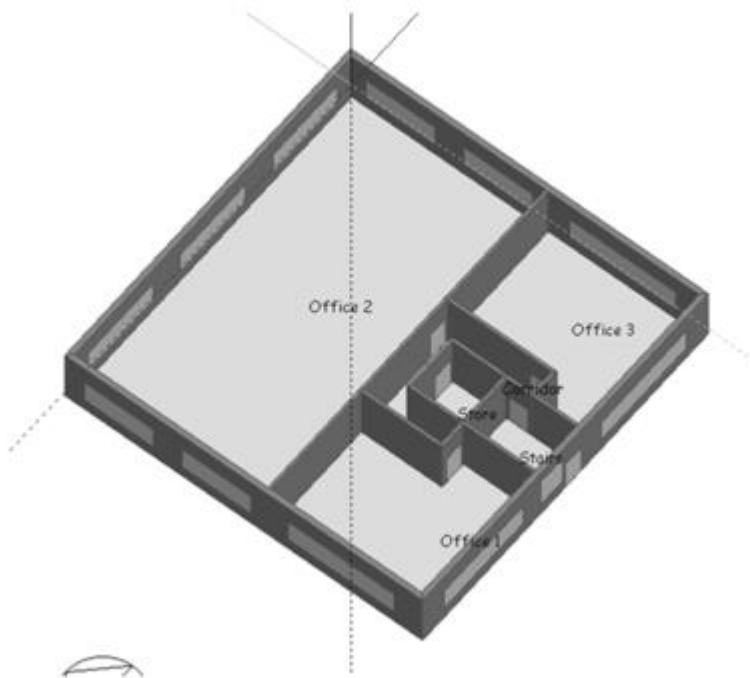


Figure 5.2. Floor plan of simple deep plan office building (Building 5.2).

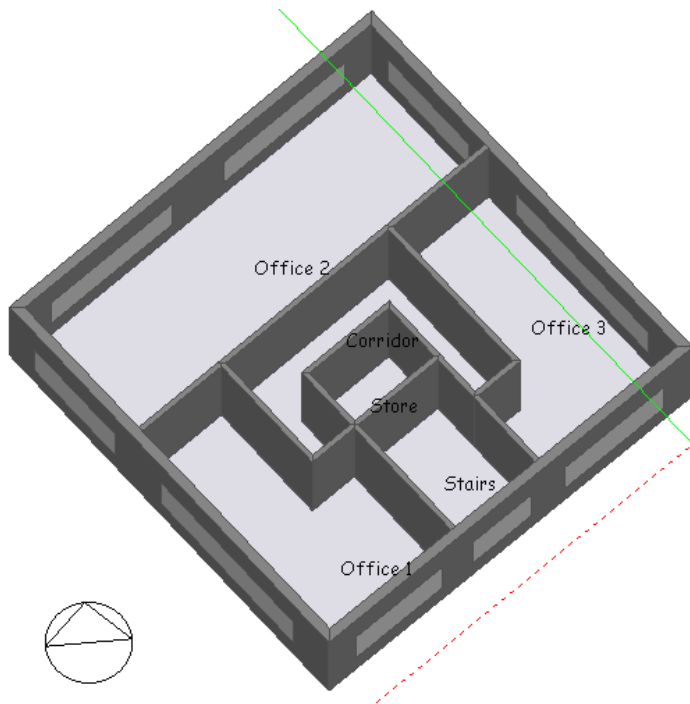


Figure 5.3. Floor plan of the simple shallow plan office building (Building 5.3).

The window openings in the building energy model correspond to horizontal sliding windows, so the opening orifice is a vertical slit the full height of the window. The dimensioning of the windows was done using the design builder preferred height method (DesignBuilder Software Ltd 2009), the windows had a standard height of 1.5m and a standard separation of 5m where the façade dimensions allowed. The exact width of the window is then defined by the percentage glazing, which was 30% for all the buildings. Also, the maximum proportion of the window area that could be opened for the purposes of natural ventilation was 5% for all the buildings.

5.3 Mixed mode cooling

The building models introduced previously all use mixed mode cooling. Mixed mode cooling is where the building's internal comfort conditions are maintained by natural ventilation as much as possible, but then supplemented with degrees of mechanical systems to maintain

thermal comfort, when needed. This strategy has been used most widely in offices. This approach was used here since pure natural ventilation would result in unacceptable levels of overheating, particularly when the ventilation openings are restricted due to noise. By using a mixed mode strategy, comfort conditions are equally maintained for all buildings and ventilation opening patterns. The environmental influences on the example buildings can then be compared; the level of mechanical cooling needed indicates how successful natural ventilation has been at maintaining these comfort conditions.

With this mixed mode strategy, natural ventilation is used until the internal temperatures reach a set-point temperature of 26°C, then the cooling strategy changes over to a fan coil cooling system. The chiller is powered by electricity and this is the basis of the results reported in this chapter. The results are calculated from the average simulation cooling load, the efficiency of the chiller (chiller CoP) and distribution loss, as given by equation (5.3).

$$\text{Chiller fuel} = (\text{Cooling Load} \times \text{Cooling distribution loss factor}) / \text{Chiller CoP} \quad (5.3)$$

where

$$\text{Cooling distribution loss factor} = 1 + (\text{Cooling Distribution Loss}) / 100 \quad (5.4)$$

and the Cooling Distribution Loss was assumed to be 5% and the Chiller CoP was set at 1.670. These were the standard values given by DesignBuilder (DesignBuilder Software Ltd 2009) and therefore considered to be appropriate for this comparative study.

5.4 Manchester noise map

The noise mapping from this study was completed using the software CadnaA (DataKustik GmbH 2006). The Calculation of Road Traffic Noise (CRTN) (DfT 1988) method was

chosen for the simulation as this has been shown to produce results that fitted well with measured noise levels at different building floor levels (Mak et al. 2010). The noise map of Manchester was one previously used for a study of urban morphology (Wang & Kang 2011). The area mapped is shown in Figure 5.4. The road and building layout for the typical 500m x 500m urban area were taken from a digital mapping service (Ordnance Survey 2012). The two sites chosen for the location of the example buildings are marked A and B. The building Location A next to a motorway was compared to the less noisy Location B. Traffic flow was measured and characterised in accordance with the best practice guidance (EC 2006), and the noise level measurements were compared with modelled values. The locations chosen have different noise exposures to enable clear comparison but are still considered representative of a normal urban environment. Positions were chosen where direct sound was dominant, avoiding situations with diffraction (i.e. behind buildings), where noise mapping could be less accurate.

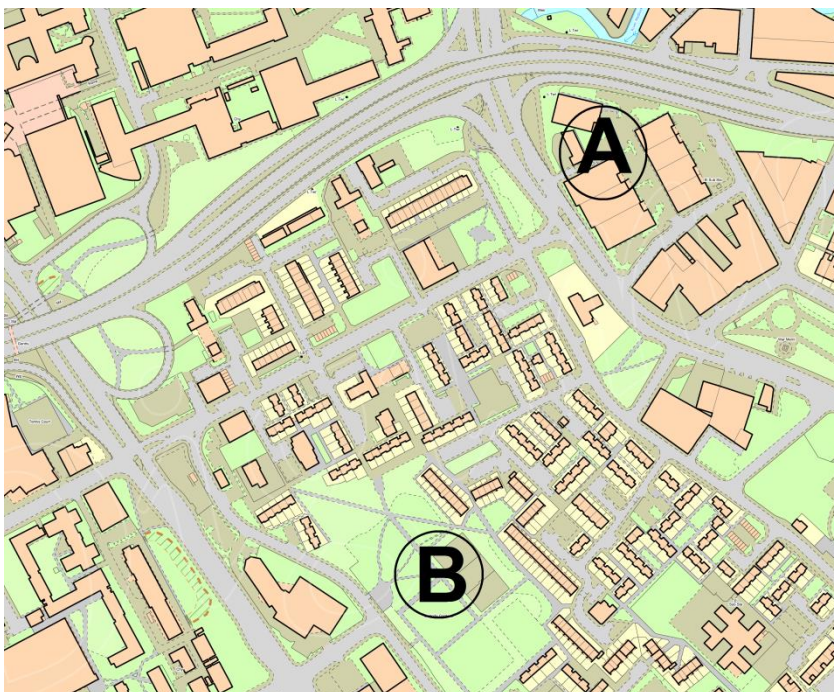


Figure 5.4. Area of Manchester used for noise mapping (Ordnance Survey 2012). The example Locations A and B are marked on the figure.

Noise mapping has become a legal requirement in Europe from Directive 2002/49/EC (European Union 2002), but there are some concerns about its accuracy since it is highly dependent on the importance of reflected noise to a specific noise map (Kang & Huang 2005; Kang 2002a; Kang 2005; Kang 2002b; Kang 2001; Kang 2000). Noise mapping does, though, present an easily available source of information about noise levels at a particular site and has been validated for a number of cases (Kang 2007; Xie & Kang 2010). Noise maps have been identified as the best sources of information available about the noise a building in an urban area is exposed too, such exposure patterns are the starting point for this investigation. Road noise is not the only possible noise source that could affect buildings. Other noise sources are, for example, aircraft, industry and energy generation, such as wind turbines or micro hydro systems. These other noise sources could also be mapped and the results integrated into the method presented here, though these sources are not considered in this study.

5.5 Building noise exposure

Figure 5.5 shows the exposure of the façades of the example buildings to road noise in the two example locations. For Building 5.1 in Location A the average noise level at a window was 74dBA. In Location B the average exposure for this same building was less, at 65dBA, and also a far greater range of noise exposure occurred. Noise levels varied progressively from 54 to 75dBA along the length of this building. An indication of what these noise exposure levels mean can be seen by comparing them to the noise exposure categories from PPG 24 (DCLG 1994). Although these categories are meant for domestic buildings and office building are less sensitive to noise, they still provide an indication of what constitute high and low exposures. Road traffic exposure of 74dBA would mean a noise exposure category of D and that planning permission should normally be refused. A drop to 65dBA would mean

Category C where planning would normally be granted if no quieter locations were available and commensurate levels of protection against noise were provided.

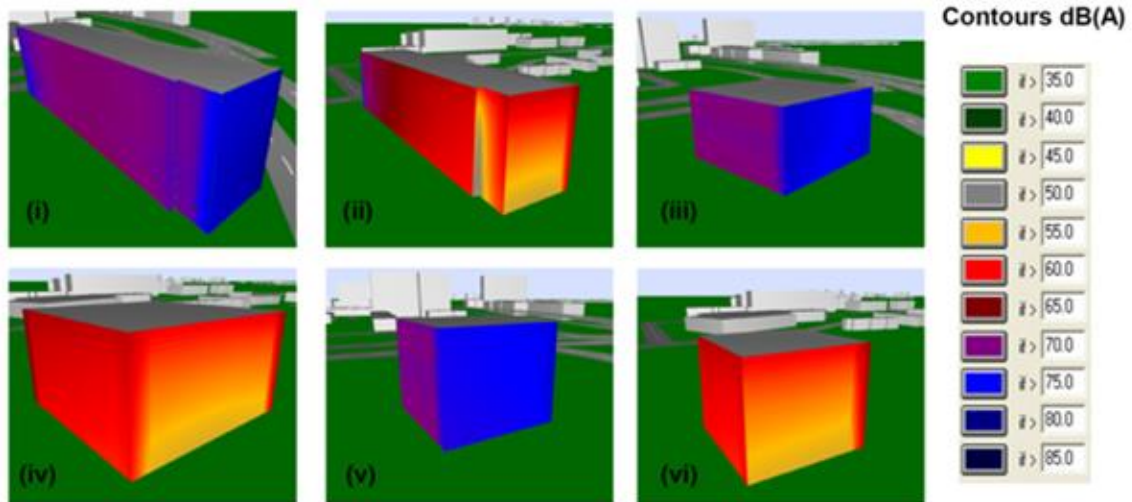


Figure 5.5. Contours of noise levels at building façade - (i) Building 5.1 in Location A. (ii) Building 5.1 in Location B. (iii) Building 5.2 in Location A. (iv) Building 5.2 in Location B. (v) Building 5.3 in Location A. (vi) Building 5.3 in Location B.

The exposure of Building 5.2 was similar to that of Building 5.3 with the average levels at Location A being 74dBA resulting in PPG24 category D. Location B results in PPG24 category B, with an average exposure of 62dBA. This means that, where appropriate, conditions would be imposed to ensure an adequate level of protection against noise. Due to the smaller perimeter length of these two buildings (compared to Building 5.1) the noise level across façades was more uniform. The exposure patterns are due to the position of noise sources and shielding objects in relation to the buildings.

5.6 Combining noise mapping and thermal building modelling

There are a number of steps in the integration of the previously introduced concepts. In this section these will be summarised before the results are introduced in the following section.

The varying road traffic noise levels at each window position on the building façade were obtained from CadnaA as single-figure, A-weighted values. To calculate attenuation from the frequency-dependant sound insulation of the façade, the single-figure façade levels were converted to a standard traffic noise spectrum. The normalized road traffic noise spectrum given in BS EN ISO 717-1:1997 (BSI 1997) and shown in Figure 5.6, was used for this.

These levels were adjusted evenly so that they matched the noise mapping level; in this way the octave-band road noise level at each window was given. Another approach could be to do the noise mapping at different frequencies, although this may not always be available if using existing noise maps produced for legislative reasons.

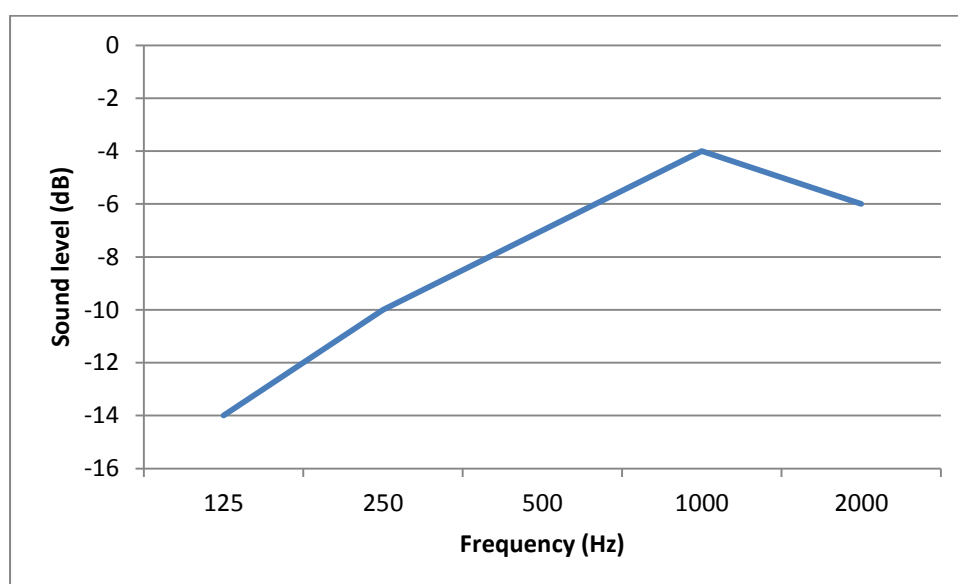


Figure 5.6. Traffic sound level spectra reproduced from (BSI 1997) levels are A-weighted and normalized to 0dB.

Attenuation from the composite façade was taken into account through equation (5.2) giving the internal octave-band noise levels. This was reduced to a single-figure value by the standard A-weighting network for all degrees of window opening at all the windows. The concept of a tolerated internal noise level was then used in the following way: The degree of opening for each window was chosen such that the internal noise levels, calculated previously, were as close to the tolerated level as possible. A separate thermal building model then corresponded to each tolerated noise level. Five tolerated levels were calculated that split the range between a fully open and fully closed façade into four segments. The thermal building model results could then be plotted against tolerated noise levels. This quantified the relationship between acoustic considerations and natural ventilation potential for the specific building and site. The results also identify where noise reduction measures can have the greatest impact.

A number of small custom BASIC scripts were written by the author to help automate some of the more repetitive procedures described above, for example to calculate the required opening of each façade window. If more wide-spread use of this method could automatically link external noise mapping and internal building conditions in a similar way to the link between CadnaA and Bastian (DataKustik GmbH 2006). Surfaces from noise mapping could be matched with the thermal building model surfaces enabling the automation of this method.

5.7 Cooling energy variation with noise tolerance results

The results presented in Figures 5.7 to 5.9 show average chiller electricity use during occupied hours of the summer period against tolerated internal noise level. The results are displayed from minimum chiller use, corresponding to the situation where all windows can be

fully open and the chiller is off, if the set point temperatures allow. Maximum chiller use corresponds to the situation where windows were sealed. These end points represent the limits of this investigation. The shapes of the curves in Figures 5.7 to 5.9 are the product of the noise exposure patterns and the window positions for the buildings.

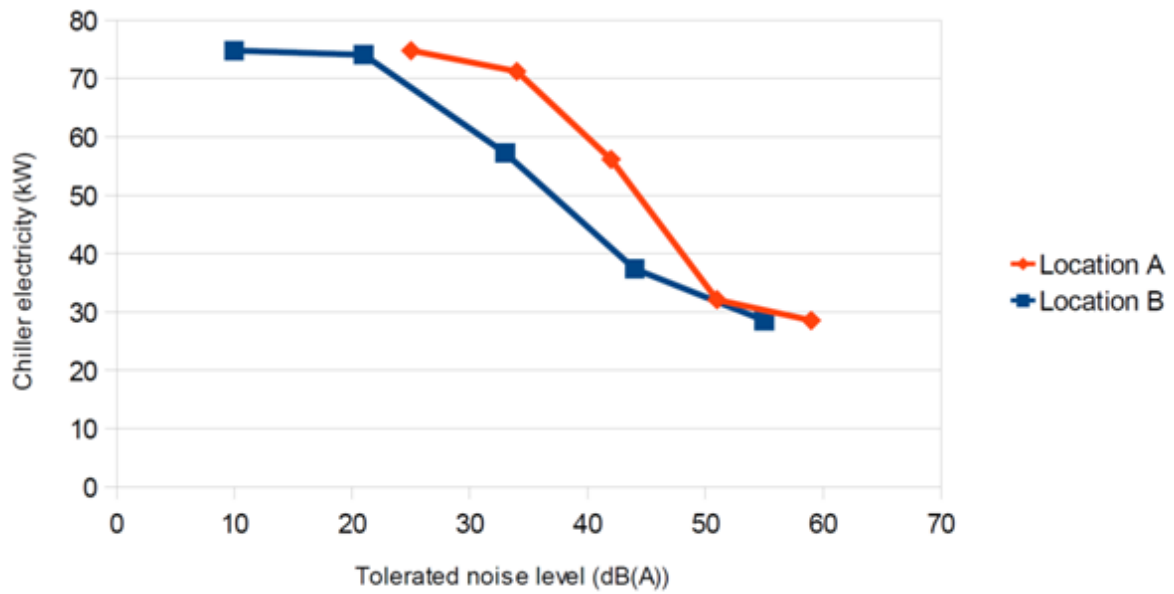


Figure 5.7. Comparison of Building 5.1 in different noise locations.

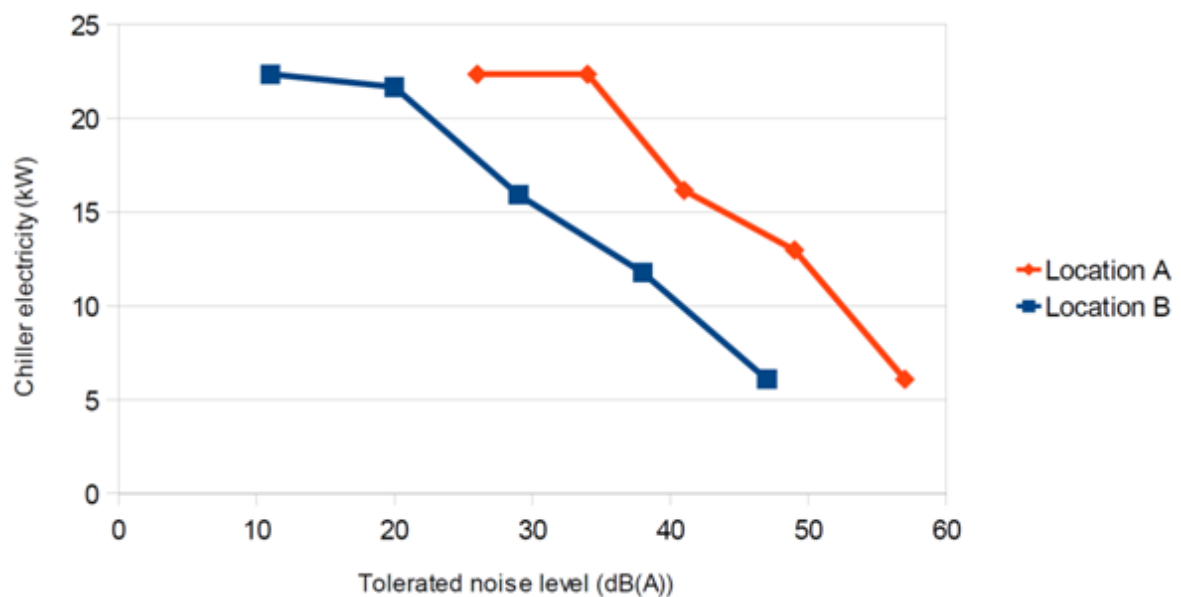


Figure 5.8. Comparison of Building 5.2 in different noise locations.

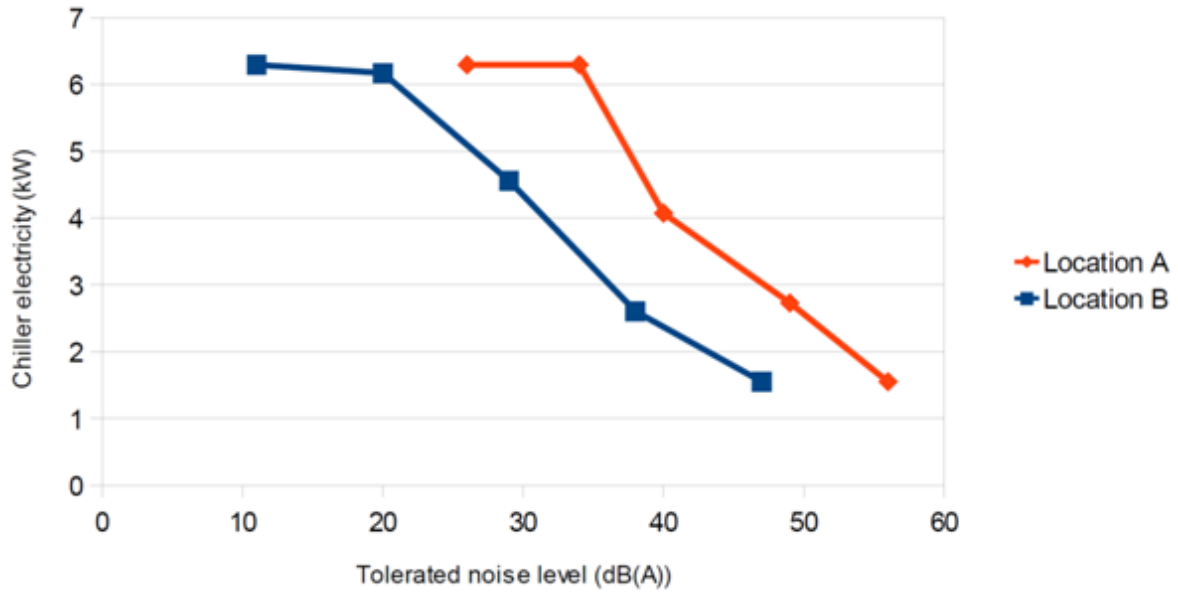


Figure 5.9. Comparison of Building 5.3 in different noise locations.

A discussion of what these results tell us about chiller use is included in section 5.8.

5.7.1 *Quantifying for location*

The differences in noise exposure between the two sites are quantified in the results by the separation of the curves. A greater tolerance of noise is needed in Location A for the same level of air conditioning used as in Location B. The distance between the curves for the buildings is related to the range of noise exposure for the buildings in each location.

Maximum exposure for Building 5.1 is relatively uniform between Locations A and B, changing from 75 to 79dBA. The minimum values for building noise exposure vary much more, from 54 to 69dBA, this being due to the length of the building and the main noise source for Location B being concentrated on one side.

There is a wide range of guidance on what level of external noise ingress is acceptable depending on different national codes or guidelines, room use, time of day etc. For England

and Wales the requirements for the acoustic design of schools are mandatory but there are no similar mandatory requirements for office buildings. To illustrate the potential use of this new method an assumed tolerated noise level was used to compare cooling energy consumption between buildings and locations. The suggested maximum noise rating of NR 35 for open plan offices (BSI 1999), which for a broad band traffic noise spectrum from BS EN ISO 717-1:1997 (BSI 1997) equates to 34dBA, was used. This represents an external noise ingress of a similar order to that, which is suggested as the maximum background noise levels generated by building services installations. Using this as the tolerated noise level, the cooling energy consumption for each building and noise location can be estimated from Figures 5.7 to 5.9.

For Building 5.1 the reduction in average cooling energy consumption between Location A and B is 22%. The change between locations for Building 5.2 is 39% and a 45% change is calculated for Building 5.3. Such information would be useful to inform decisions about which cooling strategy to implement depending on the noise exposure of a particular location. A rule of thumb for the change in noise exposure due to a change in traffic flow gives an even 3dB decrease for a halving of the traffic flow. Using the gradient of the curves in Figure 5.7 the change in cooling energy due to a halving of traffic around Building 5.1 can be estimated. For Location A this gives a 1.7% decrease and for Location B a 8.3% decrease is calculated.

5.7.2 *Quantifying for noise reduction method*

A similar method can be used to estimate the potential benefit of introducing noise mitigation measures over the whole building. Table 5.2 shows the reductions of cooling energy consumption if the 34dBA level is again used as the tolerated noise level and it is assumed

that through the application of acoustic treatments an improvement of 10dB can be made to noise levels experienced by the occupants. 10dB was chosen as the example noise reduction measure due to 20dB being reported for a natural ventilation window system (Kang & Brocklesby 2005). This is an additional 10dB on top of the 10dB which can be expected for a normal open window (Hopkins et al. 2003).

Table 5.2 Influence of a 10dB acoustic treatment on mixed mode cooling energy consumption. Percentage change relative to cooling energy consumption before the implementation of 10dB treatment and a corresponding increase in ventilation opening to maintain noise ingress at 34dBA.

	Difference (kW)		% Change	
	Location A	Location B	Location A	Location B
Building 5.1	20.4	18.0	28.7	32.6
Building 5.2	7.4	5.6	33.0	41.4
Building 5.3	2.8	1.6	44.8	45.2

Table 5.2 shows the large difference in the effectiveness of the noise reduction measure with regard to the mixed mode cooling energy consumption, depending on the location and the building. Building 5.3 in Location B benefited most from the acoustic treatment, with a 45.2% reduction in its cooling energy consumption. A combination of acoustic treatments and passive cooling strategies could remove the need for mechanical cooling for this example. The noise exposure patterns of Buildings 5.2 and 5.3 were very similar, and so the differences between these buildings were largely due to the difference in the depth of the office space. This is a key influence on the effectiveness of natural ventilation and illustrates that a natural ventilation strategy, in general, is easier to implement for buildings with shallow floor plans. For Building 5.1 the influence of the noise reduction measure was a

smaller percentage of the total cooling requirements but there was consistent improvement across the two locations. Building 5.1 had the largest variation of noise exposures at the different window positions and so applying an acoustic treatment over the whole building would not be the most effective strategy. Careful positioning of individual noise reduction measures, such as openings with higher sound insulation, would be a more effective way to maximise ventilation. For example, open areas with matching openings on either side of corners or opposite walls would develop cross ventilation. Openings concentrated on just one single wall would not encourage as much air flow. The model would have to be adjusted to represent this, but a similar method could be adopted iteratively for design optimisation.

5.7.3 *Zone level cooling*

The previous results have been based on average whole-building chiller electricity output, but it is also possible to look in more detail at individual zones of the building. Each zone is an individual room shown on the floor plans of Figure 5.1, Figure 5.2 and Figure 5.3. This is carried out in this section to gain more information about the changes to air flow characteristics when acoustic variations occur. As the noise mapping gives information about specific parts of the building and the thermal building models are zonal it makes sense to use this level of information. The steepest reduction in cooling is calculated, and the zones with unusual or contrasting behaviour are highlighted. Figure 5.10 shows the cooling use by zone level for Building 5.1 in Location A.

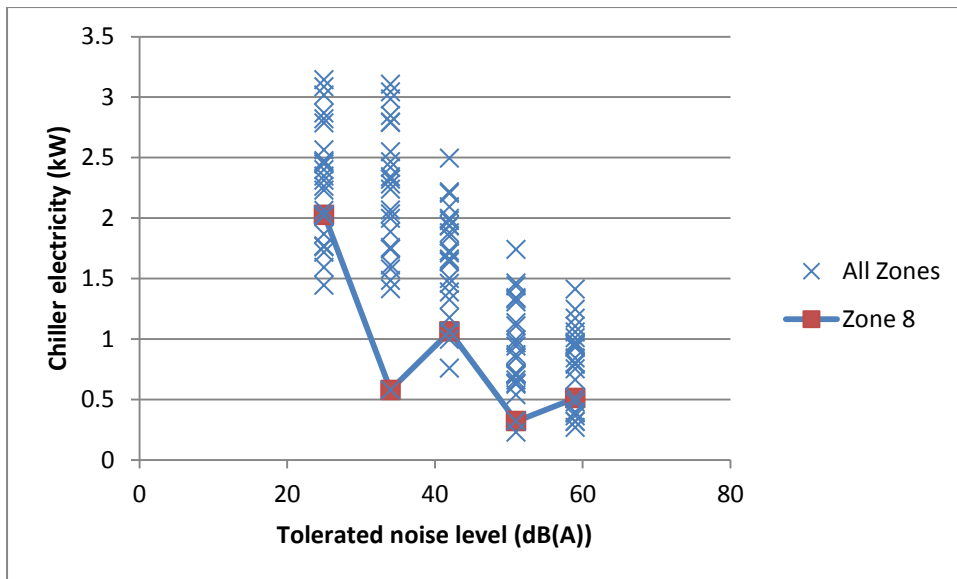


Figure 5.10. Zone level mixed mode cooling for Building 5.1 in Location A. Zone 8 from the ground floor is highlighted.

Overall the trend for a decrease in cooling load as noise tolerance increases is clear, this was seen in the average whole-building results. Some individual zones do not always follow this overall trend. The most striking example of this is Zone 8 of the ground floor which is why it has been highlighted on Figure 5.10. The first increase in tolerated noise level causes a dramatic reduction in cooling for Zone 8 on the ground floor. This dramatic decrease is about double the next steepest gradient for a zone at 0.16kW/dB and 10 times larger than the average gradient for that step in tolerated noise level. Between the tolerated noise levels of 34dB and 42dB there is an increase which goes against all other trends. To find out why this occurs the sensible cooling due to natural ventilation airflow rate is investigated

The sensible heat loss due to the external air having a lower temperature than the zone air temperature was looked at to investigate changes in the natural ventilation cooling of Zone 8. It was found that with the 34dB opening regime, Zone 8 has an average sensible heat loss rate

of 2.5kW. For the same zone but with the 42dB opening regime, this falls to 1.7kW. This is a similar proportion to the drop in air exchange rate which falls from 1.65ACH for 34dB to 1.05ACH at 42dB. This could initially be seen as unusual due to the more open façade for higher tolerated levels. However, for the step between a tolerated noise level of 34dB and 42dB the only natural ventilation opening occurs on the façade of Zone 8. The windows in the surrounding zones remained closed resulting in all ventilation air flow being concentrated in Zone 8. When more of the surrounding windows are opened the natural pressure differences are dissipated by natural ventilation flow in other zones and a decrease in ventilation cooling for Zone 8. This is a good example of the complexity resulting from uneven openings due to the noise distribution. In this special case a more open building in general does not necessarily mean better natural ventilation for this specific room.

The results for Building 5.1 in Location B are shown in Figure 5.11. This example has a more gradual change in noise exposure from one end to the other so the result curve is smoother without the anomalous zones from the previous set. An interesting point here is to compare Zones 5 and 2, the positions of which can be seen in the floor plan of Figure 5.1. Cross ventilated Zone 5 located at the noisier end of the building is contrasted to Zone 2 which has single sided ventilation and is located at the quieter end of the building. Initially Zone 5 requires more cooling as it is a larger zone and therefore has more internal gains. As the ventilation openings are increased both zones experience a reduction in cooling load. The reduction for Zone 2 levels out after 44dB as all the windows are fully open. The cooling for Zone 5 reduces further until it is below that of Zone 2, showing how much more effective cross ventilation can be. It can be seen from these results that noise mitigation measures would have most effect directed at Zone 5. Zone 5 would give 0.09kW/dB rather than 0.05kW/dB for Zone 2.

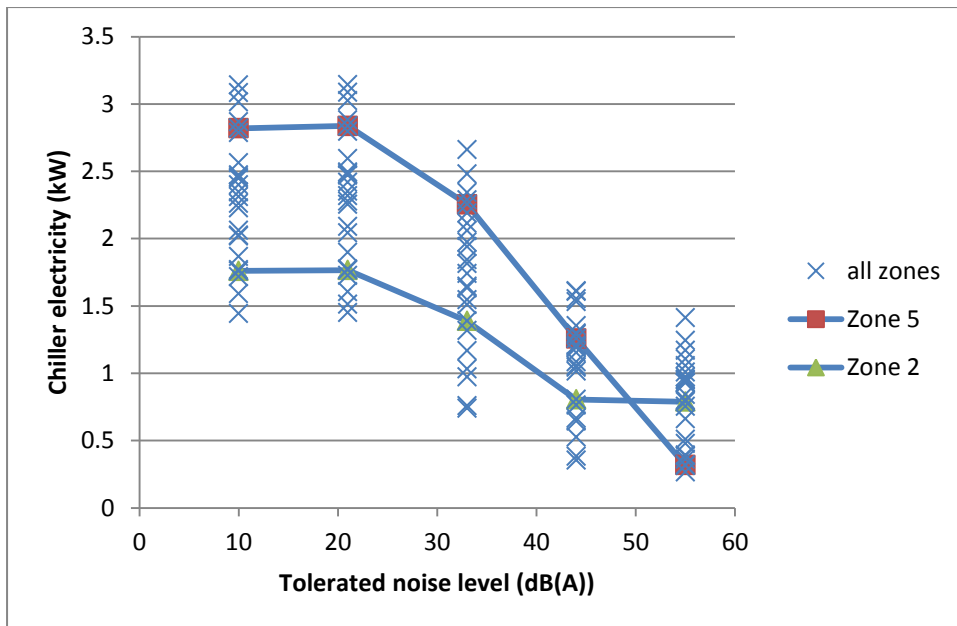


Figure 5.11. Zone level mixed mode cooling for Building 5.1 in Location B. Zones 5 and 2 from the 3rd floor is highlighted.

Zone level results for both Buildings 5.2 and 5.3 are shown in Figures 5.12 to 5.15, where it can be seen that Building 5.2 has consistently higher cooling loads. Office 1 and Office 2 for the 1st floor of the three-floor buildings have been picked out to compare behaviours. The details of these offices can be seen on the floor plans of Figure 5.2 and Figure 5.3.

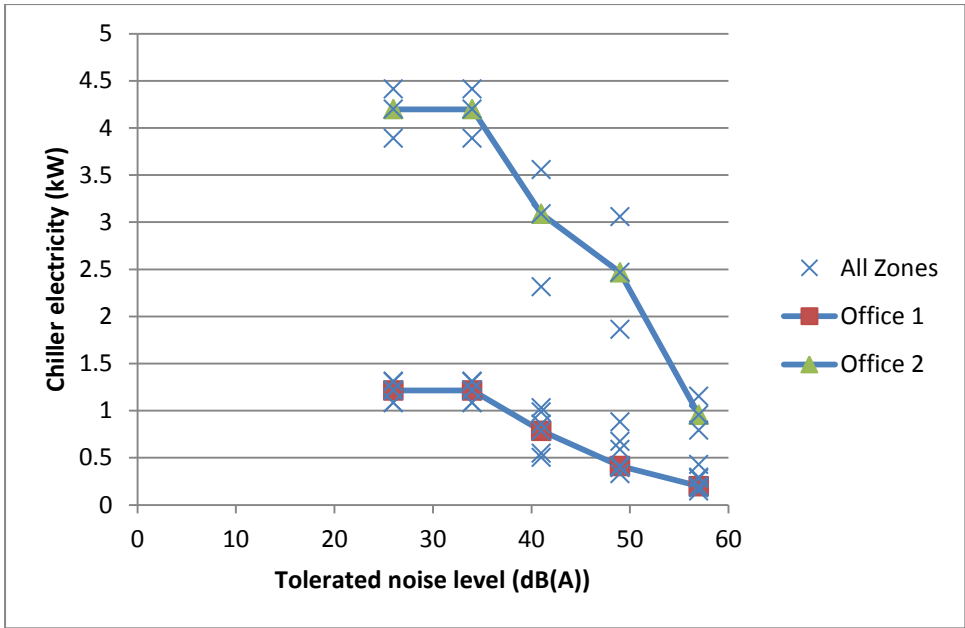


Figure 5.12. Zone level mixed mode cooling for Building 5.2 in Location A. Zones 1 and 2 from the 1st floor are highlighted.

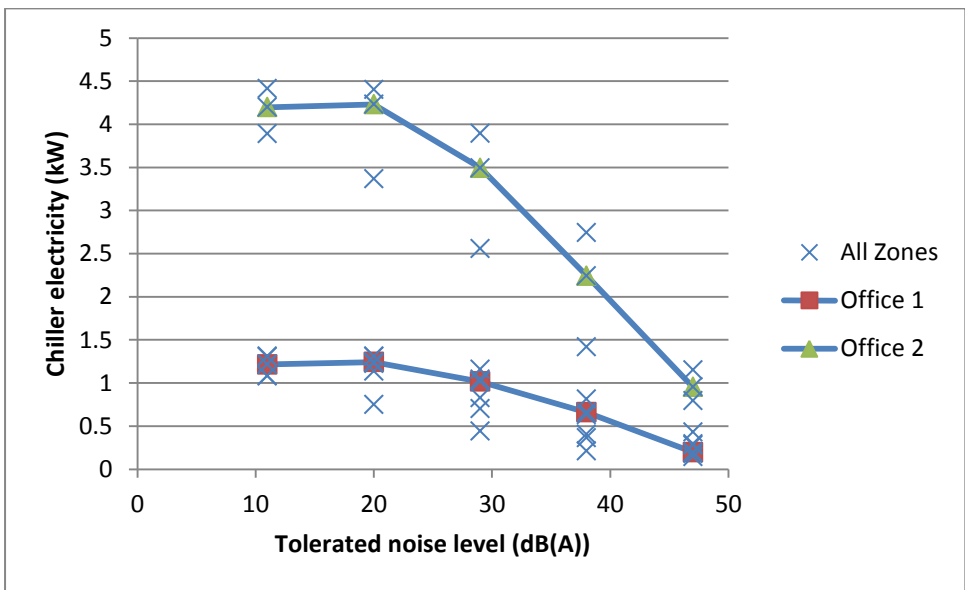


Figure 5.13. Zone level mixed mode cooling for Building 5.2 in Location B. Zones 1 and 2 from the 1st floor are highlighted.

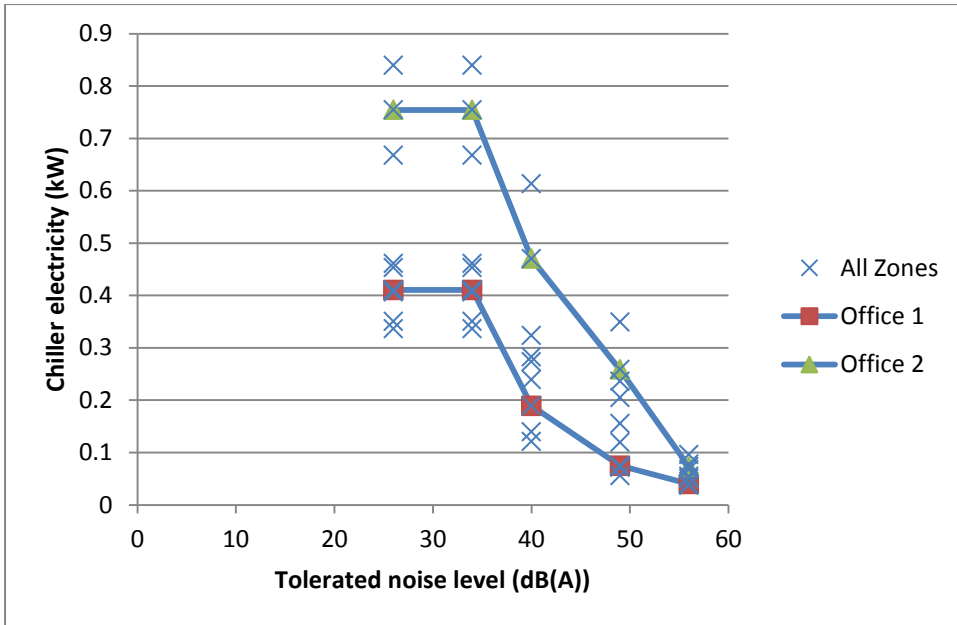


Figure 5.14. Zone level mixed mode cooling for Building 5.3 in Location A. Zones 1 and 2 from the 1st floor are highlighted.

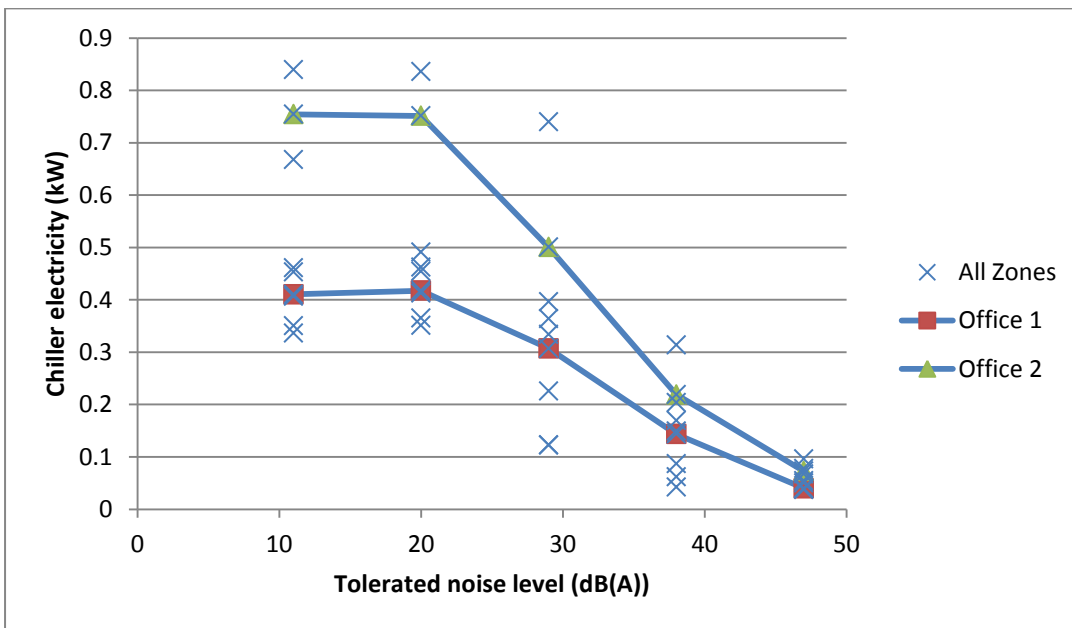


Figure 5.15. Zone level mixed mode cooling for Building 5.3 in Location B. Zones 1 and 2 from the 1st floor are highlighted.

From the above results it can be seen that the size of the acoustic affect is larger for Building 5.2 simply due to it having larger cooling loads. The gradient of the curves go up to a maximum of 0.238kW/dB compared to a much smaller maximum of 0.064kW/dB for Building 5.2. Higher gradients for the curves are important as it suggests where noise mitigation measures will have the most effect. The smaller building, Building 5.2 requires much less cooling, with full ventilation opening this building is close to being passive, and with some additional measures this could be achieved. For Office 2, Location B has a smoother curve than Location A, this is due to the noise exposure pattern and the orientation of this zone. A large amount of cross ventilation is possible for Office 2, but only when the opening pattern allows.

5.8 Discussion

A discussion of the new methods is conducted in this section. A key potential use of the gradients of the results curves (Figures 5.7 to 5.9) is to predict the appropriateness of adopting noise reduction methods. This quantifies how the acoustic requirements of a building can interact with the natural ventilation of a building and, in the case of mixed mode buildings, impact directly on the cooling load. The gradient of the curve is a useful output from this method, with higher kW per dB indicating situations where noise reduction measures would have most effect on the cooling load. As well as tolerated noise level window opening is controlled by the temperature set-points. There is a tendency for the results to follow a general shape shown in Figure 5.16.

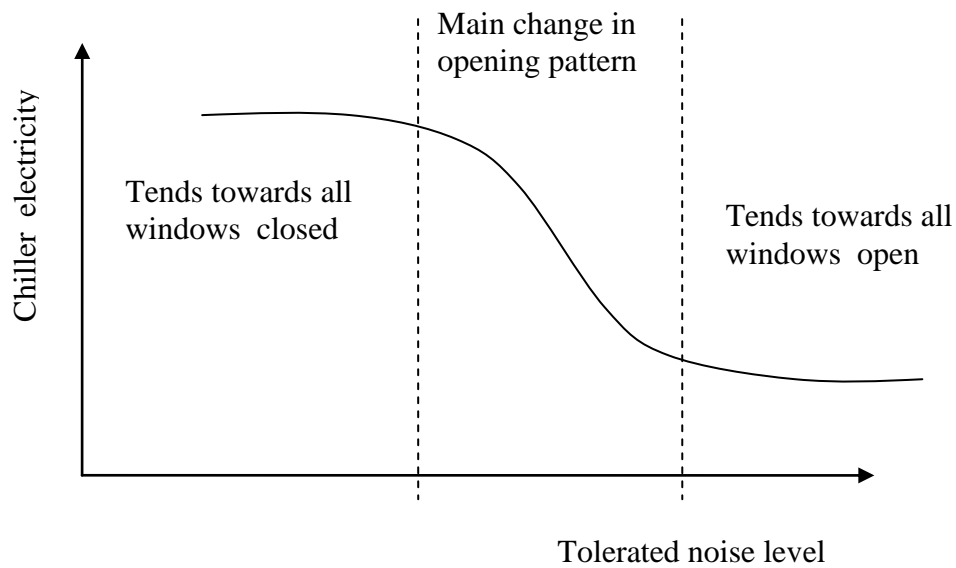


Figure 5.16. Representation of usual relationship between noise and mixed mode chiller use.

Figure 5.16 shows lower noise tolerances give a fully closed façade, as noise tolerances increase, more and more windows start to be open over the facade and the gradient of the curve steepens until there is a tendency towards maximum opening and the gradient flattens again. The most beneficial areas to implement noise mitigation measure would be in this middle section with a steeper gradient. It should also be noted that individual zones may not always follow this pattern of behaviour, due to local effects such as those illustrated in Figure 5.10.

This integrated approach could be automated within building energy calculation tools. The variation in these results demonstrated the importance of this approach when deciding where to adopt natural and mixed mode ventilation strategies and whether noise mitigation methods are worth adopting in specific cases. This is a particular issue where fixed acoustic criteria have been prescribed, as is the case for schools in the UK (Hopkins et al. 2003), where a

background noise level of 35dBA should not be exceeded. This can conflict in certain areas with the goal of reducing energy consumption and maintaining indoor air quality.

A simplification that has been used throughout this modelling is that the tolerated noise level is applied uniformly over the whole building. This is often not the case and the sensitivity to noise for many rooms would vary according to the activity going on there. The presentation of results in a whole-building curve would be complicated if this is un-even tolerance is incorporated. If the design of room locations with different noise tolerances was carried out, the method presented in this chapter could be applied iteratively to aid the organisation of the rooms. The results in Section 5.7.3 indicate the complexity of how uneven noise distribution affects the airflow patterns through a building. To increase natural ventilation the positioning of any noise reduction measures needs to take into account the way air predominantly flows through the building, as well as the noise exposure. The method presented in this chapter will be used in Chapter 7 to compare noise environment effects with those of climate change. Another issue that would affect the results is that the sound field in the room would not be perfectly diffuse. Someone working close to the window would likely experience different levels to someone on the other side of the room. This is a simplification used often used in acoustic design and is therefore thought to be appropriate for this study.

5.9 Conclusions

In conclusion the following has been accomplished in this chapter.

- Relationship between noise tolerance and thermal performance has been quantified.
- A 10dB reduction measure has been quantified in terms of thermal performance.

A method has been presented that integrates noise mapping techniques with building thermal modelling. The usefulness of this method was demonstrated for the consideration of ventilation potential for different locations, cooling energy consumption for the example buildings in the quieter noise locations were found to decrease by between 22% and 45%. Using the curves of noise tolerance against chiller electricity the example 10dB noise reduction measure was calculated to give up to a 44.8% decrease in chiller energy use.

6 Comparison of future weather data sets

In the previous chapter the results for cooling energy use were calculated with thermal building simulation driven by CIBSE TRY weather data (CIBSE & Met Office 2009b). These weather data were based on the historically observed records which aim to represent current climate. The future of the larger climate scales is considered in this chapter together with a number of options for the future weather data that represents this scale for building simulation. These options include different generations of climate projections, use of probabilistic percentile and how wind information is included. Options are compared so that a representative future weather data set can be assembled for the final comparison of acoustic and climatic environment factors. This comparison is of practical importance to building practitioners as weather data are widely used in practice, and any differences in future weather data will have direct implications for the modelling and design of naturally ventilated buildings.

Section 6.1, details the weather data sets that will be compared, and wind speed projection is then considered. An analysis of 11 member RCM wind speeds is presented in Section 6.2.1. The rest of the weather data comparison is undertaken with thermal building modelling and the example models and performance indicators are described in Section 6.3. Comparison results are presented in Section 6.4 before a discussion on the findings and conclusions end this chapter.

6.1 Details of the compared future weather data sets

In the literature review, a general background to the climate change projections was reviewed, and in this section details of the specific data compared in this chapter are covered. Two generations of climate projections (UKCIP02 and UKCP09), and the three weather data sets that are derived from them, are included here. Two weather data sets were developed by research groups affiliated with the ARCC network - COPSE (COPSE 2011) and PROMETHEUS (PROMETHEUS 2011). These use the UKCP09 weather generator outputs to produce simulation weather data. The third source was CIBSE future weather years (CIBSE & Met Office 2009b). Manchester was the chosen location for this study as all the required weather data were available and because it offers an alternative major urban location in the UK to London, which has been extensively analysed in recent years for climate change impacts.

This study concentrated on single-year hourly weather data sets that have been traditionally used as inputs for dynamic building simulation. Two types of weather file were used in this comparison from each source. The first were Test Reference Years (TRY), which are made up of typical months fitted together, and were used in this study for the comparison of building ventilation rates. The second weather file was the Design Summer Years (DSY), which represent near extreme years in terms of the summer temperature and was used in this study for the evaluation of overheating in Section 6.4.4. Methods for the production of these types of files are given by (Levermore & Parkinson 2006). Other proposed methods which use multiple year output from the UKCP09 weather generator, such as that proposed by (Jenkins et al. 2011), would not be as practical for this comparison due to the computational expense of running multi-zone airflow network models for large periods of simulation time. It is expected that yearlong reference sets of weather data will continue to be used to simulate

natural ventilation, as they are a robust representation of the climate and are appropriate to the resources typically available to professionals working in the built environment.

The CIBSE future weather years have a deterministic representation of climate change due to the type of projection available from the 2002 projections (UKCIP02). With the more recent UKCP09 climate projections introduced by (Murphy et al. 2009), a probabilistic approach has been adopted to give more information about the levels of uncertainty. Part of the output from these projections has been large volumes of synthetic weather data produced by a stochastic weather generator - see (Jones et al. 2009). Methods to use this synthetic weather data for building simulation have been a central part of a number of research projects associated with the Adaption and Resilience to Climate Change (ARCC) programme - more information on the projects can be found at the programme's website, (ARCC 2011). Some differences in approach to the incorporation of these climate change scenarios into single-year building simulation weather data have been developed, but the importance of these differences is unclear. One use of dynamic thermal building simulation is to determine whether a natural ventilation strategy is sufficient for maintaining building comfort conditions. The avoidance of mechanical cooling whenever possible will continue to be a priority, both now and in the future. This is indicated by a recent act that aims to reduce energy consumption in the built environment, the Energy Act (DECC 2011) of October 2011. There is a need, therefore, to evaluate the differences in natural ventilation characteristics due to the type of climate change information available.

6.1.1 UKCIP02

The CIBSE future weather years (CIBSE & Met Office 2009b) incorporate the UKCP02 climate scenarios (Hulme & Jenkins 2002) into the CIBSE TRY and DSY weather files by the morphing method described by (Belcher et al. 2005). The simplicity of this method has made it attractive for building evaluation and the consistency between weather variables, which is present in the original data, and which is likely to be preserved in the morphed version. Although there is an intention to update these CIBSE weather files by incorporating the later UKCP09 projections, the UKCP02 versions were included in the comparisons for reference. This was done through the adoption of CIBSE future weather years in the building simulation undertaken in Section 6.4 and directly by comparing wind speed change factors in Section 6.2.3. Additional details of the two sets that are derived from the UKCP09 projections are given in the next section.

The period used for the production of the latest CIBSE TRY weather data was from 1983 to 2005 i.e. close to the present. CIBSE weather files were also used as the baseline weather data in the future performance analysis of a case study building carried out with dynamic building simulation as part of the study by (Jentsch & Bahaj 2008). Their aim was to consider future proof options to avoid or reduce mechanical cooling in their case study building. To do this future weather files were produced using the weather generator tool produced by Jentsch & Bahaj. This tool incorporates the UK Climate Impacts Program (UKCIP) 2002 projections (Hulme & Jenkins 2002) by the morphing method (Belcher et al. 2005). A similar method was used to produce CIBSE's own future weather data (CIBSE & Met Office 2009b) and this is one of the data sets used in the comparisons presented in this chapter.

6.1.2 UKCP09

Rather than a deterministic projection, UKCP09 adopts a probabilistic approach, which means projections are based on climate model ensembles and an indication of the weight of evidence for particular climate outcomes are given. For weather data on a daily and hourly timescale a stochastic weather generator is available, reported by (Jones et al. 2009). The two sets (PROMETHEUS and COPSE) incorporating the projections from UKCP09, are made up of TRY and DSY weather files produced from the stochastic weather generator output. From the weather generator up to 100 daily or hourly time series, each 30 years long and representative of a single emission scenario and a future period, were available. The weather generator first produces rainfall data calibrated from the historical baseline period as the primary variable and then other variables are produced using inter-variable relationships as well as the climate change factors from UKCP09.

Both PROMETHEUS and COPSE data sets were produced from these 3000 year (100×30years) UKCP09 weather generator outputs with reference to the methods of TRY and DSY production by (Levermore & Parkinson 2006). COPSE and PROMETHEUS were based on different runs of the weather generator, which means that although these different runs were statistically equivalent the data at each point in time would be expected to be different due to the nature of the stochastic process. Differences in method also arose due to the representation of the wind and the climate change percentile grouping of the data from which the DSYs and TRYs were produced. These differences are examined in the sections following 6.4.1.

6.2 Wind speed projection

Wind has been a problematic variable in the UKCP09 set of climate projections due to the uncertainty in the future behaviour of this variable; it has therefore been excluded from the main UKCP09 outputs. Wind is a key driver of natural ventilation and although stack effect could be looked at in isolation of short periods for extended simulation of summer performance wind is required, for this reason issues relating to this variable will be focused on in the first sections of this chapter. From Section 6.4 onwards three weather data sets are compared and differences in wind representation and building ventilation characteristics identified, such as which data set resulted in the highest air exchange rates. In addition, the key relationships between external temperatures and overheating were investigated and differences between the weather data sets established. Where possible, differences will be related to the future weather methodologies. The comparisons in this chapter are undertaken to determine differences in future weather files so that in the final chapter design implication for future changes in climate can be investigated and quantified along with acoustic environment influences.

Values for wind speed were generated as part of the weather generator process but were not released as a matter of policy due to concerns about the projections for this variable. It was said by (Murphy et al. 2009) that wind speed projections had a high degree of variation and a lack of systematic change. This is possibly not surprising given the high natural variability of wind behaviour. The fact still remains that wind data are required to enable natural ventilation to be modelled. Wind can be important to building heat flow, particularly if the external air temperature is significantly different from the internal temperature. The lack of wind data from the weather generator output means that this source cannot be directly used for many thermal building simulation purposes.

Two approaches to investigating future wind are covered in this chapter - one is to access the 11 member RCM data for wind speed directly, and the second is to backward calculate wind from Potential Evapotranspiration (PET) variable ($\text{mm}\cdot\text{day}^{-1}$) (Ekström 2007). This variable is included in the weather generator output. The second approach is necessary as it is important that there is consistency between the other variables and wind speed. This is necessary because dynamic building energy models can attempt to control temperatures by the natural ventilation behaviour of building occupants and control systems (i.e. operation of natural ventilation or window openings). If the occurrences of high winds in the weather data coincide to an abnormal degree with heat waves then an unnatural representation of the natural ventilation could occur. Part of the stochastic weather generator process is the maintenance of inter-variable relationships, so the consistency across variables is considered. As wind speed was not a direct output of the UKCP09 weather generator the production of weather data for dynamic building simulation has required the calculation of wind speed from another variable, PET. Before results for building simulation are presented the RCM results for wind speed will be investigated.

6.2.1 11 member Regional Climate Model

The first analysis of future wind projections in this chapter is conducted with the raw RCM ensemble output data on which UKCP09 was partly based - this was accessed via the LINK project (BADC et al. 2008). This source provides 11 perturbed physics projections from the HadRM3, which has an approximately 25km horizontal resolution (Murphy et al. 2009). Each member of the ensemble is driven by the same historical and SRESA1B future emissions scenario from (Swart & Nakicenovic 2000), with one unperturbed member and 10 members with different perturbations to the atmospheric parameters. The standard atmospheric forcing includes historical levels of greenhouse gases (including methane),

sulphur and tropospheric/stratospheric ozone. The downsides to this source were that, firstly, it is not possible to check where in the probability distribution each RCM projection lies. Secondly, this ensemble represents a smaller range of sampled uncertainty than the main projections which includes modelling from a number of institutions.

Due to the variety of interests and perspectives that users of the HADRM3 data have, a number of different data formats and arrangements are used. The data were available in a number of formats CSV format is formatted data separated by commas and this was chosen as it was the most intuitive. Although CSV format data was somewhat cumbersome it didn't require the learning of new software. The data within the CSV files were not organised in a format that was very convenient for the calculation of wind speed change factors for a single location. The processing entailed accessing the large archives of compressed files within compressed files, both .tar and .zip compressed archive formats were used. Each RCM variant had a .tar file each with 1800 .zip files within it; each of these had 30 separate CSV files representing a day of the modelled period. This data set had been through several iterations of format conversion due to the range of interested parties, including the climate modelling research community, and also a range of people interested in more information about future wind speed after it had been omitted from the UKCP09 projections.

Other weather variables were available from this data set but wind speed was the only one extracted for this chapter as it was the missing variable from the weather generator output and particularly relevant to natural ventilation. A small macro program was written by the Author in BASIC which first read the required data from the large number of CSV files, before climate change factors were calculated. This is the recommended procedure, as was the case

for UKCIP02, where relative changes are calculated so that modelling biases are reduced. Relative changes from the control period of 1960 to 1990 to a number of future time slices were calculated following the UKCP convention (Hulme & Jenkins 2002). Each daily CSV file had to be accessed so that the wind speed for the Manchester grid square (1235) could be read. This was done for the entire modelled time and for all 11 variants, amounting to 594000 files that needed to be accessed.

6.2.1.1 Comparison of ensemble variant wind speed change

The initial analysis focuses on change in wind speed; Figures 6.1 to 6.4 show the percentage change in wind speed for each month of the year. Monthly percentage change is used, which is the same as UKCP02, and gives an indication of changes to wind speed across the seasons. This is the percentage change in wind speed between the 1960-1990 period (control period) and the future climate period. Each climate period covers 30 years by convention and future climate periods are labelled with the middle decade. The 2020's are shown in Figure 6.1 and this covers the period from 2010 to 2030.

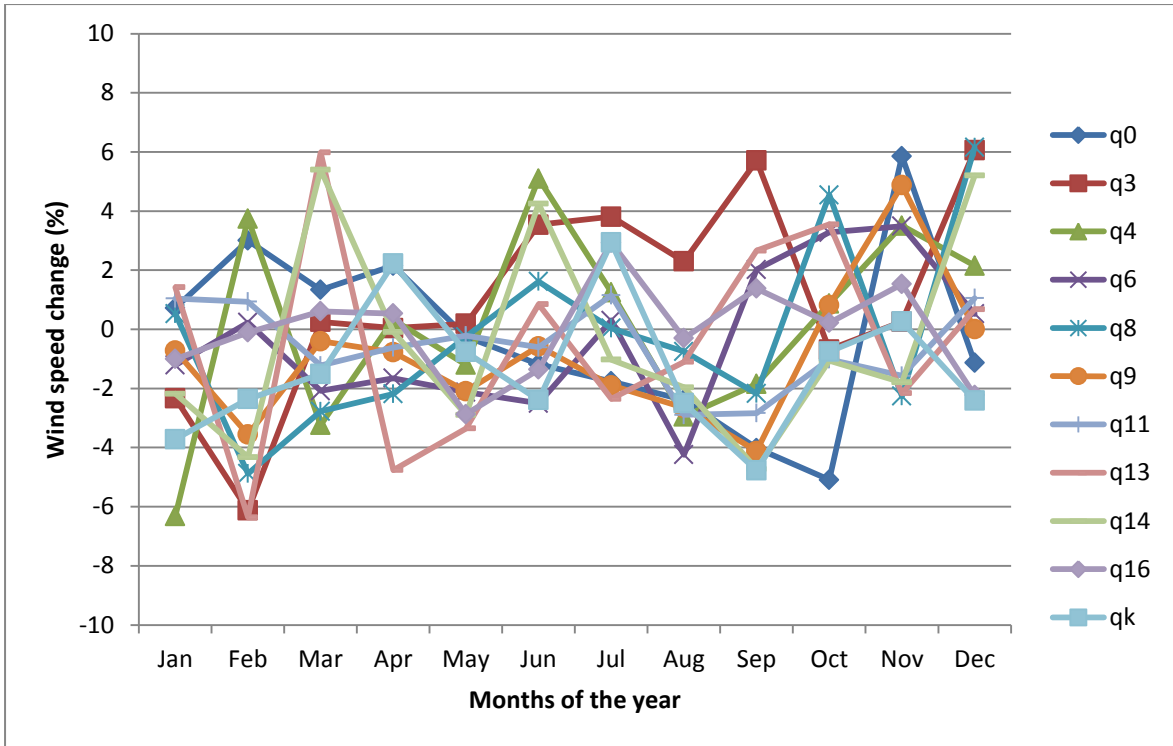


Figure 6.1. Change in wind speed between the control period and 2020 time period, for the 11 RCM variants which are indicated in the key.

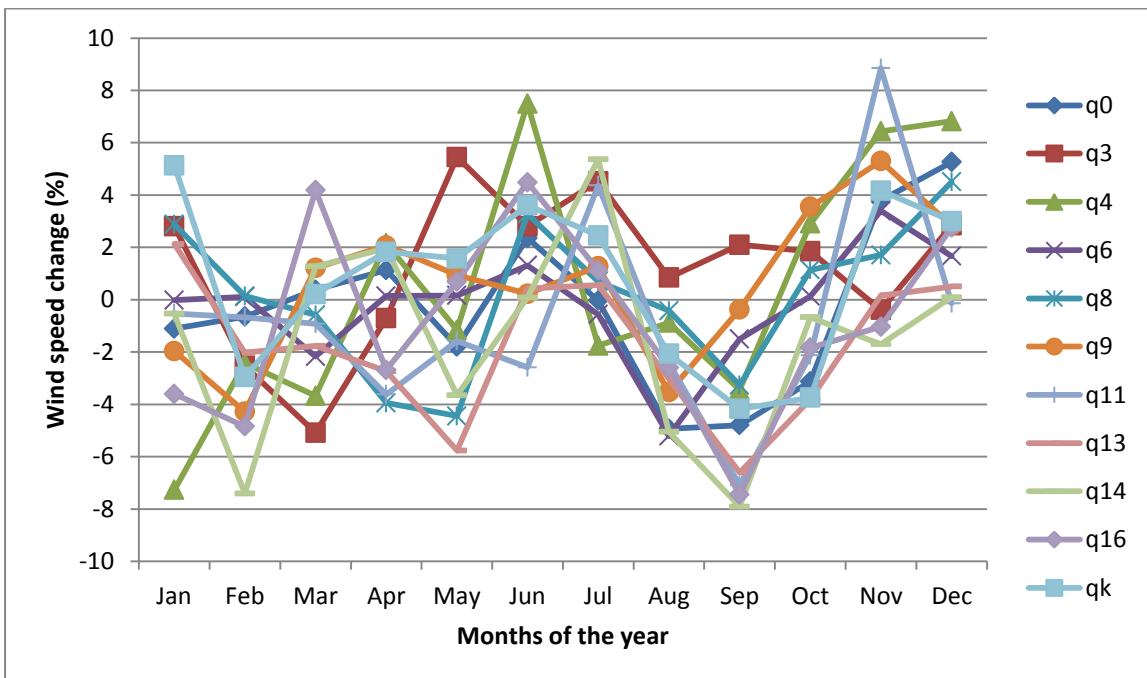


Figure 6.2. Change in wind speed between the control period and 2050 time period, for the 11 RCM variants which are indicated in the key.

By comparing Figures 6.1 and 6.2 it can be seen that some change in the profile occurs across the months. The overall mean change in wind speed is very small for both of these two time slices, with the 2020's showing a -0.30% reduction and a -0.21% reduction for the 2050's. However, the scatter is very large, with a substantial number of variants showing positive change in wind speed. Both figures have low linear regression coefficient with R^2 of 0.052 and 0.042 respectively. The spread of results increases into the future which is further illustrated by the increase in standard deviation in change in wind speed rising from 2.79 for the 2020's to 3.36 for the 2050's. The spread of the results is illustrated by the error bars in Figure 6.3.

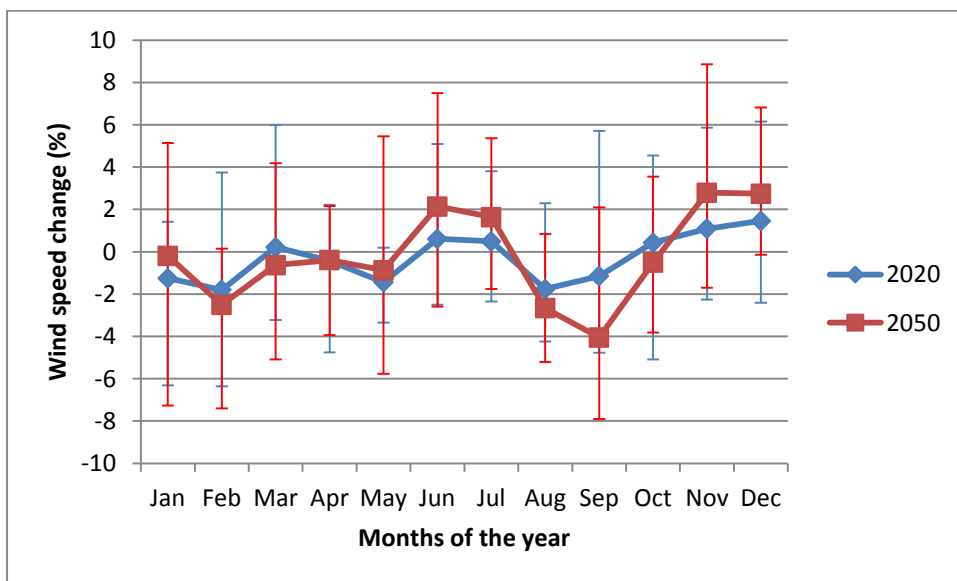


Figure 6.3. Change in wind speed between the control period and the time period indicated in the legend, for the 11 RCM. Error bars indicating scatter across the 11 member RCM.

The largest reduction in wind speed occurs around September for the 2050's, with this pattern becoming more pronounced for the 2080's. This final time slice is illustrated in Figure 6.4 where a further level of deviation from the yearly mean change can be seen, with the standard deviation rising to 3.82 for the 2080's.

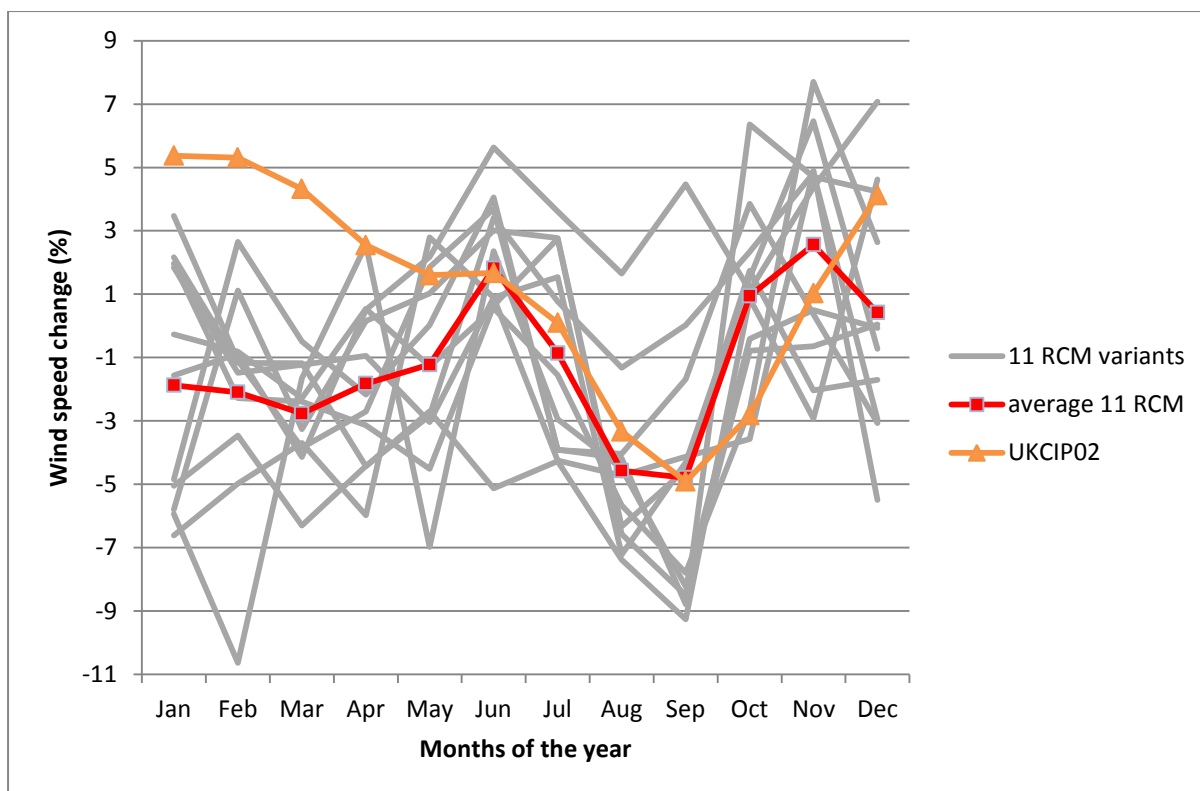


Figure 6.4. Change in wind speed between the control period and 2080 time period, for the 11 RCM variants and UKCIP02 which are indicated in the key.

The overall mean change in wind speed for the 2080's is a reduction of -1.19%, with the lowest negative change occurring around September. As well as the 11 RCM members plotted in grey, Figure 6.4 also shows the average monthly change across the variants and the single deterministic projection from UKCIP02. The agreement between the UKCIP02 change for this September low point is good but a relatively substantial difference of up to 7.4% occurs at the beginning of the year. This is likely due to developments in modelling techniques influencing the projected change in wind speed - an example of this is the incorporation of carbon feedback. Overall, it can be said from Figures 6.1 to 6.4 that the change in wind speed is strongly affected by the ensemble variants. The variation is significant with little agreement about whether change will be positive or negative for wind speed. This illustrates part of the reason why wind was excluded from the UKCP09 output. It

should also be noted that for other weather variables, such as temperature, there are clearer and more systematic trends. Information on these variables is best gained direct from UKCP09 outputs.

6.2.1.2 Climate sensitivity

Each RCM variant has a climate sensitivity associated with it that comes from the slab model (HadSM3) with the same physics perturbations as the variant of HadCM3 used to drive the RCM ensemble member. The HadSM3's climate sensitivity is defined by Rougier et al. (2009) as: the equilibrium change in globally averaged surface temperature following a doubling of the atmospheric concentration of CO₂. The following sensitivities for the 11 model variants are given in Table 6.1. These sensitivities are then plotted against wind change factors in Figure 6.5; this illustrates any correlation between climate forcing and change in wind speed.

Figure 6.5 shows some indication of a reduction in wind speed with increasing climate sensitivity, although the correlation is very poor, with an R² of 0.0802. Relationships between temperature effects on the atmosphere are complex and it would appear that there is no basis for such simple relationships. The later comparison of the RCM ensemble wind speed changes with the other data sets (in Section 6.2.3) will include only the upper and lower bounds across all the RCM variants. This comparison will include weather generator data, for which a method to backward calculate wind speed was required.

Table 6.1. Details of the 11 member RCM ensemble taken from (BADC et al. 2008).

RCM run ID	Climate Sensitivity (K) of corresponding HadSM3 variant	RCM name
afgcx	3.53	HadRM3Q0
afixa	2.58	HadRM3Q3
afixc	2.81	HadRM3Q4
afixh	3.43	HadRM3Q6
afixj	3.89	HadRM3Q8
afixi	4.39	HadRM3Q9
afixm	4.54	HadRM3Q11
afixo	4.79	HadRM3Q13
afixl	4.88	HadRM3Q14
afixq	7.11	HadRM3Q16
afixk	4.44	HadRM3Qk

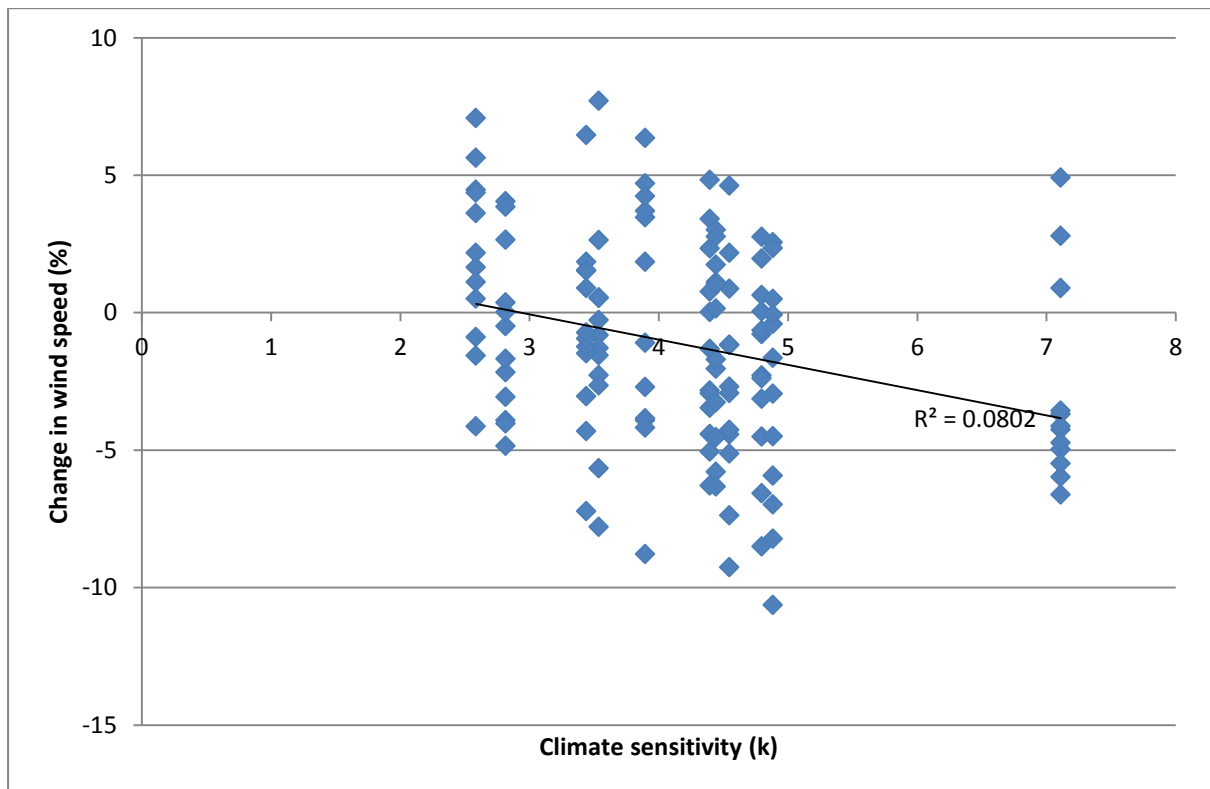


Figure 6.5. Ensemble variant change in wind speed plotted against climate sensitivity.

6.2.2 Wind from weather generator potential evapotranspiration

Wind speed from the weather generator needed to be calculated from PET so that inter-variable relationships between wind speed and the other weather generator variables could be preserved. Both the COPSE and PROMETHEUS data have wind speeds that were determined by the rearrangement of the equation from (Ekström 2007), upon which the algorithm used by the weather generator to calculate PET is based. This uses the net radiation at the crop surface, soil heat flux, mean temperature at 2m height, characteristics of the vapour pressure, and a number of constants, along with the wind speed at 2m height to calculate PET. The wind speed is the aim of the backward calculation but even after this has been calculated a number of additional steps are required. Daily time series for PET produced a consistent daily wind speed from which hourly values and a wind direction had to be produced. This was achieved through different methods for PROMETHEUS (Eames et al. 2011b) and COPSE (Watkins et al. 2011).

The COPSE and PROMETHEUS data are produced from different runs of the weather generator so instantaneous differences between the data sets should be expected due to the stochastic processes represented. The underlying statistical characteristics of the data from the weather generator should be preserved and therefore the main differences between COPSE and PROMETHEUS wind data should be due to the methods used after the backward calculation from PET. In this section the details of the two methods used to derive simulation weather data from the UKCP09 weather generator will be explained and the approach for a comparison outlined. The first issue to be dealt with after backwards calculation is cleaning of data points that do not give realistic wind speeds. There is an issue with the UKCP algorithm occasionally producing negative values of PET. This is not physically possible and therefore these data points are truncated to zero causing wind speeds which are non-realistic

after backward calculation. Both COPSE and PROMETHEUS deal with this issue in a similar way, and that is to ignore these data points and linearly interpolate from the remaining adjacent days. The similarity of the approaches for this issue means it should not result in differences between data sets.

There are some differences in the additional selection of data points to exclude; the COPSE method also excluded negative values of wind speed. PROMETHEUS focused on occasions where the differential of PET is high compared to the wind speed - this was due to PET values being rounded to two decimal places which caused errors for these cases. Both methods were tested on non UKCP09 data and calculated values of wind speed compared to observed wind speeds. For the COPSE data 94% of days were reported to be within 10% of the actual wind speed. For PROMETHEUS, 94% of the data was reported to be within 5% of the observed wind speed. Most excluded points were concentrated in the wintertime due to humidity, so in terms of natural ventilation calculation this is of less concern as natural ventilation calculations, such as those conducted in Sections 6.4.1 and 6.4.2, are conducted over the summer months.

Hourly data were recovered in the PROMETHEUS method by using observed hourly wind signals from the 1961 – 1990 base period for the weather station closest to the weather generator 5km grid reference point. The daily mean observations for the appropriate season are compared to the weather generator daily wind speed value. The observed hourly time series for which the deviations are least is chosen as the most representative. Historical recorded wind speed was also used in the COPSE method where the hourly profile was normalised and applied to the daily mean. In addition, some random variability was

introduced, below zero wind speeds were changed to zero and, finally, the 24 hourly values adjusted so the daily mean matched the PET derived value.

No information is available on the future wind direction, with this requiring more certainty about the future behaviour of the pressure systems that, to a large degree, determine the prevailing wind direction. Due to this, both methods have to assume that the relationships between wind direction, wind speed and season will stay the same as for the observed time period. In the COPSE method a frequency analysis was undertaken for 10° segments of the compass, for each month of the year over the 10 year observed period. A month's wind direction was then chosen that had the smallest sum of differences between it and the whole 10 year period for that month. The PROMETHEUS approach for wind direction was somewhat different - every six hours a wind direction is randomly generated and constrained by the probabilistic distributions of wind direction with wind speed and season. A linear relationship is then assumed between these generated wind direction values at six hour intervals and from this a complete hourly time series is produced.

As part of a validation of the PROMETHEUS method presented by (Eames et al. 2011b) fifteen TRYs were created from observed weather data using their method of pseudo wind generation. The pseudo wind was compared statistically with the observed wind data and also by means of thermal building models. From the statistical comparison it was found that the pseudo wind speed distributions were very close to the originals with the differences in distributions not being statistically significant. As well as a statistical comparison, these fifteen TRYs were compared by their use in thermal building models. This is one of the main reasons for the procedure in the first place, to allow a comparison of natural ventilation rates.

Thermal building simulation with airflow calculation was carried out for a number of buildings and all the fifteen TRY files. It was found that average differences in flow were very small between all the TRYs. Instantaneous differences could be high but the natural variability of the wind is much greater than that of the wind field generated by the PROMETHEUS method.

This validation gives some reassurance that this method produces acceptable wind data. A further investigation of this synthetic wind data will be conducted in the next sections of this chapter, along with a comparison of the alternative COPSE method and the previous generation of UKCP02 climate change weather file (CIBSE future weather years). As well as air flow characteristics of case study buildings, similar to that presented by the PROMETHEUS validation, overheating performance indicators will be examined. The differences between wind direction representations are investigated in Section 6.4.2, where wind direction frequency about the compass is analysed and the sensitivity of building natural ventilation to perturbations of the wind direction are investigated. The first step of the comparison will be a comparison of percentage change in wind speed for all weather data sets considered in this chapter.

6.2.3 Comparison of change in wind speed

Before the use of dynamic building simulations a direct comparison of the percentage changes in wind speed was carried out – see Table 6.2. The wind speed change factors between the control period (1960 to 1990) and the 2050's and 2080's for the PROMETHEUS, COPSE and CIBSE TRY weather data sets are given. Also included are the

upper and lower bound change factors for all variants of the HARM3 ensemble (BADC et al. 2008) which represent change relative to the 2080s.

Table 6.2. Monthly wind speed change factors (%).

	Jan	Feb	March	April	May	June	July	Aug	Sep	Oct	Nov	Dec
PROM. 2050	9.60	-3.25	-5.34	-1.44	16.59	3.48	-1.14	-13.60	6.69	-1.47	3.92	1.44
PROM. 2080	17.37	11.67	-11.89	2.94	15.71	-14.96	0.46	-10.12	-8.49	-10.45	3.31	-1.14
COPSE 2050	7.84	3.35	-1.86	-2.25	3.46	0.47	-11.68	-9.39	-3.43	-15.74	-2.22	18.76
COPSE 2080	-5.96	0.59	-9.22	1.97	1.11	-4.61	0.69	-18.41	-2.20	-9.79	-6.58	10.99
CIBSE 2050	3.1	3.06	2.49	1.47	0.92	0.97	0.06	-1.92	-2.83	-1.63	0.59	2.38
CIBSE 2080	5.37	5.31	4.32	2.55	1.6	1.67	0.1	-3.33	-4.91	-2.82	1.03	4.12
RCM upper	5.14	1.12	5.98	3.52	2.79	5.08	5.36	-0.30	2.66	3.55	4.91	5.20
RCM lower	-7.96	-10.63	-6.29	-5.98	-6.97	-5.57	-5.70	-8.17	-9.26	-6.71	-4.96	-5.49

PROMETHEUS and COPSE show a greater range of change factors from month to month, up to 18% compared to the same months of the control period. This can be seen as mainly a product of the stochastic weather generator’s representation of the natural variability in wind speed. Over the summer period this evens out to changes of 1.7% and -3.8%, which are within the range represented by the RCM upper and lower bounds. The average change over the summer time period for the CIBSE weather files was -0.4%. This was well within the range of the more recent climate ensemble which, although it indicates a high degree of variation for Manchester, was consistent with changes for other UK locations (Brown et al. 2009). Looking across all the periods (future and control) the average summer wind speed for both COPSE and PROMETHEUS was the same at 4.2m/s, illustrating that they derive from the same weather generator source, and for CIBSE it was 3.7m/s.

6.3 Comparison method

A key use of dynamic thermal building simulation is to determine whether a natural ventilation strategy is sufficient to maintain a building's comfort conditions and if the use of mechanical cooling can be avoided. So far comparisons have been made directly between the wind change factors from the climate projection. In the following sections, results will be presented that compare natural ventilation characteristics due to the adoption of the three different simulation weather data sources. This comparison is undertaken with two example buildings modelled using the dynamic building simulation software DesignBuilder (DesignBuilder Software Ltd 2009). DesignBuilder uses as its calculation engine EnergyPlus, a powerful thermal simulation package developed by the USA's Department of Energy which has been widely used and validated, for example by (Henninger & Witte 2009).

6.3.1 Example building models

The two example building models developed for this comparison are illustrated in Figure 6.6. The buildings were modelled as free running (no mechanical cooling) and simulations were run over a spring / summertime period from April to September. Natural ventilation rates were calculated utilising the EnergyPlus network airflow model, which is based on COMIS (LBNL 2010). Weather station wind speed is adjusted according to the method given in the ASHRAE Handbook (ASHRAE 2009) and using coefficients representing suburban terrain to give the local wind speed. In contrast to the example buildings used in Chapter 5, these buildings are free-float meaning no mechanical ventilation is utilized.

Example Building 1 was used for the comparison of air exchange rates. It is a long office building and is shown in Figure 6.6(A). The footprint is 65.4m × 13.4m and the building

consists of 45 zones, 25 of which are offices. For part of the comparison a natural ventilation set-point temperature of 24°C was used, which is a mid-value of the range of internal comfort temperatures for naturally ventilated buildings from (de Dear & Brager 2002). 30% of the façade of Building 6.1 is glazed, with 5% of this window area being assumed to be opened once the ventilation set-point is reached. Example Building 6.2 was used in the comparison of overheating and is shown in Figure 6.6(B). This is a simple three storey office building with a footprint of 13m × 13m; the building has 18 zones, 9 of which are offices. A number of passive measures have been incorporated to reduce the risk of overheating, including solar shading (depth of 1m), 30% of window area being openable and night ventilation.

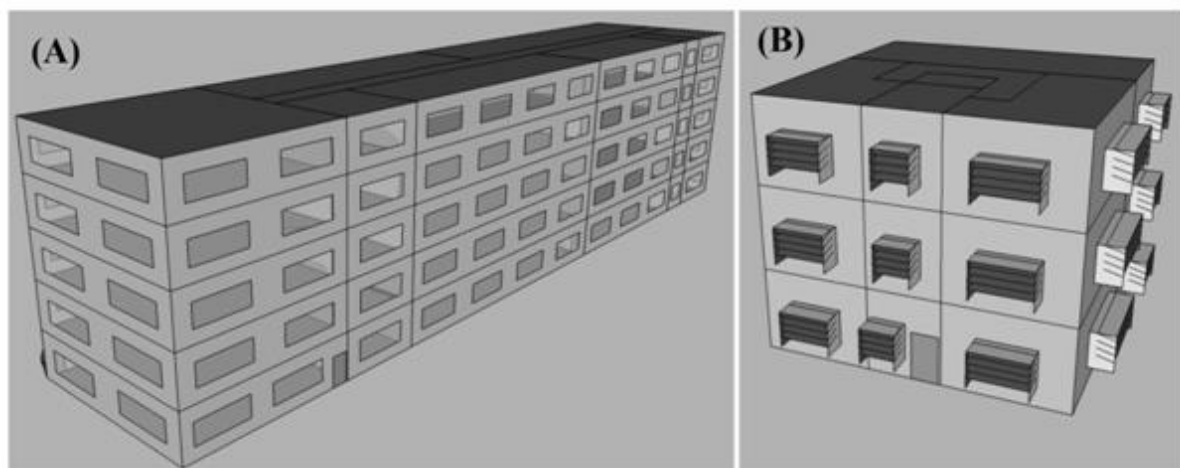


Figure 6.6. Representation of example buildings used in the study. (A) is Building 6.1 and (B) is Building 6.2 (note solar shading).

For both building models all windows were openable, which can be related to the noise exposure of the building facade and the tolerance of the occupants to noise by the methods presented by (Barclay et al. 2012). Depending on the tolerance to the surrounding noise

environment of the occupants, noise reduction measures may be necessary to ensure that the required levels of ventilation openings in these example buildings can be achieved.

6.3.2 Adaptive comfort

One performance indicator used in this chapter is overheating relative to an adaptive comfort overheating threshold. Adaptive comfort performance indicators are used for the results reported in Section 6.4.4. Information about this concept and how calculations are made for adaptive comfort are also discussed in this section.

The underlying concept of adaptive comfort is that people interact and adapt to their environment. Examples of this might be the changing of clothing, using a fan or opening a window to increase air movement. Various factors shape peoples adaptation of thermal comfort. According to Brager & de Dear (2000) these can be grouped as physiological, behavioural and psychological. Physiological adaption (which is also sometimes called acclimatization) means the biological response from prolonged exposure to relatively extreme temperatures. An example of this is the fall in the temperature that sweating is triggered at in hot climates.

Behavioural adaption refers to the actions people take to change their thermal balance, such as a change in clothing or adjusting a thermostat. The psychological component refers to the perception of thermal comfort and relates to a subject's expectations. Some degree of behavioural adaptation is represented in the percentage mean vote model via the description of clothing insulation and air movement. However, the results presented by de Dear and

Brager (2002) suggest that this does not account for all the evidence of adaptation for the occupants of naturally ventilated buildings. Rather than just considering the micro climate that effects the heat exchange of the occupants, adaptive comfort models predict comfort from a broad range of contextual factors including those connected to outdoor climate.

Studies involving the analysis of a large number of buildings in various climates around the world led to the revision of ASHRAE 55 (de Dear & Brager 2002). The creation of a standard for the collection of thermal comfort data and the adoption of this standard by a number of researchers around the world meant a large database was available for analysis. The main outputs from this analysis were weighted regressions of indoor thermal comfort temperature against the mean outdoor temperature. This was done for HVAC and naturally ventilated buildings with the regression lines being compared to the lines given by the Fanger percentage mean vote model. This regression between indoor comfort temperature and outdoor temperature represents the basis of the adaptive comfort model.

For HVAC buildings the adaptive comfort model fits very well with the traditional percentage mean vote model but for naturally ventilated buildings there are some distinct differences. The gradient of observed indoor comfort temperature against outdoor temperature is steeper for naturally ventilated buildings than for those with air conditioning. This suggests that occupants of air-conditioned buildings become more used to relatively constant conditions and prefer less deviation from this narrower set of conditions. For the occupants of naturally ventilated buildings a wider range of conditions that reflect outdoor conditions are said to be preferred.

One adaptive thermal comfort model discussed in the literature review was given in ASHRAE 55 (ASHRAE 2004), an alternative standard to this standard is the European standard BS EN 15251:2007 (CEN & BSI 2007). The main difference between the two standards is that instead of mean monthly external dry bulb temperature the European standard employs an exponentially weighted running mean Θ_{rm} . The expressions for the upper and lower limit of the 90% acceptability criteria are given in Table 6.3. The explanation of the applicability of these categories is given in Table 6.4.

Table 6.3. Category temperature limits (Θ_{max}) reproduced from Annex A of (CEN & BSI 2007) equations defining Θ_{rm} are given in the text.

Category I	Upper limit	$\Theta_{max} = 0.33\Theta_{rm} + 18.8 + 2$
	Lower limit	$\Theta_{max} = 0.33\Theta_{rm} + 18.8 - 2$
Category II	Upper limit	$\Theta_{max} = 0.33\Theta_{rm} + 18.8 + 3$
	Lower limit	$\Theta_{max} = 0.33\Theta_{rm} + 18.8 - 3$
Category III	Upper limit	$\Theta_{max} = 0.33\Theta_{rm} + 18.8 + 4$
	Lower limit	$\Theta_{max} = 0.33\Theta_{rm} + 18.8 - 4$

Table 6.4. Explanation of categories reproduced from (CEN & BSI 2007).

Category	Explanation
I	High level of expectation and is recommended for spaces occupied by very sensitive and fragile persons with special requirements like handicapped, sick, very young children and elderly persons
II	Normal level of expectation and should be used for new buildings and renovations
III	An acceptable, moderate level of expectation and may be used for existing buildings
IV	Values outside the criteria for the above categories. This category should only be accepted for a limited part of the year

The running mean Θ_{rm} is defined as follows (CEN & BSI 2007).

$$\Theta_{rm} = (1 - \alpha)\{\Theta_{ed-1} + \alpha\Theta_{ed-2} + \alpha\Theta_{ed-3} \dots\} \quad (6.1)$$

where Θ_{ed-1} is the daily mean external dry bulb temperature for the previous day, Θ_{ed-2} is the daily mean external dry bulb temperature for the day before and so on, α is a constant between 0 and 1 with 0.8 being recommended. The following approximation can also be used (CEN & BSI 2007).

$$\Theta_{rm} = (\Theta_{ed-1} + 0.8\Theta_{ed-2} + 0.6\Theta_{ed-3} + 0.5\Theta_{ed-4} + 0.4\Theta_{ed-5} + 0.3\Theta_{ed-6} + 0.2\Theta_{ed-7})/3.8 \quad (6.2)$$

The two standards were compared with respect to building energy use using a novel adaptive comfort degree day method developed by McGilligan et al. (2011). The European adaptive comfort standard was identified as having more energy saving potential compared with the ASHRAE 55. Annex F of the European standard states that the comfort conditions over time (season, year) can be based on a summation of parameters. These could be based on data measured in real buildings or dynamic computer simulations. A method that was suggested to evaluate comfort is to determine the percentage outside the comfort range. This involves calculating the number or % of occupied hours (those during which the building is occupied) when the percentage mean vote or the operative temperature is outside a specified range.

6.3.3 Performance indicators

The performance indicators used in this study were the air exchange rate in terms of the number of room ACH and the percentage of time temperatures were above a thermal comfort threshold. The air exchange rate is important for air quality and can have a strong influence on internal temperatures and thermal comfort, depending on the external temperatures. Due to

the dynamic nature of temperature changes in a building, overheating is usually defined as a proportion of time above a threshold temperature (CIBSE 2007). Two such threshold temperatures were used for the results in this chapter.

- 28°C from CIBSE Guide A (CIBSE 2007), which describes an office building as overheating if this temperature is exceeded for more than 1% of the occupied hours.
- Category II adaptive comfort temperature from European standard BS EN 15251:2007 (CEN & BSI 2007), which has a predicted percentage dissatisfied value of 10% and is recommended for new buildings.

The adaptive comfort temperature varies with the background climate and it aims to describe the thermal experience of occupants better than a single temperature; the adaptive comfort threshold temperature Θ_{\max} is defined in the following way.

$$\Theta_{\max} = 0.33\Theta_{\text{rm}} + 21.8 \quad (6.3)$$

The running mean Θ_{rm} definition from equation (6.1) is simplified to:

$$\Theta_{\text{rm}} = (1 - \alpha)\Theta_{\text{ed-1}} + \alpha\Theta_{\text{rm-1}} \quad (6.4)$$

where $\Theta_{\text{rm-1}}$ is the running mean calculated for the previous day, $\Theta_{\text{ed-1}}$ is the daily mean external dry bulb air temperature for the previous day, and α is a constant between 0 and 1, with 0.8 being recommended. Each Θ_{rm} becomes the $\Theta_{\text{rm-1}}$ for the next day.

Equations (6.3) and (6.4) were incorporated into a BASIC program written by the author to determine the threshold temperature at each day of the year, based on the external temperature history. Hourly dry bulb temperature data were averaged to a daily mean then used to calculate the running mean. Due to the running mean using temperature from the preceding days, at the start of the year (1st of January) this information is not available from a

weather file. The first seven days can be used according to the approximation given in equation (6.2). The effect of the initial year start condition was investigated by looking at the speed of convergence. This was tested by comparing the adaptive comfort temperature calculated with the seven day approximation with an adaptive comfort temperature calculated with a running mean temperature starting at zero. This can be seen as a worst case scenario for a running mean starting temperature. It was found that the convergence of these two adaptive comfort temperatures to within one decimal place occurred within a month. As overheating calculations were focused on the summer time, it was concluded that this was not an issue, although it may be relevant to winter thermal comfort.

It should be noted that there is no current guidance on what percentage of time an adaptive comfort model needs to be exceeded by to constitute building overheating. The European standard was identified by McGilligan et al. (2011) as having the most energy saving potential compared with ASHRAE 55 (ASHRAE 2004). Also, the European adaptive threshold temperature was thought to be more sensitive to climatic changes as it employs a running mean reference temperature that is continually changing and was felt to be more appropriate for this comparison of weather data. The performance indicators from the simulation of the example buildings were produced for thermal zones across the building at each hour through the summer and then average occupied values were calculated. For the adaptive comfort results an hourly time series of threshold temperatures was produced from the external temperature in each weather data set. This was then compared to the calculated internal temperature at each occupied hour.

6.4 Building performance with different weather files

From the initial investigation the differences in air exchange rates due to different wind speed predictions from the 11 member RCM are presented. The air exchange rates due to adopting RCM variants representing the upper and lower bounds for change in wind speed were calculated. Two RCM variants (3q9 and 3q11) from those presented in Section 6.2.1.1 were chosen as they were close to the upper and lower bounds of wind change factors for the mid-summer months. This was done as it is not valid to only choose the central estimate (Brown et al. 2009). The change factors represented contrasting examples of positive and negative change in wind speed and these were applied to a CIBSE TRY file using the morphing method by Belcher et al. (2005). The two weather files were run with Building 6.1 so that air exchange rates could be compared. It was found that at maximum opening of the façade the difference between the variants was 0.07ACH, which was a 3.4% change in ACH. This result was from an edited weather file. For the rest of the results given in the following sections weather files, as provided by CIBSE, COPSE and PROMETHEUS, will be used. These are the types of weather data most likely to be used by practitioners

6.4.1 Comparison of ventilation rates across TRY's

The air exchange rates were compared across the TRY's from the PROMETHEUS, COPSE and CIBSE data sets, as shown in Figure 6.7, where zone air exchange rates from Example Building 6.1 were compared between the control period, 2050's and 2080's. A high emission scenario was adopted for all future periods as this was available for all data sets and enabled a comparison to be made. The PROMETHEUS data gave a choice of climate change percentiles and in this comparison the 50th percentile was chosen as this represents the closest to the other TRY weather files. Different percentiles were investigated in more detail in the

comparison of overheating. The air exchange rates across the zones of the example building can be seen in Figure 6.7.

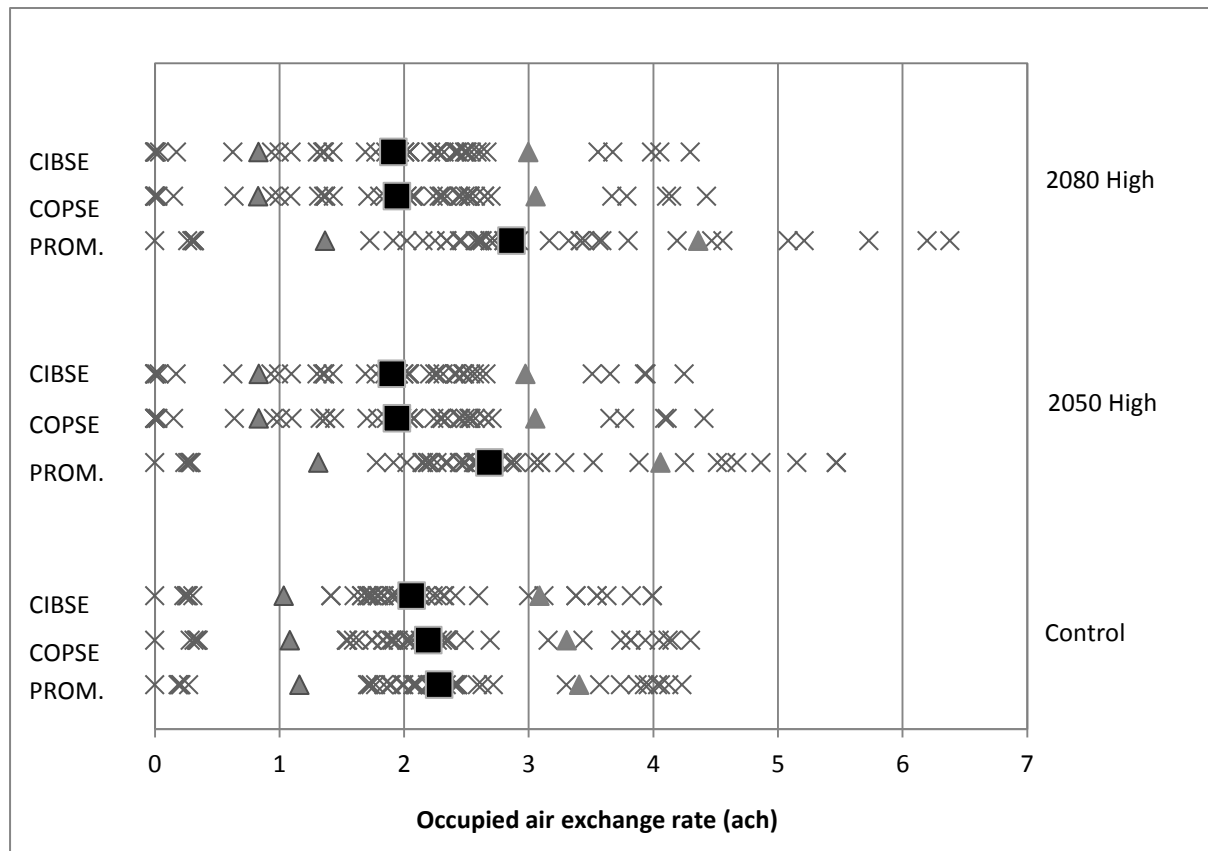


Figure 6.7. Comparison of air exchange rates for weather data sets. Crosses indicate occupied zone summer air exchange rate. Black squares indicate mean values and triangles indicate plus and minus one standard deviation.

During the control period all data sets had mean ventilation rates within 0.2ACH of each other. This difference increases in the future periods, with PROMETHEUS data up to 0.9 ACH higher than the other two data sets. With the temperature ventilation control removed the difference between the PROMETHEUS data set reduced to within 0.4ACH, indicating the degree to which removal of the ventilation temperature set-points reduced the influence of temperature on the natural ventilation rates.

6.4.2 Wind direction

For both the COPSE and PROMETHEUS weather data sets wind direction had to be generated as it was not included in the weather generator output or any projections. This was due to wind direction being highly variable and also closely related to the larger scale weather patterns which are difficult to represent robustly (Murphy et al. 2009).

Figure 6.8 shows wind direction polar plots for the control period TRYs for each of the data sets for the percentage of occurrence for 30° segments of the compass. All three weather files show the larger proportion of the time with the wind coming from the west. It can be seen that the COPSE and CIBSE wind directions are more closely matched with each other than the PROMETHEUS wind direction. Both COPSE and CIBSE have the highest frequency of wind coming from the south, with similar distributions.

The direction distribution for PROMETHEUS was smoother and this can be related to the differences in methods used to generate wind direction. The CIBSE data are based directly on measured data so the directions were inherited from these measurements. No morphing was applied to wind direction so this was also the same for future periods. The COPSE wind direction was replicated to fit the historical distribution but was independent of wind speed (Watkins et al. 2011) - this is why the COPSE and CIBSE wind direction distributions are closely matched. PROMETHEUS uses a probabilistic representation of the wind direction described by Eames et al. (2011b), where historical weather data from 1961 to 1990 are used to produce probabilistic distributions between wind speed and the season. The wind direction was generated every six hours and the other hourly directions in the series were linearly interpolated. This can be seen in Figure 6.8 and is the probable reason for the smoothness of

the distribution compared to the CIBSE and COPSE direction distributions for Manchester. Intermediate directions register a frequency even if they were not produced very often from the generator due to this linear interpolation. The directions have been linked to wind speed statistically so the occurrence of higher winds from certain directions was more likely to be preserved.

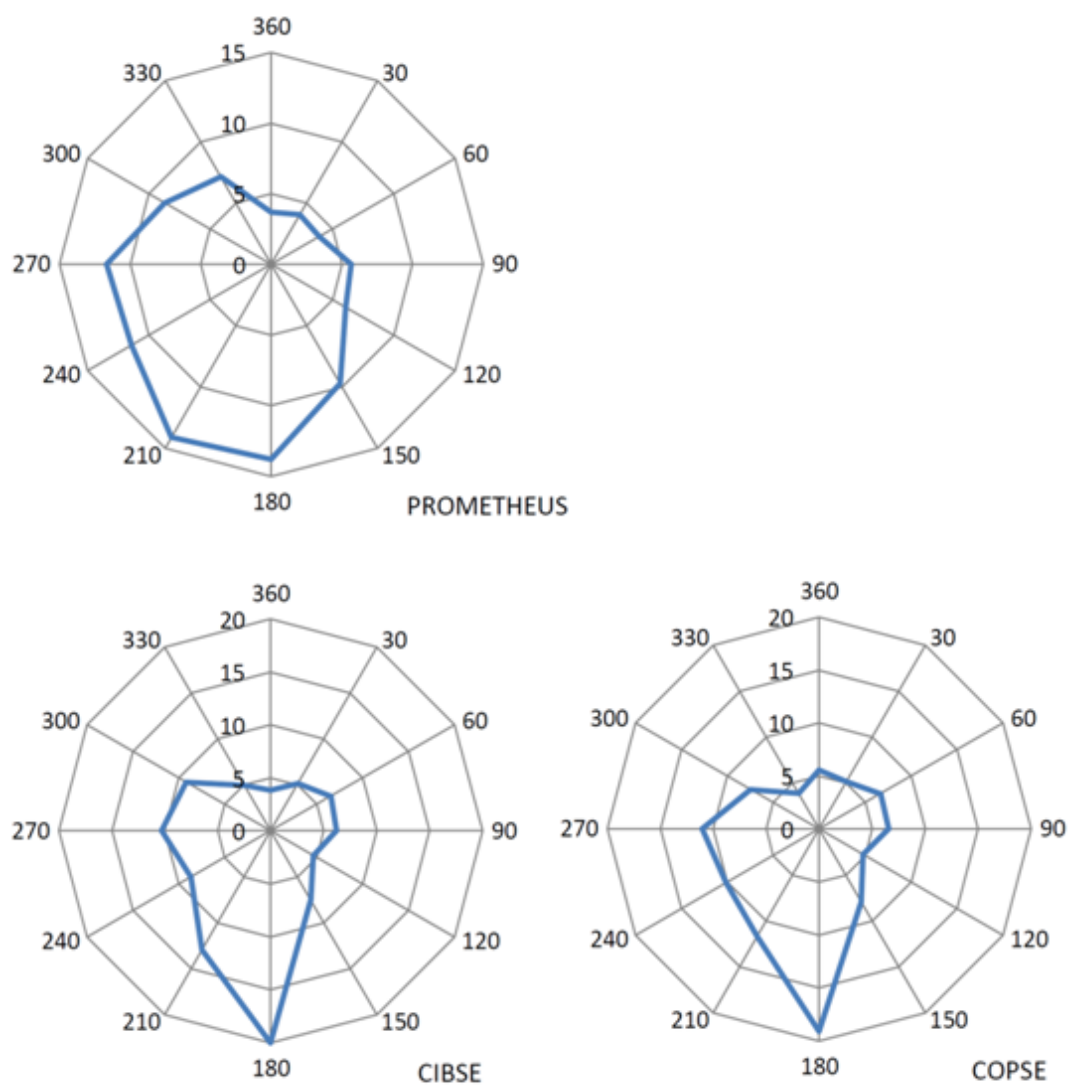


Figure 6.8. Wind direction distributions given as frequency of occurrences (%) for 30 degree increments of the compass.

6.4.3 Sensitivity to change in wind direction

In order to investigate how these differences in wind direction distribution affected ventilation rates the sensitivity to a change in direction was compared. Firstly, a number of shifts in directions were applied throughout the COPSE control TRY and ACH for this was simulated for Example Building 6.1, the results of which are given in Figure 6.9.

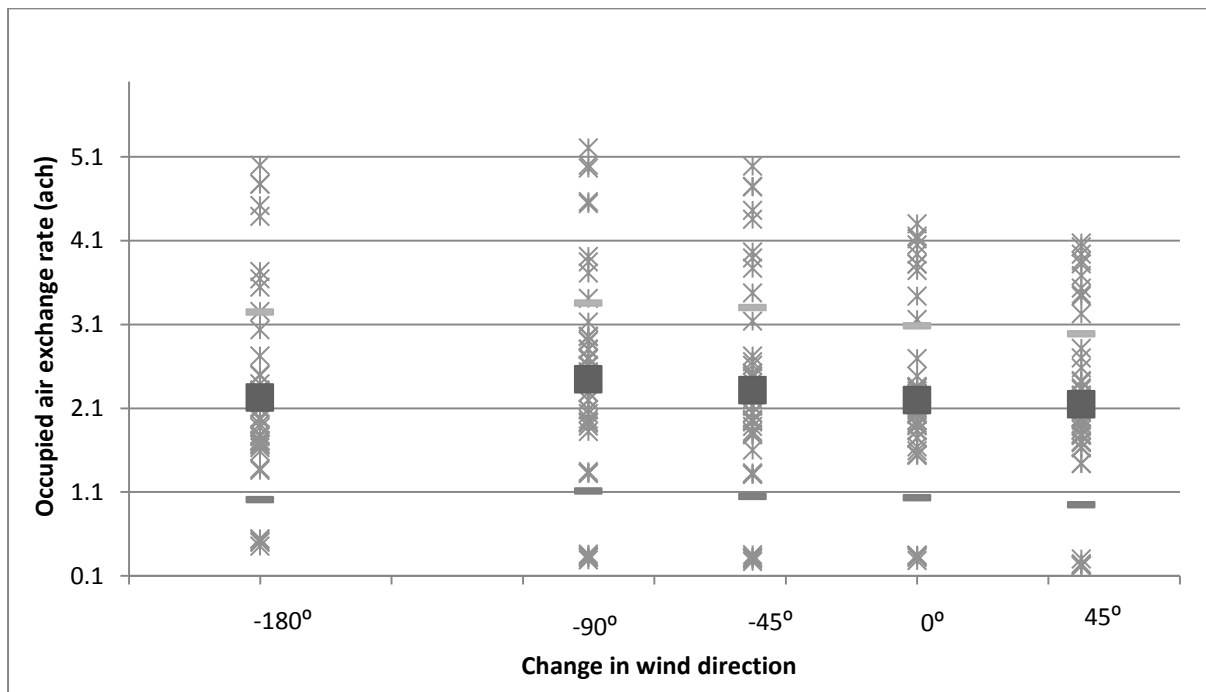


Figure 6.9. Sensitivity of air exchange rate to change in wind direction for control TRY. Black squares indicate mean values and bars represent \pm one standard deviation.

The sensitivity of the zones to a change in wind direction varies substantially. For some zones the change was negligible but for others an ACH change of up to 30% was seen. This was still somewhat less than what has been presented in the work of Horan & Finn (2008). In their CFD study the air exchange rates in a modelled atrium building were shown to vary from 2.93 to 1.0 ACH for a 45° change in wind direction with a constant wind speed of 3m/s and

single vent model. Such a dramatic change was not present between the COPSE and PROMETHEUS weather data sets.

The sensitivity of Building 6.1 was highest for changes in wind direction between 0° and 45°, and so this was chosen for the comparison of sensitivity between weather files. The long façade in Figure 6.6(A) faces south and the 45° change in wind direction is applied clockwise. Comparing the sensitivity of the PROMETHEUS and COPSE data sets to this change in direction revealed that PROMETHEUS data resulted in a 3% increase in sensitivity in the air exchange rate. Repeated measure T-test is used to determine if two sets of data are significantly different from each. A T-test supported the statistical significance of the sensitivity result. Whether the wind direction information was appropriate for the site in question depends on a variety of factors, such as topographical differences between the weather station and site and future changes in the pressure systems. These considerations are beyond the scope of this study, which was concerned with the differences between the available simulation weather data.

6.4.4 Thermal comfort

The simulation of thermal comfort conditions in a building is central to whether sole reliance on natural ventilation is possible or whether mechanical cooling will be needed. Figure 6.10 shows the percentage of occupied hours above the two different comfort threshold temperatures for the control period. Firstly, it can be seen that for Example Building 6.2 the CIBSE Guide A (CIBSE 2007) definition of overheating has for the most part been avoided, except for one zone with the CIBSE DSY which reached just over at 1.02% of occupied hours. The increase in overheating for the CIBSE control period was in keeping with the

differences in the control periods used by CIBSE and the other two data sets. The COPSE and PROMETHEUS control period comes from 1960-1990 data and the CIBSE DSY was from 1983-2004. This translates to average summer temperatures of 13.8°C for the 1960-1990 control period and 14.2°C for 1983-2004, and was an indication of the change in climate that has already occurred.

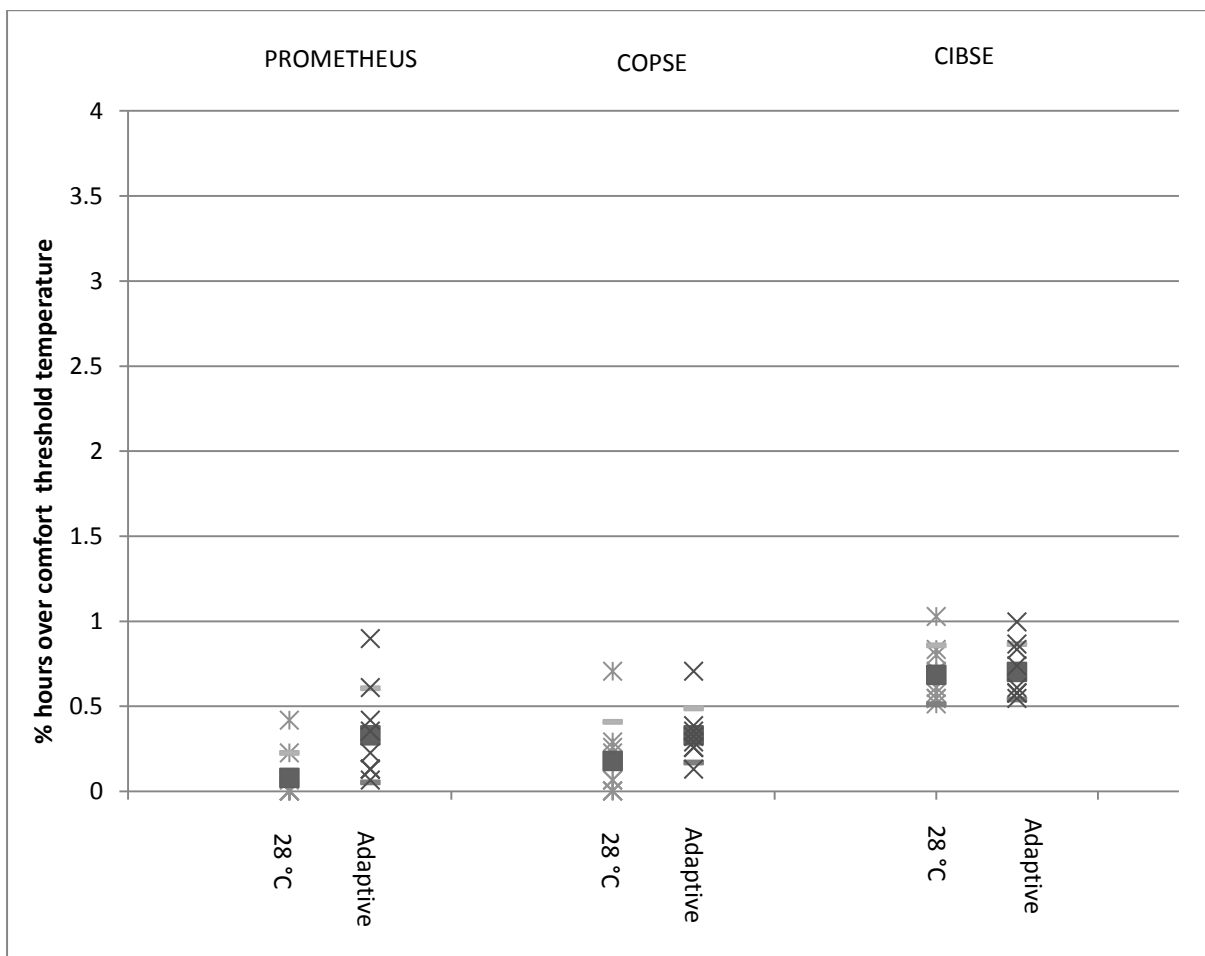


Figure 6.10. Percentage hours over threshold comfort temperature for the control period.

It can be seen from Figure 6.10 that for the control period the occurrences above the adaptive threshold temperature were larger than the occurrences above 28°C. This is reversed when future weather data was considered, as illustrated in Figures 6.11 and 6.12.

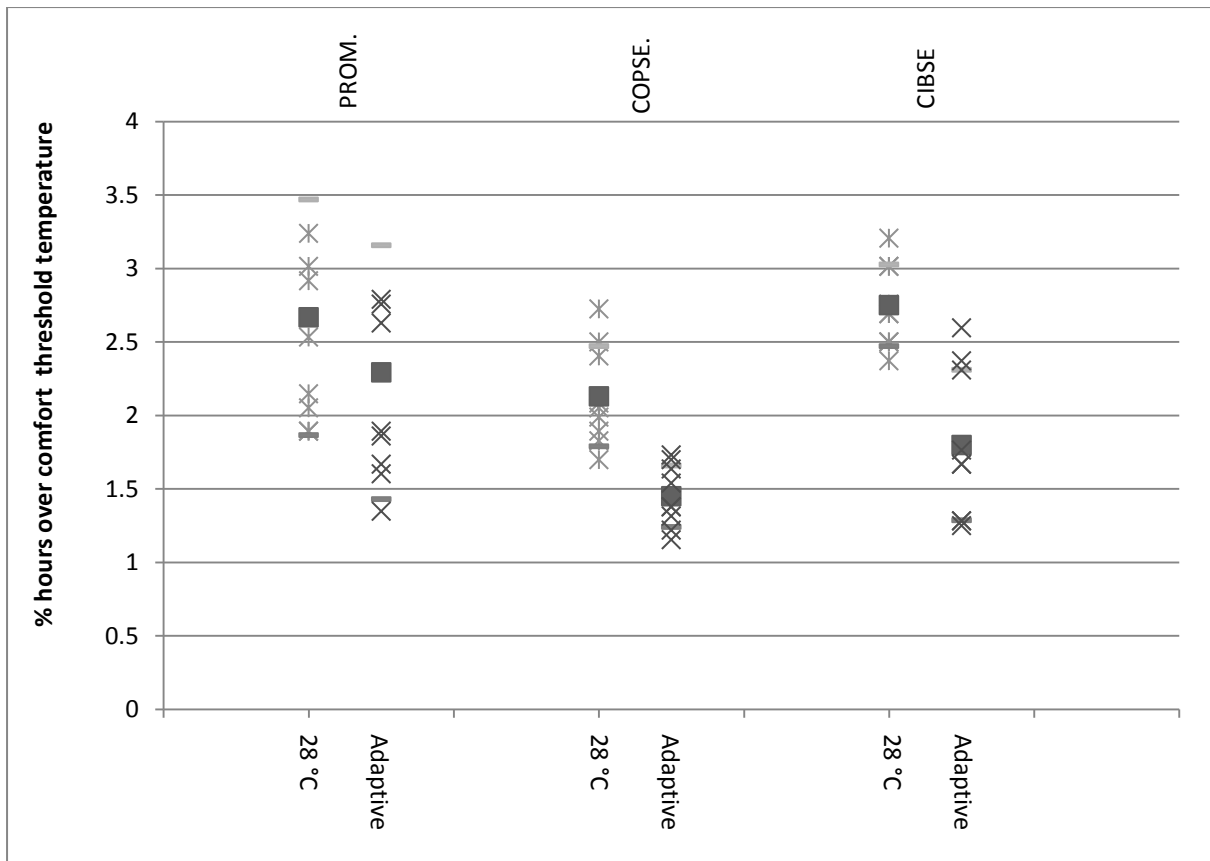


Figure 6.11. Percentage hours over threshold comfort temperature for the 2050's under the high emission scenario.

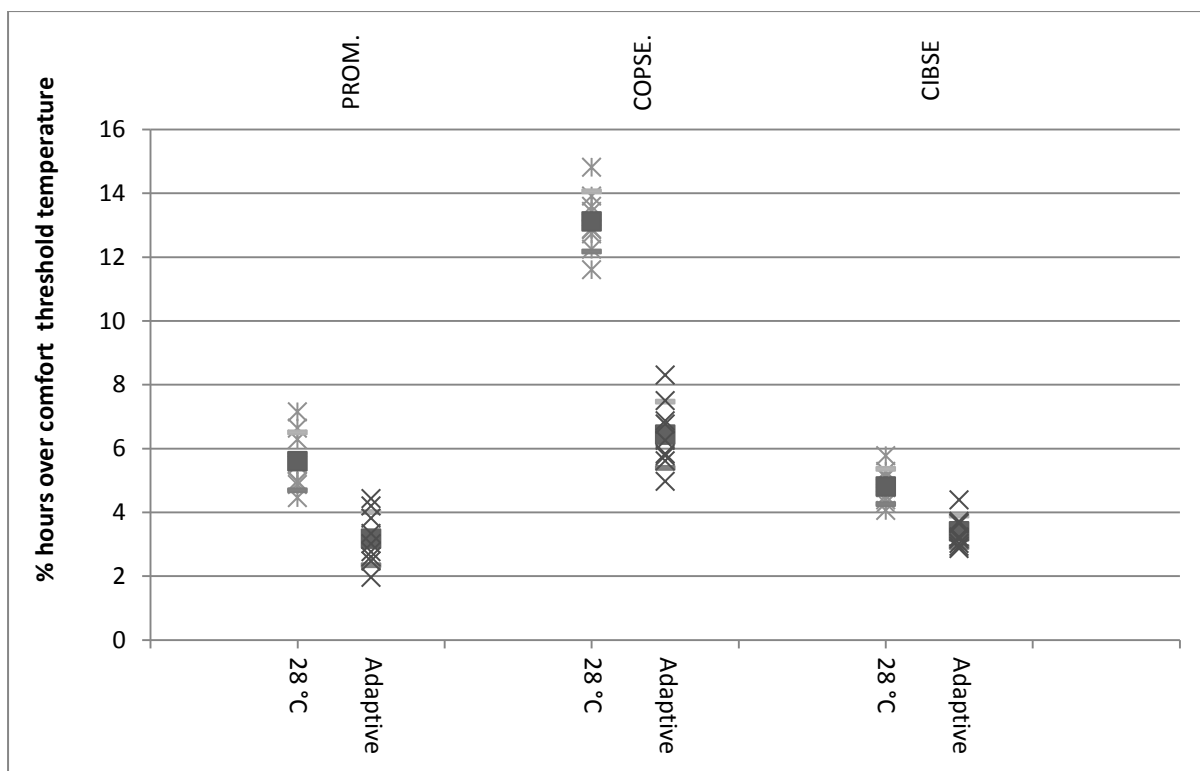


Figure 6.12. Percentage of occupied hours over threshold comfort temperature for the 2080's under the high emission scenario.

Overall, Figures 6.11 and 6.12 show a clear and substantial increase in hours above the comfort threshold temperature in to the future. The PROMETHEUS 50 percentile was only 0.1°C higher, in terms of average summer temperature, than the CIBSE DSY for the 2050's and the 2080's, indicating that the central prediction from UKCP09 was similar to the previous UKCIP02 generation of projections for this location. The published comparison by Jenkins et al. (2010), where UKCP09 was shown to give a 0.3 decrease compared to UKCIP02 for a location in Dorset, indicates differences due to location. For the results so far PROMETHEUS weather data representing the 50th percentile has been used in the comparisons, as can be seen from Figure 6.12. Substantial differences between COPSE and PROMETHEUS have developed as the comparison moves to the 2080's. One of the main differences in the production of the DSYs was the difference in approach to the percentiles of

weather generator data. This was important for external temperatures represented in the weather files and, therefore, the level of overheating. For the COPSE method developed by Watkins et al. (2011) all 3000 years produced from the 100 weather generator runs of 30 year periods were ranked according to the external temperature and a year that represents the centre of the upper quartile was chosen as the DSY. This, in effect, mixes together the natural variability in a 30 year period represented by the weather generator output and the climate change forcing from the climate modelling and often represented in the probabilistic plots. In the PROMETHEUS method (Eames et al. 2011a) a DSY was produced from each 100 of the 30 year time periods; these 100 DSY were then ranked and a number of percentiles from these 100 weather files made available. Differences within these options could be very important for buildings close to the overheating benchmark and might affect the adoption of mechanical cooling. The relationships between summer external temperature, climate percentile and overheating are illustrated in Figure 6.13. This shows the percentage of time over the comfort threshold temperature for the COPSE and PROMETHEUS data.

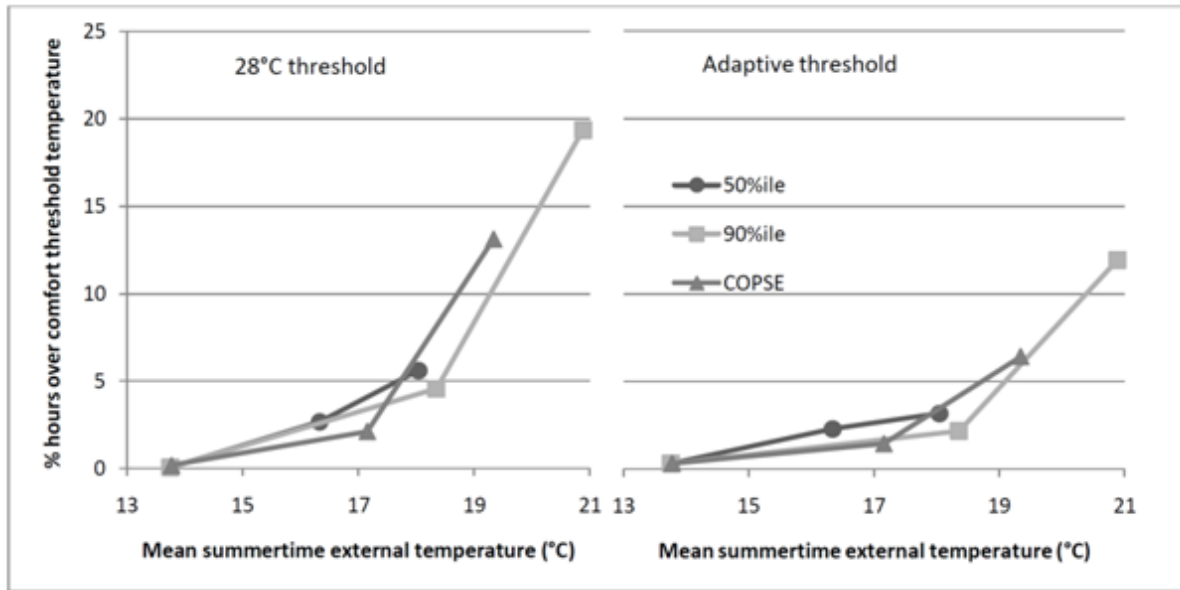


Figure 6.13. Percentage of occupied hours above thermal comfort threshold against mean summer temperature legend for two percentiles (50th and 90th) of the PROMETHEUS DSY's and the COPSE DSY. Each series consists of a control, 2050 and 2080 under the high emission scenario.

Figure 6.13 again illustrates the differences between the two approaches to the overheating threshold temperature, with the occurrence of hours above the adaptive comfort threshold temperature progressively reducing relative to the 28°C threshold as summertime temperatures increase. This is due to the running mean from equation (4.16) of the adaptive standard adjusting for some of the increase in external temperatures, as the average temperature increase so does the threshold temperature. For the other set of results 28 degrees remains the threshold temperature throughout and so the adaptive results change in relation to this. The difference in approach to future DSY generation between COPSE and PROMETHEUS can be seen in Figure 6.13. The COPSE method, in combining these two factors by ranking all 3000 years, has the benefit of simplifying the number of options available when choosing a weather file, making the comparison of building designs easier. For each time slice and emission scenario one DSY was produced. With the PROMETHEUS method a DSY is selected from the data within each climate percentile so there was the

additional choice of the following climate change percentiles: 10%, 33%, 50%, 66% and 90%. Two of these (50% and 90%) are included in Figure 6.13. It can be seen that the COPSE temperatures were between the PROMETHEUS 50th percentile and the 90th percentile temperatures. There was also a subtly different interpretation of what constitutes near extreme for DSY production. The COPSE method takes the definition of a summer representing the middle of the upper quartile so the year representing the 87.5% of the 3000 years in a weather generator run was chosen. With the PROMETHEUS method the year with the fourth warmest summer of each 30 year set was chosen as the DSY. It should be noted that there is on-going work in establishing a so called design reference year (Watkins et al. 2012), which will update the DSY methodology to use the data available. However, for the time being the DSY remains the industry standard in terms of overheating assessment.

Previous studies have found linear relationships between mean external temperatures and maximum internal temperature (Coley & Kershaw 2010). This kind of linear relationship would also be useful to simplify future performance analysis for overheating in naturally ventilated buildings. Figure 6.14 shows percentage of hours over 28°C modelled for Example Building 6.2 against mean external temperature for the full range of time periods and emission scenarios included in the CIBSE data set.

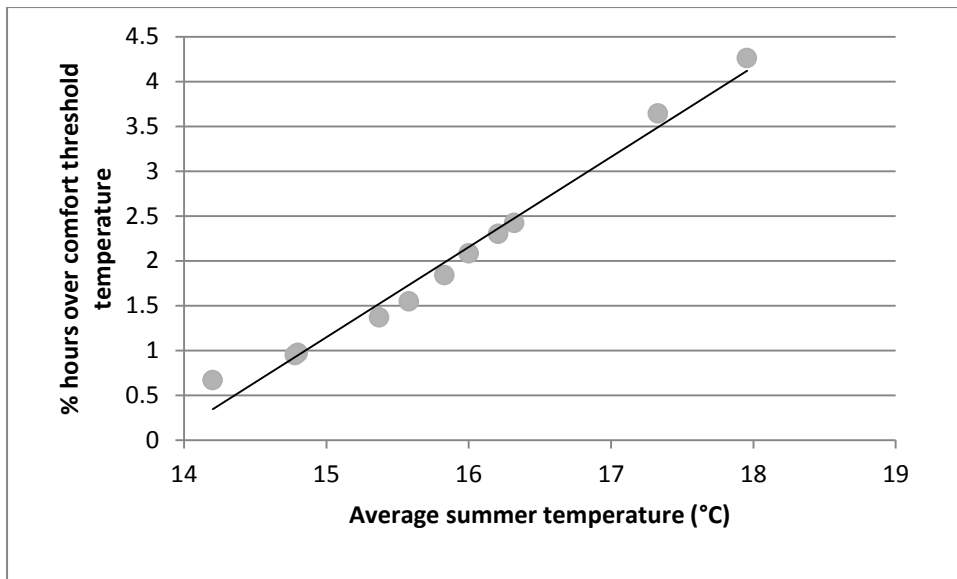


Figure 6.14. Overheating plotted against mean summer external temperatures for the CIBSE DSY weather data set.

The linear regression in Figure 6.14 fits quite well considering the complexities of overheating in a naturally ventilated building, with a correlation coefficient (R^2) of 0.9811. The closeness of fit for a linear approximation was not as strong for the UKCP09 weather generator derived weather data sets of PROMETHEUS and COPSE, results for which are given in Figure 6.15. PROMETHEUS and COPSE gave correlation coefficients of 0.7881 and 0.8314 respectively which, although indicating more scatter, are still statistically significant correlations ($p < 0.05$), where p is the probability that the result would occur by chance and this was calculated with the software R (R Development Core Team 2011). This shows that mean external summer temperature can be used to describe climate change effects on natural ventilation performance. The increased scatter would likely be due to each year of these data sets being separate synthetic time series with a different profile of peak temperatures and other variables.

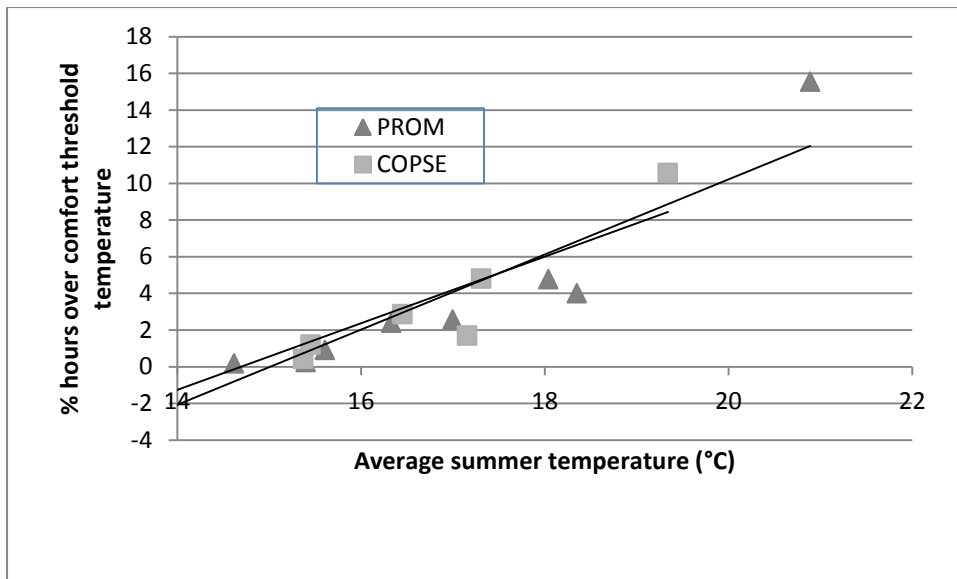


Figure 6.15. Overheating plotted against mean summer external temperatures for the weather generator derived data sets.

6.5 Discussion

Differences in wind speed, wind direction and air exchange rates have been illustrated in this chapter, with PROMETHEUS data consistently giving the highest ventilation rates, between 0.1 and 0.9 ACH higher than the other two data sets. As well as differences in wind this suggests higher internal gains and therefore more time with the windows open for natural ventilation. The need for the inclusion of wind speed data for building evaluation was less to know exactly what changes were likely in the future, due to the uncertainty and small projected change which is evident from the analysis of the 11 member RCM results. Rather, the importance of wind data is that it is needed for complete data sets that can be used with dynamic thermal models. All the sets provide this and, although differences such as those illustrated in the results exist, all sets represent plausible wind data. The higher ACH rates for PROMETHEUS could be seen as beneficial in terms of avoiding mechanical ventilation use, although the effect of climate change percentile treatment on overheating is more important. The difficulty in maintaining thermal comfort by natural ventilation alone in the future was

shown. Even with the adoption of the passive measures in Building 6.2, overheating is only avoided for the control datasets, but then increases progressively with future temperature increases. This illustrates why mixed mode cooling is used for results showing acoustic performance.

The investigation of the relationship between overheating and summer time temperatures found that results from CIBSE weather data fitted a linear regression more closely than the PROMETHEUS and COPSE results. Though the importance of external temperatures to building overheating was still clear for the UKCP09 derived data, the central reason for the differences in closeness of fit comes from the weather generator derived data having different time series for each year. Each CIBSE time series (control and future) is based on the same profile but was adjusted in to the future. The overheating results are sensitive to the details of the time series, and so use of the weather generator output for this purpose, would rely strongly on the time series of the important weather variables having a valid representation.

6.6 Conclusions

The key conclusion from this chapter is that:

- All three weather data sets can be used to represent future natural ventilation performance.

This conclusion is reached due to no difference in the plausibility of the wind data being found. Also, due to the statistically significant correlation between mean summer external temperature and overheating it is concluded that this temperature can be used to represent

climate change. Mean external summer temperature is used to rank future weather data and is the variable representing change to climate in Chapter 7.

Additional conclusions drawn from this chapter are that: the PROMETHEUS data give consistently higher ventilation rates, between 0.1 and 0.9 ACH higher than the other two data sets. The projected change for wind speed is small, with, at most, a 1.2% decrease through the year. There is high uncertainty in wind speed projection, indicated by the poor correlation between climate sensitivity and change in wind speed (R^2 of 0.0802). It can be seen from the results that under future climate scenarios, it is difficult to justify relying purely on natural ventilation, due to high levels of overheating. There is more variation in the results for overheating with the UKCP09 projections (R^2 of 0.7881 and 0.8314) as compared with the UKCIP02 projections (R^2 of 0.9811). This increased variation of overheating against external temperature is likely due to the use of the weather generator for the UKCP09 data.

7 Performance implications

As has been seen environmental factors have implications for the cooling performance of buildings. These implications are investigated in more detail in this chapter, using data and methods developed throughout the thesis. Design choices interact with environmental factors and have a central influence on the comfort and energy use of a building. Examples of such design choices include whether the cooling design is wholly reliant on natural ventilation, mixed mode or air-conditioning. The form of the building is also important (shallow plan or deep plan office space), as well as the construction materials used. Construction materials affect the thermal and acoustic performance of the building, as do the positions of ventilation openings. A central aim of this thesis is to quantify a noise reduction measure in terms of climate change mitigation, and this is done in the last section of this chapter.

The first question tackled in this chapter is how the potential for natural ventilation cooling changes under future climates, both for fully naturally ventilated and mixed mode buildings. This is investigated in detail in Section 7.1 by using the range of future weather data from Chapter 6 to determine the change in sensible cooling from natural ventilation air flows. In Section 7.2 changes in building construction are investigated with reference to past building standards and building weight. The different ways in which constructions react to a changing climate is shown as well as what effects a change in construction has on the acoustic-ventilation relationship. This uses the approach developed in Chapter 5. Section 7.3 compares the relative effect of acoustic and climatic environmental factors on mixed mode cooling. This central aim of the thesis discussed in the last section of the thesis completes the main investigation.

7.1 Climate change implications on natural ventilation cooling

Natural ventilation is used more in temperate climates as the level of cooling available is related to the temperature difference between internal and external air. Lower external temperatures mean that the inflow of external air will cool building zones more. Warming from climate change will likely reduce the cooling potential of natural ventilation, as was mentioned by Sharples & Lee (2009). This is important as it determines how much this sources of natural cooling can be relied upon and to what extent additional measures will have to be adopted.

In Chapter 6 a number of future weather data sources were compared, and in the following sections these same weather data sets will be used to look at the implications for natural ventilation cooling as weather data with warmer summer temperatures are used. This is examined in detail by considering the changes in cooling heat loss that natural ventilation offers as the summertime temperatures increase due to climate change. The previously introduced example building models from Chapters 5 and 6 will be used to investigate the natural ventilation heat loss that the future weather conditions imply. The first sets of building models all run in a free float mode (no heating or cooling), and the later results come from example building models that employ mixed mode cooling.

7.1.1 Sensible heat loss background

One of the EnergyPlus simulation output options is the sensible heat loss due to the external air and therefore only due to ventilation. Sensible heat loss is the heat loss due to the temperature change that can be sensed by temperature measurements and also experienced by the building occupants. This was chosen as the output variable that most directly describes

the cooling due to natural ventilation. It is defined as convective sensible heat loss, to the zone air corresponding to the zone infiltration volume. This is the volume of airflow from outside the building that flows into the zones through cracks, doors or windows. The airflow from this quantity is driven by natural pressure differences such as wind pressure and thermal/density differences. The output is given in terms of sensible heat loss and gain, the loss quantity being larger than the gain quantity due to the temperature set-points that control window opening.

The results in this section show sensible heat rather than latent heat, which comes from changes in the levels of water vapour in the air. To illustrate why sensible heat gain was used a brief comparison of the scale of sensible to latent heat gains was conducted with Building 5.3. The building was modelled with free float conditions and openings were unrestricted by the surrounding acoustic conditions. Sensible and latent heat losses were calculated for the CIBSE control weather years and the most extreme future year from the PROMETHEUS weather data set. In this way a full range of warming scenarios was tested. Far larger sensible heat losses were found compared with the latent heat losses from natural air exchange. An average of 8.8kW of sensible heat loss due to ventilation air exchange was found for the CIBSE control weather data compared to 5.4×10^{-7} kW of latent heat loss. The extreme 90th percentile PROMETHEUS weather year for the 2080s had the largest latent heat loss at 8.2×10^{-7} kW, but this was still 1.5×10^7 time smaller than the sensible heat gain. This represents several orders of magnitude and illustrates why sensible heat loss is focused on for the result of this section.

7.1.2 Sensible heat loss results

The first results, Figures 7.1 and 7.2, show sensible heat loss against summertime average temperature for Buildings 6.1 and 5.2 respectively. The buildings were in free float mode and were chosen as they represented a range of sizes and layouts. Building 6.1 was longer and with more zones, Building 5.2 having a square footprint and smaller area. Other aspects, such as crack template and window opening control, were the same for both buildings. The sensible heat loss was due to temperature changes from the external air coming into the zone from crack infiltration and natural ventilation through the windows. This sensible heat loss was averaged over the occupied period as this is when natural ventilation is in operation. Each weather data set is plotted as a separate series and indicated in the legend with trend lines being added to each set.

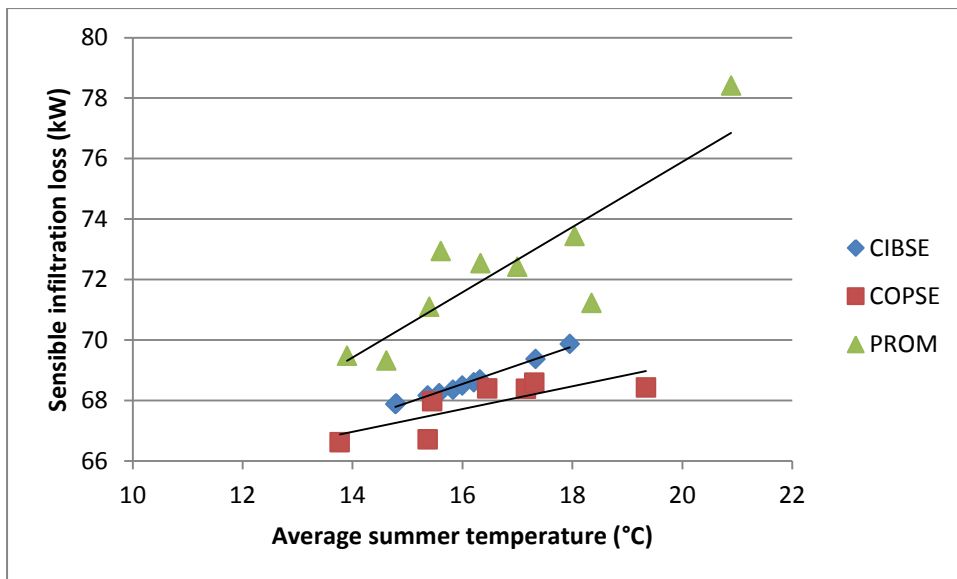


Figure 7.1. Sensible heat loss for Building 6.1 against average summertime temperature for a number of weather files from datasets marked in the legend.

From Figure 7.1 it can be seen that there is some variability in the results, as indicated by the R^2 values. The least scatter can be seen from the CIBSE results, which give an R^2 value of 0.9858, while COPSE and PROMETHEUS results showed substantially more scatter about their trend lines with R^2 values of 0.624 and 0.7419 respectively. This fits with the results from Chapter 6 where the COPSE and PROMETHEUS results showed more variation as these two data sets were derived from the stochastic weather generator. In contrast the CIBSE weather data sets are derived from a single morphed weather files and this produced more regular change as all weather files have the same base data.

The positive gradients of the trend lines in Figure 7.1 indicate a clear tendency for the sensible heat loss due to infiltration to increase with increases in temperature. This is also the case for example Building 5.2, the results of which are shown in Figure 7.2 and where positive gradients can also be seen. An outlier point at the highest summer temperature for the COPSE data set causes the gradient to be very close to zero. It is likely that the smaller volume of the building makes it more susceptible to extreme weather compared to Building 6.1 shown in the previous figure.

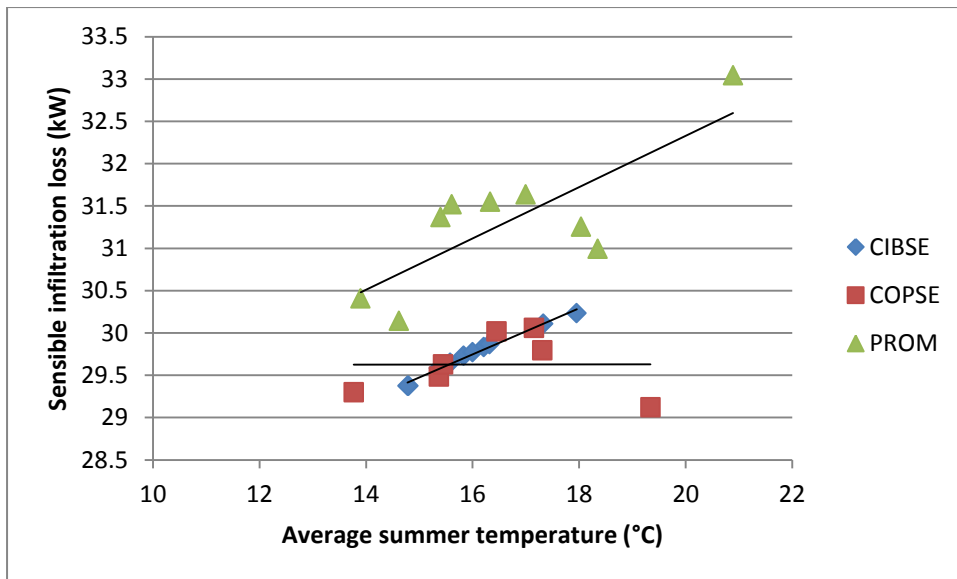


Figure 7.2. Sensible heat loss for Building 5.2 against average summertime temperature for a number of weather files from datasets marked in the legend.

Smaller sensible losses can be seen in Figure 7.2 than in Figure 7.1; this can be explained as Building 5.2 is a smaller building and therefore the volumes of air flow and the corresponding heat losses are less. There is also more variability in the results for Building 5.2 compared to Building 6.1, with the COPSE data showing a R^2 value close to zero and 0.6257 for PROMETHEUS. This is most likely due to the smaller number of zones in Building 5.2, leading to local differences having a greater effect on the whole-building values given in the results.

The increases in sensible heat loss with increasing temperatures, which are shown in Figures 7.1 and 7.2, counter intuitive. It is more logical that higher external temperatures should decrease the cooling potential of natural ventilation due to smaller temperature differences between internal and external air. A possible reason for this is that higher temperatures increase the amount of time that windows are opened. The example building models used in

this section have ventilation set-points of 24°C, which replicate occupant opening of windows or automatic control of ventilation based on temperature. In Figures 7.3 and 7.4 the average occupied air exchange rate is shown against average summer temperature for the three data sets indicated in the legend. From these figures it can be seen that as the average summer temperature increases the airflow also increases, this is due to the ventilation set-point being exceeded for more of the time, resulting in more time with the windows opened.

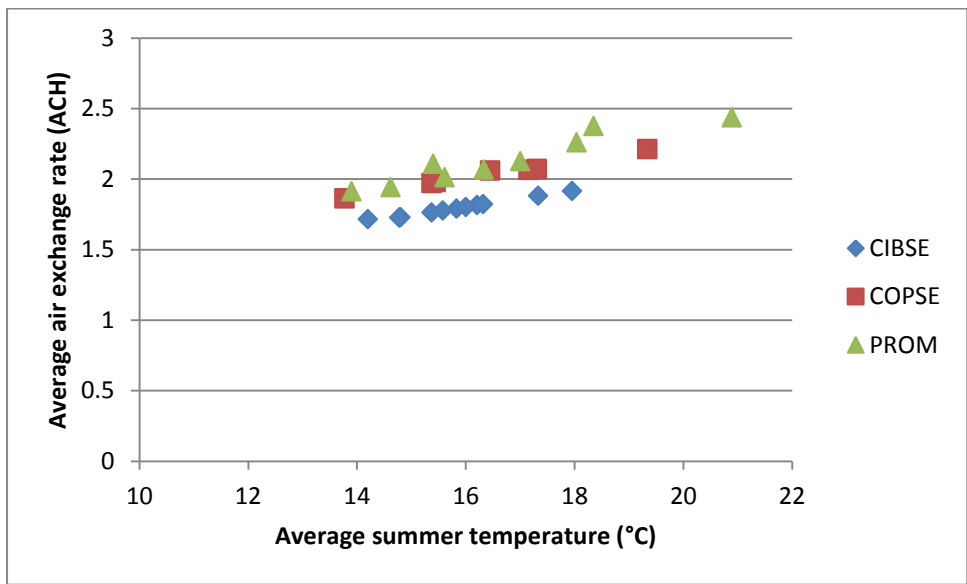


Figure 7.3. Average air exchange rate for Building 6.1 against average summertime temperature for a number of weather files from datasets marked in the legend.

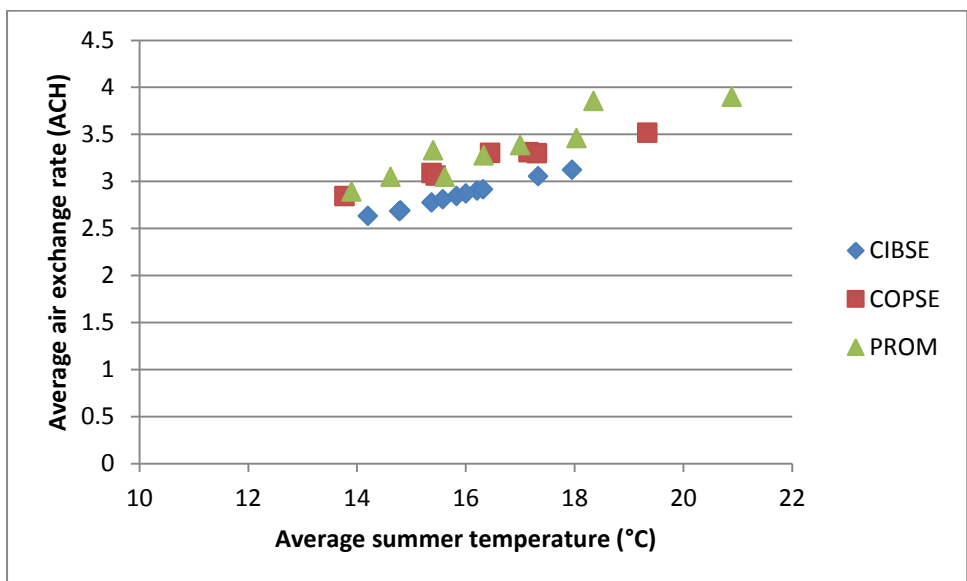


Figure 7.4. Average air exchange rate for Building 5.2 against average summertime temperature for a number of weather files from datasets marked in the legend.

Building 5.2 shows a higher ACH rate than Building 6.1; this should be due to the smaller volume for zones in Building 5.2, the air of which is exchanged more rapidly. Also Building 5.2 has a larger proportion of zones that can have cross ventilation, which increases the overall exchange rate. The variability in the results also increases along with the increase in ACH with R^2 changing from between 0.9928 to 0.9138 for Building 6.1 down to 0.8631 for Building 5.2 with PROMETHEUS data.

Further analysis is undertaken to investigate changes in sensible heat loss while taking into account the increases in natural ventilation air flow shown in Figures 7.3 and 7.4. The approach adopted for this is to calculate the sensible cooling energy per unit volume (m^3) of external air entering each zone of the building. This is calculated in the following way: at each occupied hour the sensible heat loss is divided by the infiltration volume. The infiltration volume is the volume of external air coming into the zone by infiltration and natural ventilation during that hour, which includes air flow through cracks, doors and windows. This sensible heat loss per m^3 is then averaged over the occupied time and summed over the occupied zones to give the building results illustrated in Figures 7.5 and 7.6

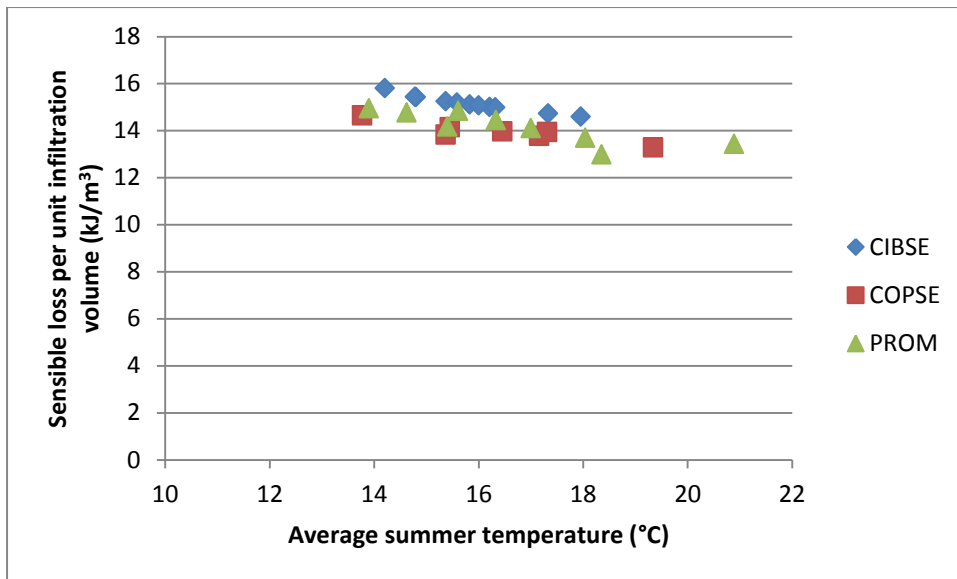


Figure 7.5. sensible heat loss per unit volume of infiltration for Building 6.1 against summer external temperature for a number of weather data sets.

In contrast to the previous results a negative gradient is seen for all data sets. This means that the sensible heat loss due to airflow into the building, once adjusted for changes in ventilation rate, decreases with an increase of temperature. The changes in airflow volume are due to the modelled ventilation control strategy, once these are taken into account the sensible heat loss due to the ventilation is then in accordance with the theory. Figure 7.5 and Figure 7.6 therefore fit with equation (2.1), as external temperatures increase the cooling potential of natural ventilation decreases. If it is assumed that the specific heat capacity of air is $1.21\text{kJ}\cdot\text{m}^{-3}\cdot\text{K}^{-1}$ and, for example, a mid-result from the graph ($14\text{kJ}/\text{m}^3$) is taken, this leads to average temperature differences of 11.6°C . It should be remembered that this is averaged over airflow volume, not time. Even so it is still relatively large and a sign that this building is overheating. This overheating is confirmed from other chapters where high levels of overheating were calculated for this building.

The same variable of sensible heat loss per m^3 of ventilation air is shown for Building 5.2 in Figure 7.6. From previous analysis of overheating it was found that Building 5.2 also exceeded overheating thresholds but less so than Building 6.1. The sensible heat gain for Building 6.1 ranges between 78.4kW to 66.6kW, for Building 5.2 it ranges from 33.0kW to 29.1kW, a substantial difference between the buildings. The difference between buildings reduces when the heat loss is adjusted for airflow volume. The sensible heat loss per m^3 is some 2 kW/m^3 less for Building 5.2 than for Building 6.1, which is only a 14% reduction.

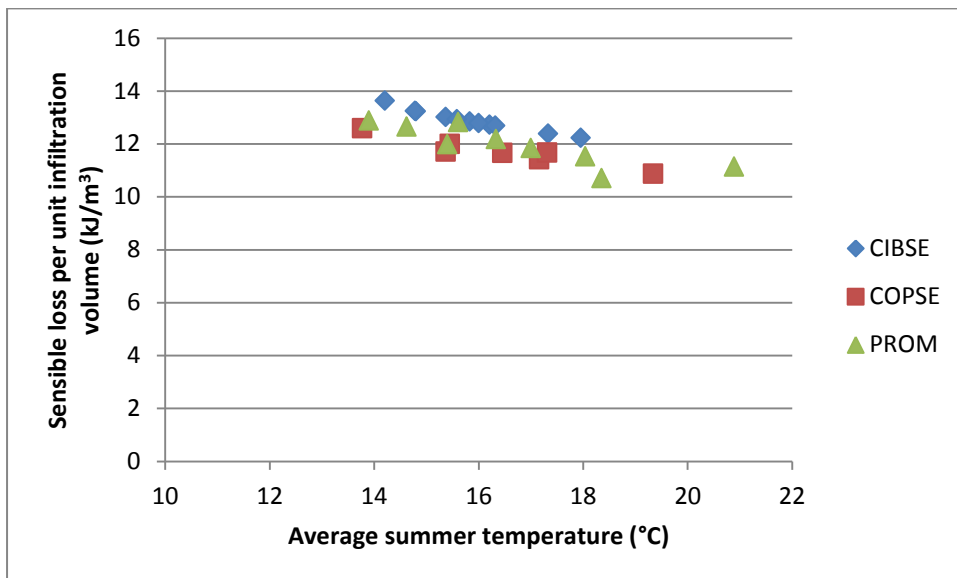


Figure 7.6. Sensible heat loss per unit volume of infiltration for Building 5.2 against summer external temperature for a number of weather data sets.

Variability in results of sensible heat loss shown in Figures 7.1 and 7.2 is relatively constant, as shown by R^2 staying between 0.9 and 0.7. Figure 7.6 indicates average temperature differences in the region of 9.9°C if $1.21\text{kJ}\cdot\text{m}^{-3}\cdot\text{K}^{-1}$ is again adopted as the specific heat capacity of air. This is a slight drop from the temperature differences suggested for Building 6.1 (11.6°C). As the external temperatures are set by the weather file and the same sets are

used for both buildings this suggests average internal temperatures in the mid to high twenties. This, as an average, is high with only a small increase needed to meet overheating criteria. This was seen from Chapter 6 and the high level of overheating for Building 6.1 where free float conditions were used but no additional measures were utilised to reduce overheating (such as window shading or mechanical cooling). This was the case for both CIBSE guide A and European adaptive comfort overheating definitions.

In addition to the two Buildings (6.1 and 5.2) which have been analysed so far the results for Building 6.2 are given in Figure 7.7. This building is different in that a number of passive cooling measures have been used; these go beyond the free float conditions of Buildings 6.1 and 5.2 but do not include mechanical cooling. These measures included the minimisation of internal heat gains, a shallow office floor plan, maximisation of ventilation openings, adoption of solar shading on all windows to depth of 1m and a night ventilation strategy. Natural ventilation was allowed to operate during the night to encourage cooling of the building fabric. With all these measures overheating criteria was avoided for the control period weather data, even though no active cooling techniques had been adopted. The sensible heat loss per unit airflow volume for this building is shown in Figure 7.7.

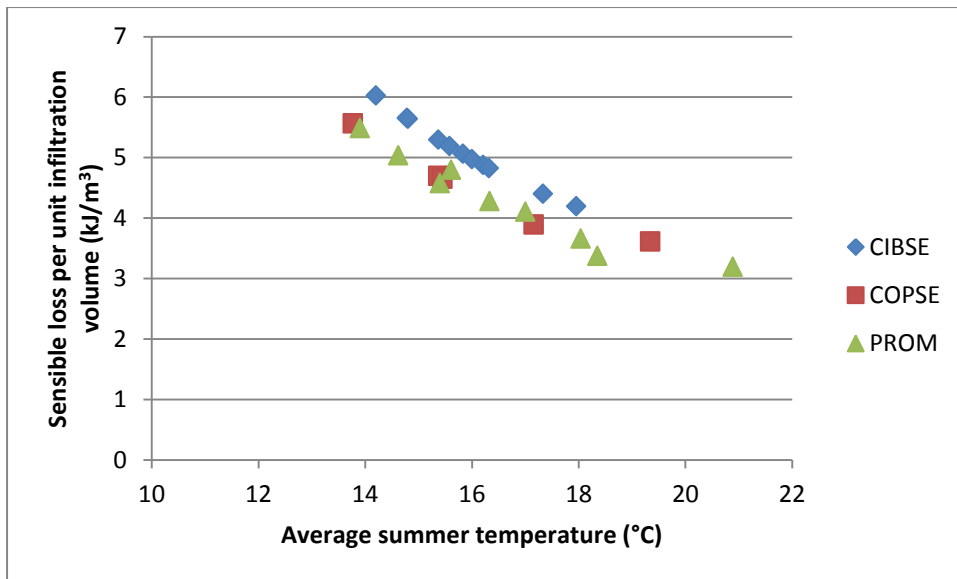


Figure 7.7. sensible heat loss per unit volume of infiltration for Building 6.2 against summer external temperature for a number of weather data sets.

The values in Figure 7.7 are much reduced, taking 4.5kJ/m^3 as a central value and $1.21\text{kJ}\cdot\text{m}^{-3}\cdot\text{K}^{-1}$ again as the specific heat capacity of air, gives an average temperature difference of 3.7°C . This is about one third of the temperature difference found for Building 6.1. The gradient is again negative and also steeper again than for both Buildings 6.1 and 5.2. A comparison of the linear regression gradients between buildings over all the weather data sets shows a gradient of -0.310 for Building 6.1 and a gradient of -0.403 for Building 6.2. The more pronounced drop for Building 6.2 suggests that the benefits of natural ventilation drop off more steeply, indicating that internal temperatures are rising faster than in the other buildings. This steep change is particularly important for this building as for the control period mechanical cooling can just be avoided. But warming in the weather files easily pushes the building over the CIBSE overheating criteria (1% of occupied hours over 28°C).

The implications from rising temperatures are greatest for buildings on the border line of satisfying comfort conditions by passive means. Additional cooling would need to be adopted to satisfy CIBSE guide A overheating criteria. For Building 6.2 the air flow is very high so any restrictions, for example because of noise ingress, would also have implications for maintaining passive cooling. In conclusion, sensible heat loss is affected by both changes in air flow and internal/external temperature differences. Overall, the cooling effect of natural ventilation airflow was found to increase with increasing summer temperatures. This is due to increases in airflow as windows are open more of the time. Once changes in air flow are taken into account the cooling per unit air flow volume then decreased with rising temperatures. This corresponds to equation (2.1) with the smaller temperature difference between internal and external air reducing heat loss due to ventilation.

7.1.3 *Mixed mode results*

In the previous section the example buildings had free float conditions, meaning natural ventilation alone was used for building cooling. Future temperature rises, as represented in future weather data sets, mean thermal comfort conditions are no longer met. An option is to use mixed mode cooling where the opening of windows for natural ventilation occurs when, for example, the zone temperature reaches 24°C, and then mechanical cooling is used once zone temperatures reach 27°C. In a sense the mixed mode approach adopted here is an adaption measure as it maintains a degree of flexibility in dealing with uncertainty about future climatic conditions. The most extreme cases of overheating can be avoided while still leaving some room to maximise passive cooling measures such as natural ventilation when this is possible.

The following results are for a building which has a mixed mode cooling strategy. This is just done for Building 6.1 and the results are shown in the following figures, Figure 7.8 shows sensible cooling and Figure 7.9 shows the ACH. For conciseness only results for this building are given although very similar patterns were found with other buildings that employed mixed mode cooling.

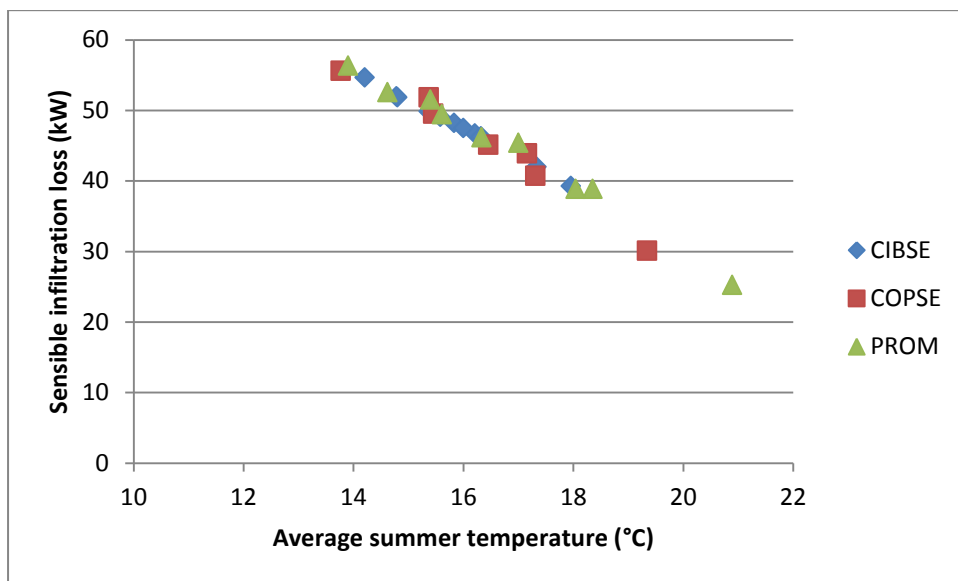


Figure 7.8. Sensible heat loss for a mixed mode Building 6.1 against average summertime temperature for a number of weather files from datasets marked in the legend.

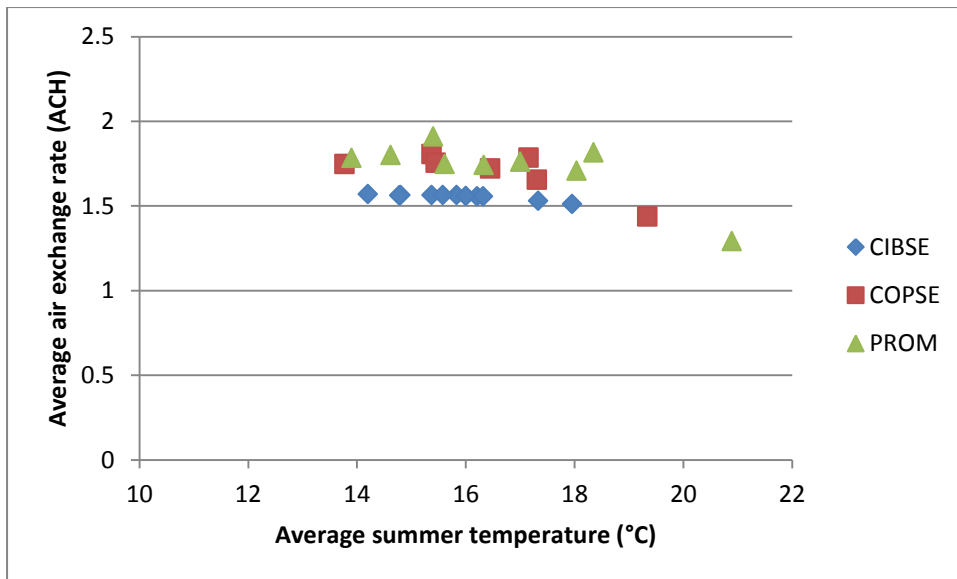


Figure 7.9. Average air exchange rate for Building 6.1 against average summertime temperature for a number of weather files from datasets marked in the legend.

A clear and steady decrease in sensible cooling can be seen from Figure 7.8 across all the weather data sets the gradient is -4.34 and variability in the results is low with an R^2 of 0.978. This is in clear contrast to Figure 7.1 which has a positive gradient and indicating the difference between free float and mixed mode buildings. Figure 7.9 shows a relatively stable air exchange rate with little change occurring for most summer temperatures. There is a slight decrease, mainly for the extreme COPSE and PROMETHEUS weather data sets, but this has not had a major effect on the results for sensible cooling. The reason for this relatively stable ACH rate would appear to be due to the two set-points controlling natural ventilation, 24°C and 27°C. Increases in temperatures did not increase average ACH rates as any increases in the amount of time windows were opened was matched by a similar increase in time windows were closed due to the change-over to mechanical cooling.

7.2 Construction materials

The thermal performance of the construction material has a key role in the cooling behaviour of buildings. Two aspects of thermal performance are investigated in this section, thermal insulation and thermal capacity. The thermal insulation or thermal resistance of the building fabric, which can be simplified as a U value, describes how easily heat travels between the building interior and outside. In the past a central concern in the UK has been the heating requirements during the winter, and this was the primary focus for the setting of minimum standards for construction materials. This is different to the thermal capacity which describes the capacity of the building fabric to store heat. For buildings using a night ventilation strategy such as Building 6.2, the thermal capacity is of particular importance to store as much of the lower night temperatures as possible so that it can be utilised through the day. Over the years changing standards and guidance mean a variety of construction materials will be present in the building stock for a number of years; with a changing climate it is interesting to see how these materials might behave. As well as thermal properties, acoustic properties of the construction materials are also relevant, with different construction materials impeding the transmission of sound to different degrees.

In this section the aim is to illustrate how construction materials change the behaviour of the building; this is done using the data and methods developed in this thesis. Firstly, thermal differences will be investigated with the same selection of thermal insulation material properties used by Chow & Levermore (2010). These give the maximum U values from building standards editions from 1965 to 2002. After 2002 a different approach was adopted - rather than prescribing U values of individual building elements, the whole-building emissions is now compared with a notional building (BRE 2010). Due to the long life cycle of buildings, those built to the past editions of the building standards U values will still be in

operation for some years to come, including the future periods covered by the weather data set from Chapter 6. The U value results will be the focus of the first part of this section, after this three levels of building weight, taken from CIBSE Guide A (CIBSE 2007), are investigated. At the end of this section acoustic ventilation interaction for two sets of construction material are compared shown.

7.2.1 Thermal performance of the construction materials

Table 7.1 Shows the U value of different components that were used in Buildings 5.2 and 5.3. These two buildings were representative of simple office buildings, with the main difference between being the depth of the office space. The building models were run with the weather files compiled in Chapter 6.

Table 7.1 Comparison of standard maximum permitted U-values of construction elements specified in UK Building Regulations from 1965 to 2002 taken from (Chow & Levermore 2010).

Year of building regulation	U-Values (W/m ² K)				
	Wall	Window	Floor	Roof	Door
1965	1.7	5.6	1.42	1.42	3
1976	1.0	5.6	1.0	0.6	3
1985	0.45	3.3	0.45	0.25	3
1995	0.45	3.0	0.35	0.2	3
2002	0.35	2.2	0.25	0.2	2.2

It can be seen that the U values have steadily decreased. The construction information of simulation building models Buildings 5.2 and 5.3 were amended so that the U values matched exactly those in Table 7.1. This was done by changing the thickness of the insulation material

layer, for example for the wall this was XPS extruded polystyrene. This produced some non-standard thicknesses of some of the materials which are unlikely to be found in practice. As this was a way of altering the U value without major change to the thermal capacity of the building components, and as this was a thermal model, some non-standard thicknesses were thought to be acceptable. Other aspects, such as layout and ventilation characteristics, were kept the same as in Chapter 5.

The building models were run with the DSY weather data set. This was used as this thesis focuses on natural ventilation and cooling, and so winter performance will not be considered. Also, with the DSY data set consistency with the previous results in Section 7.1.2 is maintained. The performance indicators used were the mixed mode cooling electricity of the building with fully opened ventilation where there is no restriction due to noise. Details of the mixed mode cooling approach for Buildings 5.2 and 5.3 are described in Chapter 5. Of particular interest is the change in performance due to the different constructions. The results in Figure 7.10 show mixed mode cooling under the incrementally warming future climate, with each of the different constructions given in Table 7.1. Each near extreme summer weather file is plotted by its average summer temperature.

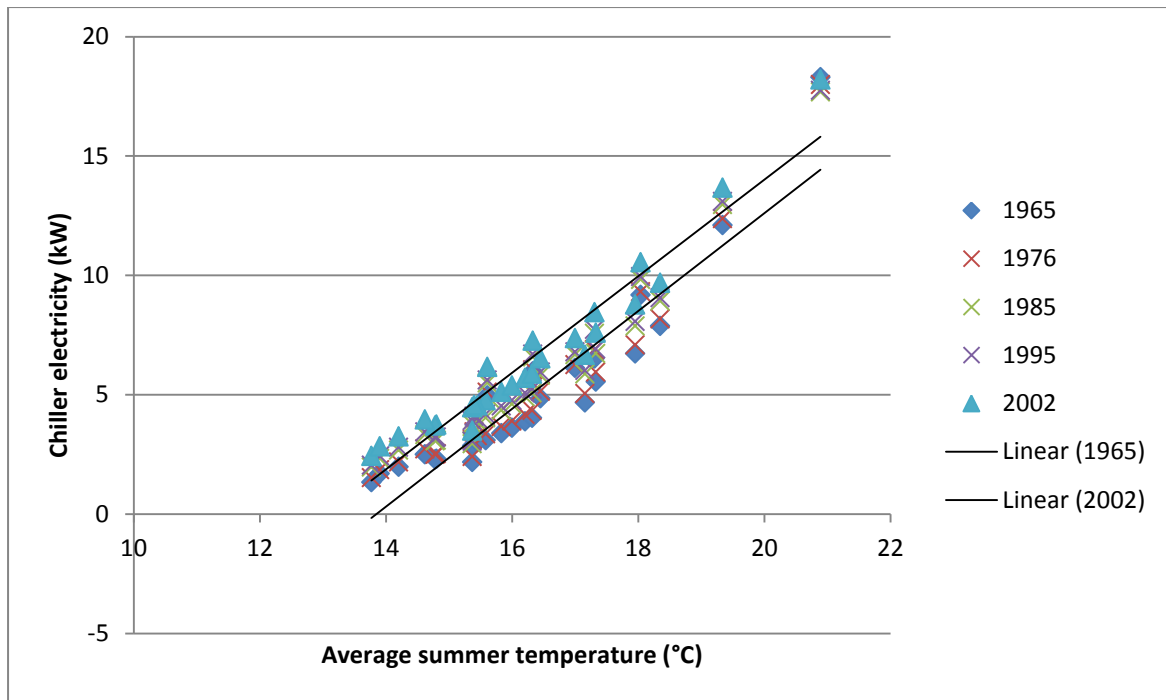


Figure 7.10. Average summer chiller electricity use against average summer temperature for Building 5.2 with the construction standards indicated in the legend.

The average difference between 1965 and 2002 is 1.504kW, which is a 29% drop from the average chiller electricity for this building. There is also considerable scatter in the results, with the 1965 insulated buildings giving an R^2 of 0.8763 and the 2002 insulated buildings having an R^2 of 0.9316. This is understandable as each plot is with an alternative weather file and the full detail of the weather data is not represented by the average summer temperature alone. The results shown in Figure 7.10 are for Building 5.2, which is the building with deeper office space; Figure 7.11 shows the results for the smaller building, Building 5.3. These results show the average difference between 1965 and 2002 is smaller, 0.209kW, which is a 14% drop from the average chiller electricity for this building. This is in keeping with the lower heating requirements needed for shallow plan office buildings.

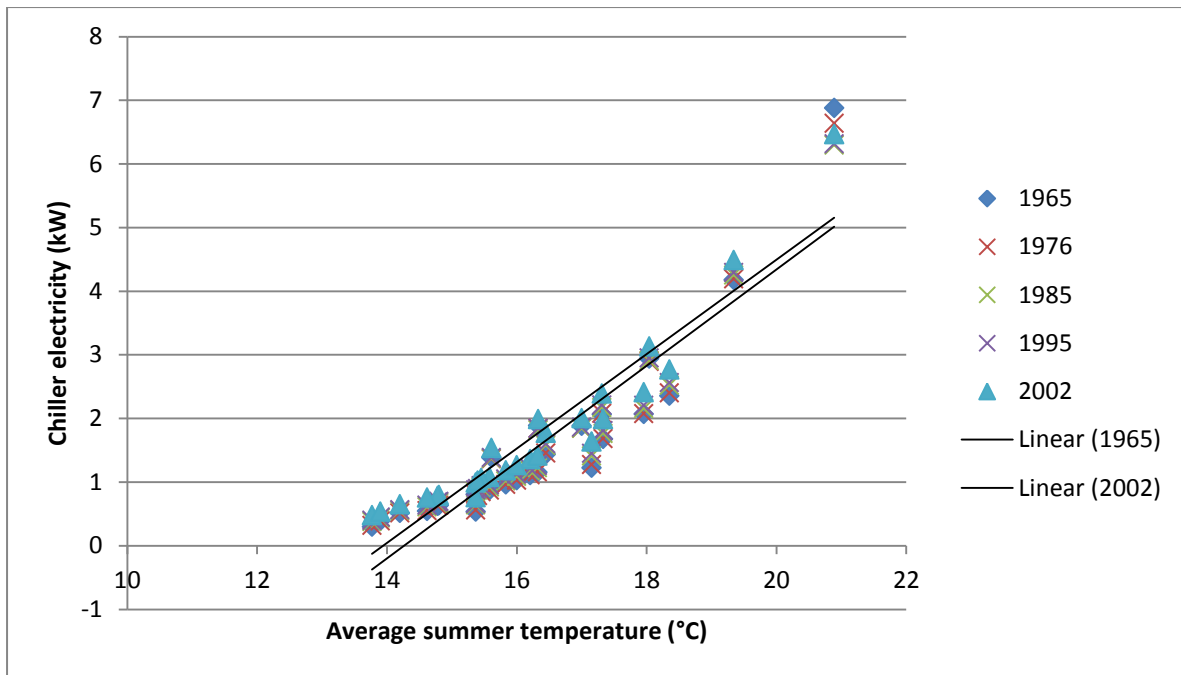


Figure 7.11. Average summer chiller electricity use against average summer temperature for Building 5.3 with the construction standards indicated in the legend.

It can be seen that the linear regression lines for Figure 7.11 do not fit very well with R^2 values of between 0.88 and 0.83. These lines are included, not to try and develop a relationship between temperature and chiller use, but to illustrate the separation between the earliest and latest editions of the building standards. It can be seen from this separation, and also from the average difference between the 1965 and 2002 editions of the building standards, that the reduction in U values increases the cooling requirements for both Building 5.2 and 5.3. This suggests that it is harder for internal gains to leave the building and any useful heat storage in the building fabric is slower to be released. It shows how in the past the regulations were aimed at reducing the winter heating use with increasing insulation rather than summer cooling use. The results with the new set of future weather data, used here, support a more flexible approach which is necessary to reduce summertime energy use, which is likely to rise. The main point to be taken from these results is that, regardless of U value, cooling demand rises sharply with the more extreme projections of future warming.

A more relevant factor than U value for the summertime cooling performance is the thermal capacity/weight of the building construction. The behaviour with a range of construction weights is investigated using a similar approach to Chow & Levermore (2010) and employing the three thermal weights from Guide A (CIBSE 2007). These are shown in Table 7.2 and their properties were applied as solid construction elements to Buildings 5.2 and 5.2. The results for Building 5.2 are then shown in Figure 7.12 and the results for Building 5.2 in Figure 7.13.

Table 7.2. Physical properties of three classes of thermal weight, reproduced from (Chow & Levermore 2010).

		Exterior wall	Exterior glazing	Internal walls	Ceiling	Floor
Heavy	Width (m)	0.3	0.01	0.02	0.2	0.2
	Conductivity (W/m/K)	0.9	1.05	0.047	1.3	1.3
	Density (kg/m ³)	1850	2500	260	2000	2000
	Cp (J/kg/k)	840	840	1260	840	840
Medium	Width (m)	0.3	0.01	0.02	0.2	0.2
	Conductivity (W/m/K)	0.6	1.05	0.047	0.32	0.32
	Density (kg/m ³)	1350	2500	260	1050	1050
	Cp (J/kg/k)	840	840	1260	840	840
Light	Width (m)	0.3	0.01	0.02	0.2	0.2
	Conductivity (W/m/K)	0.19	1.05	0.047	0.2	0.2
	Density (kg/m ³)	470	2500	260	620	620
	Cp (J/kg/k)	840	840	1260	840	840

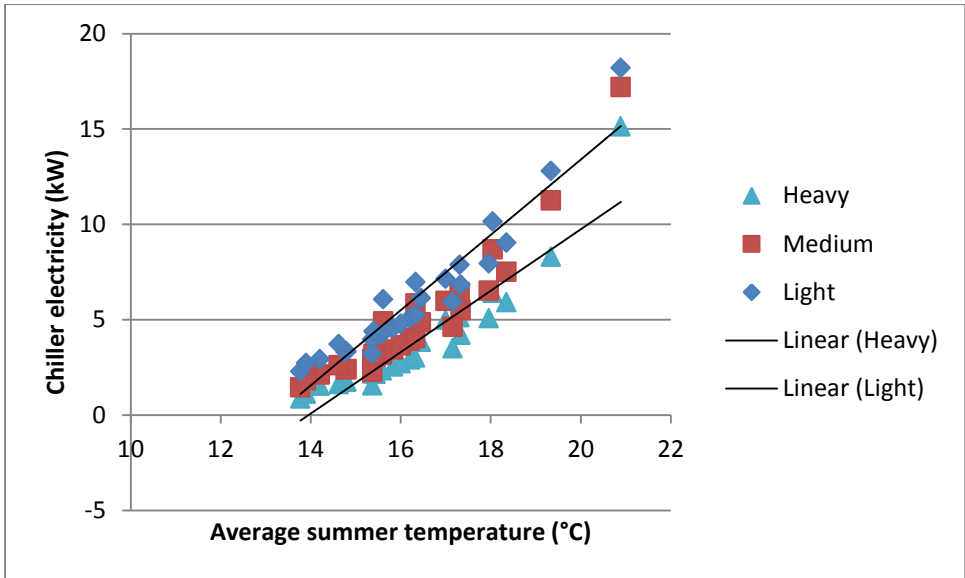


Figure 7.12. Average summer chiller electricity use against average summer temperature for Building 5.2 with the construction weight indicated in the legend.

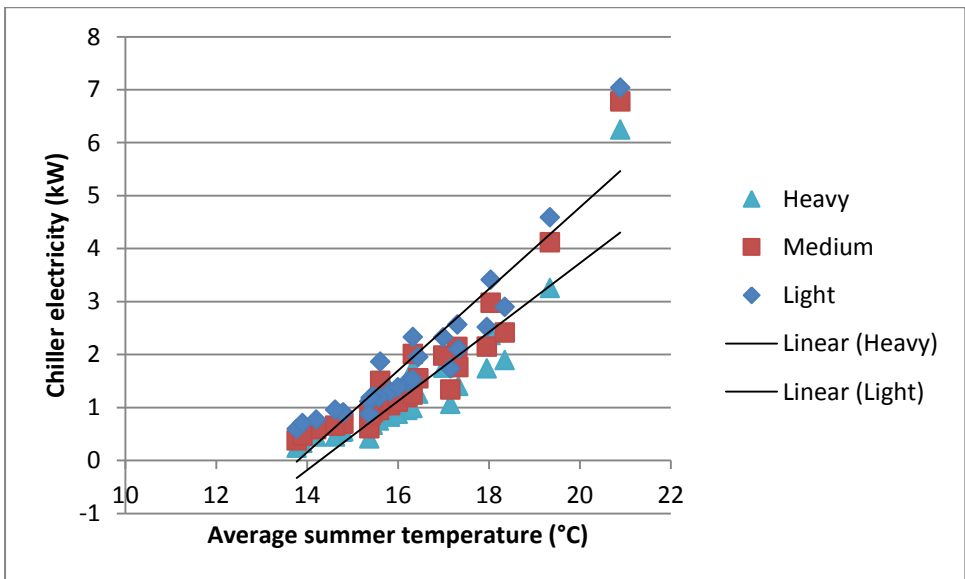


Figure 7.13. Average summer chiller electricity use against average summer temperature for Building 5.3 with the construction weight indicated in the legend.

Comparing the heavy and lightweight constructions in Figure 7.12, on average, across the weather files there is a 2.29kW increase with the lighter construction, which is a 52% increase from average cooling for Building 5.2. For Building 5.3, shown in Figure 7.13, there is a smaller increase of 0.606kW, with the lighter construction, which is a 42% increase from

the average cooling load. It is clear from these results that the building weight has a more significant influence on summer cooling than the U value investigated. With a reduction in cooling load being shown as the building thermal capacity increases, this is in contrast to what would be expected from winter performance. The gradient of the light and heavy construction regression lines show a tendency to diverge, with the lighter construction having a steeper gradient, which corresponds to this construction being more sensitive to the warming temperatures. This conclusion needs to be qualified due to the scatter, which is similar to the previous results, with R^2 ranging from 0.802 to 0.903.

7.2.2 Construction material sound insulation

As well as affecting the thermal performance of the building, differences in construction materials affect the acoustic transmission of the building façade. The previous construction from building regulations and CIBSE guide A guidance did not have the necessary acoustic transmission properties to be used with the method introduced in Chapter 5. Therefore to illustrate the effect of material on the acoustic/ventilation interaction a smaller set of two construction groups had to be used, made up of the following. Construction 1 was 4/12/4mm double glazing and two leaves of 102.5mm brickwork with a 50mm cavity, and Construction 2 was 6mm single glazing and 200mm of solid block wall. These construction materials had the measured sound insulation properties, shown in Table 7.3, and matching information in the DesignBuilder data tables.

Table 7.3. Construction material SRI values (dB). Measured according to ISO 140-3 (ISO 1995).

Construction Group		Frequency (Hz)				
		125	250	500	1000	2000
1	Double glazing (Hopkins et al. 2003)	24	20	25	35	38
2	Single glazing (DfEE 1975)	20	24	28	29	26
1	Cavity brick wall (DfEE 1975)	41	45	48	56	58
2	Solid wall (Templeton 1993)	35	38	43	49	54

A comparison of results for Construction 1 and 2 is given in Figure 7.14. With the open façade, corresponding to the lower chiller energy use, the noise ingress is similar for both constructions. This indicates how the acoustic insulations of the façades converge when opened, due to the dominant influence of the ventilation openings. With a more closed façade the variation in ingress due to the different sound insulation properties of the construction materials is apparent.

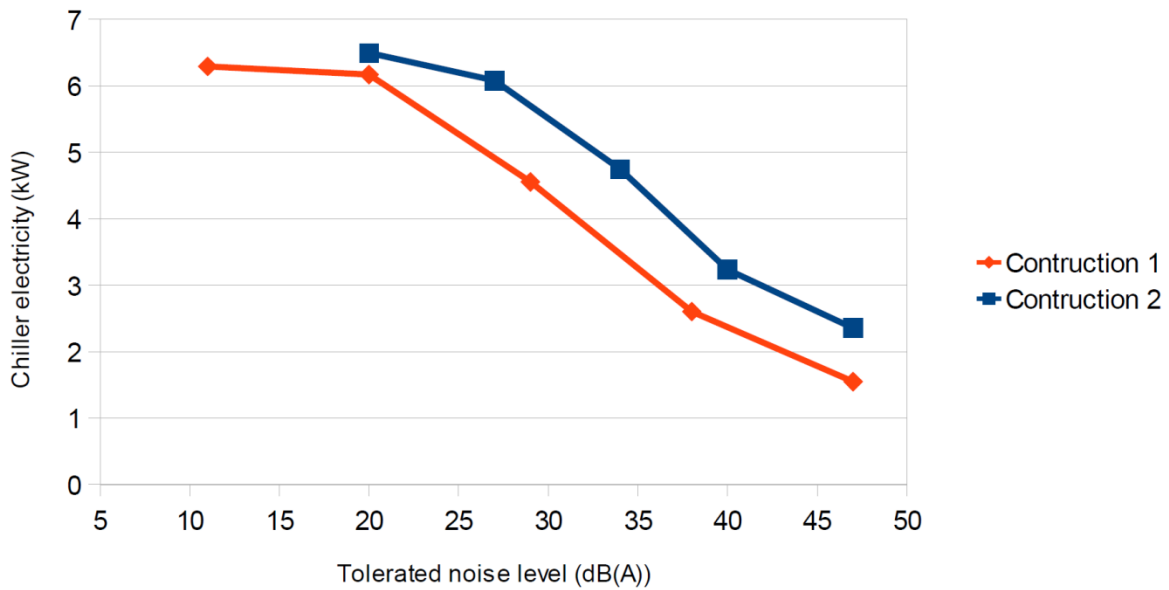


Figure 7.14. Comparison of construction materials for Building 5.3 in Location B.

The results show no large shift - construction 2, which had the least insulation, showed consistently higher chiller electricity usage. Although this converges at the minimum tolerated end of the graphs, the lowest tolerated level is when windows are closed. When windows are fully open, e.g. at the right hand side of the graphs, the difference of tolerated noise level is very small. This is due to the combined sound insulation of the façade being dominated by the opening, with the construction material making little difference to noise ingress in this case. The only difference for this situation is the thermal performance of the construction material interacting with high levels of natural ventilation and this is shown by the separation of the graphs in the y axis. At the other end of the graph windows are fully closed and so differences in acoustic insulation become apparent. This method allows the complex interactions between construction materials, ventilation and acoustics to be quantified for specific sites and buildings.

7.3 Comparing the influences of noise and climate on building thermal performance

The comparison of acoustic and climatic influences on natural ventilation is a central aim of this thesis. Determining the relative impacts of noise and climate temperature change is important, as Chapters 5 and 6 have shown that both affect a building's thermal performance. Quantifying these two influences can guide where design measures are best directed. The method of relating change in thermal performance with noise tolerance, which was presented in Chapter 5, is combined with weather data introduced in Chapter 6. A selected weather data set is compiled in Section 7.3.1 from all the sets included in the Chapter 6 comparison study. The results show that the noise tolerance / mixed mode cooling relationship for a number of climate change temperature increases. These relationships will be used to calculate the effectiveness of a noise reduction measure with different levels of climate change temperature increase. More details of the modelled noise reduction measure are given in the last section, Section 7.3.2, along with results for the main objective of determining what level of climate change temperature increase a 10dB noise reduction measure could mitigate.

7.3.1 Comparing the effects of noise tolerance and climate warming on mixed mode cooling

The method introduced in Chapter 5 can quantify the mixed mode cooling due to noise location and noise reduction measures. This is done by the noise tolerance and noise exposure affecting the ventilation opening pattern over the building façade. These opening patterns affect natural ventilation, and therefore the thermal performance of the building. Another key factor affecting the modelled thermal performance and mixed mode cooling results is the weather data drive the thermal building models. The introduction of future weather data allowed the future performance to be presented in this section. Future weather data will be introduced into the models calculating the noise tolerance to mixed mode cooling

relationships, allowing a comparison of the relative effects of these two environmental influences to be made. A reduced set of future weather data is compiled to describe a range of future climate scenarios, as shown in. The Method will focus on mixed mode performance as unrealistic overheating with the extreme future weather data will be avoided.

Table 7.4. Weather files used for the comparison ranked by their average summer temperature.

Weather data set	Time slice central decade	Emission scenario	Average summer temperature (°C)
COPSE	Control	Control	13.77
CIBSE	2050	Low	15.37
PROMETHEUS, 10 percentile	2080	High	15.61
CIBSE	2080	Medium Low	16.32
COPSE	2080	Low	17.31
PROMETHEUS, 90 percentile	2080	High	20.89

The set of selected future DSY weather files was chosen by ranking all weather files from Chapter 6 by their average summertime temperature. The reason for using these files was that they included at least two files from each set and covered a spread of summer average temperatures from the highest to the lowest and a selection from the middle. Focusing on the average summer temperature simplified the comparison as the various climate change issues, emission scenario, time slice, and probability level did not have to be explicitly shown. The six weather files used are a manageable number but still represent the wide range of change projected and have equal numbers of files from all three data sets covered in Chapter 6's comparison. DSY weather files were used as summer temperatures and cooling are the focus of this comparison.

The weather files from Table 7.4 were run with Buildings 5.1, 5.2 and 5.3 in the noise Locations A and B. More information about these example buildings and locations can be found in Chapter 5. The buildings are typical in terms of height and plan area of the example location at the edge of a city centre. More information about the cooling approach for the example thermal building models can be found in Section 5.2. Average mixed mode chiller results for a range of tolerated noise levels are given and are presented in the first set of results - see Figures 7.15 to 7.17.

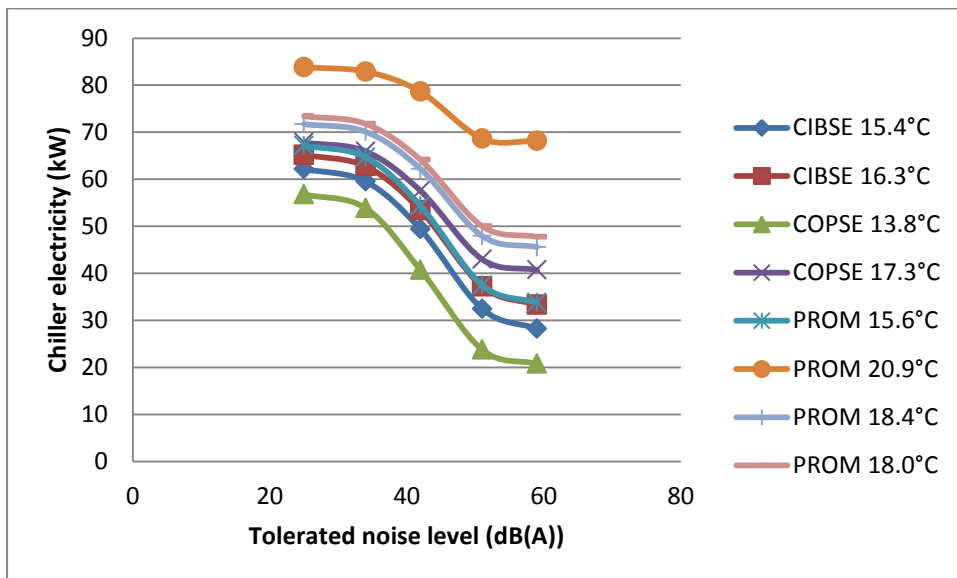


Figure 7.15. Comparison of chiller electricity for Building 5.1 in Location A and with the weather file's average summer temperature indicated in the legend.

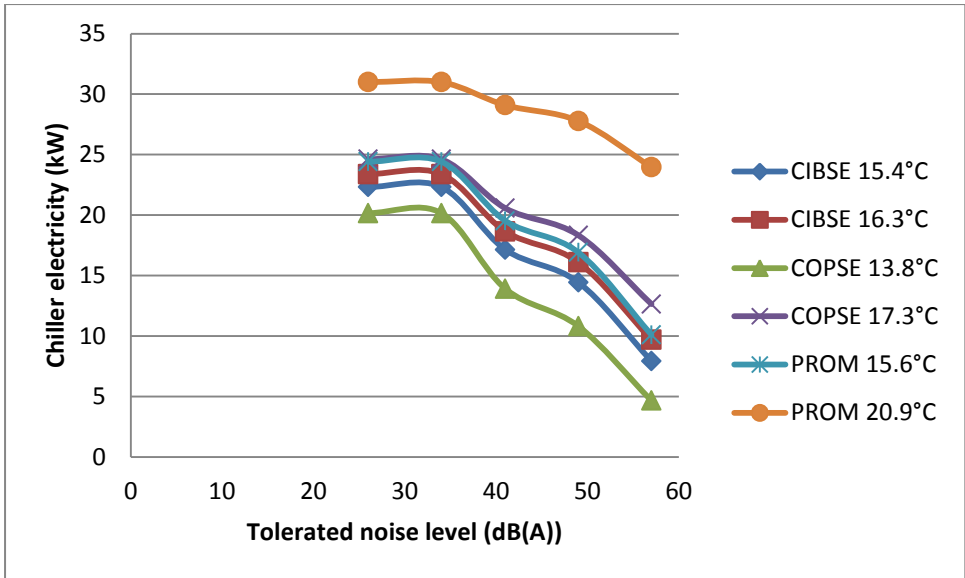


Figure 7.16. Comparison of chiller electricity for Building 5.2 in Location A and with the weather file's average summer temperature indicated in the legend.

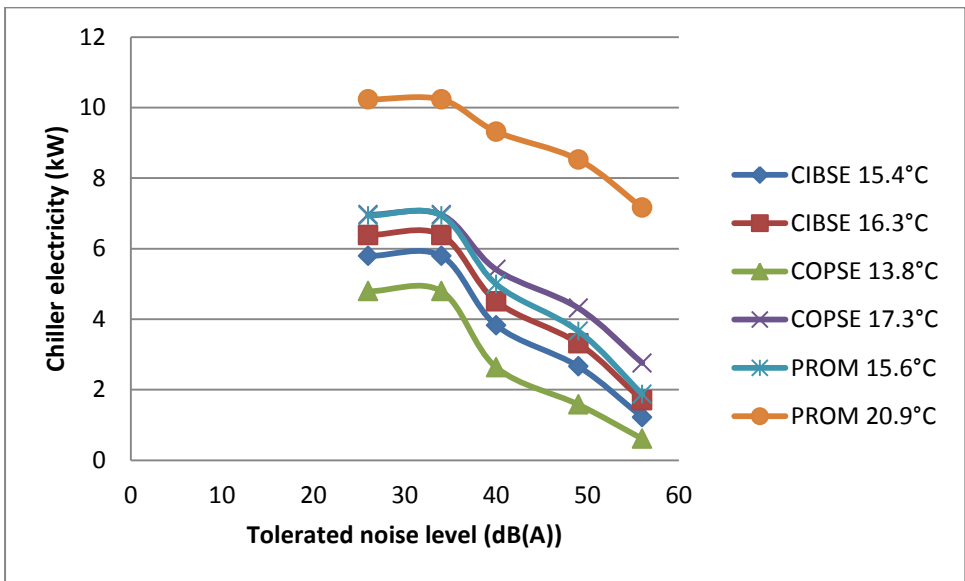


Figure 7.17. Comparison of chiller electricity for Building 5.3 in Location A and with the weather file's average summer temperature indicated in the legend.

The curves shown in Figure 7.15 follow the pattern illustrated in Figure 5.16 with the height of the curve due to the weather file used. The results for Buildings 5.1, 5.2 and 5.3 in Location B also follow this pattern and so graphs have been omitted for brevity although the results are still used for the analysis presented in Table 7.5. It can be seen from Figure 7.16 and Figure 7.17 that both Buildings 5.2 and 5.3 have a stepped trend line in the noisier Location A. This is likely due to these being small buildings, so individual windows have a large effect on the whole-building energy use. The opening and closing of key windows can only be done to each whole percentage of opening, resulting in steps. For Building 5.1 and Location B, which is the larger building and the smoother noise exposure, changes are spread over the façade more gradually and the curves are smoother. The figures show how the 90th percentile PROMETHEOUS 2080 weather file is the most extreme case; far higher cooling load is seen for all the results.

7.3.2 Quantifying the influence of a 10dB noise reduction measure

The results presented in Section 7.3.2 will be used to quantify what level of climate change temperature increase a 10dB noise reduction measure will mitigate. A 10dB noise reduction measure was chosen as an example as this is equivalent to a measure of medium effectiveness (Kang & Brocklesby 2005) from the reviewed studies in Section 2.3.4. The noise reduction measure allows more natural ventilation to occur while keeping noise levels at a 34dBA tolerated level, which is equivalent to the allowable background noise produced by many building services installations (CIBSE 2007). This example is useful as it demonstrates a method that could be used to partly justify the adoption of noise reduction measures.

There are a number of steps between noise reduction and climate temperature change mitigation, so it is worth summarising them here. Noise reduction allows more natural ventilation, as larger openings can be used before noise ingress exceeds allowable levels. In a mixed mode building this larger natural ventilation airflow leads to a reduction in the amount of time that air-conditioning chillers need to be used. The calculation of this reduction is illustrated in Figure 7.18, using the same method as that used in Section 5.7.2. Increasing summer temperatures due to climate change will lead to an increase in air-conditioning use in mixed mode buildings. By comparing the reduction in chiller use due to the noise reduction measure with the increase due to rising summer temperatures, the level of climate change temperature increase that a noise reduction measure mitigates can be calculated. The 10dB noise reduction increases the tolerated level and this is illustrated in Figure 7.18.

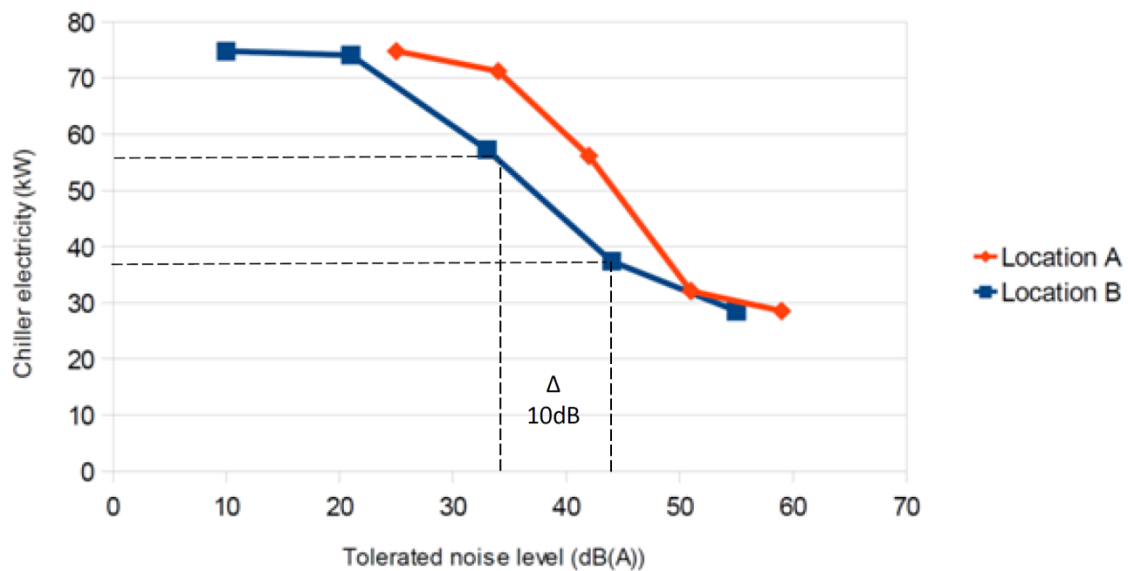


Figure 7.18. Illustration of how the change in chiller electricity due to a 10dB noise reduction measure is calculated.

The calculation of the difference due to the 10dB noise measure becomes a calculation of the difference in cooling use between a tolerated noise level of 34dB and 44dB. This - this calculation was conducted for the results shown in Figures 7.15 to 7.17. In Figure 7.19, a comparison of the increase due to climate change and the decrease due to the noise reduction measure is plotted for Building 5.1 in Location A in Figure 7.19. At a certain level of climate change warming, the saving in chiller usage attributed to the noise reduction measure is equivalent to the increase due to the warming climate and in Figure 7.19 this is the point where the lines cross. So this level of climate change temperature increase can be said to have been mitigated by the noise reduction measure.

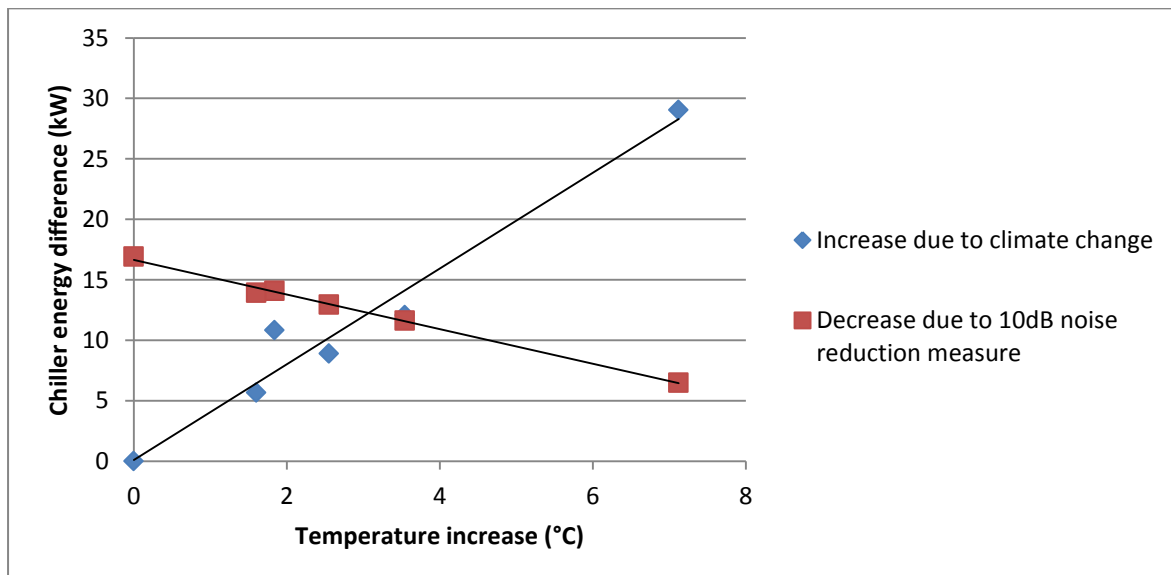


Figure 7.19. Comparison of chiller electricity difference for Building 5.1, in Location A against climate temperature increase, relative to the control period. difference due to 10dB acoustic treatment is compared with difference due to climate change temperature rise.

Similar plots to Figure 7.19 were completed for the other buildings and locations to allow similar calculations, but these are not shown here for the sake of brevity. The linear regression lines fit well: for Figure 7.19 an R^2 of 0.9497 was calculated for the climate line and 0.9957 for the noise reduction line. Similar fits were found for the other buildings and

locations. It is interesting that the results show the energy saving from adopting the 10dB noise reduction measure reducing as the temperature indicating that noise reduction measures will decrease in effectiveness in terms of energy saving, as temperatures rise. This reduction corresponds to the results found in Section 7.1.3, where the sensible cooling effect from natural ventilation decreased as the temperature increased. Figure 7.19 shows that this effect is also seen in these mixed mode buildings. The effectiveness of the noise reduction measure is related to the sensible cooling that is available from the extra natural ventilation flow. Where the regression lines cross, indicates that the climatic factors and the acoustic factors equal each other. The temperatures at which this happens for each of the buildings and locations are shown in Table 7.5.

Table 7.5. Results showing the equivalent temperature where the acoustic factors equal the climatic factors.

Building	Location	Equivalent temperature (°C)
5.1	A	3.07
	B	2.30
5.2	A	3.36
	B	2.48
5.3	A	2.96
	B	1.98

7.4 Discussion

This chapter has looked into design implications that result from the data and methods covered in the preceding chapters. The first section covered the use of future weather data to analyse the sensible cooling and see how the potential for natural ventilation changed under future climates. It was initially found that the cooling effect appeared to increase with increasing summer temperatures. This was due to an increase in ventilation flow, due to more time with the windows opened. By looking at the sensible cooling per unit of ventilation air-

flow it could be seen that the sensible cooling decreased due to a smaller temperature differences between inside and outside the building. With mixed mode cooling this decrease in cooling with higher summer temperatures was clear as the ventilation flow rate did not change considerably. This stable flow rate was because the increase in time that natural ventilation was employed was matched by the increase in time that the buildings changed over to mechanical ventilation. These effects should be kept in mind when a cooling design for the future is considered.

Constructions were varied both in terms of the insulation described by the U value and in the weight of the construction. A reduction in the U value increased the cooling requirements, whereas an increase in construction weight decreased the cooling load. This was the case for current and future climates. An example of varying construction materials for a building subject to acoustic ventilation interaction was shown in Section 7.2.2. It could be seen that both the thermal and acoustic relationships were affected by the construction materials but it is difficult to give simple conclusions from these complex interrelationships. The recommended approach for design would be the careful iteration of different material options.

The uncertainty about future climate should be remembered with updated projections being possible. This is also matched by uncertainty about the future noise environment, with differences in noise sources being possible (for example, more electric vehicles). Noise mapping is an ongoing process and future maps could take into account quieter cars, changes to local industry or power generation. The methods used in this research could be carried out with the latest data about noise and the climatic environment.

7.5 Conclusion

In this chapter design implications have been presented using the new method and data, and the following conclusions have been drawn:

- A 10dB noise reduction measure can mitigate climate change of between 2.0°C and 3.4°C.

This central finding was presented in the final section of this chapter, after outlining the method and assumptions needed to make a comparison of noise and climate on building thermal performance. At initial low levels of climate change warming the acoustic factor is dominant. As the severity of climate warming increases, mixed mode cooling increases, while at the same time the acoustic measure decreases in its effectiveness. At a certain temperature the decrease in cooling due to the acoustic treatment is equal to the increase due to climate change; this is illustrated by intersection of the trend lines in Figure 7.19. With this summer temperature increase the acoustic and climate effects are equivalent or it can be said that the acoustic measure mitigates that level of climate change temperature increase. The equivalent climate temperature increases for the example Buildings 5.1, 5.2 and 5.3 in example noise Locations A and B are given in Table 7.5.

Other conclusions drawn from this chapter are: that the modelled increase in natural ventilation cooling, corresponding to a warming climate, appears to be due to longer periods of time with the windows modelled as open. The cooling per unit of airflow decreases, most likely due to smaller differences between internal and external temperatures. A reduction in the construction material U value results in increased cooling requirements, whereas an increase in construction weight decreases the cooling load.

8 Conclusions

This thesis has examined the interaction of urban noise and a changing climate on natural ventilation cooling, to establish the level of climate change temperature rise that a noise reduction measure would mitigate. To do this, methods that focus on different scales, from individual ventilation apertures to the climate, were combined. The importance of studying these environmental effects is clear, since both have a strong impact on building conditions, and designers must have a basis by which to prioritise when making design decisions.

An example of such a design question is: how much would a noise reduction measure mitigate a temperature increase due to climate change? Climate change will provide an ever-increasing motivation for employing such measures. Such a question is highly site-specific. This study therefore concentrated on carefully chosen example cases covering a range of representative building sizes and room layouts, and contrasting noise exposures. Passive measures such as solar shading and night ventilation were also included in some of the example models. A noise reduction measure which allows more natural ventilation for the same level of noise ingress was modelled to determine the consequent reduction in air conditioning use. This air conditioning reduction was then compared with the increased need for air conditioning due to climate change temperature rise. This provided the objective of this study, the level of temperature increase that the noise reduction measure was able to mitigate. Each Chapter makes contributions to this objective, and these are outlined in the next section.

8.1 Overview of contribution

The main contribution of the thesis is given at the end of Chapter 7. A 10dB noise reduction measure was found to mitigate climate change of between 2.0°C and 3.4°C. A comparison of both climate and noise on the thermal performance was needed to reach this conclusion, involving the integration of a number of novel methods. The first novel contributions toward the main aim are described in Chapter 4, where the combined SRI for naturally ventilated facades was calculated. An FEM set-up was validated, enabling the window aperture transmission loss to be calculated. It was found that the SRI varied by up to 8dB across the frequencies considered. This was combined with construction material sound insulation to give the combined SRI of the façade. This is a new approach to such a problem and is an improvement on derived methods, as the limits on aperture configuration are avoided. It also has the flexibility to be used with a wide range of opening configurations. The results from the aperture modelling were then used in the development of the method to combine whole-building acoustic and ventilation behaviour.

The method used to combine noise mapping and building energy performance was explained in Chapter 5. This contribution enabled the relationship between noise tolerance and thermal performance to be quantified. The approach adopted elements of the method developed by De Salis et al. (2002), but noise mapping output and whole-building thermal models are used to make it specific to a building and its noise exposure. This allowed the sites to be compared with regard to natural ventilation potential. Results were presented in the form of a curve relating the mixed mode cooling use with tolerated noise level, the results of which will be of increasing importance for making design decisions in the future. These results showed the large difference in the effectiveness of a noise reduction measure, depending on the location and the building. For a tolerated road noise ingress of 34dBA, the cooling energy

consumptions for the example buildings in the quieter noise locations were found to be 22% to 45% less, compared to the noisier locations. The effect of a noise reduction measure was quantified in terms of the mixed mode cooling. A measure equal to 10dB resulted in reductions that varied from 28% to 45% of the original cooling energy consumption. These potential effects are significant, and illustrate the importance of an integrated approach.

With the noise environment quantified in terms of mixed mode cooling, it is relatively straightforward to compare this to the mixed mode cooling of the building model run with future climate weather data. There have been difficulties with the latest sets of future weather data, firstly due to the need to generate wind, and secondly due to differences in approach for processing the large amounts of data that result from the new probabilistic projections (Murphy et al. 2009). These issues are analysed in Chapter 6 where a number of future weather data sets, CIBSE, COPSE and PROMETHEUS were compared. These sets were analysed by considering the simulated natural ventilation performance that they produce, so that a representative sample of future climate weather data could be compiled. It was found that PROMETHEUS data gave consistently higher ventilation rates, between 0.1 and 0.9 ACH higher than the other two data sets. These higher rates could be seen as beneficial in terms of avoiding mechanical ventilation use, though, it should be noted that the effect of climate projection percentile on overheating is more important to whether natural ventilation is adopted or not.

The need for wind speed data was less a need to know what changes are likely in the future, but more a need for complete and consistent future weather data sets that can be used with dynamic thermal models. It was found in Chapter 6 that all three compared weather data sets

provided plausible wind data and could therefore be used to determine future thermal performance. This is a finding of significant practical importance since weather data is widely used for building evaluation by built environment practitioners. In addition, a clear conclusion from the overheating results is that it is difficult to justify passive measures alone under the future weather data, due to high levels of overheating.

In Chapter 7 weather data sets were adopted and their implications for building designers were investigated. The combined weather data sets were used to give information about the sensible cooling of natural ventilation with a warming summer time temperature. The natural ventilation cooling, per unit of ventilation air flow, was found to decrease due to a smaller difference between external and internal temperatures. In addition, the effects of different constructions were illustrated. The final set of results compared the effect of noise and climate on thermal performance and required methods and data covered throughout the thesis to be utilised. This comparison is used to quantify what level of climate temperature rise is mitigated by the introduction of a noise reduction measure. It was found that the effectiveness of the noise reduction measure reduced slightly with increasing temperatures. At a certain temperature increase the fall in cooling due to the noise reduction measure is the same as the increase due to climate change. This, in effect, is the level of climate change temperature rise that a noise reduction measure would mitigate. These equivalent temperature results are given in Table 7.4 for an example 10dB noise reduction measure. This result is a culmination of all chapters in the thesis and a useful contribution to a complex problem. It could provide part of the motivation for adopting noise reduction measures.

8.2 Future work

In the future, studies such as the one presented here would benefit from updated and more precise weather information and predictions, as knowledge of the climate system improve. The new information will likely become available and incorporated into building simulation weather data. Running the new weather files for the methods introduced in this thesis would update the results. For this study current levels of traffic noise have been used, but it is also feasible that future changes in the noise environment will occur. These could result from changes to industry, local power generation or vehicle noise emission, for example if electric cars become popular then the road noise would presumably go down. Noise mapping is an ongoing process, so maps would be updated with any future changes. The effect of more stringent planning criteria for noise on summer time building energy use would be an interesting topic of future research. Automating the method presented here would help with evaluating the effect of different potential noise mapping noise distributions.

Another useful subject for further study would be design measures that have a positive effect on both building thermal performance and noise transmission. Examples of this are solar shading devices, blinds, and green roofs (Yang et al. 2012) which can affect both building thermal performance directly and noise transmission through the façade. There is also scope for integrated acoustic/thermal simulation of specialist high-tech natural ventilation systems. It is expected, though, that simple occupant operated, or temperature operated, vents and windows will continue to be popular due to their simplicity and the familiarity of such systems. Allowing occupants to take responsibility for their comfort with such systems is likely to have wide psychological benefits. The psychological interaction between thermal and acoustic comfort is complex and needs further research. With the issue of how to cool large buildings without ever more reliance on energy use becoming more urgent in the future,

improvements and compromises will likely have to be made on a number of fronts. The comfort, in terms of both noise and thermal conditions that people can reasonably expect, will have to be carefully considered.

9 Publication list

List of publications produced during the PhD studies.

- Barclay, M, Kang, J., Sharples, S, Wang, B. & Du, H, 2010. Estimating urban natural ventilation potential by noise mapping and building energy simulation. In Proceedings of 20th International Congress on Acoustics. ICA. Sydney, Australia. Available at: http://www.acoustics.asn.au/conference_proceedings/ICA2010/cdrom-ICA2010/papers/p339.pdf.
- Barclay, M, Kang, J., Sharples, S, Wang, B. & Du, H, 2010. The challenge of balancing the demands for a comfortable thermal and acoustic built environment in a sustainable future. In Proceedings of the International Symposium on Sustainability in Acoustics. ISSA. Auckland, New Zealand.
- Barclay, M., Kang, J. & Sharples, S., 2012. Combining noise mapping and ventilation performance for non-domestic buildings in an urban area. *Building and Environment*, 52, pp.68–76.
- Barclay, M., Kang, J. & Sharples, S., 2011. Exploring Acoustic and Time-scales Issues Relating to the Thermal Physics of Buildings. In 5th International Symposium on Temporal Design. 5th ISTD. Sheffield, UK.
- Barclay, Michael, Sharples, S, Kang, J. & Watkins, R., 2012. The natural ventilation performance of buildings under alternative future weather projections. *Building Services Engineering Research and Technology*, 33(1), pp.35 –50.

10 Appendix A

In this one-dimensional case we assume the problem is a duct with prescribed acoustic amplitude p_0 at the end ($x = 0$) and a rigid barrier at the other ($x = L$) gives.

$$\left. \frac{d\hat{p}}{dx} \right|_{x=L} = 0 \quad \hat{p}|_{x=0} = p_0 = 1 \text{ Pa} \quad (10.1)$$

and

where \hat{p} is the approximate acoustic pressure which is the variable that is sought. In the Galerkin method the weighting function ϕ represents an arbitrary or virtual pressure field and is such that the boundary conditions and the following equation is satisfied

$$\int_0^L \phi \left[\frac{d^2 \hat{p}}{dx^2} + \frac{\omega^2}{c^2} \hat{p} \right] dx = 0 \quad (10.2)$$

where \tilde{p} is the approximate solution of acoustic pressure. Integrating by parts gives.

$$\phi(L) \frac{d\hat{p}}{dx}(L) - \phi(0) \frac{d\hat{p}}{dx}(0) - \int_0^L \frac{d\hat{p}}{dx} \frac{d\phi}{dx} dx + \frac{\omega^2}{c^2} \int_0^L \phi \hat{p} dx = 0 \quad (10.3)$$

One-dimensional elements are used and these have the linear shape functions. The following isoparametric relationships are derived from the shape function as shown in Figure 4.3 help with the solution of the problem.

$$\phi = \mathbf{N}\Psi, \quad \frac{d\hat{p}}{dx} = \mathbf{B}\hat{\mathbf{p}}, \quad \frac{d\phi}{dx} = \mathbf{B}\Psi \quad (10.4)$$

where $\Psi = [\psi_1, \psi_2]$, $\mathbf{N} = [N_1, N_2]$, $\mathbf{B} = \frac{1}{x_2 - x_1} [-1, 1]$, $\hat{\mathbf{p}} = [\hat{p}_1, \hat{p}_2]^T =$ Nodal pressure vector. Super script $()^T$ indicates the transpose. From these relationships the following is formulated.

$$\int_{l_e} \frac{d\hat{p}}{dx} \frac{d\phi}{dx} dx = \hat{\mathbf{p}}^T \mathbf{k} \Psi, \quad \int_{l_e} \phi \hat{p} dx = \hat{\mathbf{p}}^T \mathbf{m} \Psi \quad (10.5)$$

Where \mathbf{k} and \mathbf{m} are the acoustic stiffness and mass matrices, respectively

$$\mathbf{k} = l_e \mathbf{B}^T \mathbf{B} = \frac{1}{l_e} \begin{bmatrix} 1 & -1 \\ -1 & 1 \end{bmatrix}, \quad \mathbf{m} = \frac{l_e}{6} \begin{bmatrix} 2 & 1 \\ 1 & 2 \end{bmatrix} \quad (10.6)$$

The assembly of the global terms over the whole length gives.

$$\int_0^L \frac{d\hat{p}}{dx} \frac{d\phi}{dx} dx = \mathbf{\Psi}^T \mathbf{K} \hat{\mathbf{p}}, \int_0^L \hat{p} \phi dx = \mathbf{\Psi}^T \mathbf{M} \hat{\mathbf{p}} \quad (10.7)$$

Where the upper case notation represent the global vectors. From the conditions described in equation (10.1) and noting that $\phi(0) = 0$, the following terms can be resolved for this example.

$$\phi(L) \frac{d\hat{p}}{dx}(L) - \phi(0) \frac{d\hat{p}}{dx}(0) = 0 \quad (10.8)$$

F is assembled from the prescribed acoustic pressure at $x = 0$, p_0 which is the amplitude of the harmonic pressure source. The final system of equations is given in equation (10.9).

$$\mathbf{K} \hat{\mathbf{P}} - \frac{\omega^2}{c^2} \mathbf{M} \hat{\mathbf{P}} = \mathbf{F} \quad (10.9)$$

where \mathbf{K} is the global stiffness matrix, \mathbf{M} is the global mass matrix and \mathbf{F} is the global force vector.

11 References

- Allard, Francis, 1998. *Natural Ventilation in Buildings*, James & James (Science Publishers) Ltd.
- ARCC, 2011. ARCC Coordination network - Home. Available at: <http://www.ukcip-arcc.org.uk/> [Accessed July 13, 2011].
- Artmann, N., Gyalistra, D., Manz, H. & Heiselberg, P., 2008. Impact of climate warming on passive night cooling potential. *Building Research and Information*, 36(2), pp.111–128.
- Artmann, N., Manz, H. & Heiselberg, P., 2007. Climatic potential for passive cooling of buildings by night-time ventilation in Europe. *Applied Energy*, 84(2), pp.187–201.
- Artmann, N., Manz, H. & Heiselberg, P., 2008. Parameter study on performance of building cooling by night-time ventilation. *Renewable Energy*, 33(12), pp.2589–2598.
- ASHRAE, 2004. *ANSI/ASHRAE standard 55-2004. Thermal Environmental Conditions for Human Occupancy*, Atlanta: American Society of Heating, Refrigerating and Air-Conditioning Engineers.
- ASHRAE, 2009. *ASHRAE handbook: fundamentals*, Atlanta: American Society of Heating, Refrigeration and Air-Conditioning Engineering, Inc.
- ASHRAE, 2001. *International Weather for Energy Calculations (IWEC Weather Files) Users Manual and CD-ROM*, Atlanta: ASHRAE.
- ASHRAE, 2007. Sound and Vibration Control, in *ASHRAE Applications Handbook*, Chapter 47.
- Australian Standard, 2000. AS2107: 2000, Recommended design sound levels and reverberation times for building interiors.
- Awbi, H.B., 1991. *Ventilation of Buildings*, E & FN Spon.
- Awbi, H.B. & Hatton, A., 1999. Natural convection from heated room surfaces. *Energy and Buildings*, 30(3), pp.233–244.
- Babisch, W., 2000. *Traffic noise and cardiovascular disease : Epidemiological review and synthesis*, Available at: <http://www.noiseandhealth.org/article.asp?issn=1463-1741;year=2000;volume=2;issue=8;spage=9;epage=32;aulast=Babisch>.
- BADC, Met Office & Hadley Centre, 2008. HadRM3-PPE-UK Model Data. Available at: <http://badc.nerc.ac.uk/data/hadrm3-ppe-uk/> [Accessed January 14, 2010].
- Baird, G. & Dykes, C., 2010. Acoustic Conditions in Sustainable Buildings—Results of a Worldwide Survey of Users' Perceptions. *Building Acoustics*, 17(4), pp.291–304.

- Barclay, M., Kang, J. & Sharples, S., 2012. Combining noise mapping and ventilation performance for non-domestic buildings in an urban area. *Building and Environment*, 52, pp.68–76.
- Barclay, M., Kang, J., Sharples, S., Wang, B & Du, H, 2010. Estimating urban natural ventilation potential by noise mapping and building energy simulation. In *Proceedings of 20th International Congress on Acoustics*. ICA. Sydney, Australia. Available at: http://www.acoustics.asn.au/conference_proceedings/ICA2010/cdrom-ICA2010/papers/p339.pdf.
- Belcher, S., Hacker, J.N. & Powell, D., 2005. Constructing design weather data for future climates. *Building Services Engineering Research and Technology*, 26(1), pp.49–61.
- Bernek, L., 1971. *Noise and vibration control*, New York: McGraw-Hill.
- Betwixt, 2008. Hourly Time-series Output and Figures from the CRU Weather Generator. Available at: www.cru.uea.ac.uk/cru/projects/betwixt/cruwg_hourley.
- Blondeau, P., Spérandio, M. & Allard, F., 1997. Night ventilation for building cooling in summer. *Solar Energy*, 61(5), pp.327–335.
- Bouwkamp, C.J., 1941. *Theoretische en numerieke behandeling van de buiging door een ronde opening*. Dissertation. University of Groningen.
- Brager, G.S. & de Dear, R.J., 2000. A Standard for Natural Ventilation. *ASHRAE Journal*. Available at: <http://citeseerx.ist.psu.edu/viewdoc/download?doi=10.1.1.61.4746&rep=rep1&type=pdf>.
- BRE, 2011. Building Research Establishment Environmental Assessment Method (BREEAM) – Offices. Available at: <http://www.breeam.org/>.
- BRE, 2010. NBS Guide to Part L of the Building Regulations. Conservation of fuel and power. 2010 Edition.
- Breesch, H. & Janssens, A., 2010. Performance evaluation of passive cooling in office buildings based on uncertainty and sensitivity analysis. *Solar Energy*, 84(8), pp.1453–1467.
- Brown, S., Boorman, P., McDonald, R. & Murphy, J.M., 2009. *Interpretation for use of surface wind speed projections from the 11-member Met Office Regional Climate Model ensemble*, Available at: http://ukclimateprojections.defra.gov.uk/images/stories/Tech_notes/UKCP09_wind_technote.pdf.
- BSI, 1999. *BS 8233:1999. Sound insulation and noise reduction for buildings - Code of practice*, London: BSI: (British standards Institution).
- BSI, 2004. *BS EN 13141-1 Ventilation for buildings - Performance testing of components/products for residential ventilation. Part 1: Externally and internally mounted air transfer devices*.

- BSI, 1997. BS EN ISO 717-1:1997 - Acoustics – Rating of sound insulation in buildings and of building elements. part 1. Airborne sound insulation.
- CEN & BSI, 2007. *BS EN 15251:2007. Indoor environmental input parameters for design and assessment of energy performance of buildings addressing indoor air quality, thermal environment, lighting and acoustics*, Brussels: CEN, London: BSI: Comité Européen de Normalisation, British standards Institution.
- CEN & BSI, 2005. *BS EN ISO 7730:2005. Ergonomics of the thermal environment – Analytical determination and interpretation of thermal comfort using calculation of the PMV and PPD indices and local comfort criteria.*, Brussels: CEN, London: BSI: Comité Européen de Normalisation, British standards Institution.
- Chandrupatla, T.R. & Belegundu, A.D., 2001. *Introduction to Finite Elements in Engineering - Third edition*, Prentice Hall.
- Chow, D.H. & Levermore, G.J., 2010. The effects of future climate change on heating and cooling demands in office buildings in the UK. *Building Services Engineering Research and Technology*, 31(4), pp.307–323.
- Christensen, J., Carter, T., Rummukainen, M. & Amanatidis, G., 2007. Evaluating the performance and utility of regional climate models: the PRUDENCE project. *Climatic Change*, 81(0), pp.1–6.
- CIBSE, 2007. CIBSE Guide A: Environmental design.
- CIBSE, 2002. *Weather, solar and illuminance data CIBSE Guide J*, London: Chartered Institution of building services engineers.
- CIBSE & Met Office, 2009a. Current CIBSE TRY/DSY Hourly Weather Data Set - 14 sites. Available at: <http://www.cibse.org/index.cfm?go=publications.view&item=332>.
- CIBSE & Met Office, 2009b. Future CIBSE TRY/DSY Hourly Weather Data Set. Available at: <http://www.cibse.org/index.cfm?go=publications.view&item=406>.
- Clarke, J.A., 2001. *Energy Simulation in Building Design*, Butterworth-Heinemann.
- Clarke, J.A. & Johnstone, C.M., 2008. The role of built environment energy efficiency in a sustainable UK energy economy. *Energy Policy*, 36, pp.4605–4509.
- Coley, D. & Kershaw, T., 2010. Changes in internal temperatures within the built environment as a response to a changing climate. *Building and Environment*, 45(1), pp.89–93.
- Comsol Multiphysics, 2008. Acoustics Module, User's Guide.
- COPSE, 2011. COPSE: Co-incident probabilistic climate change weather data for a sustainable environment. Available at: <http://www.copse.manchester.ac.uk/> [Accessed July 13, 2011].

- Cóstola, D., Blocken, B. & Hensen, J.L.M., 2009. Overview of pressure coefficient data in building energy simulation and airflow network programs. *Building and Environment*, 44(10), pp.2027–2036.
- Cóstola, D., Blocken, B., Ohba, M. & Hensen, J.L.M., 2010. Uncertainty in airflow rate calculations due to the use of surface-averaged pressure coefficients. *Energy and Buildings*, 42(6), pp.881–888.
- Crawley, D.B. & Hand, J.W., 2006. Contrasting the Capabilities of building energy performance simulation programs. *Building and Environment*, 43(4), pp.661–673.
- Crawley, D.B. & Hand, J.W., 1999. Improving the Weather Information Available to Simulation Programs. In *Proceedings of the Building Simulation '99 Conference*. Kyoto, Japan.
- DataKustik GmbH, 2006. Cadna/A for Windows - User Manual.
- DCLG, 2010. National Calculation Methodology (NCM) modelling guide (for buildings other than dwellings in England and Wales) 2010 edition. Available at: <http://www.communities.gov.uk/documents/planningandbuilding/pdf/1016185.pdf>.
- DCLG, 1994. Planning Policy Guidance 24: Planning and Noise (PPG24). Available at: <http://www.communities.gov.uk/documents/planningandbuilding/pdf/156558.pdf>.
- de Dear, R.J. & Brager, G.S., 2002. Thermal comfort in naturally ventilated buildings: revisions to ASHRAE Standard 55. *Energy and Buildings*, 34(6), pp.549–561.
- DECC, 2011. *Energy act 2011*, Department of Energy and Climate Change. Available at: <http://www.legislation.gov.uk/ukpga/2011/16/contents/enacted/data.htm>.
- Defra, 2008. E-Digest of Statistics - Department for Environment Food and Rural Affairs (Defra). Available at: <http://www.defra.gov.uk/environment/statistics/globalatmos/gakf07.htmS>.
- DesignBuilder Software Ltd, 2009. DesignBuilder 2.1 User's Manual. Available at: http://www.designbuilder.co.uk/component/option,com_docman/task,cat_view/gid,20/Itemid,30/.
- DfEE, 1975. Acoustics in educational buildings, Building Bulletin 51.
- DfES, 2003. *Guidelines for environmental design in schools. 2nd edition*, School Building and Design Unit, Department for Education and Skills (DfES).
- DfT, 1988. Calculation of road traffic noise.
- DTI, 2003. *Energy White Paper: Our Energy Future — Creating a Low Carbon Economy*, Department of Trade and Industry.
- Du, H, Underwood, CP & Edge, JS, 2012. Generating design reference years from the UKCP09 projections and their application to future air-conditioning loads. *Building Services Engineering Research and Technology*, 33(1), pp.63–79.

- Du, H., Underwood, C.P. & Edge, J.S., 2011. Generating test reference years from the UKCP09 projections and their application in building energy simulations. *Building Services Engineering Research and Technology*. Available at: <http://bse.sagepub.com/content/early/2011/09/09/0143624411418132.abstract>.
- Du, Hu, Underwood, Chris & Edge, Jerry, 2010. Modelling the impact of a warming climate on commercial buildings in the UK. In *Clima 2010*. Clima 2010.
- Eames, M., Kershaw, T. & Coley, D., 2011a. On the creation of future probabilistic design weather years from UKCP09. *Building Services Engineering Research and Technology*, 32(2), pp.127 –142.
- Eames, M., Kershaw, T. & Coley, D., 2011b. The creation of wind speed and direction data for the use in probabilistic future weather files. *Building Services Engineering Research and Technology*, 32(2), pp.143 –158.
- EC, 2005. *Challenging and Changing Europe's Built Environment: A Vision for a Sustainable and Competitive Construction Sector by 2030*, European Commission (EC). Available at: www.ectp.org/documentation/ECTP-Vision2030-25Feb2005.pdf.
- EC, 2006. Working Group Assessment of Exposure to Noise (WG-AEN). Position paper – good practice guide for strategic noise mapping and the production of associated data on noise exposure, version 2. Available at: http://ec.europa.eu/environment/noise/pdf/best_practice_guide.pdf.
- EEA, 2012. Noise Observation and Information Service for Europe - NOISE. Available at: <http://noise.eionet.europa.eu/>.
- Ekström, M., 2007. Regional climate model data used within the SWURVE project. 1: previous term Projected changes next term in previous term seasonal patterns and estimation of PET. *Hydrol. Earth Syst. Sci.*, 11(3), pp.1069–1083.
- European Union, 2002. European Union, Directive 2002/49/EC. *relating to the Assessment and Management of Environmental Noise. Official Journal of the European Communities*, No. L 189.
- Fanger, P.O., 1970. *Thermal comfort : analysis and applications in environmental engineering.*, Copenhagen: Danish Technical Press.
- Feustel, H.E., 1999. COMIS--an international multizone air-flow and contaminant transport model. *Energy and Buildings*, 30(1), pp.3–18.
- Field, C., 2010. Satisfactory background noise levels in naturally ventilated buildings - challenging acoustic criteria used in the past. In *20th International Congress on Acoustics*. ICA 2010. Sydney, Australia.
- Field, C. & Digerness, J., 2008. Acoustic design criteria for naturally ventilated building. In *acousrics 08 Paris*. Euronoise. Paris. Available at: <http://intelligence.eu.com/acoustics2008/acoustics2008/cd1/data/articles/000560.pdf>.

- Field, C. & Fricke, F.R., 1998. Theory and applications of quarter-wave resonators: A prelude to their use for attenuating noise entering buildings through ventilation openings. *Applied Acoustics*, 53(1-3), pp.117–132.
- Finn, D.P., Connolly, D. & Kenny, P., 2007. Sensitivity analysis of a maritime located night ventilated library building. *Solar Energy*, 81(6), pp.697–710.
- Ford, R.D. & Kerry, G., 1973. The sound insulation of partially open double glazing. *Applied Acoustics*, 6(1), pp.57–72.
- Furbringer, J.M., Roulet, C.A. & Borchiellini, R., 1996. Technical Synthesis Report: Multizone Air Flow Modelling (COMIS) - Annex 23, Evaluation of COMIS. Available at: <http://www.ecbcs.org/annexes/annex23.htm#p>.
- GBCA, 2011. Greenstar -Office design and office as built. Available at: <http://www.gbca.org.au/>.
- Ghiaus, C. & Allard, F., 2005. *Natural Ventilation in the Urban Environment: Assessment and Design.*, London: Earthscan.
- Ghiaus, C., Allard, F., Santamouris, M., Georgakis, C. & Nicol, F., 2006. Urban environment influence on natural ventilation potential. *Building and Environment*, 41(4), pp.395–406.
- Golneshan, A.A. & Yaghoubi, M.A., 1990. Simulation of ventilation strategies of a residential building in hot arid regions of Iran. *Energy and Buildings*, 14(3), pp.201–205.
- Gomperts, M.C., 1964. The “sound insulation” of circular and slit-shaped aperture. *Acoustica*, 14(1), pp.1–16.
- Guan, L., 2009. Preparation of future weather data to study the impacts of climate change on buildings. *Building and Environment*, 44, pp.793–800.
- Hacker, J.N., 2009. CIBSE TM48 and TM49: future weather years for building simulation. Available at: nceub.commoncense.info/uploads/Hacker.pdf.
- Hacker, J.N., Capon, R. & Mylona, A., 2009. *TM48: Use of climate change scenarios for building simulation: the cibse future weather years.*, Available at: <http://www.cibse.org/index.cfm?go=publications.view&item=449>.
- Hacker, J.N. & Holmes, M.J., 2005. *TM36: Climate change and the indoor environment: impacts and adaption*, Available at: <http://www.cibse.org/index.cfm?go=publications.view&item=295>.
- Hanby, V.I. & Smith, S.T., 2012. Simulation of the future performance of low-energy evaporative cooling systems using UKCP09 climate projections. *Building and Environment*, 55(0), pp.110–116.
- Hand, J.W., 2008. *THE ESP-r COOKBOOK Strategies for Deploying Virtual Representations of the Build Environment*, Glasgow: Energy Systems Research Unit

- Department of Mechanical Engineering University of Strathclyde. Available at: http://www.esru.strath.ac.uk/Documents/ESP-r_cookbook_nov2008.pdf.
- Harpham, C. & Goodess, C.M., 2006. *The CRU Hourly Weather Generator*, Climatic Research Unit, University of East Anglia. Available at: http://www.cru.uea.ac.uk/cru/projects/betwixt/documents/BETWIXT_TBN_7_v1.pdf.
- Hartog van Banda, E. & Stapelfeldt, H., 2007. Software implementation of the harmonoise/imagine method, the various sources of uncertainty. In INTER-NOISE. Istanbul, Turkey.
- Henninger, R.H. & Witte, M.J., 2009. *EnergyPlus Testing with Building Thermal Envelope and Fabric Load Tests from ANSI/ASHRAE Standard 140-2007*, Office of Building Technologies Washington, D.C.: U.S. Department of Energy.
- Hewitt, C.D. & Goodess, C.M., 2009. Towards probabilistic projections of climate change. *Municipal Engineer*, 162(ME1), pp.33–40.
- Hewitt, C.D. & Griggs, D.J., 2004. *Ensembles-based predictions of climate changes and their impacts*, Met Office, Exeter. Available at: http://ensembles-eu.metoffice.com/tech_reports/ETR_1_vn2.pdf.
- Holmes, M.J. & Hacker, J.N., 2007. Climate change, thermal comfort and energy: Meeting the design challenges of the 21st century. *Energy and Buildings*, 39(7), pp.802–814.
- Holmes, M.J. & Hitchin, E.R., 1978. An “Example year” for the calculation of energy demand in buildings. *Building serv. Engineer*, 45(9), pp.186–189.
- Hopkins, C., Hall, R., James, A., Orłowski, R., Wise, S. & Canning, D., 2003. Building Bulletin 93 (BB93): Acoustic design of schools. Available at: www.teachernet.gov.uk/acoustics/.
- Horan, J.M. & Finn, D.P., 2008. Sensitivity of air change rates in a naturally ventilated atrium space subject to variations in external wind speed and direction. *Energy and Buildings*, 40, pp.1577–1585.
- Huang, H., 2011. Active noise attenuation in ventilation windows. *The Journal of the Acoustical Society of America*, 130(1), p.176.
- Huang, Huahua, Qiu, X. & Kang, J., 2011. Active noise attenuation in ventilation windows. *The Journal of the Acoustical Society of America*, 130(1), pp.176–188.
- Hulme, M. & Jenkins, G.J., 2002. *Climate Change Scenarios for the United Kingdom: The UKCIP02 Scientific Report*, Tyndall Centre for Climate Change Research, School of Environmental Sciences, University of East Anglia, Norwich, UK. Available at: http://www.ukcip.org.uk/index.php?id=353&option=com_content&task=view [Accessed December 1, 2008].
- IPCC, 2007. *Climate change 2007: The Physical Science Basis Working Group I Contribution to the Fourth Assessment Report of the Intergovernmental Panel on Climate Change*, Cambridge: University press.

- IPCC, 1990. *IPCC First Assessment Report 1990 (3 vols): Scientific Assessment of Climate change*, Cambridge: University press,.
- IPCC, 1995. *IPCC Second Assessment Report: Climate Change 1995: The Science of Climate Change*, Cambridge: University press,.
- IPCC, 2001. *IPCC Third Assessment Report: Climate Change 200: Synthesis Report*, Cambridge: University press,.
- ISO, 1997. ISO 140-1, Acoustics - Measurement of sound insulation in buildings and of building elements - Part 1: Requirements for laboratory test facilities with suppressed flanking transmission.
- ISO, 1995. ISO 140-3, Acoustics - Measurement of sound insulation in buildings and of building elements - Part 3: Laboratory measurements of airbourne sound insulation of building elements.
- ISO, 1998. ISO 140-4, Acoustics - Measurement of sound insulation in buildings and of building elements — Part 4: Field measurements of airborne sound insulation between rooms.
- Jakob, A. & Möser, M., 2003a. Active control of double-glazed windows. Part II: Feedback control. *Applied Acoustics*, 64(2), pp.183–196.
- Jakob, A. & Möser, M., 2003b. Active control of double-glazed windows Part I: Feedforward control. *Applied Acoustics*, 64(2), pp.163–182.
- Jenkins, D.P., 2009. The importance of office internal heat gains in reducing cooling loads in a changing climate. *International Journal of Low-Carbon Technologies*, 4(3), pp.134–140.
- Jenkins, D.P., Patidar, S., Banfill, P.F.G. & Gibson, G.J., 2011. Probabilistic climate projections with dynamic building simulation: predicting overheating in dwellings. *Energy and Buildings*, In Press, Accepted Manuscript. Available at: <http://www.sciencedirect.com/science/article/B6V2V-52FVDH8-3/2/b2f20f3ea252e850d57a420545d3f7f8>.
- Jenkins, G.J. & Lowe, J., 2003. *Handling uncertainties in the UKCIP02 scenarios of climate change*, Exeter: Met Office Hadley Centre. Available at: http://www.metoffice.gov.uk/publications/HCTN/HCTN_44.pdf.
- Jenkins, G.J., Murphy, J.M., Sexton, D., Lowe, Jason, Jones, P. & Kilsby, C., 2010. *UK Climate Projections: Briefing report*, Available at: <http://ukclimateprojections.defra.gov.uk/content/view/943/500/>.
- Jenkins, G.J., Perry, M. & Prior, J., 2009. *The climate of the United Kingdom and recent trends, Revised edition*, Hadley Centre, Met Office, Exeter. Available at: <http://ukclimateprojections.defra.gov.uk/content/view/816/500/>.
- Jentsch, M.F. & Bahaj, A.S., 2008. Climate change future proofing of buildings - Generation and assessment of building simulation weather files. *Energy and Buildings*, 40(12), pp.2148–2168.

- Jones, P.D., Kilsby, C.G., Harpham, C., Glenis, V. & Burton, A., 2009. *UK Climate Projections science report: Projections of future daily climate for the UK from the Weather Generator*, University of Newcastle, UK. Available at: <http://ukclimateprojections.defra.gov.uk/content/view/945/500>.
- Kang, J., 2002a. *Acoustics of Long Spaces: Theory and Design Practice*, London: Thomas Telford Ltd.
- Kang, J., 2002b. Numerical modelling of the sound field in urban streets with diffusely reflecting boundaries. *Journal of Sound and Vibration*, 258(5), pp.793–813.
- Kang, J., 2005. Numerical modelling of the sound fields in urban squares. *The Journal of the Acoustical Society of America*, 117(6), pp.3695–3706.
- Kang, J., 2001. Sound propagation in interconnected urban streets: a parametric study. *Environment and Planning B: Planning and Design*, 28(2), pp.281–294.
- Kang, J., 2000. Sound propagation in street canyons: Comparison between diffusely and geometrically reflecting boundaries. *The Journal of the Acoustical Society of America*, 107(3), pp.1394–1404.
- Kang, J., 2007. *Urban Sound Environment*, Taylor & Francis.
- Kang, J. & Brocklesby, M.W., 2005. Feasibility of applying micro-perforated absorbers in acoustic window systems. *Applied Acoustics*, 66(6), pp.669–689.
- Kang, J. & Huang, J., 2005. Noise-mapping: accuracy and strategic application. In *Inter noise*. Rio de Janeiro, Brazil.
- Kang, J. & Li, Z., 2007. Numerical Simulation of an Acoustic Window System Using Finite Element Method. *Acta Acustica united with Acustica*, 93(1), pp.152–163(12).
- Karava, P., Stathopoulos, T. & Athienitis, A.K., 2007. Wind-induced natural ventilation analysis. *Solar Energy*, 81(1), pp.20–30.
- Kershaw, T., Eames, M. & Coley, D., 2011. Assessing the risk of climate change for buildings: A comparison between multi-year and probabilistic reference year simulations. *Building and Environment*, 46(6), pp.1303–1308.
- Khan, N., Su, Y. & Riffat, S.B., 2008. A review on wind driven ventilation techniques. *Energy and Buildings*, 40(8), pp.1586–1604.
- Kilsby, C.G. & Jones, P.D., 2007. A daily weather generator for use in climate change studies. *Environmental Modelling & Software*, 22(12), pp.1705–1719.
- Kolokotroni, M., Giannitsaris, I. & Watkins, R., 2006. The effect of the London urban heat island on building summer cooling demand and night ventilation strategies. *Solar Energy*, 80(4), pp.383–392.
- Kurra, S. & Dal, L., 2011. Sound insulation design by using noise maps. *Building and Environment*, In Press, Accepted Manuscript. Available at: <http://www.sciencedirect.com/science/article/pii/S0360132311002149>.

- Lambert, J., Simonnet, F. & Vallet, M., 1984. Patterns of behaviour in dwellings exposed to road traffic noise. *Journal of Sound and Vibration*, 92(2), pp.159–172.
- LBNL, 2010. EnergyPlus Engineering Reference. Available at: http://apps1.eere.energy.gov/buildings/energyplus/energyplus_documentation.cfm [Accessed July 9, 2011].
- Levermore, G.J., 2008. A review of the IPCC Assessment Report Four, Part 2: Mitigation options for residential and commercial buildings. *Building Services Engineering Research and Technology*, 29(4), pp.363–374.
- Levermore, G.J. & Parkinson, J.B., 2006. Analyses and algorithms for new Test Reference Years and Design Summer Years for the UK. *Building Services Engineering Research and Technology*, 27(4), pp.311–325.
- Liddament, M.W., 1996. A guide to energy efficient ventilation. Available at: http://www.aivc.org/frameset/frameset.html?../Publications/guides/guide_to_eev.html
- Liddament, M.W., 1986. *Air infiltration calculation techniques – an applications guide*, AIVC.
- van der Linden, K., Boerstra, A.C., Raue, A.K. & Kurvers, S.R., 2002. Thermal indoor climate building performance characterized by human comfort response. *Energy and Buildings*, 34(7), pp.737–744.
- Mak, C., Leung, W. & Jiang, G., 2010. Measurement and prediction of road traffic noise at different building floor levels in Hong Kong. *Building Services Engineering Research and Technology*, 31(2), pp.131–139.
- Mao, Q. & Pietrzko, S., 2010. Experimental study for control of sound transmission through double glazed window using optimally tuned Helmholtz resonators. *Applied Acoustics*, 71(1), pp.32–38.
- McElroy, L.B., Clark, J.A. & Hand, J.W., 2001. Delivering Simulation to the Profession: The next stage? In *Seventh International IBPSA Conference*. Rio de Janeiro, Brazil.
- McGilligan, C., Natarajan, S. & Nikolopoulou, M., 2011. Adaptive Comfort Degree-Days: a metric to compare adaptive comfort standards and estimate changes in energy consumption for future UK climates. *Energy and Buildings*, 43(10), pp.2767–2778.
- Miller, K. & Montone, W.V., 1978. *Handbook of Acoustical Enclosures and Barriers*, Fairmont Press Inc., Atlanta.
- Mochida, A., Yoshino, H., Takeda, T., Kakegawa, T. & Miyauchi, S., 2005. Methods for controlling airflow in and around a building under cross-ventilation to improve indoor thermal comfort. *Journal of Wind Engineering and Industrial Aerodynamics*, 93(6), pp.437–449.
- Montazami, A., Wilson, Mike & Nicol, Fergus, 2012. Aircraft noise, overheating and poor air quality in classrooms in London primary schools. *Building and Environment*, 52(0), pp.129–141.

- Murphy, E. & King, E.A., 2010. Strategic environmental noise mapping: Methodological issues concerning the implementation of the EU Environmental Noise Directive and their policy implications. *Environment International*, 36(3), pp.290–298.
- Murphy, J.M., Sexton, D.M.H, Jenkins, G.J., Boorman, P.M., Booth, B.B.B., Brown, C.C., Clark, R.T., Collins, M., Harris, G., Kendon, E.J., Betts, R.A., Brown, S.J., Howard, T.P., Humphreys, K.A., McCarthy, M.P., McDonald, R.E., Stevens, A., Wallace, C., Warren, R., Wilby, R.L. & Wood, R.A., 2009. *UK Climate Projections Science Report: Climate change projections*, Met Office Hadley Centre, Exeter. Available at: <http://ukclimateprojections.defra.gov.uk/content/view/824/517>.
- Nijland, H.A., Van Kempen, E.E.M.M., Van Wee, G.P. & Jabben, J., 2003. Costs and benefits of noise abatement measures. *Transport Policy*, 10(2), pp.131–140.
- Nomura, Y. & Inawashiro, S., 1960. *On the transmission of acoustic waves through a circular channel of a thick wall*,
- Nota, R., Barelds, R. & van Maercke, D., 2005. *Engineering method for road traffic and railway noise after validation and fine-tuning, Technical report deliverable 18 of the harmonoise project, HAR32TR-040922-DGMR20*,
- O'Malley, V., King, E., Kenny, L. & Dilworth, C., 2009. Assessing methodologies for calculating road traffic noise levels in Ireland – Converting CRTN indicators to the EU indicators (Lden, Lnight). *Applied Acoustics*, 70(2), pp.284–296.
- Öhrström, E. & Skånberg, A., 2004. Sleep disturbances from road traffic and ventilation noise—laboratory and field experiments. *Journal of Sound and Vibration*, 271(1-2), pp.279–296.
- Oldham, D.J., Kang, J. & Brocklesby, M.W., 2005. Modelling the Acoustical and Airflow Performance of Simple Lined ventilation Apertures. *Building Acoustics*, 12(4), pp.277 – 292.
- Oldham, D.J., De Salis, M.H.F. & Sharples, S., 2004. Reducing the ingress of urban noise through natural ventilation openings. *Indoor Air*, 14, pp.118–126.
- Oldham, D.J. & Zhao, X., 1993. Measurement of the sound transmission loss of circular and slit-shaped apertures in rigid walls of finite thickness by intensimetry. *Journal of Sound and Vibration*, 161(1), pp.119–135.
- Ordnance Survey, 2012. Roam Digimap image. Available at: <http://edina.ac.uk/digimap/index.shtml>.
- Peeters, B. & Blokland, G. v, 2007. *The noise emission model for European road traffic. Deliverable 11 of IMAGINE project. Technical report IMA55TR-060821-MP10*,
- PROMETHEUS, 2011. PROMETHEUS - The Use of Probabilistic Climate Change Data to Future-proof Design Decisions in the Building Sector. Available at: <http://centres.exeter.ac.uk/cee/prometheus/> [Accessed July 13, 2011].

- R Development Core Team, 2011. *R: A Language and Environment for Statistical Computing*, Vienna, Austria: R Foundation for Statistical Computing. Available at: <http://www.R-project.org/>.
- Roberts, S., 2008. Effects of climate change on the built environment. *Energy Policy*, 36, pp.4552–4557.
- Rosenthal, D.H. & Gruenspecht, H.K., 1995. Effects of global warming on energy use for space heating and cooling in the United States. *Energy Journal*, 16(2), pp.77–96.
- Rougier, J., Sexton, David M. H., Murphy, James M. & Stainforth, D., 2009. Analyzing the Climate Sensitivity of the HadSM3 Climate Model Using Ensembles from Different but Related Experiments. *J. Climate*, 22(13), pp.3540–3557.
- De Salis, M.H.F., Oldham, D.J. & Sharples, S., 2002. Noise control strategies for naturally ventilated buildings. *Building and Environment*, 37(5), pp.471–484.
- Salomons, E. & Heimann, D., 2004. *Description of the reference model. Technical report deliverable 16 of the harmonoise project, HAR29TR-041118-TNO10*,
- Santamouris, M. & Asimakopoulos, D., 1996. *Passive Cooling of Buildings*, Earthscan.
- Santamouris, M., Papanikolaou, N., Livada, I., Koronakis, I., Georgakis, C., Argiriou, A. & Assimakopoulos, D., 2001. On the impact of urban climate on the energy consumption of buildings. *Solar Energy*, 70(3), pp.201–216.
- Santamouris, M., Sfakianaki, A. & Pavlou, K., 2010. On the efficiency of night ventilation techniques applied to residential buildings. *Energy and Buildings*, 42(8), pp.1309–1313.
- Sauter, J. & Soroka, W.W., 1970. Sound Transmission through Rectangular Slots of Finite Depth between Reverberant Rooms. *The Journal of the Acoustical Society of America*, 47(1A), pp.5–11.
- Sgard, F., Nelisse, H. & Atalla, N., 2007. On the modeling of the diffuse field sound transmission loss of finite thickness apertures. *The Journal of the Acoustical Society of America*, 122(1), pp.302–313.
- Sharples, S. & Chilengwe, N., 2006. Performance of ventilator components for natural ventilation applications. *Building and Environment*, 41(12), pp.1821–1830.
- Sharples, S. & Lee, S., 2009. Climate Change and Building Design - Chapter 19. In M. Santamouris & D. Mumovic, eds. *A Handbook of Sustainable Building Design and Engineering*. Earthscan.
- Swart, R. & Nakicenovic, N., 2000. *IPCC Special Report on Emissions Scenarios*, Geneva Switzerland: Cambridge University Press.
- Templeton, D., 1993. *Acoustics in the Built Environment*, Butterworth Architecture.
- TNO, 2010. Cp Generator. *TNO Webapplications*. Available at: <http://cpgen.bouw.tno.nl/cp/>.

- Trompette, N., Barbry, J.-L., Sgard, F. & Nelisse, H., 2009. Sound transmission loss of rectangular and slit-shaped apertures: Experimental results and correlation with a modal model. *The Journal of the Acoustical Society of America*, 125(1), pp.31–41.
- Tuohy, P., Rijal, H.B., Humphreys, M.A., Nicol, J.F., Samuel, A. & Clarke, J.A., 2007. Comfort driven adaptive window opening behaviour and the influence of building design. In *Building Simulation, 10th IBPSA Conference*. IBPSA.
- UKCP, 2009. UKCP09 User Interface manual.
- Wang, Bo & Kang, J., 2011. Effects of urban morphology on the traffic noise distribution through noise mapping: A comparative study between UK and China. *Applied Acoustics*, 72(8), pp.556–568.
- Watkins, R., Levermore, G.J. & Parkinson, J.B., 2011. Constructing a future weather file for use in building simulation using UKCP09 projections. *Building Services Engineering Research and Technology*, 32(3), pp.293–299.
- Watkins, R., Levermore, G.J. & Parkinson, J.B., 2012. The Design Reference Year – a new approach to testing a building in more extreme weather using UKCP09 projections. *Building Services Engineering Research and Technology*.
- Wiley, R.L., 2007. A Review of Climate Change Impacts on the built Environment. *Built Environment*, 33(1), pp.31–45.
- Wilks, D.S. & Wilby, R.L., 1999. The weather generation game: a review of stochastic weather models. *Progress in Physical Geography*, 23(3), pp.329–357.
- Wilson, G.P. & Soroka, W.W., 1965. Approximation to the Diffraction of Sound by a Circular Aperture in a Rigid Wall of Finite Thickness. *The Journal of the Acoustical Society of America*, 37(2), pp.286–297.
- Wilson, M. & Nicol, J.F., 1994. Tolerated noise levels in the U.K. and Pakistan and simultaneous thermal comfort. *Renewable Energy*, 5(5-8), pp.1006–1008.
- Xie, H. & Kang, J., 2010. On the Relationships Between Environmental Noise and Socio-Economic Factors in Greater London. *Acta Acustica united with Acustica*, 96(3), pp.472–481.
- Yang, H.S., Kang, J. & Choi, M.S., 2012. Acoustic effects of green roof systems on a low-profiled structure at street level. *Building and Environment*, 50(0), pp.44–55.
- Yu, C.-J. & Kang, J., 2009. Environmental impact of acoustic materials in residential buildings. *Building and Environment*, 44(10), pp.2166–2175.
- Yun, G.Y. & Steemers, K., 2010. Night-time naturally ventilated offices: Statistical simulations of window-use patterns from field monitoring. *Solar Energy*, 84(7), pp.1216–1231.
- Zannin, P.H.T. & Sant’Ana, D.Q. de, 2011. Noise mapping at different stages of a freeway redevelopment project – A case study in Brazil. *Applied Acoustics*, 72(8), pp.479–486.

Zienkiewicz, O.C. & Morgan, K., 1983. *Finite elements and approximation*, Wiley-Interscience.